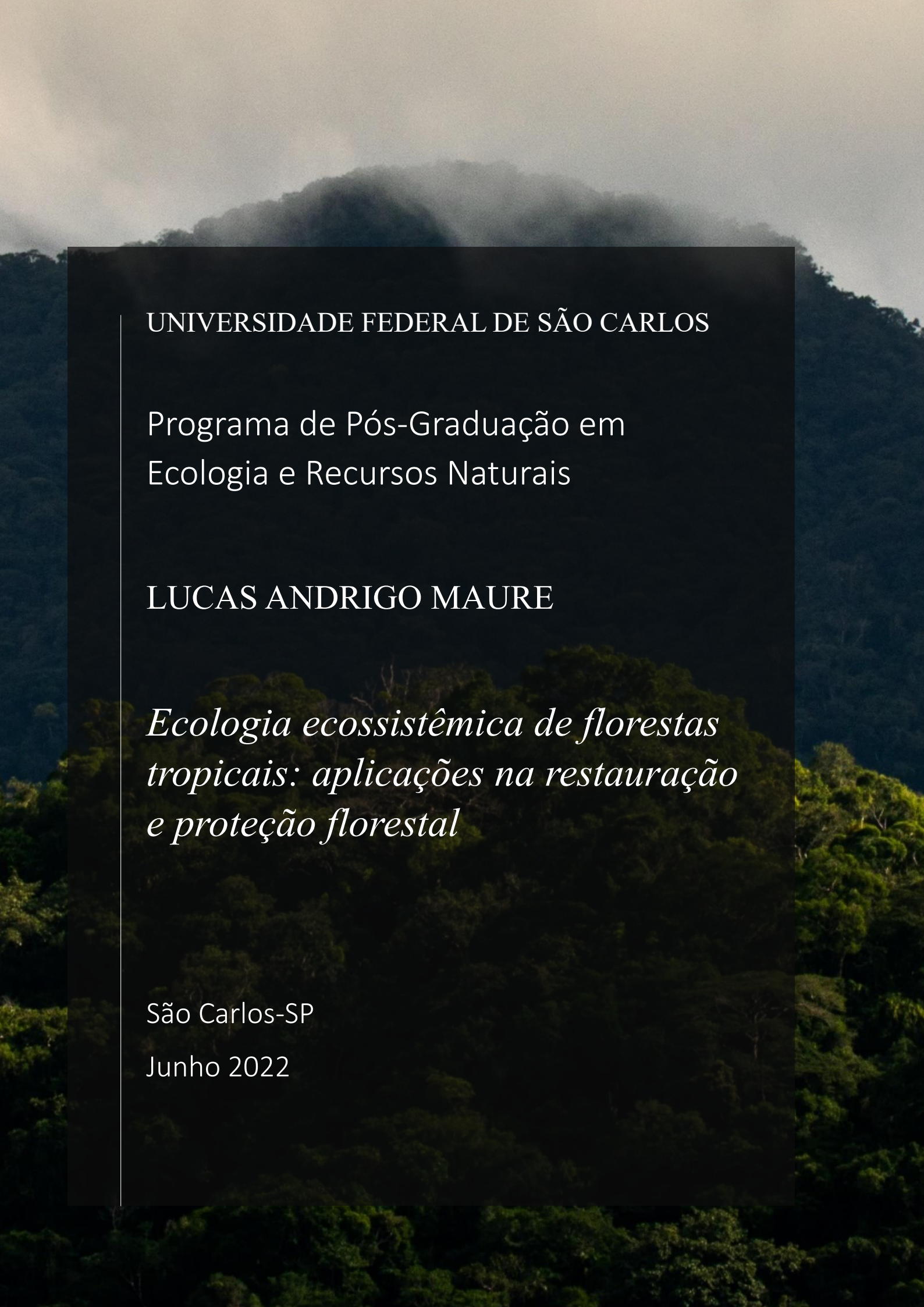

UNIVERSIDADE FEDERAL DE SÃO CARLOS

Programa de Pós-Graduação em
Ecologia e Recursos Naturais

LUCAS ANDRIGO MAURE

Ecologia ecossistêmica de florestas tropicais: aplicações na restauração e proteção florestal

São Carlos-SP

Junho 2022

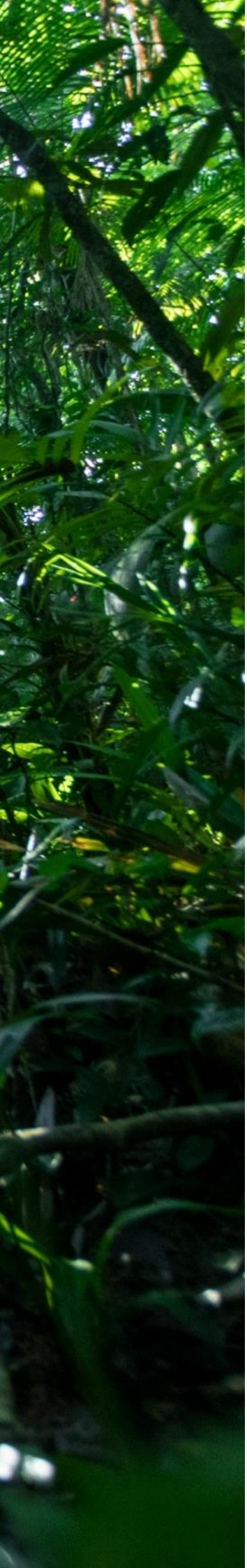

LUCAS ANDRIGO MAURE

Ecologia ecossistêmica de florestas tropicais: aplicações na restauração e proteção florestal

Tese apresentada ao Programa de Pós-Graduação em Ecologia e Recursos Naturais da Universidade Federal de São Carlos, como parte dos requisitos para obtenção do título de DOUTOR EM CIÊNCIAS, área de concentração: ECOLOGIA E RECURSOS NATURAIS.

Linha de pesquisa: Comunidades e Ecossistemas

Área de concentração do projeto: Ecologia de ecossistemas

Orientador

Fernando Rodrigues da Silva

Co-orientadora

Erica Hasui

São Carlos-SP

Junho 2022

UNIVERSIDADE FEDERAL DE SÃO CARLOS

Centro de Ciências Biológicas e da Saúde
Programa de Pós-Graduação em Ecologia e Recursos Naturais

Folha de Aprovação

Defesa de Tese de Doutorado do candidato Lucas Andrigo Maure, realizada em 10/06/2022.

Comissão Julgadora:

Prof. Dr. Fernando Rodrigues da Silva (UFSCar)

Profa. Dra. Marina Hirota (UFSC)

Prof. Dr. Pedro Henrique Santin Brancalion (ESALQ/USP)

Prof. Dr. Felipe Pimentel Lopes de Melo (UFPE)

Prof. Dr. Raísa Romênia Silva Vieira (IIS)

O Relatório de Defesa assinado pelos membros da Comissão Julgadora encontra-se arquivado junto ao Programa de Pós-Graduação em Ecologia e Recursos Naturais.

Ao tempo.

In my lifetime, I have witnessed a terrible decline. In yours, you could and should witness a wonderful recovery.

David Attenborough aos 95 anos discursando para líderes mundiais na COP26.

Agradecimentos

Agradeço ao caos. Assim como a jornada caótica do cosmos, que deu origem ao universo tal como o conhecemos e a tudo nele inserido, a vida não poderia ser diferente do que uma série de eventos aleatórios interligados e imprevisíveis. Desse modo, visto a improbabilidade da ocorrência desses eventos e a julgar pela minha jornada até agora, nesse segundo, posso me considerar um afortunado.

Isso porque nasci, ao acaso, em uma família tendo como meus pais pessoas admiráveis, Conceição e José Márcio, que me ensinaram que humildade, simplicidade e educação são as maiores virtudes que eu poderia ter. O acaso também colocou no meu caminho uma companheira, Cínthia, com quem já dividi boa parte da minha vida, cujo apoio foi fundamental para o desenvolvimento dessa tese. A ela e aos meus pais devoto o meu eterno e mais supremo sentimento de carinho e gratidão.

Não posso deixar de dedicar igual admiração e carinho a minha grande mestre e amiga, Erica Hasui, outra pessoa maravilhosa que surgiu na minha vida como um ato de providência cósmica. Desde o começo da graduação, quando me iniciou na pesquisa, ela vem me ensinando muito do que é preciso saber para fazê-la, o que fez de forma magistral como co-rientadora dessa tese. Além disso, indiretamente com ela também aprendi muito sobre a vida. Assim, após mais de dez anos de trabalho e amizade, não só muito do profissional que sou, mas muito da pessoa que sou hoje se deve a ela. E eu estou muito feliz com quem eu sou, Erica. Muito obrigado.

Desenvolver essa tese para mim foi também viver encontros e reencontros com grandes amigos que o acaso me presenteou, como a Milena Diniz que conheci há poucos anos, e como o Marco Túlio e Bruno Ribeiro, amigos desde a época da graduação. A contribuição deles para a tese foi fundamental e sempre serei grato. Também agradeço aos outros autores Milton Ribeiro, Marina Oliveira e Paulo Molin pelas importantes contribuições. Agradeço ainda ao Fernando Silva por me aceitar como aluno e me orientar nessa tese, além das importantes contribuições. Também agradeço a Marina Hirota e ao Leandro Tambosi pelas contribuições durante a qualificação.

Agradeço a outro grande amigo, Rafael Mitsuo, quem gentilmente cedeu as imagens que ilustram essa tese. Agradeço ao PPG-ERN e ao CNPq.

A todos, meus mais sinceros agradecimentos.

Sumário

Resumo

A proteção e restauração florestal têm sido apontadas como as principais soluções para conter as maiores crises ambientais do nosso tempo: a perda da biodiversidade e as mudanças climáticas. No entanto, decidir quais os locais apropriados e prioritários para proteção e restauração não é uma tarefa fácil. Desse modo, essa tese propõe uma abordagem ecossistêmica para fundamentar tais decisões na Mata Atlântica brasileira. No primeiro capítulo, testamos o efeito de variáveis ambientais na resiliência e estabilidade de florestas secundárias iniciais. Assim, predizemos a distribuição espacial de ambos parâmetros ecossistêmicos para localizar áreas com potencial ecossistêmico para a restauração florestal. No segundo capítulo, testamos o efeito de variáveis ambientais na estabilidade de florestas tardias. Com a predição da sua distribuição, visamos encontrar áreas prioritárias para a proteção e manejo florestal com foco na conservação de grande número de espécies e densidade de carbono. No terceiro capítulo, testamos o efeito do clima na estabilidade de florestas tardias. Predizendo sua distribuição com base no clima atual e futuro, localizamos áreas de ganho e perda de estabilidade florestal em decorrência das mudanças climáticas. Enquanto áreas de ganho têm grande potencial, áreas de perda de estabilidade são prioritárias para proteção e restauração florestal visando a conservação futura de espécies e estoques de carbono. Os resultados dessa tese lançam luz em decisões relacionadas a conservação de espécies e estoques de carbono por meio de uma visão ecossistêmica de seus hábitats.

Abstract

Forest protection and restoration have been singled out as major solutions to stem the biggest environmental crises of our time: the loss of biodiversity and climate change. However, deciding which sites are appropriate and priority for protection and restoration is not an easy task. Thus, this thesis proposes an ecosystem approach to substantiate such decisions in the Brazilian Atlantic Forest. In the first chapter, we tested the effect of environmental predictors on the resilience and stability of early second-growth forests. Thus, we predict the spatial distribution of both ecosystem parameters to locate areas with ecosystem potential for forest restoration. In the second chapter, we test the effect of environmental predictors on the stability of old-growth forests. By predicting their distribution, we aim to find priority areas for forest protection and management with a focus on conservation of large numbers of species and carbon density. In the third chapter, we test the effect of climate on the stability of old-growth forests. By predicting their distribution based on current and future climate, we locate areas of gain and loss of forest stability as a result of climate change. While areas of gain have great potential, areas of loss of stability are a priority for forest protection and restoration aiming at the future conservation of species and carbon stocks. The results of this thesis shed light on decisions related to conservation of species and carbon stocks through an ecosystem view of their habitats.

INTRODUÇÃO GERAL

As mudanças climáticas e o declínio da biodiversidade são as maiores crises ambientais enfrentadas atualmente pela humanidade, cujas causas se concentram criticamente nas florestas tropicais. Cobrindo apenas 7% da superfície da Terra, as florestas tropicais possuem aproximadamente metade das espécies conhecidas e desconhecidas e estocam cerca de 40% de todo o carbono de ecossistemas terrestre do planeta (Scheffers, Joppa, Pimm, & Laurance, 2012; Xu et al., 2021). Contudo, atividades antrópicas têm intensificado de forma sem precedentes a perda e degradação dessas florestas pela mudança do uso da terra.

Por conter um grande número de espécies e densidade de carbono, a devastação das florestas tropicais é considerada a principal causa antrópica da extinção de espécies e a segunda maior causa das mudanças climáticas (Harris et al., 2012, 2021; Lewis, Edwards, & Galbraith, 2015; Malhi, Gardner, Goldsmith, Silman, & Zelazowski, 2014; Sala, 2000). A degradação e a conversão do hábitat em outras formas de uso da terra têm elevado as taxas de extinção e de espécies ameaçadas, resultando no declínio da biodiversidade em ecossistemas tropicais (Lewis et al., 2015; Pimm & Raven, 2000; Sala, 2000). Assim, a maioria das áreas consideradas *hotspots* para a conservação da biodiversidade, onde é encontrado um grande número de espécies em elevado grau de ameaça, se concentram em regiões tropicais (Myers, Mittermeier, Mittermeier, da Fonseca, & Kent, 2000).

Ao derrubar e queimar a biomassa, o desmatamento contribui drasticamente para o agravamento das mudanças climáticas. Somente o desmatamento e a degradação de florestas tropicais é responsável por 15% de toda a emissão antropogênica global de carbono por ano (Houghton, Byers, & Nassikas, 2015). Ainda, a intensificação desses impactos em determinadas áreas nos últimos anos fez com que florestas tropicais alternassem o estado de sumidouro para fonte de carbono para a atmosfera (Gatti et al., 2021; Harris et al., 2021).

Nesse cenário de crescente degradação, a restauração e a proteção florestal são consideradas soluções baseadas na natureza de maior custo-benefício para conter a perda de espécies e as mudanças climáticas (Griscom et al., 2017; Leclère et al., 2020; Pettorelli et al., 2021). Isso porque enquanto a proteção promove a preservação de hábitats para espécies e garante a longevidade dos estoques de carbono, a restauração cria novos hábitats e impulsiona o sequestro de carbono da atmosfera, fixando-o em biomassa.

Florestas secundárias, como florestas restauradas naturalmente, são capazes de recuperar e manter grandes proporções das espécies presentes em florestas primárias, assim como espécies ameaçadas e endêmicas (Chazdon et al., 2009; Latawiec et al., 2016; Lennox et al., 2018; Matos et al., 2020; Rozendaal et al., 2019). Isso faz com que florestas restauradas tenham um alto valor na conservação da biodiversidade (Chazdon et al., 2009; Latawiec et al., 2016).

A restauração de florestas tropicais também tem um papel importante no balanço do carbono e redução das mudanças climáticas, devido à grande capacidade desses ecossistemas em sequestrar e estocar carbono em biomassa (Chazdon et al., 2016; Cook-patton et al., 2020; Poorter et al., 2016). Estimativas mostram que sem perturbações e desmatamento de florestas tardias, a restauração de florestas tropicais em áreas desmatadas poderia capturar até 35% de todo o carbono emitido entre 2000 e 2010 pela queima de combustíveis fósseis e produção industrial (Goodman & Herold, 2014).

Embora a restauração florestal tenha um grande potencial na conservação de espécies e na mitigação das mudanças climática, essa prática não pode substituir a proteção de florestas já existentes. Florestas primárias abrigam maior riqueza de espécies e maior número de espécies endêmicas, especialistas em florestas e ameaçadas se comparadas a florestas secundárias (Barlow, Mestre, Gardner, & Peres, 2007; Chazdon et al., 2009; Gibson et al., 2011; Matos et al., 2020). A capacidade de manter altos níveis de espécies faz com que florestas primárias tenham um valor insubstituível para a conservação e a sua proteção é fundamental para beneficiar a biodiversidade (Gibson et al., 2011).

A proteção de florestas primárias ou tardias também é insubstituível para a conservação de carbono e contenção das mudanças climáticas por estocarem grandes quantidades de carbono em biomassa, comparado a outras formações florestais (Ferreira et al., 2018; Lennox et al., 2018; Matos et al., 2020). Ainda, florestas tropicais possuem alta densidade de carbono em determinadas áreas sob condições vulneráveis cuja perda é irrecuperável em tempo viável para evitar graves impactos no clima (Goldstein et al., 2020; Noon et al., 2021). Portanto, a proteção dessas florestas é essencial para atingir os objetivos de redução de emissão e evitar drásticas alterações climáticas.

Ainda, em determinadas áreas, onde há altos níveis de riqueza de espécies e densidade ou acúmulo potencial de carbono, a restauração e a proteção florestal podem

co-beneficiar tanto a biodiversidade quanto estoques de carbono. Embora a relação entre ambos varie espacialmente e diminua de escalas globais para regionais e locais, algumas áreas apresentam sobreposição de alta biodiversidade e estoques de carbono e são consideradas prioritárias para proteção (Di Marco, Watson, Currie, Possingham, & Venter, 2018; Soto-Navarro et al., 2020). Por sua capacidade de recuperar em conjunto o número de espécies e densidade de carbono, florestas tropicais secundárias também podem apresentar co-benefícios na conservação da biodiversidade e estoques de carbono (Ferreira et al., 2018; Lennox et al., 2018; Matos et al., 2020). Assim, essas áreas são de grande importância por promoverem sinergismo na conservação, o que aumenta seu custo-benefício.

Considerando todo esse grande potencial, florestas tropicais têm sido o foco de acordos internacionais que incentivam a conservação da biodiversidade e o aumento de estoques de carbono, bem como a redução de sua emissão e captura da atmosfera, por meio da restauração e proteção florestal (Venter & Koh, 2012). Nesse contexto, estudos têm sugerido planejamentos espaciais apontando áreas adequadas e prioritárias para restauração e proteção florestal, bem como a conservação da biodiversidade e estoques de carbono. No entanto, ainda há uma carência de estudos que apresentem uma abordagem baseada no desempenho ecossistêmico de florestas tropicais.

Afim de contribuir para a tomada de decisões, nesta tese identificamos áreas com potencial ecossistêmico para a restauração florestal e para a proteção de florestas tardias, visando a conservação da biodiversidade e de estoques de carbono na Mata Atlântica brasileira, um importante *hotspot* de conservação. Esta tese é composta por três capítulos:

No primeiro capítulo, avaliamos a influência do clima, solo e topografia na distribuição espacial da resiliência (capacidade de regeneração) e a estabilidade (capacidade de manutenção da função ecossistêmica ao longo do tempo) de florestas secundárias iniciais. Também, apresentamos predições espaciais da resiliência e estabilidade e onde seus maiores e menores valores se sobrepõem para indicar locais com potencial para restauração florestal. A identificação de locais com potencial ecossistêmico para restauração florestal pode otimizá-la.

No segundo capítulo, testamos o efeito do clima, solo e topografia na distribuição espacial estabilidade de florestas tardias (acima de 33 anos). Ainda,

predizemos espacialmente a distribuição da estabilidade dessas florestas. Com essa predição, identificamos áreas com grande biodiversidade e estoque de carbono recomendadas para proteção e/ou manejo florestal. Esse planejamento espacial com abordagem ecossistêmica pode ajudar na redução das emissões de carbono e perda de espécies atuais.

No terceiro capítulo, testamos apenas o efeito do clima na distribuição espacial da estabilidade de florestas tardias para fazer predições espaciais atuais e futuras. Assim, identificamos locais de ganho e perda de estabilidade em decorrência das mudanças climáticas. Usando essa predição de mudança de estabilidade florestal, localizamos áreas apropriadas para proteção florestal, visando a conservação de grande biodiversidade e estoques de carbono. Também, localizamos áreas com potencial para restauração florestal com foco em grande capacidade de estocagem de carbono e conservação da biodiversidade. Assim, esse planejamento espacial pode ajudar nas decisões para conservação futura da biodiversidade e estoques de carbono com base no efeito das mudanças climáticas na estabilidade ecossistêmica das florestas.

REFERÊNCIAS

Barlow, J., Mestre, L. A. M., Gardner, T. A., & Peres, C. A. (2007). The value of primary, secondary and plantation forests for Amazonian birds. *Biological Conservation*, *136*(2), 212–231. https://doi.org/10.1016/j.biocon.2006.11.021

Chazdon, R. L., Broadbent, E. N., Rozendaal, D. M. A., Bongers, F., Zambrano, A. M. A., Aide, T. M., … Poorter, L. (2016). Carbon sequestration potential of second-growth forest regeneration in the Latin American tropics. *Science Advances*, *2*(5). https://doi.org/10.1126/sciadv.1501639

Chazdon, R. L., Peres, C. A., Dent, D., Sheil, D., Lugo, A. E., Lamb, D., … Miller, S. E. (2009). The potential for species conservation in tropical secondary forests. *Conservation Biology*, *23*(6), 1406–1417. https://doi.org/10.1111/j.1523-1739.2009.01338.x

Cook-patton, S. C., Leavitt, S. M., Gibbs, D., Harris, N. L., Lister, K., Anderson-teixeira, K. J., … Holl, K. D. (2020). Mapping carbon accumulation potential from global natural forest regrowth, *585*(March 2019).

Di Marco, M., Watson, J. E. M., Currie, D. J., Possingham, H. P., & Venter, O. (2018). The extent and predictability of the biodiversity–carbon correlation. *Ecology Letters*, *21*(3), 365–375. https://doi.org/10.1111/ele.12903

Ferreira, J., Lennox, G. D., Gardner, T. A., Thomson, J. R., Berenguer, E., Lees, A. C., … Barlow, J. (2018). Carbon-focused conservation may fail to protect the most biodiverse tropical forests. *Nature Climate Change*, *8*(8), 744–749. https://doi.org/10.1038/s41558-018-0225-7

Gatti, L. V., Basso, L. S., Miller, J. B., Gloor, M., Domingues, L. G., Cassol, H. L. G., … Neves, R. A. L. (2021). Amazonia as a carbon source linked to deforestation and climate change. *Nature*, *595*(July). https://doi.org/10.1038/s41586-021-03629-6

Gibson, L., Lee, T. M., Koh, L. P., Brook, B. W., Gardner, T. A., Barlow, J., … Sodhi, N. S. (2011). Primary forests are irreplaceable for sustaining tropical biodiversity. *Nature*, *478*(7369), 378–381. https://doi.org/10.1038/nature10425

Goldstein, A., Turner, W. R., Spawn, S. A., Anderson-Teixeira, K. J., Cook-Patton, S., Fargione, J., … Hole, D. G. (2020). Protecting irrecoverable carbon in Earth's ecosystems. *Nature Climate Change*, *10*(4), 287–295. https://doi.org/10.1038/s41558-020-0738-8

Goodman, R. C., & Herold, M. (2014). *Why maintaining tropical forests is essential and urgent for a stable climate. CGD Working Paper 385. Washington, DC: Center for Global Development.*

Griscom, B. W., Adams, J., Ellis, P. W., Houghton, R. A., Lomax, G., Miteva, D. A., … Fargione, J. (2017). Natural climate solutions. *Proceedings of the National Academy of Sciences of the United States of America*, *114*(44), 11645–11650. https://doi.org/10.1073/pnas.1710465114

Harris, N. L., Brown, S., Hagen, S. C., Saatchi, S. S., Petrova, S., Salas, W., … Lotsch, A. (2012). Baseline map of carbon emissions from deforestation in tropical regions. *Science*, *336*(6088), 1573–1576. https://doi.org/10.1126/science.1217962

Harris, N. L., Gibbs, D. A., Baccini, A., Birdsey, R. A., de Bruin, S., Farina, M., … Tyukavina, A. (2021). Global maps of twenty-first century forest carbon fluxes. *Nature Climate Change*. https://doi.org/10.1038/s41558-020-00976-6

Houghton, R. A., Byers, B., & Nassikas, A. A. (2015). A role for tropical forests in stabilizing atmospheric CO2. *Nature Climate Change*, *5*(12), 1022–1023. https://doi.org/10.1038/nclimate2869

Latawiec, A. E., Crouzeilles, R., Brancalion, P. H. S., Rodrigues, R. R., Sansevero, J. B., Santos, J. S. dos, … Strassburg, B. B. (2016). Natural regeneration and biodiversity: a global meta-analysis and implications for spatial planning. *Biotropica*, *48*(6), 844–855. https://doi.org/10.1111/btp.12386

Leclère, D., Obersteiner, M., Barrett, M., Butchart, S. H. M., Chaudhary, A., De Palma, A., … Young, L. (2020). Bending the curve of terrestrial biodiversity needs an integrated strategy. *Nature*. https://doi.org/10.1038/s41586-020-2705-y

Lennox, G. D., Gardner, T. A., Thomson, J. R., Ferreira, J., Berenguer, E., Lees, A. C., … Barlow, J. (2018). Second rate or a second chance? Assessing biomass and biodiversity recovery in regenerating Amazonian forests. *Global Change Biology*, *24*(12), 5680–5694. https://doi.org/10.1111/gcb.14443

Lewis, S. L., Edwards, D. P., & Galbraith, D. (2015). Increasing human dominance of tropical forests. *Science*, *349*(6250), 827–832.

Malhi, Y., Gardner, T. A., Goldsmith, G. R., Silman, M. R., & Zelazowski, P. (2014). Tropical Forests in the Anthropocene. *Annual Review of Environment and Resources*, *39*(1), 125–159. https://doi.org/10.1146/annurev-environ-030713-155141

Matos, F. A. R., Magnago, L. F. S., Aquila Chan Miranda, C., de Menezes, L. F. T., Gastauer, M., Safar, N. V. H., … Edwards, D. P. (2020). Secondary forest fragments offer important carbon and biodiversity cobenefits. *Global Change Biology*, *26*(2), 509–522. https://doi.org/10.1111/gcb.14824

Myers, N., Mittermeier, R. A., Mittermeier, C. G., da Fonseca, G. A. B., & Kent, J. (2000). Biodiversity hotspots for conservation priorities. *Nature*, *403*(6772), 853–858. https://doi.org/10.1038/35002501

Noon, M. L., Goldstein, A., Ledezma, J. C., Roehrdanz, P. R., Cook-Patton, S. C., Spawn-Lee, S. A., … Turner, W. R. (2021). Mapping the irrecoverable carbon in Earth's ecosystems. *Nature Sustainability*. https://doi.org/10.1038/s41893-021-00803-6

Pettorelli, N., Graham, N. A. J., Seddon, N., da Cunha Bustamante, M., Lowton, M. J., Sutherland, W. J., … Barlow, J. (2021). Time to integrate global climate change and biodiversity science-policy agendas. *Journal of Applied Ecology*, *n/a*(n/a). https://doi.org/https://doi.org/10.1111/1365-2664.13985

Pimm, S. L., & Raven, P. (2000). Biodiversity: extinction by numbers. *Nature*, *403*(6772), 843–845.

Poorter, L., Bongers, F., Aide, T. M., Almeyda Zambrano, A. M., Balvanera, P., Becknell, J. M., … Rozendaal, D. M. A. (2016). Biomass resilience of Neotropical secondary forests. *Nature*, *530*(7589), 211–214. https://doi.org/10.1038/nature16512

Rozendaal, D. M. A., Bongers, F., Aide, T. M., Alvarez-Dávila, E., Ascarrunz, N., Balvanera, P., … Poorter, L. (2019). Biodiversity recovery of Neotropical secondary forests. *Science Advances*, *5*(3). https://doi.org/10.1126/sciadv.aau3114

Sala, O. E. (2000). Global Biodiversity Scenarios for the Year 2100. *Science*, *287*(5459), 1770–1774. https://doi.org/10.1126/science.287.5459.1770

Scheffers, B. R., Joppa, L. N., Pimm, S. L., & Laurance, W. F. (2012). What we know and don't know about Earth's missing biodiversity. *Trends in Ecology and Evolution*, *27*(9), 501–510. https://doi.org/10.1016/j.tree.2012.05.008

Soto-Navarro, C., Ravilious, C., Arnell, A., De Lamo, X., Harfoot, M., Hill, S. L. L., … Kapos, V. (2020). Mapping co-benefits for carbon storage and biodiversity to inform conservation policy and action. *Philosophical Transactions of the Royal Society B: Biological Sciences*, *375*(1794). https://doi.org/10.1098/rstb.2019.0128

Venter, O., & Koh, L. P. (2012). Reducing emissions from deforestation and forest degradation (REDD+): Game changer or just another quick fix? *Annals of the New York Academy of Sciences*, *1249*(1), 137–150. https://doi.org/10.1111/j.1749-6632.2011.06306.x

Xu, L., Saatchi, S. S., Yang, Y., Yu, Y., Pongratz, J., Bloom, A. A., … Schimel, D. (2021). Changes in global terrestrial live biomass over the 21st century. *Science Advances*, *7*(27), eabe9829. https://doi.org/10.1126/sciadv.abe9829

CAPÍTULO I

Predicting resilience and stability of early second-growth forests

Lucas Andrigo Maure, Milena Fiuza Diniz, Marco Túlio Pacheco Coelho, Marina P. Souza de Oliveira, Milton Cezar Ribeiro, Fernando Rodrigues da Silva, Érica Hasui

Predicting resilience and stability of early second-growth forests

Lucas Andrigo Maure[1,2], Milena Fiuza Diniz[3], Marco Túlio Pacheco Coelho[3], Marina P. Souza de Oliveira[4], Milton Cezar Ribeiro[5], Fernando Rodrigues da Silva[2], Érica Hasui[4]*

[1] Programa de Pós-graduação em Ecologia e Recursos Naturais (PPGERN), Universidade Federal de São Carlos, São Carlos-SP, Brazil

[2] Laboratório de Ecologia Teórica: Integrando Tempo, Biologia e Espaço (LET.IT.BE), Departamento de Ciências Ambientais, Universidade Federal de São Carlos, Sorocaba-SP, Brazil

[3] Departamento de Ecologia, Universidade Federal de Goiás, Goânia-GO, Brazil

[4] Laboratório de Ecologia de Fragmentos (EcoFrag), Instituto de Ciências da Natureza, Universidade Federal de Alfenas, Alfenas-MG, Brazil

[5] Spatial Ecology and Conservation Lab (LEEC), Departament of Biodiversity, São Paulo State University - UNESP, Rio Claro, SP, Brazil

*Corresponding author: ericahasui@gmail.com

DOI: **https://doi.org/10.1002/rse2.256**

Abstract

Identifying deforested areas with high potential for natural forest recovery can be used as an aid for ecological restoration projects at large-scale. However, accurate predictions that infer the resilience and stability of early second-growth forests are scarce at a regional scale. Here, we investigated the effect of climate, soil, and topography on the resilience and stability of 165 early second-growth forests throughout the Brazilian Atlantic Forest. We also built prediction maps of potential resilience (i.e., recovery rate after deforestation) and stability (i.e., the ability of the ecosystem to maintain its functions) to identify where reforestation could be optimized in the early stages of forest succession. We assessed the resilience and stability through an interannual plant primary productivity time series using a normalized difference vegetation index. Our analysis reveals that resilience was mainly associated with isothermality (i.e., diurnal temperature oscillation relative to the annual temperature oscillation) and precipitation of the warmest quarter. In turn, stability was mainly associated with the probability of bedrock occurrence, annual precipitation, and precipitation seasonality. The prediction maps show a spatial pattern in which potential resilience and stability increase from north to south of the Atlantic Forest. Thus, forest restoration can be optimized in regions with high potential resilience and stability, such as an isolated area on the north coast in the Bahia state, and the southern region. However, restoration may require active practices and management in regions with low potential for both ecosystem properties, such as the north inland in the Bahia and Minas Gerais states. This ecosystemic approach can help achieve Atlantic Forest restoration commitments.

Keywords: forest succession, plant productivity, forest regeneration, secondary forests, tropical forests, NDVI

1. INTRODUCTION

Although tropical forests house over half of Earth's biodiversity and are an important regulator of global climate (Lewis et al., 2015), they are among the world's most threatened terrestrial ecosystems (Malhi et al., 2014). Currently, second-growth forests comprise 28.1% (2.4 million km^2) of land in the Latin American tropics (Chazdon et al., 2016) and this estimate is expected to increase in the future due to human-induced pressures (Chazdon, 2014; Malhi et al., 2014). This scenario of degradation has led to the creation of national and international forest restoration programs (e.g., the New York Declaration on Forests and Bonn Challenge program) to mitigate injurious climate change (e.g., the Paris Climate Agreement), reduce species extinctions, and promote ecosystem services (e.g., Aichi Targets of the Convention on Biological Diversity). For example, the Atlantic Forest Restoration Pact of 2009 established the target to restore 15 million hectares of deforested area by 2050. Under the Bonn Challenge program, Brazil's government committed to restore 1 million ha of Atlantic Forest by 2020 and 12 million ha across the country by 2030 (Crouzeilles et al., 2019). To achieve these goals, it is of utmost importance to identify areas at a regional scale where reforestation would be optimized by potential ecosystem resilience (i.e., the recovery rate of the forest after deforestation) and stability (i.e., the ability of an ecosystem to maintain its function in face of perturbations over time) at the initial stages of forest succession.

The resilience and stability of early second-growth forests can help us to understand the recovery rate of tropical forests after deforestation and their resistance to small perturbation (Jakovac et al., 2015; Poorter et al., 2016). These ecosystem properties also provide insights into the state of early second-growth forests, indicating

whether they can rapidly and successfully recover (Poorter et al., 2016) or their potential in carbon sequestration (Chazdon et al., 2016). One of the main proxies of forest recovery is field measurements of above-ground biomass accumulation over time of succession (Lohbeck et al., 2015). Biomass is directly related to the primary productivity rates that depend on the plant's ecophysiological response to local environmental resources and conditions related to climate, soil, and topography (Mulkey et al., 1996; Pau et al., 2018). Low resource availability and extreme conditions can restrict plant photosynthetic activity for long periods, limiting primary productivity and biomass accumulation (Mulkey et al., 1996). It is well known that spatial variation of resource availability and environmental conditions determine the distribution of the potential resilience and stability of a region (Pau et al., 2018; Poorter et al., 2016; Verbesselt et al., 2016). In the tropics, early second-growth forests range from around 5 to 20 years after land deforestation and abandonment (Chazdon, 2008, 2014). However, estimating ecosystem properties of early second-growth forests at a regional scale requires a long-term time series of spatially distributed sampling data from various plots, making field measurements and monitoring logistically difficult (Lennox et al., 2018; Poorter et al., 2016). Consequently, research about second-growth forests has been conducted with plots covering a microscale or a macroscale meta-analysis that may fail to capture intra-regional variation (Lennox et al., 2018).

Here, we used remote sensing and geoprocessing tools to identify areas that combine potential resilience and stability of early second-growth forests throughout the Atlantic Forest, a global biodiversity hotspot (Myers et al., 2000). This Neotropical domain originally covered c. 1.5 million km^2, of which ~ 72% has been converted for human use or degraded by anthropogenic activities (Rezende et al., 2018). Due to its wide latitudinal (from 5 to 33ºS) and longitudinal (from 35 to 55ºW) ranges, the

Atlantic Forest is a heterogeneous environment that varies in topographic (from sea level to 2200 m a.s.l.), soil characteristics, and climatic gradients such as annual rainfall (from 800 to 4000 mm) and mean annual temperature (from 15 to 25 ºC). Previous studies have demonstrated that floristic variation within and among different forest types (e.g., rainforest and semideciduous forests) in Brazilian Atlantic Forest is strongly associated with the spatial and seasonal distribution of temperature and precipitation (Morellato & Haddad, 2000; Oliveira-Filho & Fontes, 2000; Ribeiro et al., 2011, 2009). Considering that differences in rainfall regime and temperature result in distinct leaf production between forest types, it is expected that the spatial variations of climatic conditions might also be correlated with the distribution of the resilience and stability of tropical forests.

Here, we selected 165 sites of early second-growth Atlantic Forest that regrew from anthropogenic land use like pasture or agriculture after 2000 and remained as forests until 2018. Then, we tested how the spatial distributions of primary productivity resilience and stability are related to climatic, soil, and topographic predictors (Table S1). We expected that spatial variation of the climate would be the major driver of the spatial distribution of primary productivity resilience and stability of the early second-growth forests. In this case, both ecosystem properties would be positively associated with the precipitation gradient and negatively associated with the temperature gradient (Poorter et al., 2016). We also expected that temperature and precipitation seasonality negatively influence resilience and stability. For last, we built prediction maps of potential resilience and stability to identify where reforestation could be optimal for the early stages of Atlantic Forest succession.

2. METHODS

2.1 Sampling sites of early second-growth forests

Sites of early second-growth forest were identified for a 19-year range (from 2000 to 2018) using classified images (30 m resolution) of land cover in the Atlantic Forest (see Muylaert et al., 2018 for a discussion on the Atlantic Forest limits) available from MapBiomas v4.0 (http://mapbiomas.org/). For that, we reclassified the MapBiomas images setting value 1 to classes designated as natural forest formation and 0 to the remaining classes. Then, we performed three steps. First, we estimated the sites that had *forest gain* by calculating the difference between 2018 and 2000 images. The result was an output raster with values of -1 indicating areas of forest loss, 0 for unchanged areas of forests, and 1 for secondary forest areas. We reclassified this output maintaining value 1 for secondary forest areas and NA for the other values. Second, we estimated the sites that remained forest for 18 years (*stable forests*) by summing the images from 2000 to 2018. The output was reclassified setting 1 to pixels with the original value of 18 and NA to other values. Third, we used the *forest gain* reclassified output as a mask to filter out the *stable forest* reclassified output to exclude forest areas present in 2000 and that disappear in 2017. This final image was used in the sampling sites selection process.

Overall, our mapping analysis shows that early second-growth forests that emerged in 2000 and remained until 2018 encompass a total of 186,961.6 ha, and cover 0.16% of the entire Atlantic Forest. Most of these forest regeneration sizes were small (median of 0.10 ha), ranging from 0.10 to 34.81 ha. Thus, the selection of sampling sites was based on the proportion of the early second-growth forests area that intersected geographical cells of a 250 m resolution in the NDVI images (see description below).

To avoid larger influence from other land uses and commission error, we selected as sampling sites only the centroid of the NDVI cells covered with more than 60% of early second-growth forests. Then, we revised all sites using Google satellite images to exclude silviculture areas that were incorrectly classified as forest. Finally, our dataset contains 165 sites (Figure 1a) used to extract data from predictor variables and multi-temporal NDVI images to calculate the ecosystem properties.

2.2 Data

Productivity - We used the normalized difference vegetation index (NDVI) as an operational variable to measure productivity in early second-growth forests over time (Caughlin et al., 2020). Using the NDVI to monitor forest recovery is sometimes questionable due to its saturation behavior of the early successional stage, which can potentially introduce bias into the analysis (Huete et al., 2002). However, saturation may not be problematic as forests regrow take years to reach biomass concentrations in the saturated range (de Almeida et al., 2020). Forecast models show that saturation occurs after approximately 30 years of forest succession when NDVI approaches the asymptote (Caughlin et al., 2020). Furthermore, NDVI has been commonly used as a proxy of primary productivity and biomass which correlations are confirmed by field sample data (Huete et al., 2002; Nemani et al., 2003; Pettorelli et al., 2005; Saatchi et al., 2007; Verbesselt et al., 2016). It also has been used to measure forest structure dynamics during recovery (Caughlin et al., 2020).

We used an NDVI from MODIS sensor images (250 m resolution) available from the GLAM Project (http://pekko.geog.umd.edu/usda/test/). Originally, NDVI values range from -1 to 1, where negative values correspond to the absence of

vegetation and positive values to the presence of vegetation or growth. However, the GLAM Project rescaled the index from 0 to 250 indicating that values less than or equal to 50 and values greater than 250 should be interpreted as observation error and we excluded them. Considering that plant phenological periods of productivity and senescence interfere in the time series analysis (Lhermitte et al., 2011; Keersmaecker et al., 2014; Legendre & Legendre, 2012) and our aim is to detect long periods of deterministic trends and variance (standard deviation) of the NDVI, we obtained a mean value of NDVI per year between 2000 and 2018 using all available images (23 per year), instead of time series smoothing methods.

2.3 Ecosystem properties

Resilience, as the recovery rate, assumes a single basin of attraction or equilibrium state of the ecosystem and concentrates on ecosystem function near to this equilibrium state. This resilience definition is also termed "engineering resilience" and measures the returning time to the equilibrium after disturbance (Holling, 1996). However, because of our study period of 19 years (maximum extension period of the MODIS data), the NDVI time series does not reach an asymptote indicating a return to the equilibrium state, which can occur near 30 years of forest succession (Caughlin et al., 2020). Thus, we measured resilience as the increase of the primary productivity in the time series *trend* (deterministic change) (Legendre & Legendre, 2012). The trend in the inter-annual time series of the NDVI is an effective proxy for long-term vegetation growth, recovery, and succession (Caughlin et al., 2020; Fensholt & Proud, 2012; Tagesson et al., 2020; Verbesselt et al., 2010). Thus, the magnitude of the deterministic trend of the NDVI time series can indicate the recovery rate of a forest after deforestation (Caughlin et al., 2020). Data of the mean annual NDVI images of 2000–2018 intervals were

extracted from every pixel where sampling sites were located to estimate their trend using Sen's slope for time series data (Sen, 1968). This index is a non-parametric estimator of the linear regression coefficient (i.e., an estimation of the slope trend in a time series) and is less vulnerable to the data distribution and outliers. Sen's slope values can be positive or negative, indicating increasing or decreasing trends in the time series, respectively (Li, Cao, Long, Liu, & Li, 2017). Thus, positive trends of the NDVI time series are interpreted as increasing productivity and negative trends as decreasing productivity.

Stability, considered here as the ability of the ecosystem to maintain its functions over time, was measured as the total variance of the NDVI time series, which indicates vegetation resistance to frequent disturbances that affect vegetation productivity, such as extreme climatic events, grazing, and fire (Erb et al., 2018; Keersmaecker et al., 2014; Uriarte et al., 2016). The variance of primary productivity was measured by the total standard deviation of the NDVI time series (García-Palacios et al., 2018; Keersmaecker et al., 2014). However, nonstationary time series can input bias in variance metrics increasing their values due to deterministic and stochastic trends (Keersmaecker et al., 2014; Legendre & Legendre, 2012). To deal with these limitations, all the time series were detrended by a second-order difference, and the augmented Dickey-Fuller (ADF; Dickey & Fuller, 1979) test was conducted to assure stationarity. Since higher variance means low stability, we rescaled the standard deviation values by the maximum value of the standard deviation - standard deviation values * 100 / maximum value of the standard deviation. Thus, we obtained a stability index that ranged from 0 to 100, with increasing values indicating greater ecosystem stability. The statistical analysis for stability was performed only with a significant

stationary time series, which reduced the sample to 102 points (Figure 1b). The time series analysis was conducted using the *trend* R package (Pohlert, 2018).

2.4 Predictor variables

We used a total of 39 variables to predict the resilience and stability of the early second-growth forests from three environmental categories: climate, soil, and topography. Variables from these categories provide resources and conditions that are recognized as directly affecting plant productivity (Table S1).

Climatic variables – we selected a total of 21 climatic predictors, all of the 19 bioclimatic variables, and two other variables of water vapor pressure and solar radiation at a resolution of 30 seconds (~1 km) from the WorldClim v2.1 (Fick & Hijmans, 2017) database.

Soil variables – we selected 15 soil variables at 250 m resolution from the SoilGrid database (Hengl et al., 2017), which comprise physicochemical parameters of soils. The data selected represent the values of the soil parameters at a depth of 5 cm. Soil properties strongly influence plant productivity within a soil column of 0–16 cm (Goebes et al., 2019). Values for soil organic carbon stock in tons per ha were for a depth of 30 cm (OCSTHA_30cm), the lowest available depth for this variable.

Topography – we also used 3 topographic variables as environmental predictors. Elevation data, with a spatial resolution of 250 m, were obtained from the SRTM 90 m Digital Elevation Database v4.1 (Jarvis, Reuter, Nelson, & Guevara, 2008) of the Consortium for Spatial Information (CGIAR-CSI). With the elevation data, we calculated the two other topographic variables. Topographic heterogeneity was measured as the standard deviation of the elevation data using the focal statistics

method in a moving window of 3x3 cells. This index describes the variability of elevation within an area and it is strongly correlated with other measures of topographic ruggedness and slope (Amatulli et al., 2018). A topographic wetness index was calculated as $TWI = \ln(\alpha / \tan\beta + C)$, where α is flow accumulation, β is the slope and C is a constant of 0.001. This index measures the topographic control on hydrological processes and is related to terrain drainage and soil moisture (Kopecký & Čížková, 2010; Sørensen, Zinko, & Seibert, 2006). The topographic wetness index has been used to predict vegetation type and plant species richness, composition, distribution, and growth (Kopecký & Čížková, 2010; Méndez-Toribio et al., 2016; Svenning et al., 2004).

All raster maps used to obtain data for the response and predictor variables were reprojected to the South America Albers Equal Area Conic and predictor data were statistically resampled to a spatial resolution of 250 m. All geoprocessing was performed using ArcGIS (10.6.1) for early second-growth forest sites, predictor variables, and data sampling.

2.5 Selecting predictors

Due to correlation among some predictors, we selected predictors for statistical analysis by their importance and low collinearity in a procedure separately applied for resilience and stability. First, we fit a simple linear model for each of the 39 predictors and rank the models according to their estimated slope coefficient (Table S2 and Table S3). Then, we build multiple linear models adding predictors one by one from the most to the least important. For each predictor added, we check the collinearity and coefficients of all predictors in the model. We excluded the newly added predictor that elevated the

variance inflation factor (VIF) (R package *car;* Fox & Weisberg, 2018) higher than 5 (Dormann et al., 2013) and/or inverted the coefficient of any variable in the model. Coefficient inversion might indicate interactions between predictors that are out of the scope of our simple additive models. The low variance inflation factor values (Table S4) indicated that collinearity between predictors was not a problem for the resilience and stability models.

At the end of the procedure, predictors were reduced to 7 for resilience and 9 for stability. The selected predictors for resilience in order of importance were the following: isothermality (i.e., day-to-night (diurnal) temperature oscillation relative to the summer-to-winter (annual) oscillation) (BIO3), annual precipitation (BIO12), precipitation of warmest quarter (BIO18), soil organic carbon stock (OCSTHA 30cm), soil moisture based on saturated water content (AWCtS), soil organic carbon density (OCDENS), and probability of occurrence of R horizon (i.e., probability of occurrence of bedrock up to 200 cm depth) (BDRLOG). For stability, the selected predictors in order of importance were the following: precipitation seasonality (BIO15), annual precipitation (BIO12), soil organic carbon density (OCDENS), bulk density (fine earth) (BLDFIE), soil pH (PHIKCL), probability of occurrence of R horizon (BDRLOG), max temperature of the warmest month (BIO5), terrain wetness index (TWI), and solar radiation (Srad).

2.6 Statistical analysis

Here, we built multiple competitive linear models with different combinations of the selected predictor variables described above. Since prediction was the central aim of our study, we used a multi-model inference framework with model selection through the

Akaike information criterion (Burnham & Anderson, 2002). This framework of statistical inference is designed to asymptotically maximize the expected relative predictive accuracy of models (i.e., ability to fit future data). Therefore, we used this framework in our study to identify the model that maximizes predictive accuracy, thus, reducing the risk of performing predictions with overfitted models (Coelho, Diniz-Filho, & Rangel, 2019). For resilience, we compared 128 models (emerging from the combination of seven predictors), and for the stability analysis, we compared 512 models (emerging from the combination of nine predictors). These models were built using a standard multiple regression (OLS). The OLS residuals were inspected to evaluate the existence of spatial autocorrelation (Diniz-filho, Rangel, & Bini, 2008). We found no spatial autocorrelation for resilience (Moran's Index $p = 0.11$, Figure S1) models with all selected predictors. However, the stability model with all selected predictors presented significant spatial autocorrelation (Moran's Index $p = 0.01$, Figure S2a). We control the effect of spatial autocorrelation by adding the first axis of the principal coordinate analysis of neighbour matrices (PCNM) in all best-performing models ($\Delta AICc < 2$) for stability. From a distance matrix of the site's coordinates, PCNM extracts eigenvectors that maximize Moran's index and creates spatial predictors that can be used in regression models (Dray, Legendre, & Peres-Neto, 2006). After adding the first PCNM axis to each best performing model, we inspected its residuals and found no spatial autocorrelation. We identified the most important predictors for resilience and stability by the highest sum of their weights and their occurrence in all best-performing models. We also tested for a relationship between resilience and stability using Pearson's correlation. Our analyses were performed in R (R Core Team, 2020) using the packages *MuMIn* (Barton, 2019), *glmulti* (Calcagno, 2019), *fields*

(Nychka, Furrer, Paige, & Sain, 2017), *ape* (Paradis & Schliep, 2018), *vegan* (Oksanen et al., 2020) and *letsR* (Vilela & Villalobos, 2015).

2.7 Prediction maps of ecosystem properties

Models with the highest predictive accuracy were used to predict areas of potential ecosystem resilience and stability of early second-growth forests in the Atlantic Forest. Prediction maps of the ecosystem properties were built using the average estimated coefficients of the predictors of the best-performing models in the multiple linear regression equations (details in section 1.1 of the methods in Supporting Information). We classified the two prediction maps into ten classes of 10% quantiles and assembled them in a bivariate choropleth map that combines areas of different value classes of resilience and stability.

3. RESULTS

Resilience varied from -1.56 to 1.72 (Figure 1a) mainly influenced negatively by isothermality (BIO3) ($ß$ = -0.047 ± 0.014) and positively by precipitation of warmest quarter (BIO18) ($ß$ = 0.001 ± 0.000) (Table 1, Table S5). Stability varied from 0.00 to 90.20 (Figure 1b) positively influenced by the probability of occurrence of R horizon (bedrock) in soil up to 200 cm depth (BDRLOG) ($ß$ = 0.853 ± 0.262), annual precipitation (BIO12) ($ß$ = 0.023 ± 0.005), and negatively by precipitation seasonality (BIO15) ($ß$ = -0.249 ± 0.079) (Table 1, Table S6). Resilience and stability had a positive correlation (R = 0.42, p < 0.001) (Figure S3).

Both the prediction maps of potential resilience (Figure 2a) (R^2_{adj} = 0.31) (Table 1, Table S5) and stability (Figure 2b) (R^2_{adj} = 0.68) (Table 1, Table S6) show a general spatial pattern that increases from north to south across the Atlantic Forest. The lower values of potential resilience and stability occurred in larger extensions throughout the north and central regions while higher values are found in the southern region, mainly along the coastal areas (Figure 2a and b). High potential resilience and stability are also found in an isolated area on the coast of Bahia state, in the northern Atlantic Forest. These regions of contrasting values of potential resilience and stability have marked differences in the spatial distribution of their major predictors. Regions of low potential resilience have higher values of isothermality and lower values of precipitation of the warmest quarter. In turn, in regions of low potential stability lower probability of occurrence of R horizon, annual precipitation, and higher precipitation seasonality are found.

The bivariate map (Figure 3) shows a pattern of high heterogeneity of the potential resilience and stability combinations across the Atlantic Forest. Potential stability is higher than resilience in the northern region states of Alagoas, Pernambuco, Bahia and Paraíba (Figure 4a). A large area of high potential resilience and stability is found on the coast of Bahia state, bordering an inland area that has a combination of the lowest values for both ecosystem properties (Figure 4b). The resilience extends into the central region of the Atlantic Forest, where isolated areas of high value for both ecosystem properties are found. In the south region, the combination of high potential resilience and stability extends over a large area along the coast of São Paulo state and in isolated inland areas (Figure 4c). The greatest extension of high values for both ecosystem properties is found in the southern regions, mainly inland, near the coast, and in the far south (Figure 4d).

4. DISCUSSION

In 19 years of succession, the early second-growth forests showed high spatial variation in their resilience and stability that were positively correlated across the Atlantic Forest. Both ecosystem properties present a general spatial pattern of increment from north to south. The recovery rate of primary productivity in early second-growth forests is higher in regions where diurnal temperature oscillation is less relative to the annual temperature oscillations (i.e., low isothermality) and where precipitation of the warmest quarter months is high. Primary productivity in early second-growth forests is not only more stable in regions with a higher probability of occurrence of bedrock up to 200 cm depth, and precipitation throughout the year, but also higher on less precipitation seasonality. This ecosystemic approach sheds light on the relationship between the environment and early second-growth forest ecosystems in terms of recovery rate and resistance to perturbations after deforestation. Projecting these results on prediction maps of potential resilience and stability provides practical support to forest restoration. By indicating areas where natural regrowth could be improved by high potential resilience and stability, and where active restoration and forest management are recommended due to the low potential of ecosystem properties, this mapping can help decisions in trade-off scenarios of resource allocation for restoration.

4.1 Predictors effect and ecosystem implications

Although isothermality has a negative effect on the resilience of early second-growth forests, this predictor positively influences the distribution of species richness, traits, and height of plants worldwide (Keil & Chase, 2019; Moles et al., 2009; Wieczynski et

al., 2019). However, high isothermality occurs mainly in regions with elevated annual temperatures in the Atlantic Forest ($R = 0.48$, $p < 0.001$; Pearson's correlation for resilience data). Thus, the early second-growth forests found in higher isothermality may face stressful conditions of long periods of constantly elevated diurnal and annual temperatures, constraining growth and making the recovery rate slower. Higher diurnal temperatures increase plant evapotranspiration leading to stomatal closure to avoid water loss, which reduces photosynthesis rates, carbon uptake, and the net primary productivity in tropical forests (Doughty & Goulden, 2009; Goulden et al., 2004; Pau et al., 2018). This growth constraint may be more severe in the early stages of succession, considering the high frequency of pioneer species which have physiological attributes such as high photosynthetic rates and evapotranspiration that confer vulnerability to elevated temperature (Uriarte et al., 2016).

While productivity in tropical forests is restricted by elevated temperatures this restriction is attenuated by precipitation, which could explain why forests are more resilient in regions with high precipitation in the warmest quarter of year (Sullivan et al., 2020). Precipitation in the warmer months provides a water resource that mitigates the effects of temperature on tree growth rates in tropical second-growth forests (Uriarte et al., 2016). Also, precipitation is the main predictor with positive effect on the biomass resilience of neotropical second-growth forests and tree cover resilience, and negative effect on slowing down of tropical forest ecosystem worldwide (Hirota et al., 2011; Poorter et al., 2016; Toledo et al., 2011; Verbesselt et al., 2016). Therefore, less diurnal temperature variations and precipitation in the warmer months can ameliorate physiological stress on plants, allowing higher recovery rates of early second-growth forests.

Contrary to our expectations, the spatial distribution of stability was influenced primarily by a soil predictor. Early second-growth forests are more stable when the probability of occurrence of bedrock up to 200 cm is high. Although the bedrock restricts root growth downwards, the weathering of its minerals is a major source of soil phosphorus (P) which determines productivity distribution in tropical forests (Mercado et al., 2011; Vitousek et al., 2010; Wright et al., 2011). Soil P content is directly related to its foliar concentrations that strongly influence photosynthetic rates, carbon gain, and growth in tropical forests trees (Mercado et al., 2011). In addition, the bedrock has water storage capacity which is used as a resource mainly by evergreen trees of early successional stages during the dry seasons in tropical forests (Hasselquist et al., 2010; Querejeta et al., 2007).

Both annual precipitation and precipitation seasonality also have an important effect on the stability of primary productivity in early second-growth forests. Low precipitation and intense dry season cause hydraulic stress conditions that also trigger ecophysiological mechanisms in plants to control water loss by transpiration, such as stomatal regulation, reducing plant productivity in tropical forests (Oliveira et al., 2021). Thus, the occurrence of the bedrock and precipitation may provide nutrients and water allowing constant productivity of trees during the year. The availability of these resources may contribute to make early second-growth forests more resistant to stochastic perturbations that affect primary productivity and even control tree mortality, such as heat waves, drought, fire, and grazing (Erb et al., 2018; Uriarte et al., 2016). This resistance to perturbance confers more stability to the early second-growth forests, that is, the ability to maintain its function over time.

4.2 Predictive mapping and its applications

Beyond understanding how ecosystem properties of the early second-growth forests respond to spatial variation of resources and conditions of the environment, our results provide practical support for restoration actions throughout the Atlantic Forest. Overall, our prediction maps (Figure 2a and b) highlight continuous values of potential resilience and stability of early second-growth forests. Despite the correlation between resilience and stability, the bivariate choropleth map (Figure 3 and 4) identifies regions of the combination of different value classes of both ecosystem properties. These maps can indicate the appropriate restoration and management approach for a determined location. Thus, the costs of both practices can be mitigated due to the region's higher potential of resilience and/or stability provided by optimal conditions and higher resource availability.

Forest restoration by natural regrowth can be enhanced due to the higher potential of resilience and stability in locations such as the southern region of the Atlantic Forest and its coastal areas (Figure 2a and b, Figure 3, and Figure 4c and d), and the coastal area of the north region (Figure 2a and b, Figure 3, and Figure 4b). The higher potential of stability of these regions also means low management interventions to prevent perturbations are required, as well as in the northern region with only high stability (Figure 2b, Figure 3, and Figure 4a). Otherwise, in regions with low potential resilience and stability, like the inland areas in the northern region of the Atlantic Forest (Figure 2a and b, Figure 3, and Figure 4b), the active restoration and management interventions are recommended. Thus, this ecosystem-based spatial planning prioritizing areas for forest restoration could help Brazil's commitment to the Atlantic Forest Restoration Pact and Bonn Challenge (Crouzeilles et al., 2019; Verdone & Seidl, 2017). This ecosystem approach could also be useful in the upcoming United Nations'

Decade on Ecosystem Restoration (2021–2030) and in the post-2020 agendas for biodiversity conservation and climate change mitigation.

We emphasize that our intent here is not to propose an ultimate and definitive prioritization for forest restoration in the Atlantic Forest. Instead, to optimize recovery, we provide an ecosystemic view of the early stages of forest succession that can be used in association with studies that address other important factors related to forest restoration. Such factors can be biodiversity conservation, carbon accumulation, tree cover potential, landscape properties, and land use, as well as socio-economic and political matters (Bastin et al., 2019; Brancalion et al., 2019; Cook-patton et al., 2020; Crouzeilles et al., 2019; Hayek et al., 2020; Leclère et al., 2020; Strassburg et al., 2019, 2020; Tambosi et al., 2014). Moreover, our study searched for high and low potential resilience and stability only in the Atlantic Forest domain, which in general has a high potential for restoration compared to other biomes, as pointed out by the studies cited above. Thus, we strongly encourage forest restoration even in regions with low potential resilience and stability identified here.

4.3 Limitations and perspectives

Despite rigorous procedures to avoid bias in the results (see details in the methods), some potential confounding factors may arise. First, is the use of NDVI pixels not fully covered by early second-growth forest. This limitation can be avoided by using higher resolution data, which would reduce the commission error and allow measuring the ecosystem properties of forest areas smaller than a 250 m pixel. Second, although the climate and soil data used in this study are widely recognized as drivers of tropical forest recovery and productivity worldwide, they were not sampled at early second-

growth forest sites and do not correspond to the study period. Tropical forests productivity and growth are directly linked to the local meteorological variations (Clark et al., 2003). Also, both climate and soil data were generated interpolating on space data from sampling sites, which could limit the predictive accuracy of the models and the prediction maps. In addition to improving the methodological limitations cited above, future works should consider using other ecosystem metrics, such as those that consider multiple ecosystem stable states and measure the chance of transition between them. Ecosystems tend to slowly recover back to their original equilibrium state after small perturbations when they are close to the tipping point of transition to another stable state or even to the collapse. This phenomenon is known as critical slowing down (Scheffer et al., 2015). Therefore, critical slowing down indicators could infer how close early second-growth tropical forests are to shift to a state of savannah-like forest (Verbesselt et al., 2016).

CONCLUSION

In the Brazilian Atlantic Forest, the spatial distribution of resilience and stability of early second-growth forests was mainly driven by climate and soil predictors, respectively. Areas of high potential resilience and stability are found mainly in the south while areas of low potential resilience and stability are found mainly in the northern region of the Atlantic Forest. Thus, reserving areas of high resilience and stability for natural regrowth and areas of low resilience and stability for active forest restoration and management could optimize restoration plans. This ecosystem-based approach could make regional forest restoration more cost-effective, helping in resource allocation decisions and therefore contributing to the Brazilian government achieving its forest restoration commitments.

ACKNOWLEDGMENTS

Lucas Andrigo Maure thanks CNPq for the Ph.D. funding (141255/2018-8). Milton Cezar Ribeiro thanks CNPq (Brazilian Government Research Council) for the research grants (312045/2013-1, 312292/2016-3, 442147/2020-1, 402765/2021-4, and 313016/2021-6) and FAPESP (processes 2013/50421-2, 2020/1779-5, #2021/08534-0) and CAPES (Procad project 88881.068425/2014-0) for the financial support.

DATA AVAILABILITY

The data that support the findings of this study are openly available in [repository name] at http://doi.org/[doi], reference number [reference number].

AUTHORS' CONTRIBUTION

LM, EH and MD conceived the ideas and designed methodology; LM collected the data; LM and MC analyzed the data; LM led the writing of the manuscript. All authors contributed critically to the drafts and gave final approval for publication.

REFERENCE

Amatulli, G., Domisch, S., Tuanmu, M. N., Parmentier, B., Ranipeta, A., Malczyk, J., & Jetz, W. (2018). Data Descriptor: A suite of global, cross-scale topographic variables for environmental and biodiversity modeling. Scientific Data, 5, 1–15. https://doi.org/10.1038/sdata.2018.40

Barton, K. (2019). MuMIn: Multi-Model Inference. R package version 1.43.15.

Https://CRAN.R-Project.Org/Package=MuMIn.

Bastin, J. F., Finegold, Y., Garcia, C., Mollicone, D., Rezende, M., Routh, D., … Crowther, T. W. (2019). The global tree restoration potential. Science, 364(6448), 76–79. https://doi.org/10.1126/science.aax0848

Brancalion, P. H. S., Niamir, A., Broadbent, E., Crouzeilles, R., Barros, F. S. M., Almeyda Zambrano, A. M., … Chazdon, R. L. (2019). Global restoration opportunities in tropical rainforest landscapes. Science Advances, 5(7), 1–12. https://doi.org/10.1126/sciadv.aav3223

Brando, P. M., Balch, J. K., Nepstad, D. C., Morton, D. C., Putz, F. E., Coe, M. T., … Soares-Filho, B. S. (2014). Abrupt increases in Amazonian tree mortality due to drought-fire interactions. Proceedings of the National Academy of Sciences of the United States of America, 111(17), 6347–6352. https://doi.org/10.1073/pnas.1305499111

Burnham, K. P., & Anderson, D. R. (2003). Model selection and multimodel inference: a practical information-theoretic approach. Springer Science & Business Media.

Calcagno, V. (2019). glmulti: Model Selection and Multimodel Inference Made Easy. R package version 1.0.7.1. Https://CRAN.R-Project.Org/Package=glmulti.

Caughlin, T. T., Barber, C., Asner, G. P., Glenn, N. F., Bohlman, S. A., & Wilson, C. H. (2020). Monitoring tropical forest succession at landscape scales despite uncertainty in Landsat time series. Ecological Applications, 31(1), 1–18. https://doi.org/10.1002/eap.2208

Chazdon, R. L. (2008). Chance and Determinism in Tropical Forest Succession. In TROPICAL FOREST COMMUNITY ECOLOGY (pp. 384–408). Blackwell Publishing Ltd.

Chazdon, R. L. (2014). Second growth : the promise of tropical forest regeneration in an age of deforestation. The University of Chicago Press. https://doi.org/10.1007/BF02394968

Chazdon, R. L., Broadbent, E. N., Rozendaal, D. M. A., Bongers, F., Zambrano, A. M. A., Aide, T. M., … Poorter, L. (2016). Carbon sequestration potential of second-growth forest regeneration in the Latin American tropics. Science Advances, 2(5).

https://doi.org/10.1126/sciadv.1501639

Clark, D. A., Piper, S. C., Keeling, C. D., & Clark, D. B. (2003). Tropical rain forest tree growth and atmospheric carbon dynamics linked to interannual temperature variation during 1984-2000. Proceedings of the National Academy of Sciences of the United States of America, 100(10), 5852–5857. https://doi.org/10.1073/pnas.0935903100

Coelho, M. T. P., Diniz-Filho, J. A., & Rangel, T. F. (2019). A parsimonious view of the parsimony principle in ecology and evolution. Ecography, 42(5), 968–976. https://doi.org/10.1111/ecog.04228

Cook-patton, S. C., Leavitt, S. M., Gibbs, D., Harris, N. L., Lister, K., Anderson-teixeira, K. J., … Holl, K. D. (2020). Mapping carbon accumulation potential from global natural forest regrowth, 585(March 2019).

Crouzeilles, R., Barros, F. S. M., Molin, P. G., Ferreira, M. S., Junqueira, A. B., Chazdon, R. L., … Brancalion, P. H. S. (2019). A new approach to map landscape variation in forest restoration success in tropical and temperate forest biomes. Journal of Applied Ecology, 56(12), 2675–2686. https://doi.org/10.1111/1365-2664.13501

Crouzeilles, R., Santiami, E., Rosa, M., Pugliese, L., Brancalion, P. H. S., Rodrigues, R. R., … Pinto, S. (2019). There is hope for achieving ambitious Atlantic Forest restoration commitments. Perspectives in Ecology and Conservation, 17(2), 80–83. https://doi.org/10.1016/j.pecon.2019.04.003

de Almeida, D. R. A., Stark, S. C., Valbuena, R., Broadbent, E. N., Silva, T. S. F., de Resende, A. F., … Brancalion, P. H. S. (2020). A new era in forest restoration monitoring. Restoration Ecology, 28(1), 8–11. https://doi.org/10.1111/rec.13067

Dickey, D. A., & Fuller, W. A. (1979). Distribution of the Estimators for Autoregressive Time Series With a Unit Root. Journal of the American Statistical Association, 74(366), 427–431. https://doi.org/10.2307/2286348

Diniz-filho, J. A. F., Rangel, T. F. L. V. B., & Bini, L. M. (2008). Model selection and information theory in geographical ecology. Global Ecology and Biogeography, 17(4), 479–488. https://doi.org/10.1111/j.1466-8238.2008.00395.x

Dormann, C. F., Elith, J., Bacher, S., Buchmann, C., Carl, G., Carré, G., … Lautenbach, S. (2013). Collinearity: A review of methods to deal with it and a simulation study evaluating their performance. Ecography, 36(1), 27–46. https://doi.org/10.1111/j.1600-0587.2012.07348.x

Doughty, C. E., & Goulden, M. L. (2009). Are tropical forests near a high temperature threshold? Journal of Geophysical Research: Biogeosciences, 114(1), 1–12. https://doi.org/10.1029/2007JG000632

Dray, S., Legendre, P., & Peres-Neto, P. R. (2006). Spatial modelling: a comprehensive framework for principal coordinate analysis of neighbour matrices (PCNM). Ecological Modelling, 196(3–4), 483–493. https://doi.org/10.1016/j.ecolmodel.2006.02.015

Erb, K. H., Kastner, T., Plutzar, C., Bais, A. L. S., Carvalhais, N., Fetzel, T., … Luyssaert, S. (2018). Unexpectedly large impact of forest management and grazing on global vegetation biomass. Nature, 553(7686), 73–76. https://doi.org/10.1038/nature25138

Fensholt, R., & Proud, S. R. (2012). Evaluation of Earth Observation based global long term vegetation trends - Comparing GIMMS and MODIS global NDVI time series. Remote Sensing of Environment, 119, 131–147. https://doi.org/10.1016/j.rse.2011.12.015

Fick, S. E., & Hijmans, R. J. (2017). WorldClim 2: new 1-km spatial resolution climate surfaces for global land areas. International Journal of Climatology, 37(12), 4302–4315. https://doi.org/doi:10.1002/joc.5086

Fox, J., & Weisberg, S. (2018). An R companion to applied regression. Sage publications.

García-Palacios, P., Gross, N., Gaitán, J., & Maestre, F. T. (2018). Climate mediates the biodiversity–ecosystem stability relationship globally. Proceedings of the National Academy of Sciences of the United States of America, 115(33), 8400–8405. https://doi.org/10.1073/pnas.1800425115

Goebes, P., Schmidt, K., Seitz, S., Both, S., Bruelheide, H., Erfmeier, A., … Kühn, P. (2019). The strength of soil-plant interactions under forest is related to a Critical Soil Depth. Scientific Reports, 9(8635), 1–12. https://doi.org/10.1038/s41598-019-

45156-5

Goulden, M. L., Miller, S. D., Da Rocha, H. R., Menton, M. C., De Freitas, H. C., E Silva Figueira, A. M., & Dias De Sousa, C. A. (2004). Diel and seasonal patterns of tropical forest CO2 exchange. Ecological Applications, 14(4 SUPPL.), 42–54. https://doi.org/10.1890/02-6008

Hasselquist, N. J., Allen, M. F., & Santiago, L. S. (2010). Water relations of evergreen and drought-deciduous trees along a seasonally dry tropical forest chronosequence. Oecologia, 164(4), 881–890. https://doi.org/10.1007/s00442-010-1725-y

Hayek, M. N., Harwatt, H., Ripple, W. J., & Mueller, N. D. (2020). The carbon opportunity cost of animal-sourced food production on land. Nature Sustainability, 10–13. https://doi.org/10.1038/s41893-020-00603-4

Hengl, T., De Jesus, J. M., Heuvelink, G. B. M., Gonzalez, M. R., Kilibarda, M., Blagotić, A., … Kempen, B. (2017). SoilGrids250m: Global gridded soil information based on machine learning. PLoS ONE, 12(2), 1–40. https://doi.org/10.1371/journal.pone.0169748

Hirota, M., Holmgren, M., Van Nes, E. H., & Scheffer, M. (2011). Global resilience of tropical forest and savanna to critical transitions. Science, 334(6053), 232–235. https://doi.org/10.1126/science.1210657

Holling, C. S. (1996). Engineering resilience versus ecological resilience. In Engineering within ecological constraints (Vol. 31, p. 32).

Huete, A., Didan, K., Miura, T., Rodriguez, E. P., Gao, X., & Ferreira, L. G. (2002). Overview of the radiometric and biophysical performance of the MODIS vegetation indices. Remote Sensing of Environment, 83(1), 195–213. https://doi.org/https://doi.org/10.1016/S0034-4257(02)00096-2

Jakovac, C. C., Peña-Claros, M., Kuyper, T. W., & Bongers, F. (2015). Loss of secondary-forest resilience by land-use intensification in the Amazon. Journal of Ecology, 103(1), 67–77. https://doi.org/10.1111/1365-2745.12298

Jarvis, A., Reuter, H., Nelson, A., & Guevara, E. (2008). Hole-filled SRTM for the globe version 3, from the CGIAR-CSI SRTM 90m database. See Http://Srtm. Csi. Cgiar. Org.

Keersmaecker, W. De, Lhermitte, S., & Honnay, O. (2014). How to measure ecosystem stability? An evaluation of the reliability of stability metrics based on remote sensing time series across the major global ecosystems. Global Change Biology, 2149–2161. https://doi.org/10.1111/gcb.12495

Keil, P., & Chase, J. M. (2019). Global patterns and drivers of tree diversity integrated across a continuum of spatial grains. Nature Ecology & Evolution, 3(3), 390–399. https://doi.org/10.1038/s41559-019-0799-0

Kopecký, M., & Čížková, Š. (2010). Using topographic wetness index in vegetation ecology: Does the algorithm matter? Applied Vegetation Science, 13(4), 450–459. https://doi.org/10.1111/j.1654-109X.2010.01083.x

Leclère, D., Obersteiner, M., Barrett, M., Butchart, S. H. M., Chaudhary, A., De Palma, A., … Young, L. (2020). Bending the curve of terrestrial biodiversity needs an integrated strategy. Nature. https://doi.org/10.1038/s41586-020-2705-y

Legendre, P., & Legendre, L. F. J. (2012). Numerical ecology. Elsevier.

Lennox, G. D., Gardner, T. A., Thomson, J. R., Ferreira, J., Berenguer, E., Lees, A. C., … Barlow, J. (2018). Second rate or a second chance? Assessing biomass and biodiversity recovery in regenerating Amazonian forests. Global Change Biology, 24(12), 5680–5694. https://doi.org/10.1111/gcb.14443

Lewis, S. L., Edwards, D. P., & Galbraith, D. (2015). Increasing human dominance of tropical forests. Science, 349(6250), 827–832.

Lhermitte, S., Verbesselt, J., Verstraeten, W. W., & Coppin, P. (2011). A comparison of time series similarity measures for classification and change detection of ecosystem dynamics. Remote Sensing of Environment, 115(12), 3129–3152. https://doi.org/10.1016/j.rse.2011.06.020

Li, Y., Cao, Z., Long, H., Liu, Y., & Li, W. (2017). Dynamic analysis of ecological environment combined with land cover and NDVI changes and implications for sustainable urban e rural development : The case of Mu Us Sandy Land , China. Journal of Cleaner Production, 142, 697–715. https://doi.org/10.1016/j.jclepro.2016.09.011

Lohbeck, M., Poorter, L., Martínez-Ramos, M., & Bongers, F. (2015). Biomass is the

main driver of changes in ecosystem process rates during tropical forest succession. Ecology, (96), 1242–1252. https://doi.org/10.1890/14-0472.1

Malhi, Y., Gardner, T. A., Goldsmith, G. R., Silman, M. R., & Zelazowski, P. (2014). Tropical Forests in the Anthropocene. Annual Review of Environment and Resources, 39(1), 125–159. https://doi.org/10.1146/annurev-environ-030713-155141

Méndez-Toribio, M., Meave, J. A., Zermeño-Hernández, I., & Ibarra-Manríquez, G. (2016). Effects of slope aspect and topographic position on environmental variables, disturbance regime and tree community attributes in a seasonal tropical dry forest. Journal of Vegetation Science, 27(6), 1094–1103. https://doi.org/10.1111/jvs.12455

Mercado, L. M., Patiño, S., Domingues, T. F., Fyllas, N. M., Weedon, G. P., Sitch, S., … Lloyd, J. (2011). Variations in Amazon forest productivity correlated with foliar nutrients and modelled rates of photosynthetic carbon supply. Philosophical Transactions of the Royal Society B: Biological Sciences, 366(1582), 3316–3329. https://doi.org/10.1098/rstb.2011.0045

Moles, A. T., Warton, D. I., Warman, L., Swenson, N. G., Laffan, S. W., Zanne, A. E., … Leishman, M. R. (2009). Global patterns in plant height. Journal of Ecology, 97(5), 923–932. https://doi.org/10.1111/j.1365-2745.2009.01526.x

Morellato, L. P. C., & Haddad, C. F. B. (2000). Introduction: The Brazilian Atlantic Forest. Biotropica, 32(4b), 786–792. https://doi.org/10.1111/j.1744-7429.2000.tb00618.x

Mulkey, S. S., Chazdon, R. L., & Smith, A. P. (1996). Tropical forest plant ecophysiology. New York: Chapman & Hall. https://doi.org/10.1007/978-1-4613-1163-8

Muylaert, R. de L., Vancine, M. H., Bernardo, R., Oshima, J. E. F., Sobral-Souza, T., Tonetti, V. R., … Ribeiro, M. C. (2018). Uma nota sobre os limites territorialis da mata atlantica - A note on the territorial limits of the Atlantic Forest. Oecologia Australis, 22(3), 302–311.

Myers, N., Mittermeier, R. A., Mittermeier, C. G., Da Fonseca, G. A. B., & Kent, J. (2000). Biodiversity hotspots for conservation priorities. Nature, 403(6772), 853–

858.

Nemani, R. R., Keeling, C. D., Hashimoto, H., Jolly, W. M., Piper, S. C., Tucker, C. J., … Running, S. W. (2003). Climate-driven increases in global terrestrial net primary production from 1982 to 1999. Science, 300(5625), 1560–1563. https://doi.org/10.1126/science.1082750

Nychka, D., Furrer, R., Paige, J., & Sain, S. (2017). fields: Tools for spatial data. R package version 10.3. <URL: Https://Github.Com/NCAR/Fields>. https://doi.org/10.5065/D6W957CT

Oksanen, J., Blanchet, F. G., Kindt, R., Legendre, P., Minchin, P. R., O'hara, R. B., … Wagner, H. (2020). vegan: Community Ecology Package 2.5-7. Retrieved from https://cran.r-project.org/package=vegan

Oliveira-Filho, A. T., & Fontes, M. A. L. (2000). Patterns of Floristic Differentiation among Atlantic Forests in Southeastern Brazil and the Influence of Climate. Biotropica, 32(4b), 793–810. https://doi.org/doi:10.1111/j.1744-7429.2000.tb00619.x

Oliveira, R. S., Eller, C. B., Barros, F. de V., Hirota, M., Brum, M., & Bittencourt, P. (2021). Linking plant hydraulics and the fast-slow continuum to understand resilience to drought in tropical ecosystems. New Phytologist. https://doi.org/10.1111/nph.17266

Paradis, E., & Schliep, K. (2018). ape 5.0: an environment for modern phylogenetics and evolutionary analyses in R. Bioinformatics, 35(3), 526–528.

Pau, S., Detto, M., Kim, Y., & Still, C. J. (2018). Tropical forest temperature thresholds for gross primary productivity. Ecosphere, 9(7), 1–12. https://doi.org/10.1002/ecs2.2311

Pettorelli, N., Vik, J. O., Mysterud, A., Gaillard, J. M., Tucker, C. J., & Stenseth, N. C. (2005). Using the satellite-derived NDVI to assess ecological responses to environmental change. Trends in Ecology and Evolution. https://doi.org/10.1016/j.tree.2005.05.011

Pohlert, T. (2018). trend: Non-Parametric Trend Tests and Change-Point Detection. R package version 1.1.1. Https://CRAN.R-Project.Org/Package=trend.

Poorter, L., Bongers, F., Aide, T. M., Almeyda Zambrano, A. M., Balvanera, P., Becknell, J. M., … Rozendaal, D. M. A. (2016). Biomass resilience of Neotropical secondary forests. Nature, 530(7589), 211–214. https://doi.org/10.1038/nature16512

Querejeta, J. I., Estrada-Medina, H., Allen, M. F., & Jiménez-Osornio, J. J. (2007). Water source partitioning among trees growing on shallow karst soils in a seasonally dry tropical climate. Oecologia, 152(1), 26–36. https://doi.org/10.1007/s00442-006-0629-3

R Core Team. (2020). R: A language and environment for statistical computing. R Foundation for Statistical Computing, Vienna, Austria.

Rezende, C. L., Scarano, F. R., Assad, E. D., Joly, C. A., Metzger, J. P., Strassburg, B. B. N., … Mittermeier, R. A. (2018). From hotspot to hopespot: An opportunity for the Brazilian Atlantic Forest. Perspectives in Ecology and Conservation, 16(4), 208–214. https://doi.org/10.1016/j.pecon.2018.10.002

Ribeiro, M. C., Metzger, J. P., Martensen, A. C., Ponzoni, F. J., & Hirota, M. M. (2009). The Brazilian Atlantic Forest: How much is left, and how is the remaining forest distributed? Implications for conservation. Biological Conservation, 142(6), 1141–1153. https://doi.org/10.1016/j.biocon.2009.02.021

Ribeiro, M., Martensen, A., Metzger, J., Tabarelli, M., Scarano, F., & Fortin, M.-J. (2011). The Brazilian Atlantic Forest: A Shrinking Biodiversity Hotspot. In Biodiversity Hotspots: Distribution and Protection of Conservation Priority Areas (pp. 405–434). https://doi.org/10.1007/978-3-642-20992-5_21

Saatchi, S., Houghton, R. A., Dos Santos Alvalá, R. C., Soares, J. V., & Yu, Y. (2007). Distribution of aboveground live biomass in the Amazon basin. Global Change Biology, 13(4), 816–837. https://doi.org/10.1111/j.1365-2486.2007.01323.x

Scheffer, M., Carpenter, S. R., Dakos, V., & van Nes, E. H. (2015). Generic Indicators of Ecological Resilience: Inferring the Chance of a Critical Transition. Annual Review of Ecology, Evolution, and Systematics, 46(1), 145–167. https://doi.org/10.1146/annurev-ecolsys-112414-054242

Sen, P. K. (1968). Estimates of the Regression Coefficient Based on Kendall's Tau. Journal of the American Statistical Association, 63(324), 1379–1389.

https://doi.org/10.2307/2285891

Sørensen, R., Zinko, U., & Seibert, J. (2006). On the calculation of the topographic wetness index: Evaluation of different methods based on field observations. Hydrology and Earth System Sciences, 10(1), 101–112. https://doi.org/10.5194/hess-10-101-2006

Strassburg, B. B. N., Beyer, H. L., Crouzeilles, R., Iribarrem, A., Barros, F., de Siqueira, M. F., … Uriarte, M. (2019). Strategic approaches to restoring ecosystems can triple conservation gains and halve costs. Nature Ecology and Evolution, 3(1), 62–70. https://doi.org/10.1038/s41559-018-0743-8

Strassburg, B. B. N., Iribarrem, A., Beyer, H. L., Cordeiro, C. L., Crouzeilles, R., Jakovac, C. C., … Visconti, P. (2020). Global priority areas for ecosystem restoration. Nature, (August 2019). https://doi.org/10.1038/s41586-020-2784-9

Sullivan, M. J. P., Lewis, S. L., Affum-Baffoe, K., Castilho, C., Costa, F., Sanchez, A. C., … Phillips, O. L. (2020). Long-term thermal sensitivity of Earth's tropical forests. Science, in press(800), 869–874. https://doi.org/10.1126/science.aaw7578

Svenning, J. C., Kinner, D. A., Stallard, R. F., Engelbrecht, B. M. J., & Wright, S. J. (2004). Ecological determinism in plant community structure across a tropical forest landscape. Ecology, 85(9), 2526–2538. https://doi.org/10.1890/03-0396

Tagesson, T., Tian, F., Schurgers, G., Horion, S., Scholes, R., Ahlström, A., … Fensholt, R. (2020). A physiology-based Earth observation model indicate stagnation in the global gross primary production during recent decades. Global Change Biology, (July), 1–19. https://doi.org/10.1111/gcb.15424

Tambosi, L. R., Martensen, A. C., Ribeiro, M. C., & Metzger, J. P. (2014). A framework to optimize biodiversity restoration efforts based on habitat amount and landscape connectivity. Restoration Ecology, 22(2), 169–177. https://doi.org/10.1111/rec.12049

Toledo, M., Poorter, L., Peña-Claros, M., Alarcón, A., Balcázar, J., Leaño, C., … Bongers, F. (2011). Climate is a stronger driver of tree and forest growth rates than soil and disturbance. Journal of Ecology, 99(1), 254–264. https://doi.org/10.1111/j.1365-2745.2010.01741.x

Uriarte, M., Schwartz, N., Powers, J. S., Marín-Spiotta, E., Liao, W., & Werden, L. K. (2016). Impacts of climate variability on tree demography in second growth tropical forests: the importance of regional context for predicting successional trajectories. Biotropica. https://doi.org/10.1111/btp.12380

Verbesselt, J., Hyndman, R., Newnham, G., & Culvenor, D. (2010). Detecting trend and seasonal changes in satellite image time series. Remote Sensing of Environment, 114(1), 106–115. https://doi.org/10.1016/j.rse.2009.08.014

Verbesselt, J., Umlauf, N., Hirota, M., Holmgren, M., Van Nes, E. H., Herold, M., … Scheffer, M. (2016). Remotely sensed resilience of tropical forests. Nature Climate Change, 6(11), 1028–1031. https://doi.org/10.1038/nclimate3108

Verdone, M., & Seidl, A. (2017). Time, space, place, and the Bonn Challenge global forest restoration target. Restoration Ecology, 25(6), 903–911. https://doi.org/10.1111/rec.12512

Vilela, B., & Villalobos, F. (2015). letsR: a new R package for data handling and analysis in macroecology. Methods in Ecology and Evolution, 6(10), 1229–1234. https://doi.org/https://doi.org/10.1111/2041-210X.12401

Vitousek, P. M., Porder, S., Houlton, B. Z., & Chadwick, O. A. (2010). Terrestrial phosphorus limitation: mechanisms, implications, and nitrogen–phosphorus interactions. Ecological Applications, 20(1), 5–15. https://doi.org/https://doi.org/10.1890/08-0127.1

Wieczynski, D. J., Boyle, B., Buzzard, V., Duran, S. M., Henderson, A. N., Hulshof, C. M., … Savage, V. M. (2019). Correction: Climate shapes and shifts functional biodiversity in forests worldwide. Proceedings of the National Academy of Sciences of the United States of America. https://doi.org/10.1073/pnas.1904390116

Wright, S. J., Yavitt, J. B., Wurzburger, N., Turner, B. I., Tanner, E. V. J., Sayer, E. J., … Corre, M. D. (2011). Potassium, phosphorus, or nitrogen limit root allocation, tree growth, or litter production in a lowland tropical forest. Ecology, 92(8), 1616–1625. https://doi.org/10.1890/10-1558.1

FIGURES

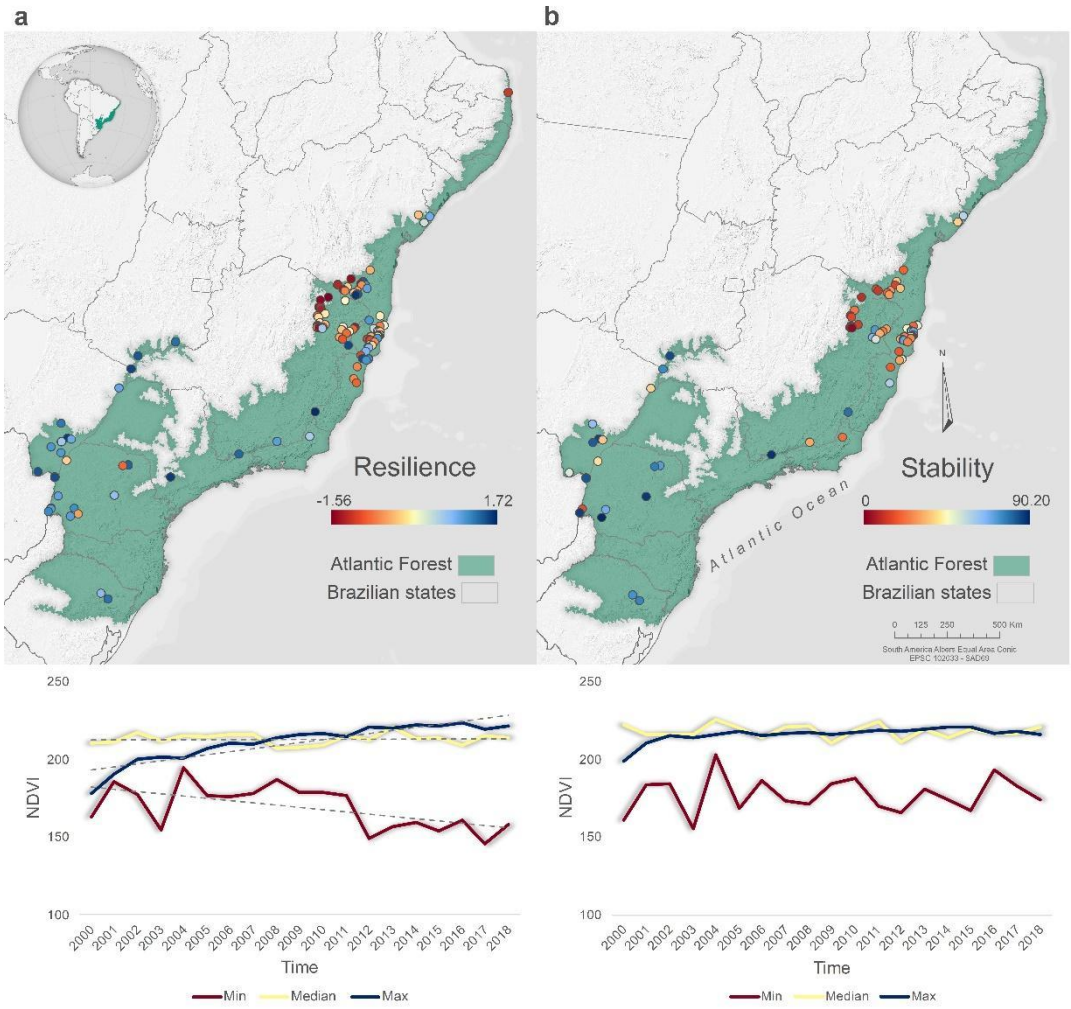

Figure 1. Above, sample points of early second-growth forests were obtained from land-use images of MapBiomas for the resilience (a) and stability (b) dataset. Colors of the points indicate values of each ecosystem property. Resilience was measured by the time series deterministic trend using Sen's slope and stability was measured by the total standard deviation of the stationary time series. Below, interannual time series of raw NDVI data for the maximum (blue), median (yellow), and minimum (red) values of resilience (a) and stability (b). Dashed lines of the resilience graph (a) represent linear trends of the NDVI time series.

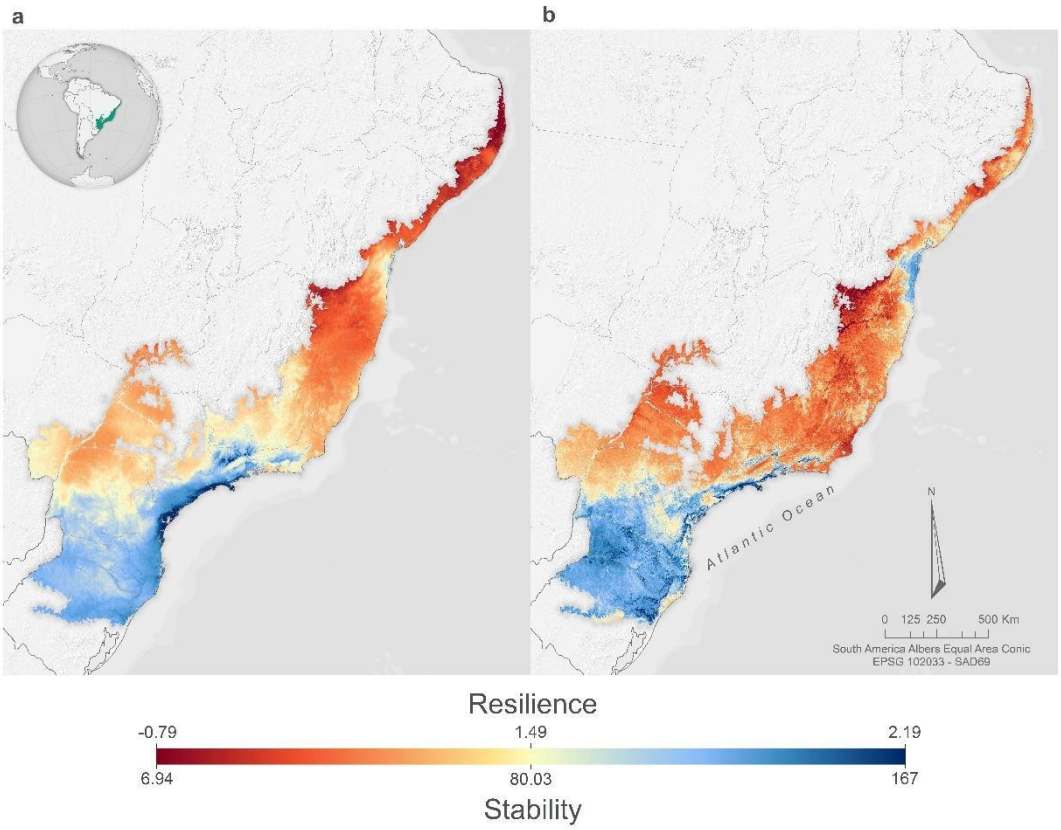

Figure 2. Prediction map of potential resilience (a) and stability (b). Maps were built with averaged coefficients of the predictors of the highest predictive accuracy models of each ecosystem's properties. In both maps, red represents regions with low ecosystem potential while blue represents regions with high ecosystem potential of early second-growth forests.

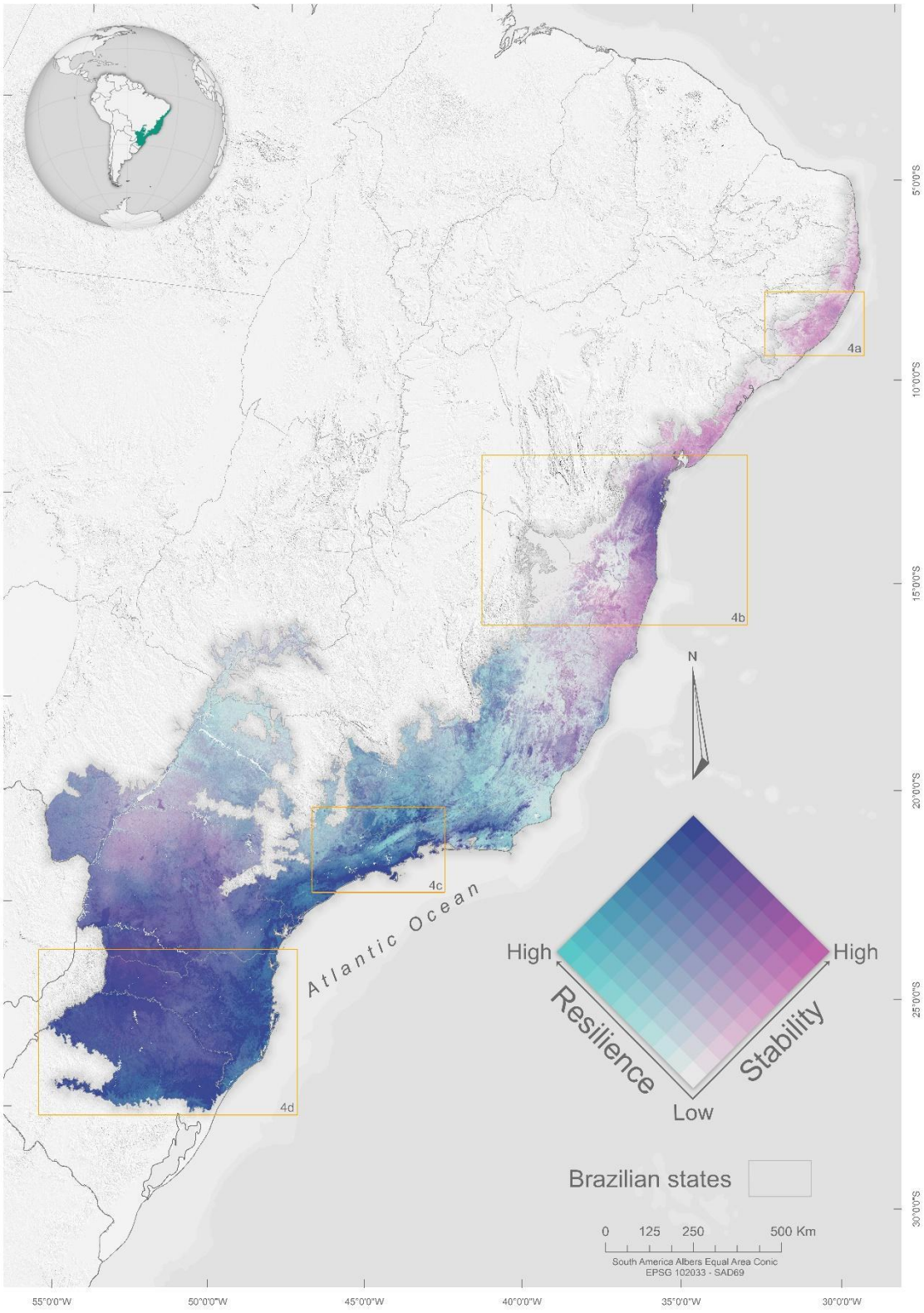

Figure 3. Bivariate map showing the combination of the ten resilience (blue) and stability (purple) classes, obtained by dividing the values of each ecosystem property into 10% quantiles. Resilience increases from gray to light blue, stability from gray to purple and the combination of both from gray to deep blue. Yellow boxes are extent indicators of highlighted regions in Figure 4.

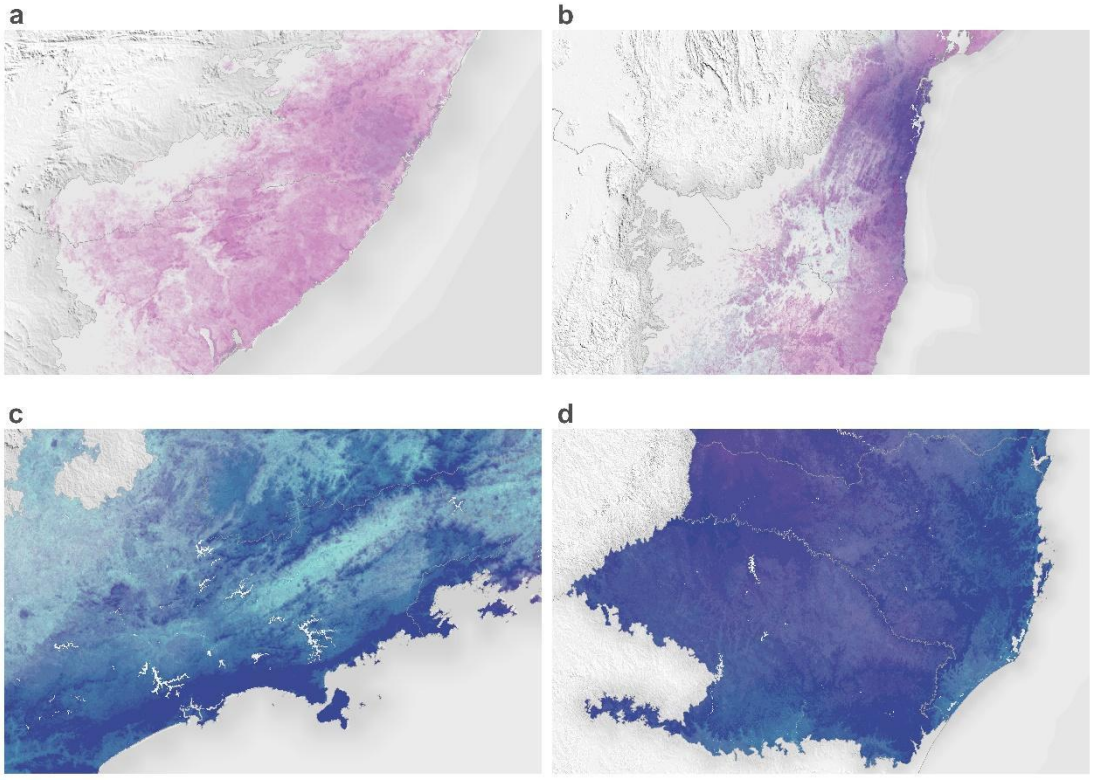

Figure 4. Highlighted regions of the bivariate map showing high stability in the north (a), the combination of higher values of resilience and stability in the coast and lower values in the interior of the north (b), and combination of higher values of both ecosystem properties in the coast and interior of the south (c) and in the southern region (d).

TABLES

Table 1. Averaged coefficients of predictors (BIO3 = isothermality, BIO12 = annual precipitation, BIO15 = Precipitation Seasonality, BIO18 = precipitation of warmest quarter, AWCtS = Derived saturated water content, BDRLOG = Probability of occurrence of R horizon (bedrock), BLDFIE = bulk density (fine earth), OCDENS = Soil organic carbon density in kg per cubic-m at depth 0.05 m, OCSTHA_30cm = Soil organic carbon stock in tons per ha, PHIKCL = Soil pH x 10 in KCl) of the best performing models for resilience and stability.

RESILIENCE					
		B	*SE*	*t*	*P*
	Intercept	2.065	1.504	1.365	0.172
	BIO3	-0.048	0.014	3.319	< 0.001 ***
	BIO12	< 0.001	< 0.001	0.301	0.763
	BIO18	0.001	< 0.001	2.895	0.003 **
	AWCtS	0.010	0.019	0.527	0.598
	BDRLOG	0.002	0.005	0.494	0.621
	OCDENS	< 0.001	0.001	0.489	0.625
	OCSTHA_30cm	0.001	0.002	0.389	0.697

STABILITY					
		B	*SE*	*t*	*P*
	Intercept	83.228	52.507	1.577	0.115
	BIO12	0.024	0.006	3.981	< 0.001 ***
	BIO15	-0.250	0.079	3.118	0.002 **
	BDRLOG	0.854	0.263	3.220	0.001 **
	BLDFIE	-0.014	0.027	0.499	0.617
	OCDENS	0.021	0.035	0.594	0.553
	PHIKCL	-0.977	0.710	1.366	0.172

Supporting information

Predicting resilience and stability on early second-growth forests

Lucas Andrigo Maure[1,2], Milena Fiuza Diniz[3], Marina P. Souza de Oliveira[4], Marco Túlio Pacheco Coelho[3], Milton César Ribeiro[5], Fernando Rodrigues da Silva[2], Erica Hasui[4]*

[1] Programa de Pós-graduação em Ecologia e Recursos Naturais (PPGERN), Universidade Federal de São Carlos, São Carlos-SP, Brazil

[2] Laboratório de Ecologia Teórica: Integrando Tempo, Biologia e Espaço (LET.IT.BE), Departamento de Ciências Ambientais, Universidade Federal de São Carlos, Sorocaba-SP, Brazil

[3] Departamento de Ecologia, Universidade Federal de Goiás, Goânia-GO, Brazil

[4] Laboratório de Ecologia de Fragmentos (EcoFrag), Instituto de Ciências da Natureza, Universidade Federal de Alfenas, Alfenas-MG, Brazil

[5] Spatial Ecology and Conservation Lab (LEEC), Departament of Biodiversity, São Paulo State University - UNESP, Rio Claro, SP, Brazil

*Corresponding author: ericahasui@gmail.com

1. METHODS

1.1 Prediction maps of ecosystem properties

For resilience, the regression equation was: *resilience* = 2.065 + 0.01017 * derived saturated water content + 0.001213 * precipitation of warmest quarter + (-0.04787 * isothermality) + 0.0003446 * soil organic carbon density + 0.0008228 * soil organic carbon stock in tons per ha + 0.002349 * probability of occurrence of R horizon + 0.00003224 * annual precipitation.

For stability, the regression equation was: *stability* = 83.227569 + 0.853995 * probability of occurrence of R horizon + (-0.977300 * soil pH) + 0.023777 * annual precipitation + (-0.249758 * precipitation seasonality) + (-0.013514 * bulk density) + 0.020929 * soil organic carbon stock in tons per ha.

TABLES

Table S1. All the 39 predictors selected a priori and the effect of their category on plant productivity.

Category	Variable	Description	Effect on plant productivity
Climate			
	BIO1	Annual Mean Temperature	
	BIO2	Mean Diurnal Range (Mean of monthly (max temp - min temp))	
	BIO3	Isothermality (BIO2/BIO7) (×100)	Temperature and precipitation affect plant productivity by ecophysiological responses that constrains photosynthesis. Higher temperature increases plant evaporation leading to stomatal closure reducing photosynthesis and the net primary productivity, forest growth, and above ground biomass (Baldocchi & Amthor, 2001; Clark, 2004; Cowling & Shin, 2006; Feeley, Joseph Wright, Nur Supardi, Kassim, & Davies, 2007; Sullivan et al., 2020). Water stress caused by low precipitation also increases the time of stomatal closure to avoid plant water loss, reducing plant productivity and growth. In extreme situations, water stress increases the mortality risk by hydraulic failure and carbon starvation (da Costa et al., 2010; McDowell et al., 2018, 2008; Nepstad, 2002; Oliveira et al., 2021).
	BIO4	Temperature Seasonality (standard deviation ×100)	
	BIO5	Max Temperature of Warmest Month	
	BIO6	Min Temperature of Coldest Month	
	BIO7	Temperature Annual Range (BIO5-BIO6)	
	BIO8	Mean Temperature of Wettest Quarter	
	BIO9	Mean Temperature of Driest Quarter	
	BIO10	Mean Temperature of Warmest Quarter	
	BIO11	Mean Temperature of Coldest Quarter	
	BIO12	Annual Precipitation	
	BIO13	Precipitation of Wettest Month	
	BIO14	Precipitation of Driest Month	
	BIO15	Precipitation Seasonality (Coefficient of Variation)	
	BIO16	Precipitation of Wettest Quarter	
	BIO17	Precipitation of Driest Quarter	
	BIO18	Precipitation of Warmest Quarter	
	BIO19	Precipitation of Coldest Quarter	
	Vapr	Water vapor pressure (kPa)	
	Srad	Solar Radiation (kJ m-2 day-1)	
Soil			
	AWCtS	Derived saturated water content (volumetric fraction) teta-S	Edaphic chemical parameters determine nutrients availability, water content, and stressor conditions (Jakovac, Peña-Claros, Kuyper, & Bongers, 2015; Laurance et al., 1999; Poorter et al., 2016; Santiago-García, Finegan, & Bosque-Pérez, 2019). Whilst, edaphic physical parameters like soil texture control the roots growth and length, affecting plant nutrients and water uptake (Bengough, 2003; Bennett, Penman, Arndt, Roxburgh, & Bennett, 2020; Stirzaker, Passioura, & Wilms, 1996). Both physical and chemical soil parameters influence biomass and forest structure distribution, and recovery in second-growth tropical forests (Jakovac et al.,
	BDRLOG	Probability of occurrence of R horizon	
	BDTICM	Absolute depth to bedrock	
	BLDFIE	Bulk density (fine earth)	
	CECSOL	Cation exchange capacity (CEC)	
	CLYPPT	Clay content (0-2 micro meter) mass fraction	
	OCDENS	Soil organic carbon density in kg per cubic-m at depth 0.05 m	
	OCSTHA_30cm	Soil organic carbon stock in tons per ha	
	OCSTHA_sd2	Soil organic carbon stock	
	ORCDRC	Soil organic carbon content (fine earth fraction)	
	PHIHOX	Soil pH in H2O	
	PHIKCL	Soil pH x 10 in KCl	

	SLTPPT	Silt content (2-50 micro meter) mass fraction	2015; Poorter et al., 2016; Santiago-García et al., 2019).
	SNDPPT	Sand content (50-2000 micro meter) mass fraction	
	WWP	Derived available soil water capacity (volumetric fraction) until wilting point	
Topographic			Topography modulates climate and determine water and nutrient availability in soil affecting tree productivity, biomass and forest structure in the tropics (de Castilho et al., 2006; Ediriweera, Singhakumara, & Ashton, 2008; Kitayama & Aiba, 2002; Raich, Russell, & Vitousek, 1997; Sattler, Murray, Kirchner, & Lindner, 2014).
	Elevation	Altitude (m)	
	Topographic heterogeneity (TH)	Standard deviation of elevation measures the elevational variability within an area	
	Terrain wetness index (TWI)	Quantify topographic control on hydrological processes	

Table S2. Predictors rank for resilience by AICc.

	df	logLik	AICc	delta	weight
BIO3	3	-102.24	210.62	0	1
BIO12	3	-109.39	224.94	14.32	0
BIO18	3	-112.52	231.19	20.57	0
OCSTHA_30cm	3	-114.46	235.07	24.44	0
BLDFIE	3	-114.88	235.91	25.29	0
BIO4	3	-115.44	237.03	26.41	0
OCSTHA_sd2	3	-115.6	237.34	26.72	0
AWCtS	3	-117.31	240.78	30.16	0
OCDENS	3	-118.05	242.25	31.63	0
ORCDRC	3	-119.12	244.39	33.77	0
BDTICM	3	-121.57	249.29	38.66	0
BIO17	3	-121.67	249.48	38.86	0
BDRLOG	3	-121.96	250.07	39.44	0
BIO15	3	-121.99	250.13	39.51	0
BIO19	3	-122.94	252.03	41.41	0
BIO14	3	-123.06	252.26	41.64	0
BIO13	3	-123.56	253.27	42.65	0
CECSOL	3	-124.05	254.25	43.63	0
BIO16	3	-124.33	254.81	44.19	0
BIO11	3	-124.92	255.99	45.37	0
BIO9	3	-125.74	257.63	47	0
BIO6	3	-126.83	259.82	49.19	0
WWP	3	-126.99	260.14	49.52	0
BIO1	3	-127.02	260.2	49.58	0
Srad	3	-127.44	261.02	50.4	0
PHIKCL	3	-127.61	261.37	50.75	0
SLTPPT	3	-127.62	261.39	50.77	0
PHIHOX	3	-127.64	261.44	50.82	0
BIO7	3	-127.85	261.85	51.22	0
Vapr	3	-128.73	263.61	52.99	0
SNDPPT	3	-128.77	263.69	53.07	0
BIO8	3	-128.93	264	53.38	0
BIO5	3	-129.06	264.26	53.64	0
Elevation	3	-129.58	265.31	54.69	0
TH	3	-129.64	265.43	54.81	0
BIO10	3	-129.67	265.49	54.87	0
CLYPPT	3	-129.68	265.51	54.89	0
TWI	3	-129.72	265.58	54.96	0
BIO2	3	-129.81	265.77	55.14	0

Table S3. Predictors rank for stability by AICc.

	df	logLik	AICc	delta	weight
BIO15	3	-424.01	854.26	0	0.62
BIO12	3	-424.58	855.41	1.15	0.35
BIO17	3	-427.17	860.58	6.33	0.03
OCDENS	3	-428.65	863.55	9.29	0.01
BIO14	3	-430.27	866.79	12.54	0
BIO19	3	-430.68	867.6	13.34	0
BLDFIE	3	-433.32	872.88	18.62	0
OCSTHA_30cm	3	-435.02	876.28	22.02	0
AWCtS	3	-435.34	876.92	22.66	0
OCSTHA_sd2	3	-435.42	877.08	22.82	0
PHIKCL	3	-439.07	884.39	30.13	0
BIO3	3	-439.54	885.32	31.07	0
CECSOL	3	-440.03	886.3	32.05	0
ORCDRC	3	-440.29	886.82	32.56	0
PHIHOX	3	-442.14	890.53	36.28	0
BIO2	3	-445.35	896.95	42.69	0
BDRLOG	3	-446.28	898.81	44.55	0
BDTICM	3	-448.59	903.43	49.18	0
WWP	3	-448.72	903.69	49.43	0
SLTPPT	3	-450.32	906.88	52.63	0
BIO18	3	-450.82	907.88	53.62	0
BIO4	3	-451.42	909.09	54.83	0
BIO5	3	-451.56	909.36	55.11	0
SNDPPT	3	-453.13	912.51	58.25	0
BIO7	3	-453.63	913.51	59.25	0
Elevation	3	-454.06	914.36	60.1	0
BIO11	3	-454.51	915.26	61.01	0
BIO1	3	-454.82	915.89	61.63	0
BIO8	3	-454.99	916.22	61.97	0
TWI	3	-455.18	916.61	62.35	0
CLYPPT	3	-455.29	916.82	62.56	0
BIO13	3	-455.47	917.19	62.94	0
BIO16	3	-455.53	917.31	63.05	0
Vapr	3	-455.56	917.37	63.11	0
BIO6	3	-455.64	917.52	63.26	0
BIO9	3	-455.71	917.66	63.4	0
BIO10	3	-455.76	917.77	63.51	0
Srad	3	-455.76	917.77	63.52	0
TH	3	-455.77	917.79	63.53	0

Table S4. Variance inflation factor (VIF) of all selected predictors for resilience and stability analysis.

Resilience	VIF
BIO3	2.60
BIO12	3.29
BIO18	1.95
AWCtS	3.21
BDRLOG	1.65
OCEDENS	4.26
OCSTHA_30cm	4.60
Stability	**VIF**
BIO5	1.65
BIO12	1.83
BIO15	3.19
Srad	1.21
BDRLOG	2.14
BLDFIE	3.57
OCEDENS	3.63
PHIKCL	2.34
TWI	1.72

Table S5. Selection of 128 models emerging from the combination of the seven predictors for resilience.

Models	df	logLik	AICc	deltaAICc	weight
Resilience ~ AWCtS + BIO18 + BIO3	5	-96.32	203.03	0.00	0.08
Resilience ~ OCDENS + BIO18 + BIO3	5	-96.39	203.16	0.13	0.08
Resilience ~ OCSTHA_30cm + BIO18 + BIO3	5	-96.63	203.64	0.61	0.06
Resilience ~ BDRLOG + BIO18 + BIO3	5	-96.72	203.82	0.79	0.05
Resilience ~ BIO18 + BIO3	4	-97.92	204.09	1.06	0.05
Resilience ~ BDRLOG + BIO12 + BIO18 + BIO3	6	-95.83	204.19	1.16	0.05
Resilience ~ BDRLOG + OCSTHA_30cm + BIO18 + BIO3	6	-95.91	204.35	1.32	0.04
Resilience ~ AWCtS + BDRLOG + BIO18 + BIO3	6	-95.96	204.45	1.42	0.04
Resilience ~ BDRLOG + OCDENS + BIO18 + BIO3	6	-95.99	204.50	1.47	0.04
Resilience ~ AWCtS + BIO12 + BIO18 + BIO3	6	-96.02	204.57	1.54	0.04
Resilience ~ AWCtS + OCSTHA_30cm + BIO18 + BIO3	6	-96.05	204.63	1.60	0.04
Resilience ~ AWCtS + OCDENS + BIO18 + BIO3	6	-96.08	204.69	1.67	0.04
Resilience ~ OCDENS + BIO12 + BIO18 + BIO3	6	-96.10	204.73	1.70	0.03
Resilience ~ OCDENS + OCSTHA_30cm + BIO18 + BIO3	6	-96.22	204.98	1.95	0.03
Resilience ~ BIO12 + BIO18 + BIO3	5	-97.33	205.03	2.00	0.03
Resilience ~ AWCtS + BDRLOG + BIO12 + BIO18 + BIO3	7	-95.42	205.56	2.53	0.02
Resilience ~ BDRLOG + OCDENS + BIO12 + BIO18 + BIO3	7	-95.45	205.62	2.59	0.02
Resilience ~ OCSTHA_30cm + BIO12 + BIO18 + BIO3	6	-96.57	205.66	2.64	0.02
Resilience ~ BDRLOG + OCSTHA_30cm + BIO12 + BIO18 + BIO3	7	-95.61	205.93	2.90	0.02
Resilience ~ AWCtS + BDRLOG + OCSTHA_30cm + BIO18 + BIO3	7	-95.68	206.07	3.05	0.02
Resilience ~ BDRLOG + OCDENS + OCSTHA_30cm + BIO18 + BIO3	7	-95.78	206.28	3.25	0.02
Resilience ~ AWCtS + BDRLOG + OCDENS + BIO18 + BIO3	7	-95.80	206.32	3.30	0.02
Resilience ~ AWCtS + OCDENS + BIO12 + BIO18 + BIO3	7	-95.82	206.36	3.33	0.02
Resilience ~ AWCtS + OCSTHA_30cm + BIO12 + BIO18 + BIO3	7	-95.93	206.57	3.54	0.01
Resilience ~ AWCtS + OCDENS + OCSTHA_30cm + BIO18 + BIO3	7	-95.97	206.66	3.64	0.01
Resilience ~ BDRLOG + BIO12 + BIO3	5	-98.18	206.74	3.71	0.01
Resilience ~ OCDENS + OCSTHA_30cm + BIO12 + BIO18 + BIO3	7	-96.07	206.85	3.83	0.01
Resilience ~ AWCtS + BDRLOG + OCDENS + BIO12 + BIO18 + BIO3	8	-95.34	207.60	4.58	0.01
Resilience ~ AWCtS + BDRLOG + OCSTHA_30cm + BIO12 + BIO18 + BIO3	8	-95.38	207.69	4.66	0.01
Resilience ~ BDRLOG + OCDENS + OCSTHA_30cm + BIO12 + BIO18 + BIO3	8	-95.44	207.80	4.78	0.01
Resilience ~ BIO12 + BIO3	4	-99.86	207.97	4.95	0.01
Resilience ~ AWCtS + BDRLOG + OCDENS + OCSTHA_30cm + BIO18 + BIO3	8	-95.66	208.24	5.21	0.01
Resilience ~ AWCtS + OCDENS + OCSTHA_30cm + BIO12 + BIO18 + BIO3	8	-95.81	208.55	5.53	0.01
Resilience ~ AWCtS + BDRLOG + BIO12 + BIO3	6	-98.13	208.78	5.76	0.00
Resilience ~ AWCtS + BIO12 + BIO3	5	-99.22	208.81	5.78	0.00
Resilience ~ BDRLOG + OCSTHA_30cm + BIO12 + BIO3	6	-98.15	208.83	5.80	0.00
Resilience ~ BDRLOG + OCDENS + BIO12 + BIO3	6	-98.17	208.88	5.85	0.00

Resilience ~ OCDENS + BIO12 + BIO3	5	-99.46	209.29	6.26	0.00
Resilience ~ AWCtS + BDRLOG + OCDENS + OCSTHA_30cm + BIO12 + BIO18 + BIO3	9	-95.34	209.83	6.80	0.00
Resilience ~ OCSTHA_30cm + BIO12 + BIO3	5	-99.81	209.99	6.97	0.00
Resilience ~ BDRLOG + BIO3	4	-101.10	210.46	7.43	0.00
Resilience ~ BIO3	3	-102.24	210.62	7.59	0.00
Resilience ~ AWCtS + BDRLOG + OCSTHA_30cm + BIO12 + BIO3	7	-98.01	210.72	7.70	0.00
Resilience ~ AWCtS + OCSTHA_30cm + BIO12 + BIO3	6	-99.14	210.82	7.79	0.00
Resilience ~ AWCtS + BIO3	4	-101.30	210.86	7.83	0.00
Resilience ~ BDRLOG + OCDENS + OCSTHA_30cm + BIO12 + BIO3	7	-98.07	210.86	7.83	0.00
Resilience ~ AWCtS + OCDENS + BIO12 + BIO3	6	-99.21	210.94	7.92	0.00
Resilience ~ AWCtS + BDRLOG + OCDENS + BIO12 + BIO3	7	-98.12	210.95	7.92	0.00
Resilience ~ BDRLOG + OCDENS + BIO12 + BIO18	6	-99.32	211.17	8.14	0.00
Resilience ~ OCDENS + OCSTHA_30cm + BIO12 + BIO3	6	-99.36	211.26	8.23	0.00
Resilience ~ BDRLOG + OCSTHA_30cm + BIO18	5	-100.51	211.40	8.37	0.00
Resilience ~ BDRLOG + OCSTHA_30cm + BIO12 + BIO18	6	-99.43	211.40	8.37	0.00
Resilience ~ OCDENS + BIO12 + BIO18	5	-100.54	211.46	8.44	0.00
Resilience ~ AWCtS + OCSTHA_30cm + BIO18	5	-100.55	211.48	8.45	0.00
Resilience ~ OCSTHA_30cm + BIO3	4	-101.62	211.49	8.47	0.00
Resilience ~ AWCtS + BDRLOG + BIO12 + BIO18	6	-99.49	211.51	8.48	0.00
Resilience ~ OCDENS + BIO3	4	-101.64	211.53	8.50	0.00
Resilience ~ OCSTHA_30cm + BIO18	4	-101.73	211.70	8.68	0.00
Resilience ~ AWCtS + BIO12 + BIO18	5	-100.75	211.88	8.85	0.00
Resilience ~ AWCtS + BDRLOG + BIO3	5	-100.79	211.96	8.94	0.00
Resilience ~ BDRLOG + OCSTHA_30cm + BIO3	5	-100.80	211.98	8.96	0.00
Resilience ~ OCDENS + OCSTHA_30cm + BIO18	5	-100.90	212.17	9.14	0.00
Resilience ~ BDRLOG + BIO12 + BIO18	5	-100.95	212.27	9.25	0.00
Resilience ~ BDRLOG + OCDENS + BIO3	5	-100.97	212.32	9.29	0.00
Resilience ~ AWCtS + OCDENS + BIO12 + BIO18	6	-99.93	212.38	9.36	0.00
Resilience ~ AWCtS + OCSTHA_30cm + BIO12 + BIO18	6	-99.93	212.40	9.37	0.00
Resilience ~ AWCtS + BDRLOG + OCSTHA_30cm + BIO18	6	-100.00	212.54	9.51	0.00
Resilience ~ AWCtS + BDRLOG + OCSTHA_30cm + BIO12 + BIO18	7	-98.97	212.64	9.62	0.00
Resilience ~ BDRLOG + OCDENS + OCSTHA_30cm + BIO12 + BIO18	7	-99.05	212.81	9.78	0.00
Resilience ~ AWCtS + BDRLOG + OCDENS + BIO12 + BIO18	7	-99.05	212.82	9.79	0.00
Resilience ~ AWCtS + OCSTHA_30cm + BIO3	5	-101.22	212.82	9.79	0.00
Resilience ~ AWCtS + OCDENS + OCSTHA_30cm + BIO12 + BIO3	7	-99.06	212.84	9.81	0.00
Resilience ~ OCDENS + OCSTHA_30cm + BIO12 + BIO18	6	-100.16	212.85	9.83	0.00
Resilience ~ OCSTHA_30cm + BIO12 + BIO18	5	-101.25	212.88	9.85	0.00
Resilience ~ AWCtS + BDRLOG + OCDENS + OCSTHA_30cm + BIO12 + BIO3	8	-97.99	212.91	9.88	0.00
Resilience ~ AWCtS + OCDENS + BIO3	5	-101.29	212.95	9.93	0.00

Resilience ~ BDRLOG + OCDENS + OCSTHA_30cm + BIO18	6	-100.22	212.97	9.94	0.00
Resilience ~ AWCtS + OCDENS + OCSTHA_30cm + BIO18	6	-100.40	213.34	10.31	0.00
Resilience ~ OCDENS + OCSTHA_30cm + BIO3	5	-101.52	213.41	10.39	0.00
Resilience ~ OCDENS + BIO18	4	-102.63	213.52	10.49	0.00
Resilience ~ AWCtS + OCDENS + BIO18	5	-101.73	213.84	10.81	0.00
Resilience ~ AWCtS + BDRLOG + OCSTHA_30cm + BIO3	6	-100.70	213.94	10.91	0.00
Resilience ~ AWCtS + OCDENS + OCSTHA_30cm + BIO12 + BIO18	7	-99.68	214.07	11.04	0.00
Resilience ~ AWCtS + BDRLOG + OCDENS + BIO3	6	-100.79	214.12	11.09	0.00
Resilience ~ BDRLOG + OCDENS + OCSTHA_30cm + BIO3	6	-100.80	214.14	11.11	0.00
Resilience ~ BDRLOG + OCDENS + BIO18	5	-102.05	214.48	11.45	0.00
Resilience ~ AWCtS + BIO18	4	-103.17	214.58	11.55	0.00
Resilience ~ AWCtS + BDRLOG + OCDENS + OCSTHA_30cm + BIO18	7	-99.95	214.61	11.58	0.00
Resilience ~ AWCtS + BDRLOG + OCDENS + OCSTHA_30cm + BIO12 + BIO18	8	-98.85	214.62	11.60	0.00
Resilience ~ AWCtS + OCDENS + OCSTHA_30cm + BIO3	6	-101.22	214.97	11.94	0.00
Resilience ~ AWCtS + BDRLOG + OCDENS + BIO18	6	-101.42	215.36	12.33	0.00
Resilience ~ AWCtS + BDRLOG + BIO18	5	-102.56	215.50	12.48	0.00
Resilience ~ AWCtS + BDRLOG + OCDENS + OCSTHA_30cm + BIO3	7	-100.68	216.06	13.04	0.00
Resilience ~ BDRLOG + BIO12	4	-104.11	216.47	13.45	0.00
Resilience ~ AWCtS + BDRLOG + BIO12	5	-103.48	217.33	14.30	0.00
Resilience ~ BDRLOG + OCDENS + BIO12	5	-103.59	217.55	14.53	0.00
Resilience ~ BDRLOG + OCSTHA_30cm + BIO12	5	-103.83	218.04	15.01	0.00
Resilience ~ BIO12 + BIO18	4	-105.49	219.23	16.20	0.00
Resilience ~ AWCtS + BDRLOG + OCDENS + BIO12	6	-103.41	219.34	16.32	0.00
Resilience ~ AWCtS + BDRLOG + OCSTHA_30cm + BIO12	6	-103.46	219.45	16.43	0.00
Resilience ~ BDRLOG + OCDENS + OCSTHA_30cm + BIO12	6	-103.59	219.70	16.68	0.00
Resilience ~ AWCtS + BIO12	4	-105.82	219.89	16.87	0.00
Resilience ~ OCDENS + BIO12	4	-106.18	220.61	17.58	0.00
Resilience ~ AWCtS + OCDENS + BIO12	5	-105.49	221.37	18.34	0.00
Resilience ~ AWCtS + BDRLOG + OCDENS + OCSTHA_30cm + BIO12	7	-103.40	221.52	18.50	0.00
Resilience ~ AWCtS + OCSTHA_30cm + BIO12	5	-105.73	221.84	18.82	0.00
Resilience ~ OCDENS + OCSTHA_30cm + BIO12	5	-106.17	222.71	19.69	0.00
Resilience ~ OCSTHA_30cm + BIO12	4	-107.38	223.02	19.99	0.00
Resilience ~ BDRLOG + BIO18	4	-107.46	223.17	20.14	0.00
Resilience ~ AWCtS + OCDENS + OCSTHA_30cm + BIO12	6	-105.49	223.52	20.49	0.00
Resilience ~ BIO12	3	-109.39	224.94	21.91	0.00
Resilience ~ BIO18	3	-112.52	231.19	28.17	0.00
Resilience ~ BDRLOG + OCSTHA_30cm	4	-112.52	233.29	30.26	0.00
Resilience ~ AWCtS + BDRLOG + OCSTHA_30cm	5	-112.13	234.64	31.62	0.00
Resilience ~ AWCtS + OCSTHA_30cm	4	-113.22	234.69	31.66	0.00
Resilience ~ OCSTHA_30cm	3	-114.46	235.07	32.04	0.00

Resilience ~ BDRLOG + OCDENS + OCSTHA_30cm	5	-112.51	235.40	32.38	0.00
Resilience ~ OCDENS + OCSTHA_30cm	4	-114.13	236.51	33.49	0.00
Resilience ~ AWCtS + BDRLOG + OCDENS + OCSTHA_30cm	6	-112.08	236.68	33.66	0.00
Resilience ~ AWCtS + OCDENS + OCSTHA_30cm	5	-113.22	236.82	33.79	0.00
Resilience ~ AWCtS + BDRLOG	4	-116.09	240.42	37.40	0.00
Resilience ~ AWCtS + OCDENS	4	-116.21	240.68	37.65	0.00
Resilience ~ AWCtS	3	-117.31	240.78	37.75	0.00
Resilience ~ AWCtS + BDRLOG + OCDENS	5	-115.34	241.07	38.04	0.00
Resilience ~ BDRLOG + OCDENS	4	-116.55	241.34	38.31	0.00
Resilience ~ OCDENS	3	-118.05	242.25	39.22	0.00
Resilience ~ BDRLOG	3	-121.96	250.07	47.04	0.00
Resilience ~ NA + NA + NA + NA + NA + NA	2	-129.89	263.85	60.83	0.00

Table S6. Selection of 512 models emerging from the combination of nine predictors for stability.

Models	df	logLik	AICc	deltaAICc	weight
Stability ~ BDRLOG + PHIKCL + BIO12 + BIO15	6	-401.07	815.02	0.00	0.12
Stability ~ BDRLOG + OCDENS + PHIKCL + BIO12 + BIO15	7	-400.61	816.41	1.38	0.06
Stability ~ BDRLOG + BLDFIE + PHIKCL + BIO12 + BIO15	7	-400.67	816.53	1.50	0.06
Stability ~ BDRLOG + OCDENS + BIO12 + BIO15	6	-401.99	816.86	1.84	0.05
Stability ~ BDRLOG + PHIKCL + BIO12 + BIO15 + BIO5	7	-400.93	817.04	2.02	0.04
Stability ~ BDRLOG + PHIKCL + BIO12 + BIO15 + Srad	7	-400.99	817.17	2.14	0.04
Stability ~ BDRLOG + PHIKCL + PHIKCL + BIO12 + BIO15	7	-401.07	817.33	2.31	0.04
Stability ~ BDRLOG + BIO12 + BIO15	5	-403.46	817.54	2.51	0.03
Stability ~ BDRLOG + BLDFIE + BIO12 + BIO15	6	-402.41	817.70	2.68	0.03
Stability ~ BDRLOG + BIO12 + BIO15 + BIO5	6	-402.66	818.20	3.18	0.02
Stability ~ BDRLOG + BLDFIE + OCDENS + PHIKCL + BIO12 + BIO15	8	-400.53	818.60	3.58	0.02
Stability ~ BDRLOG + OCDENS + PHIKCL + BIO12 + BIO15 + BIO5	8	-400.59	818.74	3.71	0.02
Stability ~ BDRLOG + OCDENS + PHIKCL + BIO12 + BIO15 + Srad	8	-400.60	818.75	3.73	0.02
Stability ~ BDRLOG + OCDENS + PHIKCL + PHIKCL + BIO12 + BIO15	8	-400.61	818.76	3.74	0.02
Stability ~ BDRLOG + BLDFIE + PHIKCL + PHIKCL + BIO12 + BIO15	8	-400.63	818.80	3.78	0.02
Stability ~ BDRLOG + BLDFIE + PHIKCL + BIO12 + BIO15 + Srad	8	-400.66	818.86	3.84	0.02
Stability ~ BDRLOG + BLDFIE + PHIKCL + BIO12 + BIO15 + BIO5	8	-400.66	818.87	3.85	0.02
Stability ~ BDRLOG + OCDENS + BIO12 + BIO15 + BIO5	7	-401.86	818.92	3.90	0.02
Stability ~ BDRLOG + BLDFIE + OCDENS + BIO12 + BIO15	7	-401.88	818.95	3.92	0.02
Stability ~ BDRLOG + OCDENS + PHIKCL + BIO12 + BIO15	7	-401.91	819.00	3.98	0.02
Stability ~ BDRLOG + OCDENS + BIO12 + BIO15 + Srad	7	-401.99	819.17	4.14	0.02
Stability ~ BDRLOG + PHIKCL + BIO12 + BIO15 + BIO5 + Srad	8	-400.88	819.30	4.28	0.01
Stability ~ BDRLOG + BLDFIE + PHIKCL + BIO12 + BIO15	7	-402.08	819.35	4.33	0.01
Stability ~ BDRLOG + PHIKCL + PHIKCL + BIO12 + BIO15 + BIO5	8	-400.91	819.37	4.35	0.01
Stability ~ BDRLOG + BIO12 + BIO15 + Srad	6	-403.27	819.43	4.41	0.01
Stability ~ BDRLOG + PHIKCL + PHIKCL + BIO12 + BIO15 + Srad	8	-400.98	819.52	4.49	0.01
Stability ~ BDRLOG + PHIKCL + BIO12 + BIO15	6	-403.34	819.56	4.54	0.01
Stability ~ BDRLOG + BLDFIE + BIO12 + BIO15 + BIO5	7	-402.24	819.67	4.65	0.01
Stability ~ BDRLOG + BLDFIE + BIO12 + BIO15 + Srad	7	-402.40	819.99	4.96	0.01
Stability ~ BDRLOG + PHIKCL + BIO12 + BIO15 + BIO5	7	-402.40	820.00	4.98	0.01
Stability ~ BDRLOG + BIO12 + BIO15 + BIO5 + Srad	7	-402.59	820.38	5.35	0.01
Stability ~ BDRLOG + BLDFIE + OCDENS + PHIKCL + BIO12 + BIO15	8	-401.71	820.97	5.94	0.01
Stability ~ BDRLOG + BLDFIE + OCDENS + PHIKCL + PHIKCL + BIO12 + BIO15	9	-400.51	820.97	5.94	0.01
Stability ~ BDRLOG + OCDENS + PHIKCL + BIO12 + BIO15 + BIO5	8	-401.72	821.00	5.97	0.01
Stability ~ BDRLOG + BLDFIE + OCDENS + PHIKCL + BIO12 + BIO15 + Srad	9	-400.53	821.01	5.98	0.01
Stability ~ BDRLOG + BLDFIE + OCDENS + PHIKCL + BIO12 + BIO15 + BIO5	9	-400.53	821.01	5.98	0.01

Stability ~ BDRLOG + OCDENS + PHIKCL + PHIKCL + BIO12 + BIO15 + BIO5	9	-400.59	821.13	6.11	0.01
Stability ~ BDRLOG + OCDENS + PHIKCL + BIO12 + BIO15 + BIO5 + Srad	9	-400.59	821.14	6.11	0.01
Stability ~ BDRLOG + OCDENS + PHIKCL + PHIKCL + BIO12 + BIO15 + Srad	9	-400.60	821.16	6.13	0.01
Stability ~ BDRLOG + BLDFIE + OCDENS + BIO12 + BIO15 + BIO5	8	-401.81	821.17	6.15	0.01
Stability ~ BDRLOG + BLDFIE + PHIKCL + PHIKCL + BIO12 + BIO15 + Srad	9	-400.61	821.18	6.16	0.01
Stability ~ BDRLOG + BLDFIE + PHIKCL + PHIKCL + BIO12 + BIO15 + BIO5	9	-400.61	821.18	6.16	0.01
Stability ~ BDRLOG + BLDFIE + PHIKCL + BIO12 + BIO15 + BIO5 + Srad	9	-400.65	821.26	6.24	0.01
Stability ~ BDRLOG + OCDENS + BIO12 + BIO15 + BIO5 + Srad	8	-401.86	821.28	6.25	0.01
Stability ~ BDRLOG + BLDFIE + PHIKCL + BIO12 + BIO15 + BIO5	8	-401.88	821.30	6.28	0.01
Stability ~ BDRLOG + BLDFIE + OCDENS + BIO12 + BIO15 + Srad	8	-401.88	821.30	6.28	0.01
Stability ~ BDRLOG + OCDENS + PHIKCL + BIO12 + BIO15 + Srad	8	-401.90	821.35	6.33	0.01
Stability ~ BDRLOG + PHIKCL + BIO12 + BIO15 + Srad	7	-403.11	821.42	6.39	0.00
Stability ~ BDRLOG + PHIKCL + PHIKCL + BIO12 + BIO15 + BIO5 + Srad	9	-400.85	821.66	6.64	0.00
Stability ~ BDRLOG + BLDFIE + PHIKCL + BIO12 + BIO15 + Srad	8	-402.06	821.67	6.64	0.00
Stability ~ BDRLOG + BLDFIE + BIO12 + BIO15 + BIO5 + Srad	8	-402.23	822.01	6.99	0.00
Stability ~ BDRLOG + PHIKCL + BIO12 + BIO15 + BIO5 + Srad	8	-402.31	822.17	7.14	0.00
Stability ~ OCDENS + BIO12 + BIO15	5	-405.96	822.55	7.52	0.00
Stability ~ BDRLOG + OCDENS + PHIKCL + BIO12	6	-404.89	822.67	7.65	0.00
Stability ~ BDRLOG + BLDFIE + OCDENS + PHIKCL + BIO12 + BIO15 + BIO5	9	-401.61	823.18	8.16	0.00
Stability ~ BDRLOG + BLDFIE + PHIKCL + BIO12	6	-405.20	823.28	8.25	0.00
Stability ~ BDRLOG + PHIKCL + BIO12	5	-406.33	823.29	8.26	0.00
Stability ~ BDRLOG + BLDFIE + OCDENS + PHIKCL + BIO12 + BIO15 + Srad	9	-401.71	823.37	8.35	0.00
Stability ~ BDRLOG + OCDENS + PHIKCL + BIO12 + BIO15 + BIO5 + Srad	9	-401.72	823.40	8.37	0.00
Stability ~ BDRLOG + BLDFIE + OCDENS + PHIKCL + PHIKCL + BIO12 + BIO15 + BIO5	10	-400.50	823.42	8.40	0.00
Stability ~ BDRLOG + BLDFIE + OCDENS + PHIKCL + PHIKCL + BIO12 + BIO15 + Srad	10	-400.50	823.43	8.40	0.00
Stability ~ BDRLOG + BLDFIE + OCDENS + PHIKCL + BIO12 + BIO15 + BIO5 + Srad	10	-400.52	823.47	8.44	0.00
Stability ~ BDRLOG + BLDFIE + OCDENS + BIO12 + BIO15 + BIO5 + Srad	9	-401.81	823.58	8.56	0.00
Stability ~ BDRLOG + OCDENS + PHIKCL + PHIKCL + BIO12 + BIO15 + BIO5 + Srad	10	-400.58	823.58	8.56	0.00
Stability ~ BDRLOG + BLDFIE + PHIKCL + PHIKCL + BIO12 + BIO15 + BIO5 + Srad	10	-400.60	823.62	8.60	0.00
Stability ~ BDRLOG + BLDFIE + PHIKCL + BIO12 + BIO15 + BIO5 + Srad	9	-401.86	823.67	8.65	0.00
Stability ~ OCDENS + BIO12 + BIO15 + BIO5	6	-405.40	823.68	8.66	0.00
Stability ~ OCDENS + PHIKCL + BIO12 + BIO15	6	-405.41	823.70	8.68	0.00
Stability ~ BDRLOG + OCDENS + PHIKCL + BIO12 + Srad	7	-404.39	823.97	8.95	0.00

Stability ~ BDRLOG + OCDENS + PHIKCL + BIO12 + BIO5	7	-404.60	824.39	9.37	0.00
Stability ~ BLDFIE + OCDENS + BIO12 + BIO15	6	-405.84	824.56	9.54	0.00
Stability ~ OCDENS + PHIKCL + BIO12 + BIO15	6	-405.84	824.57	9.54	0.00
Stability ~ BDRLOG + BLDFIE + OCDENS + PHIKCL + BIO12	7	-404.72	824.63	9.61	0.00
Stability ~ BDRLOG + BLDFIE + PHIKCL + BIO12 + Srad	7	-404.75	824.69	9.67	0.00
Stability ~ OCDENS + BIO12 + BIO15 + Srad	6	-405.95	824.78	9.76	0.00
Stability ~ BDRLOG + OCDENS + PHIKCL + PHIKCL + BIO12	7	-404.80	824.80	9.77	0.00
Stability ~ BDRLOG + BLDFIE + PHIKCL + BIO12 + BIO5	7	-404.81	824.81	9.78	0.00
Stability ~ BDRLOG + BLDFIE + PHIKCL + PHIKCL + BIO12	7	-404.86	824.91	9.88	0.00
Stability ~ OCDENS + PHIKCL + PHIKCL + BIO12 + BIO15	7	-404.98	825.16	10.13	0.00
Stability ~ BDRLOG + PHIKCL + BIO12 + Srad	6	-406.16	825.21	10.19	0.00
Stability ~ BDRLOG + PHIKCL + PHIKCL + BIO12	6	-406.25	825.38	10.35	0.00
Stability ~ OCDENS + PHIKCL + BIO12 + BIO15 + BIO5	7	-405.10	825.38	10.36	0.00
Stability ~ BDRLOG + PHIKCL + BIO12 + BIO5	6	-406.32	825.52	10.50	0.00
Stability ~ BDRLOG + BLDFIE + OCDENS + PHIKCL + BIO12 + BIO15 + BIO5 + Srad	10	-401.61	825.64	10.62	0.00
Stability ~ BDRLOG + BLDFIE + OCDENS + PHIKCL + BIO12 + Srad	8	-404.14	825.83	10.81	0.00
Stability ~ OCDENS + PHIKCL + BIO12 + BIO15 + BIO5	7	-405.33	825.85	10.83	0.00
Stability ~ BDRLOG + BLDFIE + OCDENS + PHIKCL + PHIKCL + BIO12 + BIO15 + BIO5 + Srad	11	-400.50	825.94	10.91	0.00
Stability ~ OCDENS + PHIKCL + BIO12 + BIO15 + Srad	7	-405.37	825.94	10.92	0.00
Stability ~ BDRLOG + OCDENS + PHIKCL + BIO12 + BIO5 + Srad	8	-404.20	825.96	10.93	0.00
Stability ~ OCDENS + BIO12 + BIO15 + BIO5 + Srad	7	-405.38	825.96	10.93	0.00
Stability ~ BLDFIE + OCDENS + PHIKCL + BIO12 + BIO15	7	-405.39	825.96	10.94	0.00
Stability ~ BLDFIE + OCDENS + BIO12 + BIO15 + BIO5	7	-405.39	825.97	10.94	0.00
Stability ~ BDRLOG + BLDFIE + OCDENS + PHIKCL + BIO12 + BIO5	8	-404.23	826.01	10.99	0.00
Stability ~ BDRLOG + OCDENS + PHIKCL + PHIKCL + BIO12 + Srad	8	-404.36	826.27	11.25	0.00
Stability ~ BDRLOG + BLDFIE + PHIKCL + BIO12 + BIO5 + Srad	8	-404.47	826.48	11.46	0.00
Stability ~ BDRLOG + BLDFIE + PHIKCL + PHIKCL + BIO12 + Srad	8	-404.50	826.55	11.53	0.00
Stability ~ BDRLOG + BLDFIE + OCDENS + PHIKCL + PHIKCL + BIO12	8	-404.51	826.57	11.55	0.00
Stability ~ BLDFIE + OCDENS + PHIKCL + BIO12 + BIO15	7	-405.73	826.65	11.62	0.00
Stability ~ BDRLOG + OCDENS + PHIKCL + PHIKCL + BIO12 + BIO5	8	-404.58	826.71	11.69	0.00
Stability ~ BDRLOG + BLDFIE + PHIKCL + PHIKCL + BIO12 + BIO5	8	-404.59	826.73	11.71	0.00
Stability ~ BLDFIE + OCDENS + BIO12 + BIO15 + Srad	7	-405.81	826.82	11.79	0.00
Stability ~ OCDENS + PHIKCL + BIO12 + BIO15 + Srad	7	-405.83	826.85	11.83	0.00
Stability ~ OCDENS + PHIKCL + PHIKCL + BIO12 + BIO15 + BIO5	8	-404.81	827.17	12.15	0.00
Stability ~ BIO12 + BIO15 + BIO5	5	-408.36	827.35	12.33	0.00
Stability ~ BDRLOG + PHIKCL + PHIKCL + BIO12 + Srad	7	-406.11	827.42	12.40	0.00
Stability ~ OCDENS + PHIKCL + PHIKCL + BIO12 + BIO15 + Srad	8	-404.94	827.43	12.41	0.00
Stability ~ BLDFIE + OCDENS + PHIKCL + PHIKCL + BIO12 + BIO15	8	-404.98	827.51	12.48	0.00
Stability ~ BDRLOG + PHIKCL + BIO12 + BIO5 + Srad	7	-406.16	827.52	12.49	0.00

Stability ~ BDRLOG + BLDFIE + OCDENS + PHIKCL + BIO12 + BIO5 + Srad	9	-403.78	827.52	12.50	0.00
Stability ~ OCDENS + PHIKCL + BIO12 + BIO15 + BIO5 + Srad	8	-405.06	827.67	12.65	0.00
Stability ~ BLDFIE + BIO12 + BIO15 + BIO5	6	-407.40	827.68	12.65	0.00
Stability ~ BDRLOG + PHIKCL + PHIKCL + BIO12 + BIO5	7	-406.25	827.68	12.66	0.00
Stability ~ BLDFIE + OCDENS + PHIKCL + BIO12 + BIO15 + BIO5	8	-405.10	827.74	12.72	0.00
Stability ~ BDRLOG + BLDFIE + OCDENS + PHIKCL + PHIKCL + BIO12 + Srad	9	-404.03	828.01	12.99	0.00
Stability ~ OCDENS + PHIKCL + BIO12 + BIO15 + BIO5 + Srad	8	-405.31	828.18	13.15	0.00
Stability ~ BLDFIE + OCDENS + PHIKCL + BIO12 + BIO15 + BIO5	8	-405.32	828.18	13.16	0.00
Stability ~ BDRLOG + BLDFIE + OCDENS + PHIKCL + PHIKCL + BIO12 + BIO5	9	-404.14	828.24	13.21	0.00
Stability ~ BLDFIE + OCDENS + PHIKCL + BIO12 + BIO15 + Srad	8	-405.34	828.24	13.21	0.00
Stability ~ BLDFIE + OCDENS + BIO12 + BIO15 + BIO5 + Srad	8	-405.37	828.28	13.26	0.00
Stability ~ BLDFIE + BIO12 + BIO15	5	-408.83	828.28	13.26	0.00
Stability ~ BDRLOG + OCDENS + PHIKCL + PHIKCL + BIO12 + BIO5 + Srad	9	-404.20	828.36	13.33	0.00
Stability ~ OCDENS + PHIKCL + BIO12	5	-408.89	828.41	13.39	0.00
Stability ~ BDRLOG + BLDFIE + PHIKCL + PHIKCL + BIO12 + BIO5 + Srad	9	-404.30	828.56	13.54	0.00
Stability ~ PHIKCL + BIO12 + BIO15 + BIO5	6	-407.96	828.81	13.79	0.00
Stability ~ BLDFIE + OCDENS + PHIKCL + BIO12 + BIO15 + Srad	8	-405.70	828.96	13.93	0.00
Stability ~ PHIKCL + BIO12 + BIO15 + BIO5	6	-408.18	829.25	14.22	0.00
Stability ~ BIO12 + BIO15 + BIO5 + Srad	6	-408.24	829.36	14.34	0.00
Stability ~ BDRLOG + OCDENS + BIO12 + Srad	6	-408.26	829.41	14.39	0.00
Stability ~ OCDENS + PHIKCL + PHIKCL + BIO12 + BIO15 + BIO5 + Srad	9	-404.77	829.50	14.48	0.00
Stability ~ BLDFIE + OCDENS + PHIKCL + PHIKCL + BIO12 + BIO15 + BIO5	9	-404.81	829.57	14.55	0.00
Stability ~ BLDFIE + PHIKCL + BIO12 + BIO15 + BIO5	7	-407.19	829.58	14.56	0.00
Stability ~ OCDENS + PHIKCL + BIO12 + Srad	6	-408.35	829.58	14.56	0.00
Stability ~ BLDFIE + PHIKCL + BIO12 + BIO15	6	-408.35	829.59	14.57	0.00
Stability ~ BDRLOG + OCDENS + BIO12	5	-409.50	829.63	14.60	0.00
Stability ~ BLDFIE + PHIKCL + BIO12 + BIO15 + BIO5	7	-407.25	829.69	14.67	0.00
Stability ~ BDRLOG + PHIKCL + PHIKCL + BIO12 + BIO5 + Srad	8	-406.11	829.77	14.75	0.00
Stability ~ BLDFIE + OCDENS + PHIKCL + PHIKCL + BIO12 + BIO15 + Srad	9	-404.94	829.83	14.80	0.00
Stability ~ BDRLOG + BLDFIE + OCDENS + PHIKCL + PHIKCL + BIO12 + BIO5 + Srad	10	-403.74	829.89	14.87	0.00
Stability ~ OCDENS + BIO12	4	-410.75	829.91	14.89	0.00
Stability ~ OCDENS + PHIKCL + PHIKCL + BIO12	6	-408.53	829.94	14.92	0.00
Stability ~ BLDFIE + PHIKCL + BIO12 + BIO15	6	-408.54	829.96	14.93	0.00
Stability ~ BLDFIE + BIO12 + BIO15 + BIO5 + Srad	7	-407.39	829.96	14.94	0.00
Stability ~ PHIKCL + PHIKCL + BIO12 + BIO15 + BIO5	7	-407.42	830.02	15.00	0.00
Stability ~ BLDFIE + OCDENS + PHIKCL + BIO12 + BIO15 + BIO5 + Srad	9	-405.06	830.08	15.06	0.00

Stability ~ OCDENS + BIO12 + Srad	5	-409.73	830.09	15.06	0.00
Stability ~ BLDFIE + OCDENS + PHIKCL + BIO12	6	-408.70	830.28	15.25	0.00
Stability ~ BDRLOG + PHIKCL + BIO15	5	-409.84	830.30	15.27	0.00
Stability ~ BDRLOG + OCDENS + PHIKCL + BIO12	6	-408.73	830.35	15.32	0.00
Stability ~ BLDFIE + PHIKCL + PHIKCL + BIO12 + BIO15	7	-407.61	830.40	15.38	0.00
Stability ~ BLDFIE + BIO12 + BIO15 + Srad	6	-408.81	830.50	15.48	0.00
Stability ~ BLDFIE + OCDENS + PHIKCL + BIO12 + BIO15 + BIO5 + Srad	9	-405.30	830.55	15.53	0.00
Stability ~ OCDENS + PHIKCL + BIO12 + BIO5	6	-408.89	830.66	15.64	0.00
Stability ~ BDRLOG + BLDFIE + PHIKCL + BIO15	6	-408.91	830.70	15.68	0.00
Stability ~ BDRLOG + BLDFIE + OCDENS + BIO12 + Srad	7	-407.81	830.81	15.79	0.00
Stability ~ OCDENS + PHIKCL + PHIKCL + BIO12 + Srad	7	-407.82	830.82	15.80	0.00
Stability ~ BDRLOG + OCDENS + PHIKCL + BIO12 + Srad	7	-407.85	830.90	15.87	0.00
Stability ~ PHIKCL + BIO12 + BIO15 + BIO5 + Srad	7	-407.88	830.96	15.93	0.00
Stability ~ BDRLOG + OCDENS + PHIKCL + BIO15	6	-409.11	831.11	16.08	0.00
Stability ~ BLDFIE + PHIKCL + PHIKCL + BIO12 + BIO15 + BIO5	8	-406.80	831.16	16.13	0.00
Stability ~ BDRLOG + PHIKCL + BIO15 + Srad	6	-409.15	831.18	16.15	0.00
Stability ~ BDRLOG + BLDFIE + OCDENS + PHIKCL + BIO12	7	-408.00	831.20	16.18	0.00
Stability ~ BDRLOG + BLDFIE + OCDENS + BIO12	6	-409.18	831.24	16.22	0.00
Stability ~ BDRLOG + OCDENS + BIO15	5	-410.31	831.25	16.23	0.00
Stability ~ PHIKCL + BIO12 + BIO15 + BIO5 + Srad	7	-408.06	831.32	16.29	0.00
Stability ~ BLDFIE + OCDENS + PHIKCL + BIO12 + Srad	7	-408.07	831.33	16.31	0.00
Stability ~ BDRLOG + BLDFIE + BIO15	5	-410.39	831.41	16.39	0.00
Stability ~ BLDFIE + OCDENS + BIO12 + Srad	6	-409.33	831.54	16.51	0.00
Stability ~ BLDFIE + OCDENS + BIO12	5	-410.46	831.54	16.51	0.00
Stability ~ BDRLOG + BLDFIE + PHIKCL + BIO12	6	-409.37	831.62	16.60	0.00
Stability ~ BDRLOG + OCDENS + BIO12 + BIO5	6	-409.37	831.63	16.60	0.00
Stability ~ BDRLOG + OCDENS + BIO12 + BIO5 + Srad	7	-408.22	831.64	16.61	0.00
Stability ~ BDRLOG + BLDFIE + PHIKCL + BIO15	6	-409.40	831.68	16.65	0.00
Stability ~ BDRLOG + BLDFIE + OCDENS + PHIKCL + BIO12 + Srad	8	-407.08	831.70	16.68	0.00
Stability ~ OCDENS + PHIKCL + BIO12 + BIO5 + Srad	7	-408.31	831.82	16.79	0.00
Stability ~ BLDFIE + PHIKCL + BIO12 + BIO15 + Srad	7	-408.34	831.88	16.85	0.00
Stability ~ BLDFIE + PHIKCL + BIO12 + BIO15 + BIO5 + Srad	8	-407.19	831.92	16.90	0.00
Stability ~ BLDFIE + OCDENS + PHIKCL + PHIKCL + BIO12 + BIO15 + BIO5 + Srad	10	-404.77	831.96	16.93	0.00
Stability ~ BLDFIE + PHIKCL + BIO12 + BIO15 + BIO5 + Srad	8	-407.24	832.03	17.01	0.00
Stability ~ BDRLOG + BLDFIE + PHIKCL + PHIKCL + BIO15	7	-408.44	832.06	17.04	0.00
Stability ~ BLDFIE + OCDENS + PHIKCL + PHIKCL + BIO12	7	-408.45	832.09	17.07	0.00
Stability ~ OCDENS + PHIKCL + BIO12	5	-410.74	832.11	17.08	0.00
Stability ~ OCDENS + BIO12 + BIO5	5	-410.75	832.13	17.10	0.00
Stability ~ PHIKCL + PHIKCL + BIO12 + BIO15	6	-409.63	832.13	17.11	0.00
Stability ~ OCDENS + PHIKCL + PHIKCL + BIO12 + BIO5	7	-408.50	832.20	17.17	0.00

Stability ~ BLDFIE + PHIKCL + BIO12 + BIO15 + Srad	7	-408.52	832.22	17.20	0.00
Stability ~ BDRLOG + PHIKCL + PHIKCL + BIO15	6	-409.67	832.23	17.20	0.00
Stability ~ PHIKCL + PHIKCL + BIO12 + BIO15 + BIO5 + Srad	8	-407.36	832.27	17.24	0.00
Stability ~ OCDENS + BIO12 + BIO5 + Srad	6	-409.71	832.30	17.28	0.00
Stability ~ OCDENS + PHIKCL + BIO12 + Srad	6	-409.71	832.30	17.28	0.00
Stability ~ BDRLOG + BLDFIE + PHIKCL + BIO15 + Srad	7	-408.60	832.40	17.37	0.00
Stability ~ BDRLOG + PHIKCL + BIO15 + BIO5	6	-409.76	832.40	17.38	0.00
Stability ~ BDRLOG + BLDFIE + PHIKCL + BIO12 + Srad	7	-408.69	832.57	17.55	0.00
Stability ~ BLDFIE + OCDENS + PHIKCL + BIO12 + BIO5	7	-408.69	832.58	17.55	0.00
Stability ~ BDRLOG + OCDENS + PHIKCL + BIO12 + BIO5	7	-408.71	832.62	17.59	0.00
Stability ~ BDRLOG + OCDENS + PHIKCL + BIO15	6	-409.89	832.67	17.64	0.00
Stability ~ BDRLOG + OCDENS + PHIKCL + BIO15 + Srad	7	-408.77	832.74	17.72	0.00
Stability ~ BLDFIE + PHIKCL + PHIKCL + BIO12 + BIO15 + Srad	8	-407.60	832.75	17.73	0.00
Stability ~ BDRLOG + BIO15	4	-412.17	832.76	17.73	0.00
Stability ~ BDRLOG + BLDFIE + OCDENS + BIO15	6	-409.94	832.77	17.75	0.00
Stability ~ BDRLOG + BLDFIE + OCDENS + PHIKCL + BIO15	7	-408.79	832.77	17.75	0.00
Stability ~ BDRLOG + BLDFIE + OCDENS + BIO12 + BIO5 + Srad	8	-407.63	832.82	17.79	0.00
Stability ~ BDRLOG + BLDFIE + PHIKCL + BIO15 + BIO5	7	-408.86	832.92	17.89	0.00
Stability ~ BDRLOG + BLDFIE + OCDENS + BIO12 + BIO5	7	-408.87	832.92	17.90	0.00
Stability ~ BDRLOG + OCDENS + BIO15 + Srad	6	-410.03	832.94	17.92	0.00
Stability ~ BLDFIE + OCDENS + PHIKCL + PHIKCL + BIO12 + Srad	8	-407.70	832.95	17.93	0.00
Stability ~ BDRLOG + PHIKCL + PHIKCL + BIO15 + Srad	7	-408.88	832.96	17.93	0.00
Stability ~ BDRLOG + OCDENS + PHIKCL + PHIKCL + BIO15	7	-408.92	833.04	18.02	0.00
Stability ~ BDRLOG + BLDFIE + BIO15 + Srad	6	-410.08	833.05	18.02	0.00
Stability ~ BDRLOG + BIO15 + Srad	5	-411.24	833.11	18.09	0.00
Stability ~ OCDENS + PHIKCL + PHIKCL + BIO12 + BIO5 + Srad	8	-407.81	833.17	18.14	0.00
Stability ~ BDRLOG + OCDENS + PHIKCL + BIO12 + BIO5 + Srad	8	-407.85	833.25	18.22	0.00
Stability ~ BDRLOG + BLDFIE + PHIKCL + BIO15 + Srad	7	-409.04	833.27	18.24	0.00
Stability ~ BDRLOG + BLDFIE + OCDENS + PHIKCL + BIO12 + BIO5	8	-407.88	833.30	18.28	0.00
Stability ~ BDRLOG + OCDENS + PHIKCL + BIO15 + BIO5	7	-409.11	833.40	18.38	0.00
Stability ~ BDRLOG + PHIKCL + BIO15 + BIO5 + Srad	7	-409.13	833.44	18.42	0.00
Stability ~ BDRLOG + OCDENS + BIO15 + BIO5	6	-410.29	833.46	18.44	0.00
Stability ~ BLDFIE + PHIKCL + PHIKCL + BIO12 + BIO15 + BIO5 + Srad	9	-406.80	833.56	18.53	0.00
Stability ~ BDRLOG + BLDFIE + OCDENS + PHIKCL + BIO15	7	-409.19	833.58	18.55	0.00
Stability ~ PHIKCL + BIO12 + BIO15	5	-411.49	833.60	18.57	0.00
Stability ~ BDRLOG + BLDFIE + BIO15 + BIO5	6	-410.38	833.65	18.62	0.00
Stability ~ BLDFIE + OCDENS + PHIKCL + BIO12 + BIO5 + Srad	8	-408.07	833.69	18.66	0.00
Stability ~ BLDFIE + OCDENS + PHIKCL + BIO12	6	-410.40	833.69	18.67	0.00
Stability ~ BDRLOG + BIO15 + BIO5	5	-411.54	833.71	18.69	0.00
Stability ~ BLDFIE + OCDENS + BIO12 + BIO5	6	-410.42	833.73	18.71	0.00

Stability ~ BDRLOG + BLDFIE + PHIKCL + PHIKCL + BIO15 + Srad	8	-408.09	833.74	18.71	0.00
Stability ~ BLDFIE + OCDENS + BIO12 + BIO5 + Srad	7	-409.32	833.84	18.82	0.00
Stability ~ BLDFIE + OCDENS + PHIKCL + BIO12 + Srad	7	-409.33	833.84	18.82	0.00
Stability ~ BDRLOG + BLDFIE + BIO12 + Srad	6	-410.49	833.86	18.83	0.00
Stability ~ BDRLOG + BLDFIE + PHIKCL + BIO12 + BIO5	7	-409.35	833.90	18.87	0.00
Stability ~ BDRLOG + BLDFIE + PHIKCL + BIO15 + BIO5	7	-409.36	833.91	18.89	0.00
Stability ~ BDRLOG + PHIKCL + BIO15	5	-411.66	833.94	18.92	0.00
Stability ~ BDRLOG + BLDFIE + OCDENS + PHIKCL + BIO12 + BIO5 + Srad	9	-407.00	833.96	18.93	0.00
Stability ~ BDRLOG + BLDFIE + BIO12	5	-411.67	833.97	18.94	0.00
Stability ~ PHIKCL + PHIKCL + BIO12 + BIO15 + Srad	7	-409.41	834.01	18.98	0.00
Stability ~ BDRLOG + PHIKCL + BIO15 + Srad	6	-410.57	834.02	19.00	0.00
Stability ~ BDRLOG + OCDENS + PHIKCL + BIO15 + Srad	7	-409.51	834.21	19.18	0.00
Stability ~ BDRLOG + PHIKCL + PHIKCL + BIO15 + BIO5	7	-409.51	834.21	19.19	0.00
Stability ~ BDRLOG + BLDFIE + OCDENS + PHIKCL + PHIKCL + BIO15	8	-408.38	834.31	19.29	0.00
Stability ~ BLDFIE + OCDENS + PHIKCL + PHIKCL + BIO12 + BIO5	8	-408.40	834.34	19.32	0.00
Stability ~ OCDENS + PHIKCL + BIO12 + BIO5	6	-410.74	834.36	19.34	0.00
Stability ~ BDRLOG + BLDFIE + PHIKCL + PHIKCL + BIO15 + BIO5	8	-408.43	834.40	19.38	0.00
Stability ~ BDRLOG + PHIKCL + BIO15 + BIO5	6	-410.79	834.46	19.44	0.00
Stability ~ BDRLOG + OCDENS + PHIKCL + PHIKCL + BIO15 + Srad	8	-408.52	834.58	19.56	0.00
Stability ~ OCDENS + PHIKCL + BIO12 + BIO5 + Srad	7	-409.70	834.59	19.57	0.00
Stability ~ BDRLOG + BIO15 + BIO5 + Srad	6	-410.85	834.59	19.57	0.00
Stability ~ BDRLOG + BLDFIE + OCDENS + PHIKCL + BIO15 + Srad	8	-408.54	834.63	19.61	0.00
Stability ~ BDRLOG + BLDFIE + PHIKCL + BIO15 + BIO5 + Srad	8	-408.55	834.65	19.63	0.00
Stability ~ BDRLOG + BLDFIE + OCDENS + BIO15 + Srad	7	-409.75	834.69	19.66	0.00
Stability ~ BLDFIE + PHIKCL + BIO12	5	-412.07	834.77	19.75	0.00
Stability ~ BDRLOG + OCDENS + PHIKCL + BIO15 + BIO5	7	-409.79	834.78	19.76	0.00
Stability ~ BDRLOG + BLDFIE + PHIKCL + BIO12 + BIO5 + Srad	8	-408.69	834.93	19.90	0.00
Stability ~ BDRLOG + BLDFIE + OCDENS + PHIKCL + BIO15 + BIO5	8	-408.72	834.98	19.96	0.00
Stability ~ PHIKCL + BIO12 + BIO15 + Srad	6	-411.09	835.06	20.04	0.00
Stability ~ BDRLOG + BLDFIE + OCDENS + BIO15 + BIO5	7	-409.94	835.08	20.05	0.00
Stability ~ BDRLOG + OCDENS + PHIKCL + BIO15 + BIO5 + Srad	8	-408.77	835.08	20.06	0.00
Stability ~ BDRLOG + PHIKCL + PHIKCL + BIO15 + BIO5 + Srad	8	-408.80	835.16	20.13	0.00
Stability ~ BDRLOG + PHIKCL + BIO15 + BIO5 + Srad	7	-409.99	835.16	20.14	0.00
Stability ~ BDRLOG + OCDENS + BIO15 + BIO5 + Srad	7	-410.01	835.21	20.19	0.00
Stability ~ BLDFIE + OCDENS + PHIKCL + PHIKCL + BIO12 + BIO5 + Srad	9	-407.68	835.31	20.29	0.00
Stability ~ BDRLOG + BLDFIE + BIO15 + BIO5 + Srad	7	-410.07	835.34	20.31	0.00
Stability ~ BDRLOG + BLDFIE + OCDENS + PHIKCL + BIO15 + Srad	8	-408.92	835.39	20.37	0.00
Stability ~ BDRLOG + OCDENS + PHIKCL + PHIKCL + BIO15 + BIO5	8	-408.92	835.39	20.37	0.00
Stability ~ BDRLOG + BLDFIE + PHIKCL + BIO15 + BIO5 + Srad	8	-409.00	835.56	20.53	0.00

Stability ~ BIO12 + BIO15	4	-413.66	835.74	20.72	0.00
Stability ~ BDRLOG + BLDFIE + OCDENS + PHIKCL + BIO15 + BIO5	8	-409.19	835.92	20.90	0.00
Stability ~ BLDFIE + OCDENS + PHIKCL + BIO12 + BIO5	7	-410.39	835.98	20.95	0.00
Stability ~ BDRLOG + BLDFIE + BIO12 + BIO5	6	-411.55	835.99	20.97	0.00
Stability ~ BDRLOG + BLDFIE + BIO12 + BIO5 + Srad	7	-410.44	836.08	21.06	0.00
Stability ~ BDRLOG + BLDFIE + OCDENS + PHIKCL + PHIKCL + BIO15 + Srad	9	-408.08	836.12	21.09	0.00
Stability ~ BDRLOG + BLDFIE + PHIKCL + PHIKCL + BIO15 + BIO5 + Srad	9	-408.08	836.12	21.10	0.00
Stability ~ BLDFIE + OCDENS + PHIKCL + BIO12 + BIO5 + Srad	8	-409.32	836.20	21.17	0.00
Stability ~ PHIKCL + BIO12 + BIO15	5	-412.86	836.34	21.32	0.00
Stability ~ BIO12 + BIO15 + Srad	5	-412.86	836.34	21.32	0.00
Stability ~ BDRLOG + OCDENS + PHIKCL + BIO15 + BIO5 + Srad	8	-409.41	836.37	21.34	0.00
Stability ~ BLDFIE + PHIKCL + PHIKCL + BIO12	6	-411.75	836.38	21.36	0.00
Stability ~ BLDFIE + PHIKCL + BIO12 + Srad	6	-411.78	836.44	21.42	0.00
Stability ~ BLDFIE + PHIKCL + BIO12 + BIO5	6	-411.89	836.66	21.63	0.00
Stability ~ BDRLOG + BLDFIE + OCDENS + PHIKCL + PHIKCL + BIO15 + BIO5	9	-408.36	836.68	21.65	0.00
Stability ~ BDRLOG + BLDFIE + OCDENS + PHIKCL + BIO15 + BIO5 + Srad	9	-408.47	836.90	21.88	0.00
Stability ~ BDRLOG + OCDENS + PHIKCL + PHIKCL + BIO15 + BIO5 + Srad	9	-408.52	836.99	21.96	0.00
Stability ~ BDRLOG + BLDFIE + OCDENS + BIO15 + BIO5 + Srad	8	-409.75	837.04	22.02	0.00
Stability ~ PHIKCL + BIO12 + BIO15 + Srad	6	-412.15	837.18	22.16	0.00
Stability ~ OCDENS + BIO15	4	-414.68	837.76	22.74	0.00
Stability ~ BDRLOG + BLDFIE + OCDENS + PHIKCL + BIO15 + BIO5 + Srad	9	-408.91	837.78	22.76	0.00
Stability ~ BLDFIE + PHIKCL + PHIKCL + BIO12 + Srad	7	-411.35	837.90	22.87	0.00
Stability ~ BLDFIE + PHIKCL + BIO12 + BIO5 + Srad	7	-411.50	838.20	23.17	0.00
Stability ~ BLDFIE + BIO12	4	-414.98	838.38	23.36	0.00
Stability ~ BDRLOG + BLDFIE + OCDENS + PHIKCL + PHIKCL + BIO15 + BIO5 + Srad	10	-408.06	838.54	23.52	0.00
Stability ~ BLDFIE + PHIKCL + PHIKCL + BIO12 + BIO5	7	-411.68	838.55	23.53	0.00
Stability ~ BLDFIE + BIO12 + Srad	5	-414.22	839.07	24.05	0.00
Stability ~ BLDFIE + OCDENS + BIO15	5	-414.27	839.17	24.15	0.00
Stability ~ OCDENS + BIO15 + BIO5	5	-414.35	839.32	24.29	0.00
Stability ~ OCDENS + PHIKCL + BIO15	5	-414.46	839.54	24.52	0.00
Stability ~ OCDENS + BIO15 + Srad	5	-414.51	839.64	24.61	0.00
Stability ~ OCDENS + PHIKCL + BIO15	5	-414.62	839.86	24.84	0.00
Stability ~ BLDFIE + PHIKCL + PHIKCL + BIO12 + BIO5 + Srad	8	-411.24	840.03	25.00	0.00
Stability ~ BLDFIE + BIO12 + BIO5	5	-414.85	840.33	25.31	0.00
Stability ~ BLDFIE + PHIKCL + BIO12	5	-414.86	840.35	25.32	0.00
Stability ~ PHIKCL + BIO12 + BIO5	5	-415.08	840.78	25.76	0.00

Stability ~ BLDFIE + BIO12 + BIO5 + Srad	6	-413.96	840.81	25.79	0.00
Stability ~ BLDFIE + OCDENS + BIO15 + BIO5	6	-414.12	841.13	26.10	0.00
Stability ~ BDRLOG + PHIKCL + BIO12 + BIO5	6	-414.12	841.13	26.11	0.00
Stability ~ BDRLOG + PHIKCL + BIO12	5	-415.26	841.15	26.13	0.00
Stability ~ BLDFIE + OCDENS + BIO15 + Srad	6	-414.17	841.23	26.21	0.00
Stability ~ BLDFIE + OCDENS + PHIKCL + BIO15	6	-414.18	841.24	26.22	0.00
Stability ~ OCDENS + BIO15 + BIO5 + Srad	6	-414.18	841.25	26.23	0.00
Stability ~ BLDFIE + PHIKCL + BIO12 + Srad	6	-414.19	841.27	26.25	0.00
Stability ~ BLDFIE + OCDENS + PHIKCL + BIO15	6	-414.23	841.34	26.31	0.00
Stability ~ OCDENS + PHIKCL + BIO15 + BIO5	6	-414.25	841.38	26.36	0.00
Stability ~ OCDENS + PHIKCL + PHIKCL + BIO15	6	-414.28	841.44	26.41	0.00
Stability ~ OCDENS + PHIKCL + BIO15 + BIO5	6	-414.32	841.52	26.49	0.00
Stability ~ OCDENS + PHIKCL + BIO15 + Srad	6	-414.32	841.52	26.50	0.00
Stability ~ PHIKCL + PHIKCL + BIO12 + BIO5	6	-414.40	841.69	26.67	0.00
Stability ~ OCDENS + PHIKCL + BIO15 + Srad	6	-414.45	841.78	26.75	0.00
Stability ~ PHIKCL + PHIKCL + BIO12	5	-415.64	841.90	26.88	0.00
Stability ~ BLDFIE + PHIKCL + BIO12 + BIO5	6	-414.62	842.11	27.09	0.00
Stability ~ BDRLOG + BIO12	4	-416.94	842.29	27.27	0.00
Stability ~ BDRLOG + PHIKCL + BIO12 + BIO5 + Srad	7	-413.75	842.68	27.66	0.00
Stability ~ PHIKCL + BIO12 + BIO5 + Srad	6	-414.96	842.80	27.77	0.00
Stability ~ BLDFIE + BIO15	4	-417.20	842.81	27.79	0.00
Stability ~ BLDFIE + PHIKCL + BIO12 + BIO5 + Srad	7	-413.86	842.91	27.89	0.00
Stability ~ BDRLOG + PHIKCL + BIO12 + Srad	6	-415.08	843.04	28.02	0.00
Stability ~ BDRLOG + BIO12 + BIO5	5	-416.25	843.12	28.09	0.00
Stability ~ BLDFIE + OCDENS + BIO15 + BIO5 + Srad	7	-414.01	843.22	28.19	0.00
Stability ~ BLDFIE + OCDENS + PHIKCL + PHIKCL + BIO15	7	-414.05	843.29	28.27	0.00
Stability ~ BLDFIE + BIO15 + BIO5	5	-416.35	843.32	28.29	0.00
Stability ~ BLDFIE + OCDENS + PHIKCL + BIO15 + BIO5	7	-414.07	843.33	28.31	0.00
Stability ~ BLDFIE + OCDENS + PHIKCL + BIO15 + Srad	7	-414.09	843.36	28.34	0.00
Stability ~ BLDFIE + OCDENS + PHIKCL + BIO15 + BIO5	7	-414.09	843.37	28.35	0.00
Stability ~ OCDENS + PHIKCL + BIO15 + BIO5 + Srad	7	-414.11	843.41	28.38	0.00
Stability ~ BLDFIE + OCDENS + PHIKCL + BIO15 + Srad	7	-414.12	843.44	28.41	0.00
Stability ~ OCDENS + PHIKCL + PHIKCL + BIO15 + Srad	7	-414.14	843.47	28.45	0.00
Stability ~ OCDENS + PHIKCL + PHIKCL + BIO15 + BIO5	7	-414.14	843.48	28.45	0.00
Stability ~ OCDENS + PHIKCL + BIO15 + BIO5 + Srad	7	-414.15	843.50	28.47	0.00
Stability ~ BDRLOG + BIO12 + Srad	5	-416.48	843.59	28.56	0.00
Stability ~ PHIKCL + PHIKCL + BIO12 + BIO5 + Srad	7	-414.20	843.59	28.56	0.00
Stability ~ BDRLOG + BIO12 + BIO5 + Srad	6	-415.52	843.92	28.89	0.00
Stability ~ PHIKCL + PHIKCL + BIO12 + Srad	6	-415.58	844.05	29.02	0.00
Stability ~ BLDFIE + BIO15 + Srad	5	-416.83	844.29	29.27	0.00

Stability ~ PHIKCL + BIO12	4	-418.06	844.53	29.50	0.00
Stability ~ BLDFIE + PHIKCL + BIO15	5	-417.02	844.66	29.64	0.00
Stability ~ BLDFIE + PHIKCL + BIO15	5	-417.09	844.81	29.78	0.00
Stability ~ BLDFIE + BIO15 + BIO5 + Srad	6	-416.00	844.89	29.87	0.00
Stability ~ BLDFIE + PHIKCL + BIO15 + BIO5	6	-416.26	845.40	30.37	0.00
Stability ~ BLDFIE + OCDENS + PHIKCL + PHIKCL + BIO15 + Srad	8	-413.96	845.46	30.44	0.00
Stability ~ BLDFIE + OCDENS + PHIKCL + BIO15 + BIO5 + Srad	8	-413.97	845.49	30.46	0.00
Stability ~ BIO15 + BIO5	4	-418.54	845.49	30.46	0.00
Stability ~ BLDFIE + OCDENS + PHIKCL + BIO15 + BIO5 + Srad	8	-413.98	845.51	30.48	0.00
Stability ~ BLDFIE + OCDENS + PHIKCL + PHIKCL + BIO15 + BIO5	8	-413.98	845.51	30.49	0.00
Stability ~ BLDFIE + PHIKCL + BIO15 + BIO5	6	-416.33	845.54	30.52	0.00
Stability ~ OCDENS + PHIKCL + PHIKCL + BIO15 + BIO5 + Srad	8	-414.00	845.56	30.53	0.00
Stability ~ BIO15 + BIO5 + Srad	5	-417.58	845.79	30.77	0.00
Stability ~ BLDFIE + PHIKCL + BIO15 + Srad	6	-416.65	846.19	31.16	0.00
Stability ~ BLDFIE + PHIKCL + BIO15 + Srad	6	-416.74	846.37	31.35	0.00
Stability ~ BLDFIE + PHIKCL + PHIKCL + BIO15	6	-416.75	846.38	31.36	0.00
Stability ~ PHIKCL + BIO12 + Srad	5	-418.04	846.70	31.68	0.00
Stability ~ BLDFIE + PHIKCL + BIO15 + BIO5 + Srad	7	-415.91	847.02	31.99	0.00
Stability ~ BLDFIE + PHIKCL + BIO15 + BIO5 + Srad	7	-415.99	847.18	32.15	0.00
Stability ~ PHIKCL + BIO15 + BIO5	5	-418.38	847.39	32.37	0.00
Stability ~ PHIKCL + BIO15 + BIO5	5	-418.41	847.44	32.42	0.00
Stability ~ BLDFIE + PHIKCL + PHIKCL + BIO15 + BIO5	7	-416.18	847.55	32.53	0.00
Stability ~ BLDFIE + OCDENS + PHIKCL + PHIKCL + BIO15 + BIO5 + Srad	9	-413.88	847.72	32.70	0.00
Stability ~ PHIKCL + BIO15 + BIO5 + Srad	6	-417.46	847.80	32.78	0.00
Stability ~ PHIKCL + BIO15 + BIO5 + Srad	6	-417.49	847.86	32.84	0.00
Stability ~ BLDFIE + PHIKCL + PHIKCL + BIO15 + Srad	7	-416.41	848.01	32.99	0.00
Stability ~ BDRLOG + BLDFIE + PHIKCL + PHIKCL + BIO5	7	-416.89	848.97	33.94	0.00
Stability ~ PHIKCL + PHIKCL + BIO15 + BIO5	6	-418.07	849.02	33.99	0.00
Stability ~ BIO12 + BIO5	4	-420.32	849.06	34.03	0.00
Stability ~ BLDFIE + PHIKCL + PHIKCL + BIO15 + BIO5 + Srad	8	-415.85	849.25	34.22	0.00
Stability ~ BDRLOG + BLDFIE + PHIKCL + PHIKCL	6	-418.23	849.35	34.33	0.00
Stability ~ BDRLOG + BLDFIE + PHIKCL + BIO5	6	-418.31	849.51	34.49	0.00
Stability ~ PHIKCL + PHIKCL + BIO15 + BIO5 + Srad	7	-417.22	849.63	34.61	0.00
Stability ~ BDRLOG + BLDFIE + OCDENS + PHIKCL + BIO5	7	-417.29	849.77	34.74	0.00
Stability ~ BDRLOG + BLDFIE + OCDENS + PHIKCL + PHIKCL + BIO5	8	-416.31	850.17	35.15	0.00
Stability ~ BIO12 + BIO5 + Srad	5	-419.81	850.25	35.22	0.00
Stability ~ BDRLOG + OCDENS + PHIKCL + BIO5	6	-419.04	850.96	35.93	0.00
Stability ~ BDRLOG + BLDFIE + OCDENS + PHIKCL + PHIKCL	7	-417.89	850.98	35.95	0.00
Stability ~ PHIKCL + BIO12 + BIO5	5	-420.19	851.00	35.98	0.00
Stability ~ BDRLOG + BLDFIE + PHIKCL + PHIKCL + BIO5 + Srad	8	-416.81	851.17	36.15	0.00

Stability ~ BDRLOG + BLDFIE + PHIKCL + PHIKCL + Srad	7	-418.07	851.33	36.31	0.00
Stability ~ BDRLOG + BLDFIE + PHIKCL + BIO5 + Srad	7	-418.17	851.53	36.50	0.00
Stability ~ BDRLOG + BLDFIE + OCDENS + PHIKCL + BIO5 + Srad	8	-417.04	851.62	36.60	0.00
Stability ~ BDRLOG + BLDFIE + PHIKCL	5	-420.57	851.76	36.74	0.00
Stability ~ PHIKCL + PHIKCL + BIO15 + Srad	6	-419.45	851.79	36.77	0.00
Stability ~ BIO15 + Srad	4	-421.72	851.85	36.82	0.00
Stability ~ PHIKCL + BIO15 + Srad	5	-420.67	851.97	36.95	0.00
Stability ~ BDRLOG + OCDENS + PHIKCL	5	-420.67	851.97	36.95	0.00
Stability ~ BDRLOG + OCDENS + PHIKCL + PHIKCL	6	-419.55	851.98	36.96	0.00
Stability ~ BDRLOG + BLDFIE + OCDENS + PHIKCL + PHIKCL + BIO5 + Srad	9	-416.16	852.29	37.26	0.00
Stability ~ PHIKCL + PHIKCL + BIO15	5	-420.85	852.32	37.29	0.00
Stability ~ BDRLOG + OCDENS + PHIKCL + PHIKCL + BIO5	7	-418.57	852.34	37.31	0.00
Stability ~ PHIKCL + BIO12 + BIO5 + Srad	6	-419.75	852.39	37.37	0.00
Stability ~ BDRLOG + BLDFIE + OCDENS + PHIKCL	6	-419.80	852.48	37.46	0.00
Stability ~ BDRLOG + BLDFIE + OCDENS + PHIKCL + PHIKCL + Srad	8	-417.64	852.84	37.81	0.00
Stability ~ PHIKCL + BIO15 + Srad	5	-421.14	852.91	37.89	0.00
Stability ~ BDRLOG + OCDENS + PHIKCL + BIO5 + Srad	7	-418.88	852.94	37.92	0.00
Stability ~ PHIKCL + BIO15	4	-422.39	853.20	38.17	0.00
Stability ~ BDRLOG + BLDFIE + PHIKCL + Srad	6	-420.22	853.33	38.30	0.00
Stability ~ BDRLOG + OCDENS + PHIKCL + Srad	6	-420.32	853.53	38.50	0.00
Stability ~ BDRLOG + BLDFIE + OCDENS + PHIKCL + Srad	7	-419.31	853.80	38.78	0.00
Stability ~ BDRLOG + OCDENS + PHIKCL + PHIKCL + Srad	7	-419.38	853.95	38.92	0.00
Stability ~ BIO15	3	-424.01	854.26	39.23	0.00
Stability ~ BDRLOG + OCDENS + PHIKCL + PHIKCL + BIO5 + Srad	8	-418.47	854.50	39.47	0.00
Stability ~ PHIKCL + BIO15	4	-423.29	855.00	39.97	0.00
Stability ~ BIO12	3	-424.58	855.41	40.38	0.00
Stability ~ BDRLOG + PHIKCL + PHIKCL	5	-422.99	856.61	41.58	0.00
Stability ~ OCDENS + PHIKCL	4	-424.17	856.75	41.73	0.00
Stability ~ BDRLOG + PHIKCL	4	-424.22	856.84	41.82	0.00
Stability ~ BDRLOG + BLDFIE + OCDENS + PHIKCL	6	-422.07	857.02	41.99	0.00
Stability ~ PHIKCL + BIO12	4	-424.36	857.12	42.10	0.00
Stability ~ BLDFIE + OCDENS + PHIKCL	5	-423.25	857.13	42.11	0.00
Stability ~ BDRLOG + BLDFIE + OCDENS + PHIKCL + BIO5	7	-421.07	857.33	42.30	0.00
Stability ~ BIO12 + Srad	4	-424.55	857.51	42.49	0.00
Stability ~ BLDFIE + OCDENS + PHIKCL + BIO5	6	-422.36	857.61	42.58	0.00
Stability ~ BDRLOG + BLDFIE + PHIKCL	5	-423.56	857.74	42.72	0.00
Stability ~ BDRLOG + BLDFIE + OCDENS + PHIKCL + Srad	7	-421.44	858.07	43.05	0.00
Stability ~ OCDENS + PHIKCL + BIO5	5	-423.72	858.07	43.05	0.00
Stability ~ OCDENS + PHIKCL + Srad	5	-423.78	858.18	43.15	0.00
Stability ~ BDRLOG + PHIKCL + BIO5	5	-423.81	858.24	43.21	0.00

Stability ~ BLDFIE + OCDENS + PHIKCL + Srad	6	-422.71	858.31	43.28	0.00
Stability ~ BDRLOG + BLDFIE + OCDENS + PHIKCL + BIO5 + Srad	8	-420.55	858.65	43.62	0.00
Stability ~ BDRLOG + PHIKCL + PHIKCL + BIO5	6	-422.89	858.66	43.64	0.00
Stability ~ BDRLOG + BLDFIE + PHIKCL + BIO5	6	-422.98	858.85	43.83	0.00
Stability ~ BDRLOG + PHIKCL + PHIKCL + Srad	6	-422.99	858.86	43.84	0.00
Stability ~ OCDENS + PHIKCL + PHIKCL	5	-424.15	858.92	43.90	0.00
Stability ~ BDRLOG + PHIKCL + Srad	5	-424.20	859.02	44.00	0.00
Stability ~ BLDFIE + OCDENS + PHIKCL + PHIKCL	6	-423.09	859.06	44.04	0.00
Stability ~ BLDFIE + OCDENS + PHIKCL + BIO5 + Srad	7	-421.97	859.12	44.10	0.00
Stability ~ PHIKCL + BIO12 + Srad	5	-424.26	859.15	44.12	0.00
Stability ~ BDRLOG + BLDFIE + PHIKCL + Srad	6	-423.14	859.16	44.13	0.00
Stability ~ OCDENS + PHIKCL + BIO5 + Srad	6	-423.43	859.75	44.73	0.00
Stability ~ BLDFIE + OCDENS + PHIKCL + PHIKCL + BIO5	7	-422.36	859.90	44.88	0.00
Stability ~ OCDENS + PHIKCL + PHIKCL + BIO5	6	-423.70	860.29	45.27	0.00
Stability ~ BDRLOG + OCDENS + PHIKCL	5	-424.88	860.38	45.35	0.00
Stability ~ BLDFIE + OCDENS + PHIKCL + PHIKCL + Srad	7	-422.61	860.42	45.39	0.00
Stability ~ OCDENS + PHIKCL + PHIKCL + Srad	6	-423.77	860.43	45.41	0.00
Stability ~ BDRLOG + BLDFIE + PHIKCL + BIO5 + Srad	7	-422.65	860.48	45.46	0.00
Stability ~ BDRLOG + PHIKCL + BIO5 + Srad	6	-423.81	860.50	45.47	0.00
Stability ~ BDRLOG + PHIKCL + PHIKCL + BIO5 + Srad	7	-422.88	860.94	45.92	0.00
Stability ~ BLDFIE + OCDENS + PHIKCL	5	-425.37	861.37	46.35	0.00
Stability ~ BLDFIE + OCDENS + PHIKCL + PHIKCL + BIO5 + Srad	8	-421.97	861.48	46.46	0.00
Stability ~ BDRLOG + OCDENS + PHIKCL + Srad	6	-424.35	861.58	46.55	0.00
Stability ~ BDRLOG + OCDENS + PHIKCL + BIO5	6	-424.49	861.87	46.84	0.00
Stability ~ OCDENS + PHIKCL + PHIKCL + BIO5 + Srad	7	-423.39	861.98	46.96	0.00
Stability ~ BDRLOG + BLDFIE + OCDENS + BIO5	6	-424.57	862.03	47.01	0.00
Stability ~ BLDFIE + OCDENS + PHIKCL + Srad	6	-424.60	862.08	47.06	0.00
Stability ~ BDRLOG + BLDFIE + OCDENS + BIO5 + Srad	7	-423.46	862.11	47.09	0.00
Stability ~ BLDFIE + OCDENS + BIO5	5	-425.84	862.31	47.29	0.00
Stability ~ BLDFIE + OCDENS + Srad	5	-425.94	862.50	47.48	0.00
Stability ~ BLDFIE + OCDENS + PHIKCL + BIO5	6	-424.84	862.56	47.54	0.00
Stability ~ BLDFIE + OCDENS + BIO5 + Srad	6	-424.84	862.56	47.54	0.00
Stability ~ BLDFIE + PHIKCL	4	-427.20	862.82	47.79	0.00
Stability ~ BLDFIE + OCDENS	4	-427.30	863.01	47.98	0.00
Stability ~ OCDENS + PHIKCL	4	-427.30	863.02	48.00	0.00
Stability ~ BDRLOG + OCDENS + PHIKCL + BIO5 + Srad	7	-424.03	863.25	48.23	0.00
Stability ~ OCDENS + Srad	4	-427.52	863.46	48.44	0.00
Stability ~ BLDFIE + OCDENS + PHIKCL + BIO5 + Srad	7	-424.14	863.48	48.45	0.00
Stability ~ BDRLOG + BLDFIE + OCDENS + Srad	6	-425.33	863.55	48.53	0.00
Stability ~ OCDENS	3	-428.65	863.55	48.53	0.00

Stability ~ OCDENS + PHIKCL + Srad	5	-426.64	863.91	48.88	0.00
Stability ~ OCDENS + BIO5	4	-427.87	864.14	49.12	0.00
Stability ~ BDRLOG + BLDFIE + OCDENS	5	-426.85	864.32	49.30	0.00
Stability ~ BDRLOG + OCDENS + BIO5	5	-426.97	864.57	49.54	0.00
Stability ~ BLDFIE + PHIKCL + Srad	5	-426.98	864.58	49.56	0.00
Stability ~ OCDENS + BIO5 + Srad	5	-427.00	864.62	49.60	0.00
Stability ~ BDRLOG + OCDENS + Srad	5	-427.00	864.63	49.61	0.00
Stability ~ BLDFIE + PHIKCL + BIO5	5	-427.02	864.67	49.65	0.00
Stability ~ BLDFIE + PHIKCL + PHIKCL	5	-427.08	864.79	49.77	0.00
Stability ~ OCDENS + PHIKCL + BIO5	5	-427.10	864.82	49.80	0.00
Stability ~ BDRLOG + OCDENS	4	-428.26	864.93	49.91	0.00
Stability ~ BDRLOG + OCDENS + BIO5 + Srad	6	-426.03	864.95	49.92	0.00
Stability ~ OCDENS + PHIKCL + BIO5 + Srad	6	-426.48	865.85	50.83	0.00
Stability ~ BLDFIE + PHIKCL + BIO5 + Srad	6	-426.85	866.59	51.56	0.00
Stability ~ BLDFIE + PHIKCL + PHIKCL + Srad	6	-426.90	866.68	51.66	0.00
Stability ~ BLDFIE + PHIKCL + PHIKCL + BIO5	6	-426.98	866.85	51.83	0.00
Stability ~ BLDFIE + PHIKCL + PHIKCL + BIO5 + Srad	7	-426.82	868.84	53.81	0.00
Stability ~ BDRLOG + BLDFIE + BIO5	5	-429.42	869.46	54.43	0.00
Stability ~ BDRLOG + BLDFIE + BIO5 + Srad	6	-428.45	869.78	54.76	0.00
Stability ~ BLDFIE + PHIKCL	4	-430.81	870.04	55.01	0.00
Stability ~ BDRLOG + BLDFIE + Srad	5	-429.77	870.17	55.15	0.00
Stability ~ BDRLOG + BLDFIE	4	-431.07	870.55	55.52	0.00
Stability ~ BLDFIE + PHIKCL + Srad	5	-430.41	871.44	56.41	0.00
Stability ~ BLDFIE + PHIKCL + BIO5	5	-430.81	872.24	57.21	0.00
Stability ~ BLDFIE	3	-433.32	872.88	57.85	0.00
Stability ~ BLDFIE + Srad	4	-432.39	873.20	58.17	0.00
Stability ~ BLDFIE + PHIKCL + BIO5 + Srad	6	-430.41	873.70	58.67	0.00
Stability ~ BLDFIE + BIO5	4	-432.93	874.27	59.25	0.00
Stability ~ BLDFIE + BIO5 + Srad	5	-432.17	874.96	59.93	0.00
Stability ~ PHIKCL + BIO5	4	-436.89	882.19	67.17	0.00
Stability ~ PHIKCL + PHIKCL + BIO5	5	-436.78	884.18	69.16	0.00
Stability ~ PHIKCL + BIO5 + Srad	5	-436.88	884.38	69.35	0.00
Stability ~ PHIKCL	3	-439.07	884.39	69.36	0.00
Stability ~ PHIKCL + PHIKCL	4	-438.04	884.49	69.47	0.00
Stability ~ BDRLOG + PHIKCL + BIO5	5	-437.16	884.95	69.92	0.00
Stability ~ BDRLOG + PHIKCL	4	-438.40	885.21	70.19	0.00
Stability ~ PHIKCL + Srad	4	-438.81	886.03	71.01	0.00
Stability ~ PHIKCL + PHIKCL + BIO5 + Srad	6	-436.77	886.43	71.40	0.00
Stability ~ PHIKCL + PHIKCL + Srad	5	-437.96	886.54	71.51	0.00
Stability ~ BDRLOG + PHIKCL + BIO5 + Srad	6	-437.14	887.17	72.15	0.00

Stability ~ BDRLOG + PHIKCL + Srad	5	-438.40	887.42	72.40	0.00
Stability ~ BDRLOG	3	-446.28	898.81	83.78	0.00
Stability ~ BDRLOG + BIO5	4	-445.89	900.20	85.17	0.00
Stability ~ BDRLOG + Srad	4	-446.07	900.56	85.54	0.00
Stability ~ BDRLOG + BIO5 + Srad	5	-445.55	901.73	86.71	0.00
Stability ~ PHIKCL + BIO5	4	-448.75	905.92	90.90	0.00
Stability ~ PHIKCL + BIO5 + Srad	5	-448.73	908.09	93.07	0.00
Stability ~ BIO5	3	-451.56	909.36	94.34	0.00
Stability ~ BIO5 + Srad	4	-451.38	911.17	96.15	0.00
Stability ~ NA + NA + NA + NA + NA + NA	2	-455.77	915.67	100.65	0.00
Stability ~ PHIKCL	3	-455.18	916.61	101.59	0.00
Stability ~ Srad	3	-455.76	917.77	102.75	0.00
Stability ~ PHIKCL + Srad	4	-455.09	918.60	103.57	0.00

FIGURES

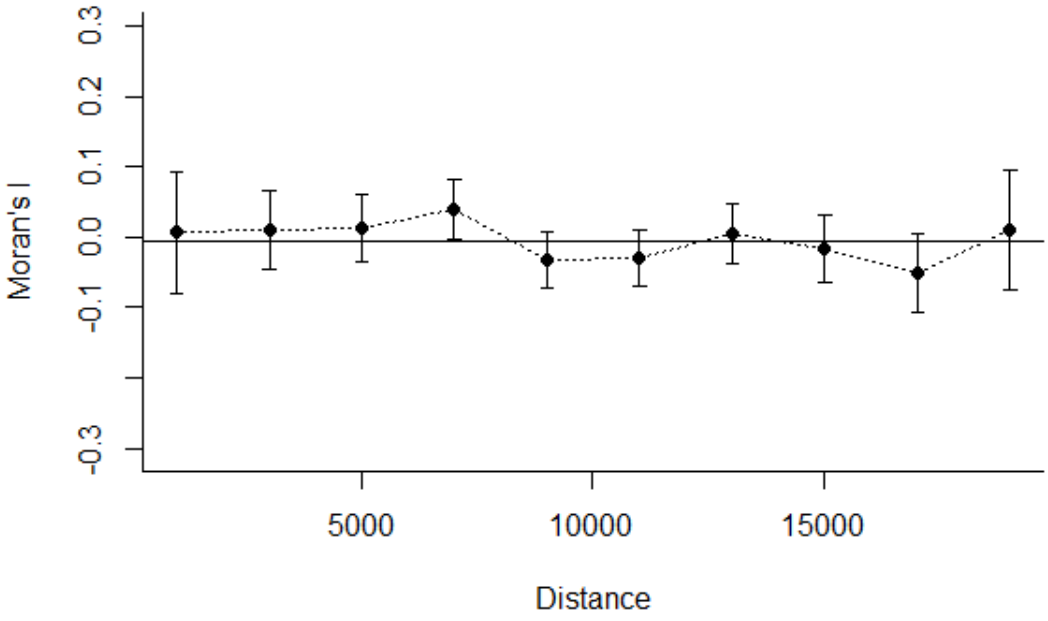

Figure S1. Correlogram of the Moran's index for the residuals of the linear regression of selected predictors and resilience indicating no spatial autocorrelation (p = 0.11) in a distance range of 20000 m between sample points.

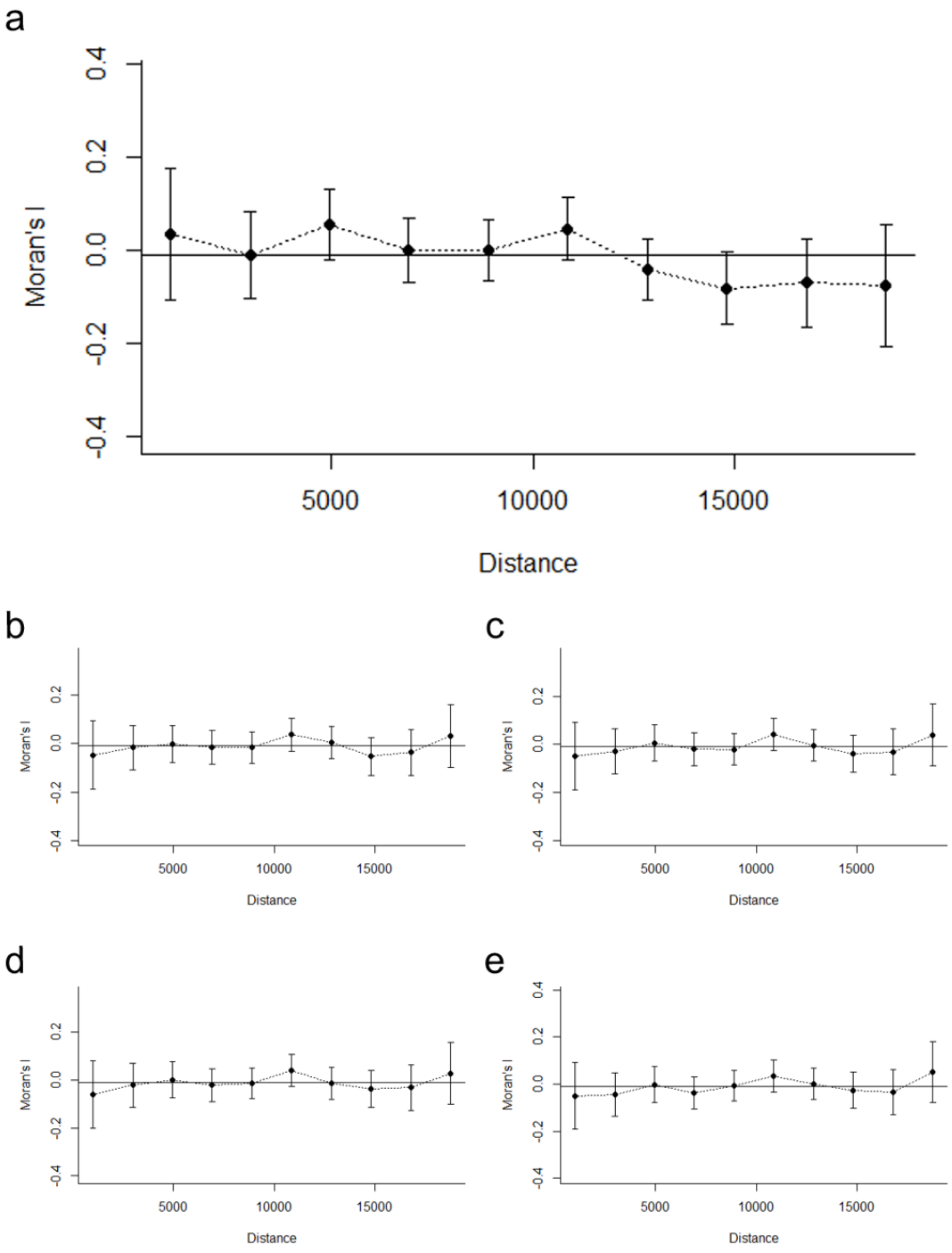

Figure S2. Above, correlogram of the Moran's index for the residuals of the linear regression of selected predictors and stability indicating spatial autocorrelation (p = 0.01) in a distance range of 20000 m between sample points (a). Below, correlogram of the Moran's index for the residuals of the first (a, p = 0.90), second (b, p = 0.71), third (b, p = 0.77), and fourth (b, p = 0.40) of the best performing models with controlled effect of the spatial autocorrelation.

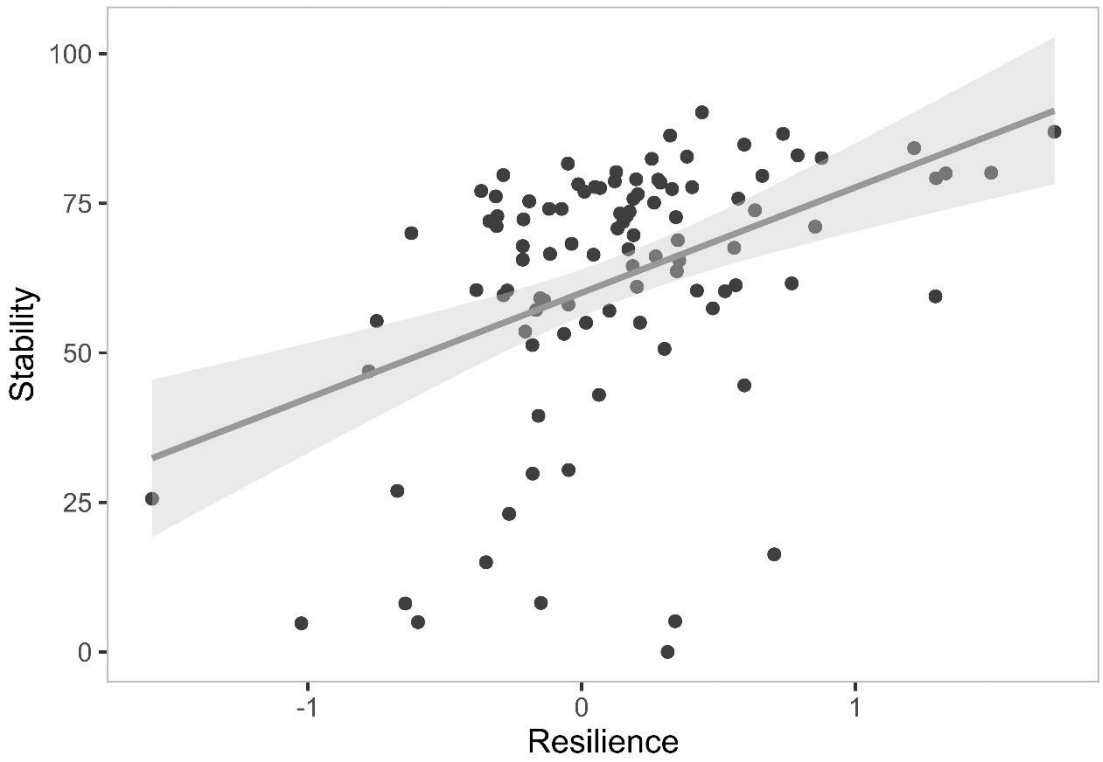

Figure S3. Scatter plot showing the positive correlation ($R = 0.42$, $p < 0.001$) between resilience and stability. The 95% confidence intervals are given as shading.

REFERENCES

Barlow, J., Mestre, L. A. M., Gardner, T. A., & Peres, C. A. (2007). The value of primary, secondary and plantation forests for Amazonian birds. *Biological Conservation*, *136*(2), 212–231. https://doi.org/10.1016/j.biocon.2006.11.021

Chazdon, R. L., Broadbent, E. N., Rozendaal, D. M. A., Bongers, F., Zambrano, A. M. A., Aide, T. M., … Poorter, L. (2016). Carbon sequestration potential of second-growth forest regeneration in the Latin American tropics. *Science Advances*, *2*(5). https://doi.org/10.1126/sciadv.1501639

Chazdon, R. L., Peres, C. A., Dent, D., Sheil, D., Lugo, A. E., Lamb, D., … Miller, S. E. (2009). The potential for species conservation in tropical secondary forests. *Conservation Biology*, *23*(6), 1406–1417. https://doi.org/10.1111/j.1523-1739.2009.01338.x

Cook-patton, S. C., Leavitt, S. M., Gibbs, D., Harris, N. L., Lister, K., Anderson-teixeira, K. J., … Holl, K. D. (2020). Mapping carbon accumulation potential from global natural forest regrowth, *585*(March 2019).

Di Marco, M., Watson, J. E. M., Currie, D. J., Possingham, H. P., & Venter, O. (2018). The extent and predictability of the biodiversity–carbon correlation. *Ecology Letters*, *21*(3), 365–375. https://doi.org/10.1111/ele.12903

Ferreira, J., Lennox, G. D., Gardner, T. A., Thomson, J. R., Berenguer, E., Lees, A. C., … Barlow, J. (2018). Carbon-focused conservation may fail to protect the most biodiverse tropical forests. *Nature Climate Change*, *8*(8), 744–749. https://doi.org/10.1038/s41558-018-0225-7

Gatti, L. V., Basso, L. S., Miller, J. B., Gloor, M., Domingues, L. G., Cassol, H. L. G., … Neves, R. A. L. (2021). Amazonia as a carbon source linked to deforestation and climate change. *Nature*, *595*(July). https://doi.org/10.1038/s41586-021-03629-6

Gibson, L., Lee, T. M., Koh, L. P., Brook, B. W., Gardner, T. A., Barlow, J., … Sodhi, N. S. (2011). Primary forests are irreplaceable for sustaining tropical biodiversity. *Nature*, *478*(7369), 378–381. https://doi.org/10.1038/nature10425

Goldstein, A., Turner, W. R., Spawn, S. A., Anderson-Teixeira, K. J., Cook-Patton, S.,

Fargione, J., … Hole, D. G. (2020). Protecting irrecoverable carbon in Earth's ecosystems. *Nature Climate Change*, *10*(4), 287–295. https://doi.org/10.1038/s41558-020-0738-8

Goodman, R. C., & Herold, M. (2014). *Why maintaining tropical forests is essential and urgent for a stable climate. CGD Working Paper 385. Washington, DC: Center for Global Development.*

Griscom, B. W., Adams, J., Ellis, P. W., Houghton, R. A., Lomax, G., Miteva, D. A., … Fargione, J. (2017). Natural climate solutions. *Proceedings of the National Academy of Sciences of the United States of America*, *114*(44), 11645–11650. https://doi.org/10.1073/pnas.1710465114

Harris, N. L., Brown, S., Hagen, S. C., Saatchi, S. S., Petrova, S., Salas, W., … Lotsch, A. (2012). Baseline map of carbon emissions from deforestation in tropical regions. *Science*, *336*(6088), 1573–1576. https://doi.org/10.1126/science.1217962

Harris, N. L., Gibbs, D. A., Baccini, A., Birdsey, R. A., de Bruin, S., Farina, M., … Tyukavina, A. (2021). Global maps of twenty-first century forest carbon fluxes. *Nature Climate Change*. https://doi.org/10.1038/s41558-020-00976-6

Houghton, R. A., Byers, B., & Nassikas, A. A. (2015). A role for tropical forests in stabilizing atmospheric CO2. *Nature Climate Change*, *5*(12), 1022–1023. https://doi.org/10.1038/nclimate2869

Latawiec, A. E., Crouzeilles, R., Brancalion, P. H. S., Rodrigues, R. R., Sansevero, J. B., Santos, J. S. dos, … Strassburg, B. B. (2016). Natural regeneration and biodiversity: a global meta-analysis and implications for spatial planning. *Biotropica*, *48*(6), 844–855. https://doi.org/10.1111/btp.12386

Leclère, D., Obersteiner, M., Barrett, M., Butchart, S. H. M., Chaudhary, A., De Palma, A., … Young, L. (2020). Bending the curve of terrestrial biodiversity needs an integrated strategy. *Nature*. https://doi.org/10.1038/s41586-020-2705-y

Lennox, G. D., Gardner, T. A., Thomson, J. R., Ferreira, J., Berenguer, E., Lees, A. C., … Barlow, J. (2018). Second rate or a second chance? Assessing biomass and biodiversity recovery in regenerating Amazonian forests. *Global Change Biology*, *24*(12), 5680–5694. https://doi.org/10.1111/gcb.14443

Lewis, S. L., Edwards, D. P., & Galbraith, D. (2015). Increasing human dominance of tropical forests. *Science*, *349*(6250), 827–832.

Malhi, Y., Gardner, T. A., Goldsmith, G. R., Silman, M. R., & Zelazowski, P. (2014). Tropical Forests in the Anthropocene. *Annual Review of Environment and Resources*, *39*(1), 125–159. https://doi.org/10.1146/annurev-environ-030713-155141

Matos, F. A. R., Magnago, L. F. S., Aquila Chan Miranda, C., de Menezes, L. F. T., Gastauer, M., Safar, N. V. H., … Edwards, D. P. (2020). Secondary forest fragments offer important carbon and biodiversity cobenefits. *Global Change Biology*, *26*(2), 509–522. https://doi.org/10.1111/gcb.14824

Myers, N., Mittermeier, R. A., Mittermeier, C. G., da Fonseca, G. A. B., & Kent, J. (2000). Biodiversity hotspots for conservation priorities. *Nature*, *403*(6772), 853–858. https://doi.org/10.1038/35002501

Noon, M. L., Goldstein, A., Ledezma, J. C., Roehrdanz, P. R., Cook-Patton, S. C., Spawn-Lee, S. A., … Turner, W. R. (2021). Mapping the irrecoverable carbon in Earth's ecosystems. *Nature Sustainability*. https://doi.org/10.1038/s41893-021-00803-6

Pettorelli, N., Graham, N. A. J., Seddon, N., da Cunha Bustamante, M., Lowton, M. J., Sutherland, W. J., … Barlow, J. (2021). Time to integrate global climate change and biodiversity science-policy agendas. *Journal of Applied Ecology*, *n/a*(n/a). https://doi.org/https://doi.org/10.1111/1365-2664.13985

Pimm, S. L., & Raven, P. (2000). Biodiversity: extinction by numbers. *Nature*, *403*(6772), 843–845.

Poorter, L., Bongers, F., Aide, T. M., Almeyda Zambrano, A. M., Balvanera, P., Becknell, J. M., … Rozendaal, D. M. A. (2016). Biomass resilience of Neotropical secondary forests. *Nature*, *530*(7589), 211–214. https://doi.org/10.1038/nature16512

Rozendaal, D. M. A., Bongers, F., Aide, T. M., Alvarez-Dávila, E., Ascarrunz, N., Balvanera, P., … Poorter, L. (2019). Biodiversity recovery of Neotropical secondary forests. *Science Advances*, *5*(3). https://doi.org/10.1126/sciadv.aau3114

Sala, O. E. (2000). Global Biodiversity Scenarios for the Year 2100. *Science*, *287*(5459), 1770–1774. https://doi.org/10.1126/science.287.5459.1770

Scheffers, B. R., Joppa, L. N., Pimm, S. L., & Laurance, W. F. (2012). What we know and don't know about Earth's missing biodiversity. *Trends in Ecology and Evolution*, *27*(9), 501–510. https://doi.org/10.1016/j.tree.2012.05.008

Soto-Navarro, C., Ravilious, C., Arnell, A., De Lamo, X., Harfoot, M., Hill, S. L. L., … Kapos, V. (2020). Mapping co-benefits for carbon storage and biodiversity to inform conservation policy and action. *Philosophical Transactions of the Royal Society B: Biological Sciences*, *375*(1794). https://doi.org/10.1098/rstb.2019.0128

Venter, O., & Koh, L. P. (2012). Reducing emissions from deforestation and forest degradation (REDD+): Game changer or just another quick fix? *Annals of the New York Academy of Sciences*, *1249*(1), 137–150. https://doi.org/10.1111/j.1749-6632.2011.06306.x

Xu, L., Saatchi, S. S., Yang, Y., Yu, Y., Pongratz, J., Bloom, A. A., … Schimel, D. (2021). Changes in global terrestrial live biomass over the 21st century. *Science Advances*, *7*(27), eabe9829. https://doi.org/10.1126/sciadv.abe9829

CAPÍTULO II

Biodiversity and carbon conservation under the ecosystem stability of tropical forests

Lucas Andrigo Maure, Milena Fiuza Diniz, Marco Túlio Pacheco Coelho, Paulo Guilherme Molin, Fernando Rodrigues da Silva, Erica Hasui

Biodiversity and carbon conservation under the ecosystem stability of tropical forests

Lucas Andrigo Maure[1,2], Milena Fiuza Diniz[3], Marco Túlio Pacheco Coelho[4], Paulo Guilherme Molin[5], Fernando Rodrigues da Silva[2], Erica Hasui[6]*

[1]Programa de Pós-graduação em Ecologia e Recursos Naturais (PPGERN), Universidade Federal de São Carlos, São Carlos-SP, Brazil

[2]Laboratório de Ecologia Teórica: Integrando Tempo, Biologia e Espaço (LET.IT.BE), Departamento de Ciências Ambientais, Universidade Federal de São Carlos, Sorocaba-SP, Brazil

[3]Departamento de Ecologia, Universidade Federal de Goiás, Goânia-GO, Brazil

[4]Swiss Federal Institute for Forest, Snow and Landscape, Birmensdorf, Switzerland

[5]Centro de Ciências da Natureza, Universidade Federal de São Carlos, Buri-SP, Brasil

[6]Laboratório de Ecologia de Fragmentos (EcoFrag), Instituto de Ciências da Natureza, Universidade Federal de Alfenas-MG, Brazil

***Corresponding author:** ericahasui@gmail.com

Abstract

Although efforts to protect high levels of biodiversity and carbon storage can greatly increase the effectiveness of species loss and climate change mitigation, there is evidence indicating a trade-off scenario for their conservation at regional scale. Decisions making in trade-off scenarios can be supported by including information on the ecosystem stability of tropical forests (i.e., the ability of the ecosystem to maintain its function over time). Forest stability may affect biodiversity integrity and the residence time of carbon stored in tree biomass. Here, we used remote sensing and geoprocessing tools to analyze the overlap among forest-specialist vertebrate species richness, carbon density, and stability of old-growth forest throughout the Brazilian Atlantic Forest. We used model selection to find environmental predictors of the stability of primary productivity and build a predictive map of potential stability. Then, we overlapped maps of potential stability, species richness of forest-specialist vertebrates, and carbon density to identify hotspot areas of biodiversity and carbon density occurring at highest and lowest potential stability. We found that forest stability increases from north to south along the Atlantic Forest. High biodiversity occurs mainly at low stability while high carbon stock at high stability. Spatial overlap of the hotspots, where conservation co-benefits high biodiversity and carbon stock, occurs mostly at high stability in a large area along part of the coast and in smaller inland areas of the southern region. Most of the hotspots with low stability for biodiversity, carbon stock and combination of both are found in unprotected areas. Thus, species loss and carbon emission could be mitigated if prioritizing forest protection in unprotected hotspots, management in protected hotspots of low stability, and protection and management in unprotected hotspots of low stability. This ecosystem-based planning can also help

Brazil’s government to achieve its commitments in biodiversity conservation and carbon emission reduction.

Keywords: Atlantic Forest, protected area, carbon density, conservation trade-offs, rainforest, climate change

1. INTRODUCTION

Understanding the relationship between biodiversity, carbon storage and the tropical forest ecosystem can help find and design protected areas to mitigate species loss and carbon emission. Tropical forests have gained special attention because of their greater biodiversity and carbon stored in the aboveground biomass of the world's terrestrial ecosystems, conferring a high potential to conserve both (Dixon et al., 1994; Xu et al., 2021). However, the biodiversity-carbon relationship shows high spatial variation and decreases from global to regional and local scales. Thus, the ideal scenario of co-benefit is limited and a trade-off scenario for conservation arises (Armenteras, Rodríguez, & Retana, 2015; Murray et al., 2015; Sullivan et al., 2017; Di Marco et al., 2018). In trade-off scenarios, conservation focused only on carbon storage may not be sufficient to protect most of the biodiversity in tropical forests (Ferreira et al., 2018).

Despite many proposals for prone areas for biodiversity and carbon conservation, studies have not yet taken into account the stability of tropical forests (i.e., the ability of the ecosystem to maintain its function over time). Forest stability could affect biodiversity integrity and the residence time of carbon stored in tree biomass (Sales, Galetti, & Pires, 2020; Xu et al., 2021). An ecosystem-based approach can substantially improve spatial planning by indicating where conservation in synergy or trade-off scenarios can be enhanced by taking into account forest stability. This

approach may also introduce an important new element to help decisions in trade-off scenarios, as conservation would potentially be more cost-effective in areas that combine high forest stability with high biodiversity and/or carbon density.

For example, mitigation of climate change by ecosystems is based on net carbon which depends on the stability of carbon stocks (Díaz, Hector, & Wardle, 2009). Not only deforestation, but also eventual perturbations affect the residence time of the carbon stored in forest biomass, making forests turn from sink to source of carbon (Aragão et al., 2018; Gatti et al., 2021; Xu et al., 2021). Also, stable forests may contribute to reducing local extinctions of forest-specialists vertebrates due to the drastic decrease in their suitable range as a consequence of perturbations increase (Sales, Galetti, & Pires, 2020). Species loss and reduced residence time of carbon storage undermines policies and governmental commitments of international biodiversity and carbon conservation agendas. Thus, such ecosystem-based spatial planning would be of uttermost importance for biodiversity-carbon conservation, especially for regions with high concentration of threatened biodiversity, advanced forest degradation due to a long history of human land use, biomass erosion, and constant perturbations like the Brazilian Atlantic Forest (Brooks et al., 2002; Ribeiro et al., 2009, 2011; Rezende et al., 2018; de Lima et al., 2020; Soto-Navarro et al., 2020).

Here, we used remote sensing and geoprocessing tools to analyze the overlap among forest-specialist vertebrate species richness, carbon density, and stability of old-growth forest throughout the Atlantic Forest. We selected 3934 old-growth forest sites in the Atlantic Forest to test the relationship of climate, soil, and topography on the spatial distribution of the primary productivity stability of these forests. We provided a prediction map of the potential forest stability and overlapped it with maps of forest-specialist vertebrate species richness and carbon density. Finally, we identified hotspot

areas where high biodiversity and carbon density overlap with the highest and lowest values of potential stability. These hotspots would be of particular relevance for policy decisions on conservation to mitigate species loss and climate change.

2. METHODS

2.1 Study area

The study covers the Brazilian Atlantic Forest, one of the most important global hotspots for conservation due to its high levels of biodiversity, endemism, and threatened species (Myers et al., 2000; Brooks et al., 2002; Ribeiro et al., 2009, 2011). Only ~28% of the Brazilian Atlantic Forest surface (c. 1.5 million km^2) is currently covered by native vegetation (Rezende et al., 2018). Furthermore, most of the forest remnants in the Brazilian Atlantic Forest are facing constant anthropogenic perturbation such as grazing, logging, hunting, and fire that severely impact their biodiversity and ecosystem (Tabarelli, Pinto, Silva, Hirota, & Bedê, 2005; Ribeiro et al., 2011; Barlow et al., 2016; Erb et al., 2018; de Lima et al., 2020).

2.2 Data

Sampling sites - To identify sites of old-growth forest, we used classified images from 1985 to 2018 (33-year range) of 30 m resolution for the land cover in the Brazilian Atlantic Forest available from MapBiomas v4.0 (http://mapbiomas.org/). Our mapping showed that old-growth forests have a total area of 21,444,900 ha, covering 19.37% of the entire extension of the Brazilian Atlantic Forest. We intersected the forest areas with a 250 m gridded map. We selected as sampling sites only the centroid coordinates of the

geographical cells totally covered by forest area. To reduce the number of sampling sites and improve computational tractability, we selected a total of 14,569 cells out of 920,603 remained after we performed a random selection of cells with a minimum arbitrary distance of 5 km to each other.

Response variable - We measured stability of the primary productivity of old-growth forests by calculating the standard deviation of interannual time series of 19 years (time range of available images) of the Normalized Difference Vegetation Index (NDVI) (De Keersmaecker et al., 2014; García-Palacios et al., 2018). NDVI is a remote sensing vegetation index derived from satellite images that measure vegetation greenness, used as indicator of primary productivity and biomass (Pettorelli et al., 2005; Saatchi et al., 2007; Verbesselt et al., 2016; Caughlin et al., 2020). We used NDVI data at 250m resolution available in the GLAM Project (http://pekko.geog.umd.edu/usda/test/) extracted from MODIS sensor images, in which values from observation error were excluded. With all 23 available images per year between 2000-2018, we used mean NDVI values for each year to obtain interannual time series. Thus, we avoided intra-annual fluctuations caused by the seasonality of the plant productivity phenology, which may influence our main objective to detect long-term variations in primary productivity.

To measure forest stability by the standard deviation, we first detrended all time series by a second-order difference to avoid long-term or stochastic trends variation in nonstationary time series (Legendre & Legendre, 2012; De Keersmaecker et al., 2014). We ensure stationarity of time series using the Augmented Dickey Fuller test (ADF; Dickey & Fuller, 1979) from the trend R package trend (Pohlert, 2018) and we selected only significant stationary time series for statistical analysis, which reduced the dataset

to 8,974 sampling points. Because high variation means low stability, we rescaled standard deviation values to range from 0 to 100 in which higher values indicate higher forest stability. To promote regular distribution of the sites we applied a new random selection based on a minimum distance of 10 km, which is the mean distance between all sites. Regular spatial distribution of the samples contributes to reaching a gradient-wide range of the variables values and to avoid spatial autocorrelation (Dale & Fortin, 2014; Fletcher & Fortin, 2018). At last, we obtained a dataset of 3,934 sites regularly distributed across the Brazilian Atlantic Forest (Figure 1).

2.3 Predictors

To build the models for predicting the stability of old-growth forests, we used a total of 39 variables from three categories (Appendix S1): 21 climatic, 15 soil, and 3 topographical variables. These categories constitute resources and conditions that directly affect plant productivity (Laurance et al., 1999; Sattler et al., 2014; Sullivan et al., 2020). A detailed description of the three categories and the calculation of topography variables are available as supporting information. In summary, climatic variables were downloaded at a resolution of 30 seconds (~1 km) from the WorldClim v2.1 (Fick & Hijmans, 2017) database. Soil variables were downloaded at 250 m resolution from the SoilGrid database (Hengl et al., 2017) with soil organic carbon stock in tons per ha obtained for a depth of 30 cm (OCSTHA_30cm), the lowest available depth for this variable. Topographic variables were obtained from the SRTM 90 m Digital Elevation Database v4.1 (Jarvis et al., 2008) of the Consortium for Spatial Information (CGIAR-CSI). All raster maps were reprojected to the South America Albers Equal Area Conic and predictor data were statistically resampled to a spatial resolution of 250 m. All geoprocessing was performed using ArcGIS (10.6.1).

Predictor selection - To avoid correlation between predictors we first build simple linear models for each of the 39 predictors and rank them according to their importance by the estimated slope coefficient. Then, we built a multiple linear model adding predictors one by one following their importance rank. For each added predictor we checked the collinearity and the coefficients of the model. We excluded the newly added predictor that elevate the variance inflation factor (VIF) (R package *car;* Fox & Weisberg, 2018) higher than 5, which indicates predictors collinearity (Dormann et al., 2013), and/or inverted the coefficient of any variable in the model. Coefficient inversion might indicate predictors interaction, which is out of scope of our simple additive model framework. At the end of the procedure, the selected predictors in order of importance were: temperature seasonality (BIO4), isothermality (BIO3), mean temperature of coldest quarter (BIO11), annual precipitation (BIO12), absolute depth to bedrock (BDTICM), and soil organic carbon stock (OCSTHA_30cm). The low VIF values (≤ 4.93) (Appendix S2) between selected predictors indicated the collinearity observed in our selected variables.

2.4 Statistical analysis

We used a multi-model inference framework with model selection through the Akaike information criterion (Burnham & Anderson, 2001, 2002). This framework of statistical inference is designed to asymptotically maximize the expected relative predictive accuracy of models (i.e., the ability to fit future data). Therefore, this framework identifies the model that maximizes predictive accuracy, reducing the risk of performing predictions with overfitted models (Coelho, Diniz-Filho, & Rangel, 2019). We

compared 64 models, emerging from the combination of the six selected predictors, which were built using a standard multiple regression (OLS). Models with ΔAICc values less than 2 were considered to have higher predictive accuracy and the importance of their predictors was assessed by the sum of their weights and the number of models containing them. We inspected the OLS residuals of the model with all selected predictors to evaluate the existence of spatial autocorrelation (Diniz-filho, Rangel, & Bini, 2008), which showed no evidence for it (Moran's Index $p = 0.57$, Appendix S3). We performed our analyses in R (R Core Team, 2020) using the packages *MuMIn* (Barton, 2019), *glmulti* (Calcagno, 2019), *fields* (Nychka, Furrer, Paige, & Sain, 2017), *ape* (Paradis & Schliep, 2018), and *letsR* (Vilela & Villalobos, 2015).

2.5 Mapping

We built bivariate maps that overlap classes of either species richness of forest-specialist vertebrates or carbon density of aboveground biomass with potential stability. Then, we constructed maps of hotspot areas that highlight the highest values of the bivariate maps of biodiversity and carbon density overlaid with the highest and lowest values of potential stability. Because carbon density aboveground biomass and potential stability could be associated with species richness, we confronted species richness against these variables to understand their functional association with vertebrate richness. Initial visual inspections of the association of these variables indicate non-linear relationships. Therefore, to capture the non-linearity in these relationships we use General Additive Models (GAMs) with penalized smooth functions through Generalized Cross Validation (GCV, Wood, Pya, and Säfken, 2016; Wood, 2017).

Potential stability map - to obtain the potential stability map, we used the average estimated coefficients of the predictors of all models with the highest predictive accuracy (ΔAICc < 2) in the multiple linear regression equations (details in section 1.2 of the methods in supporting information). To estimate the prediction power of the potential stability map, we calculated Pearson's correlation between predicted and observed stability. Because the equation uses the predictors' data, the potential stability map is at a spatial resolution of 250 m.

Biodiversity and potential stability bivariate map - Here, vertebrate diversity is measured by species richness for each grid cell. For the biodiversity map, we used species' range from the International Union for Conservation of Nature database (IUCN, www.iucnredlist.org) for birds (ranges from BirdLife International), mammals, and amphibians of Brazil and occupant of all forest habitats categories. These species are classified as forest-specialists and are more vulnerable to forest perturbations (Sales et al., 2020). We restricted the range maps for the Brazilian Atlantic Forest, which resulted in a total of 732 birds, 293 mammals, and 445 amphibians. Then, we converted the distribution range of each taxon in a species richness raster map with 5 km resolution using the R package *lestR* (Vilela & Villalobos, 2015). Given the high correlation between the richness maps ($r > 0.94$), we summed them to obtain a single map of the total species richness for the three taxa (1,470) (Appendix S4a). We resampled the map of potential stability to 5 km resolution using bilinear interpolation to fit the species richness map. Then, we classified both maps in ten classes by 10% quantiles and assembled them in a bivariate choropleth map that combines areas of the different classes of species richness and potential stability maps. However, local species

richness may omit species of high conservation concern. Hence, we repeated the process above using ranges of threatened forest-specialist species from the IUCN red list categories of critically endangered (CE), endangered (EN), and vulnerable (VU) species for the three taxa. Maps of the threatened species richness present a moderate correlation between the three taxa ($r > 0.50$) and we also summed them (Appendix S4b). Because maps of species richness and threatened species richness had a high correlation ($r = 0.89$), we moved the bivariate map of the threatened species richness to supporting information (Appendix S5).

Carbon density and potential stability bivariate map - For the carbon map, we used a harmonized global map of aboveground biomass carbon density (MgC/ha) for the reference year 2010 at ~328 m resolution (Spawn et al., 2020). This data comprises the carbon stored in living plant tissues found above the earth's surface. We resampled the potential stability map to the same resolution of the carbon density map using bilinear interpolation. Then, we joined both maps in a bivariate choropleth map that overlaps ten classes of 10% quantiles of the values of carbon density and potential stability.

Hotspot maps – Based on bivariate maps we built three hotspot maps; one for biodiversity, one for carbon density, and one for the overlapped hotspot areas of both, which are areas of co-benefit conservation. First, we define hotspot areas in two classes, one class for the highest and other for the lowest 20% values of potential stability that overlap with the highest 20% values of biodiversity and carbon density (Armenteras, Rodríguez, & Retana, 2015, Soto-Navarro 2020). The map of co-benefit conservation shows the spatial overlap of the two classes of the biodiversity and carbon hotspot map.

To build this map, the map of carbon hotspots was resampled to a 5 km resolution using nearest interpolation to fit the biodiversity hotspot map resolution. Then, we combined the both hotspot maps of biodiversity and carbon density. We quantified the species number and carbon stock for the two classes of each of the three maps. For the carbon stock quantification, we obtained absolute values in MgC by multiplying the total MgC/ha value in each of the two hotspots classes by 10.77, which is the pixel area in ha of the carbon density dataset. We also quantified the proportion of the hotspot areas for each of the two classes of the three maps located in protected and unprotected areas, according to the World Database on Protected Areas (WDPA) (UNEP-WCMC & IUCN, 2022). Finally, each hotspot map has four classes that highlight areas of high potential stability 1) currently protected; and 2) unprotected, considered as refuge for high biodiversity and/or carbon storage that are suitable for protection. Also, areas of low potential stability 3) currently protected but forest management is required; and 4) unprotected, considered as vulnerable areas for high biodiversity and/or carbon storage where forest protection and management are recommended.

3. RESULTS

3.1 Predictors of forest stability and potential stability map

Stability varied from 0 to 96.5 in which values increase from north to south in a general pattern of spatial distribution across the Atlantic Forest (Figure 1). Two nested models with $\Delta AICc < 2$ and weight of 71% (nested model with five variables) and 26,6% (six variables) best fitted the data (Appendix S6). Based on the more complex model, the spatial distribution of stability was associated positively with temperature seasonality (BIO4) ($ß = 0.038 \pm 0.004$), soil organic carbon stock (OCSTHA_30cm) ($ß = 0.025 \pm$

0.008) and annual precipitation (BIO12) (ß = 0.006 ± 0.000), and negatively with isothermality (BIO3) (ß = -0.309 ± 0.053) and absolute depth to bedrock (BDTICM) (ß = -0.001 ± 0.000), Appendices S6 and S7).

The prediction map of potential stability (Figure 2) shows a general pattern of spatial distribution that increases from north to south across the Brazilian Atlantic Forest and a moderate correlation with the observed values (r = 0.56). Higher values of potential stability are found in: i) the Serra do Mar region in the south coast, ii) isolated areas of the mountain chains of Serra da Mantiqueira in Minas Gerais state and Serra dos Orgãos in Rio de Janeiro state, and iii) Bahia state coast in the northern region. The species richness map of forest-specialists presents higher values along the Atlantic Forest coast of the Brazilian southeastern region (Appendix S4a). However, higher values of the threatened species richness of forest-specialists concentrates along coastal regions of the Atlantic Forest, mainly in the Espírito Santo and Bahia states (Appendix S4b).

3.2 Spatial overlap of biodiversity, carbon density and potential stability

In both bivariate maps, areas of high species richness (Figure 3) and carbon density (Figure 4) with high potential stability are found mainly along the south coast and in an isolated area at the Bahia state coast. Covering 1.14% of the entire Brazilian Atlantic Forest along the Serra do Mar and Serra da Mantiqueira regions, hotspot areas of high potential stability harbor 860 species (58.50%) (Figure 5a, Table 1). These hotspots have 29.65% of its area unprotected. Also occurring in these same regions and in other areas over the Brazilian south, hotspots of high potential stability contain a total carbon stock of 4,920,818,211 MgC (40.90%) (Figure 5b, Table 1). Its area represents 6.27%

of the Brazilian Atlantic Forest; however, 75.72% are found in unprotected areas. In turn, where hotspot areas of high biodiversity, carbon density and potential stability overlap along the Serra do Mar and Serra da Mantiqueira are found 860 species (58.50%) and 729,776,936 MgC (6.06%), covering 0.94% of the biome domain (Figure 5c, Table 1). These hotspots of co-benefit conservation have 25.32% of its area unprotected.

Bivariate maps show that areas of high species richness (Figures 3) and carbon density (Figures 4) overlapping with low potential stability are found mainly in the central and northern regions of the Atlantic Forest, respectively. At low potential stability, hotspots for species richness contain 896 species (60.95%) and cover 1.72% of the Atlantic Forest in which 95.11% is unprotected (Figure 5a, Table 1). For carbon density these areas hold 1,275,363,082 MgC (10.60%) in 1.77% of the entire biome domain where 91.08% is found unprotected (Figure 5b, Table 1). Areas where high biodiversity, carbon density and low potential stability overlap represent only 0.02% of the Atlantic Forest (Figure 5c, Table 1). These areas occur near the coast of the Rio de Janeiro state, and in the Espírito Santo and Minas Gerais states. Although they are few and small, and have a carbon stock of only 7,823,610 MgC (0.06%), they contain an expressive number of 776 species (52.79%). Also, 83.71% of its area is unprotected.

3.3 Stability, biodiversity and carbon relationship

GAM model for stability and carbon density explained 43.3% (r^2_{adj} = 0.44) of birds, 62.4% (r^2_{adj} = 0.64) of mammals, 38% (r^2_{adj} = 0.44) for amphibians and 47.2% (r^2_{adj} = 0.47) of all groups deviance of species richness. Generally, species richness presents a unimodal distribution with stability (Appendix S8a, c, e and g), while increases with

carbon density (Appendix S8b, d, f and h). The effect of stability and carbon density on distribution of species richness is underestimated in highly rich regions like the central coast and overestimated in the Atlantic Forest interior for all groups and each of them (Appendix S9).

4. DISCUSSION

The current scenario of advanced devastation and constant perturbations of forests makes spatial planning for conservation of utmost importance to avoid biodiversity decline and carbon emission in the Brazilian Atlantic Forest. We demonstrated that an ecosystem-based planning brings new alternatives to conservation by prioritizing areas and guiding strategies according to forest stability, preserving a great number of species and carbon stocks. Our results allow us to locate unprotected refuge areas where biodiversity and carbon stocks may be safe by high potential stability of the forest ecosystem. These areas are suitable for protection and low intervention may be necessary. Most importantly, it is possible to identify unprotected areas where biodiversity and carbon stocks may be in vulnerable conditions due to low potential stability. In these areas, forest protection and management associated with conservation actions are recommended to avoid severe degradation by perturbations of forests that house large amounts of species and carbon. In trade-off scenarios of biodiversity and carbon storage conservation, our results can help policy makers, conservation institutions, and stakeholders to allocate effort and resources to conservation and forest management.

Implemented in Brazilian Atlantic Forest, our results may further contribute to the achievement of current and post-2020 agendas for biodiversity conservation and

carbon emission reduction. Beyond conservation, forest restoration can also be optimized by this ecosystem-based approach, prioritizing areas of high potential stability and directing management efforts and resources to areas of low potential stability. This approach could also help Brazil's government to achieve its commitment in the Brazilian Atlantic Forest Restoration Pact, Bonn Challenge, and the upcoming United Nations' Decade on Ecosystem Restoration (2021–2030) (Melo et al., 2013; Verdone & Seidl, 2017; Crouzeilles et al., 2019; Bonn Challenge, 2020).

4.1 Predictors of forest stability and potential stability map

In general, forest stability increases from north to south across Brazilian Atlantic Forest mainly as a function of temperature seasonality, soil organic carbon stock, and annual precipitation, and decreases in function of isothermality and depth to bedrock. Discussion about the effect of some predictors on primary productivity and its stability is found as supporting information. In general, the spatial distribution of the environmental conditions of temperature and resources availability such as water and nutrients influence forest stability in a given location, determining its ability to maintain primary productivity constant over time. The projection of these results indicates the potential stability throughout the Brazilian Atlantic Forest, helping direct forest management for biodiversity and carbon stocks conservation.

4.2 Spatial overlap of biodiversity, carbon density and potential stability

The overlap between biodiversity maps and carbon density with potential stability display areas where forest protection and management are urgent in the Brazilian

Atlantic Forest. Forests located in areas of high potential stability that house greater biodiversity or have higher carbon density found at coastal areas along the south region and at Bahia state, may require low interventions. Forests in these areas may present low variation in primary productivity indicating that they are more resistant, withstanding eventual perturbations without severe changes in their functions. Because high potential stability may confer to these forests the status of refugee for biodiversity and carbon storage, conservation can be directed specifically at threatened species and low forest management may contribute to the preservation of carbon stocks.

However, areas of low potential stability overlapping with high biodiversity or carbon density extends over different regions. For biodiversity, a larger area of high species richness with low potential stability occurs in the central region of the Atlantic Forest and along the coast at Rio de Janeiro state in the southern region. As our selected species are specialized in forest habitat, the vulnerability of the less stable forests puts the biodiversity and threatened species that inhabit it at risk. Thus, conservation actions and forest management could avoid the loss of forest-specialist species and a faunal savanization after perturbations such as fire and drought (Sales et al., 2020).

Similarly, areas of high carbon density and low stability are found throughout the northern region but mainly in its interior. Because forests located in areas of low potential stability may be more vulnerable to fire and edge effects, forest management can prevent the emission of the carbon stored in above ground biomass caused by these perturbations (Brinck et al., 2017; Aragão et al., 2018; Armenteras et al., 2021; Gatti et al., 2021; Kruid et al., 2021; Xu et al., 2021). Overall, without forest management and conservation actions in these areas, especially for threatened species, biodiversity loss

and emission of stored carbon can undermine REDD+ agreements (Aragão & Shimabukuro, 2010; Venter & Koh, 2012).

4.3 Priority areas for conservation

The hotspot maps highlight unprotected areas where forest protection and management should be prioritized to preserve greater biodiversity and/or carbon density. Carbon density hotspots have the largest proportion of unprotected areas with high potential stability, in which 75.72% of its area is found out of protection mainly across the Brazilian southern region. The total area of this hotspot has 40.90% (4,920,818,211 MgC) of all carbon storage of the aboveground biomass present in the forest areas found in this study. With 58.50% (860) of all our selected species, hotspots for high biodiversity and potential stability occur in the Serra do Mar and Serra da Mantiqueira regions and are 29.65% unprotected. Also in these regions, areas of overlapping biodiversity-carbon, where conservation co-benefit both, is found in its majority at higher potential stability and have 25.32% of its area unprotected. This hotspot hosts 58.50% (860) of all species and 6.06% (729,776,935 MgC) of carbon storage. In unprotected areas of all the hotspots mentioned above, the high potential for forest stability can optimize conservation of the large biodiversity and carbon stocks, making it more cost-effective because low forest management is required. Thus, these areas can be considered as refugees and should be prioritized for forest protection.

In turn, the largest proportion of unprotected areas for the low potential stability class occur in biodiversity hotspots, which in its total host 60.95% (896) of all species of this study. This hotspot with a great number of forest-specialists species living in unstable forests is 95.11% unprotected. These areas are found discontinuously

distributed mainly near the coast of the Rio de Janeiro state but also in the Espírito Santo and Minas Gerais states. The carbon density hotspot at lower potential stability has 91.07% of its area unprotected, the second large proportion. In total, they contain 10.60% (1,275,363,082 MgC) of the forest carbon storage and are found across the central and northern regions of the Atlantic Forest. Covering only 0.02% of the Atlantic Forest, co-benefit areas at lower potential stability are few, small and sparsely distributed with 83.71% of its area unprotected. Despite their small size, these areas harbor 52.79% (776) of all species but contain only 0.06% (7,823,610 MgC) of all carbon stock found in forest areas. All these hotspots are considered as vulnerable areas for high biodiversity and carbon storage because their forests may be less stable. Thus, forest management to avoid perturbations for the entire area and forest protection for its unprotected areas are urgently needed, especially for biodiversity conservation in their hotspots.

Overall, biodiversity and carbon stock hotspots overlap in 9.34% of their total area, meaning that co-benefit conservation on high levels of species richness and carbon density is limited to small areas in Atlantic Forest. The majority of these areas found in the Serra do Mar and Serra da Mantiqueira regions have high potential stability and are mostly protected (74.68%). This finding was expected for two reasons. First, because Atlantic Forest is highly fragmented and these regions concentrate the greatest expansions of old-growth forest remnants which store more carbon, and the highest levels of biodiversity, both at protection areas (Saatchi et al., 2007; Ribeiro et al., 2009, 2011, Ferreira et al., 2018). In fragmented landscapes, field surveys show that the size and proximity of forest remnants have a positive effect on carbon stock and biodiversity (Magnago et al., 2015). Second, the biodiversity-carbon correlation becomes weaker from global to regional scales and hotspots areas of co-benefit for conservation tend to

be small and sparsely distributed (Armenteras, Rodríguez, & Retana, 2015; Murray et al., 2015; Sullivan et al., 2017; Di Marco et al., 2018).

Therefore, because co-benefit areas are scarce, its protection needs to be expanded to unprotected areas found here for conservation of its high biodiversity and carbon stock. Moreover, this low spatial overlap of the hotspots suggest that conservation should mainly be implemented separately for biodiversity and carbon stocks in the Atlantic Forest, following a trade-off approach (Gardner et al., 2012; Phelps, Friess, et al., 2012; Phelps, Webb, et al., 2012). In this case, decisions can be supported by the spatial planning based on the forest ecosystem stability and the priority areas for conservation of biodiversity and carbon stocks discussed above.

5. CONCLUSION

The ecosystem stability of the old-growth forest increased from north to south in the Brazilian Atlantic Forest and this spatial pattern was associated mainly with climate and soil predictors. Combining knowledge of the prediction map of potential stability with maps of biodiversity and aboveground biomass can greatly increase the effectiveness of attempts to mitigate both the climate and biodiversity crises. Hotspot areas of higher species richness and carbon density occur mainly at higher potential stability along the south coast of the Atlantic Forest. The protection of the forests located in these areas can serve both biodiversity and carbon conservation purposes. However, the low spatial overlap of the hotspot areas of biodiversity and carbon stock means that there is a trade-off between protecting biodiversity and carbon storage in the Brazilian Atlantic Forest. In this trade-off scenario, hotspot maps can help policy decisions by indicating priority and unprotected areas, and the conservation strategy. In hotspot areas for biodiversity

and carbon stock, forest protection at higher potential stability is recommended. In turn, forest protection and management, and conservation especially of threatened species, should be implemented at low potential stability. This ecosystem approach can optimize conservation planning making it more cost-effective and contribute to avoiding a massive species loss and carbon emission by perturbations.

SUPPORTING INFORMATION

Additional supporting information may be found in the online version of the article at the publisher's website.

REFERENCES

Aragão, L. E. O. C., Anderson, L. O., Fonseca, M. G., Rosan, T. M., Vedovato, L. B., Wagner, F. H., … Saatchi, S. (2018). 21st Century drought-related fires counteract the decline of Amazon deforestation carbon emissions. *Nature Communications*, *9*(1), 1–12. https://doi.org/10.1038/s41467-017-02771-y

Aragão, L. E. O. C., & Shimabukuro, Y. E. (2010). The incidence of fire in Amazonian forests with implications for REDD. *Science*, *328*(5983), 1275–1278.

Armenteras, D., Dávalos, L. M., Barreto, J. S., Miranda, A., Hernández-Moreno, A., Zamorano-Elgueta, C., … Retana, J. (2021). Fire-induced loss of the world's most biodiverse forests in Latin America. *Science Advances*, *7*(33), 2–10. https://doi.org/10.1126/sciadv.abd3357

Armenteras, D., Rodríguez, N., & Retana, J. (2015). National and regional relationships of carbon storage and tropical biodiversity. *Biological Conservation*, *192*, 378–386. https://doi.org/10.1016/j.biocon.2015.10.014

Barlow, J., Lennox, G. D., Ferreira, J., Berenguer, E., Lees, A. C., Nally, R. Mac, … Gardner, T. A. (2016). Anthropogenic disturbance in tropical forests can double biodiversity loss from deforestation. *Nature*, *535*(7610), 144–147. https://doi.org/10.1038/nature18326

Bonn Challenge. (2020). https://infoflr.org/countries/brazil.

Brinck, K., Fischer, R., Groeneveld, J., Lehmann, S., Dantas De Paula, M., Pütz, S., … Huth, A. (2017). High resolution analysis of tropical forest fragmentation and its impact on the global carbon cycle. *Nature Communications*, *8*. https://doi.org/10.1038/ncomms14855

Brooks, T. M., Mittermeier, R. A., Mittermeier, C. G., Da Fonseca, G. A. B., Rylands, A. B., Konstant, W. R., … Hilton-Taylor, C. (2002). Habitat Loss and Extinction in the Hotspots of Biodiversity. *Conservation Biology*, *16*(4), 909–923. https://doi.org/10.1046/j.1523-1739.2002.00530.x

Caughlin, T. T., Barber, C., Asner, G. P., Glenn, N. F., Bohlman, S. A., & Wilson, C. H. (2020). Monitoring tropical forest succession at landscape scales despite uncertainty in Landsat time series. *Ecological Applications*, *31*(1), 1–18. https://doi.org/10.1002/eap.2208

Coelho, M. T. P., Diniz-Filho, J. A., and Rangel, T. F. (2019). A parsimonious view of the parsimony principle in ecology and evolution. Ecography, 42(5), 968–976. https://doi.org/10.1111/ecog.04228

Crouzeilles, R., Santiami, E., Rosa, M., Pugliese, L., Brancalion, P. H. S., Rodrigues, R. R., … Pinto, S. (2019). There is hope for achieving ambitious Atlantic Forest restoration commitments. *Perspectives in Ecology and Conservation*, *17*(2), 80–83. https://doi.org/10.1016/j.pecon.2019.04.003

Dale, M. R. T., & Fortin, M.-J. (2014). *Spatial analysis: a guide for ecologists*. Cambridge University Press.

De Keersmaecker, W., Lhermitte, S., & Honnay, O. (2014). How to measure ecosystem stability? An evaluation of the reliability of stability metrics based on remote sensing time series across the major global ecosystems. *Global Change Biology*,

2149–2161. https://doi.org/10.1111/gcb.12495

de Lima, R. A. F., Oliveira, A. A., Pitta, G. R., de Gasper, A. L., Vibrans, A. C., Chave, J., … Prado, P. I. (2020). The erosion of biodiversity and biomass in the Atlantic Forest biodiversity hotspot. *Nature Communications*, *11*(1), 6347. https://doi.org/10.1038/s41467-020-20217-w

Di Marco, M., Watson, J. E. M., Currie, D. J., Possingham, H. P., & Venter, O. (2018). The extent and predictability of the biodiversity–carbon correlation. *Ecology Letters*, *21*(3), 365–375. https://doi.org/10.1111/ele.12903

Díaz, S., Hector, A., & Wardle, D. A. (2009). Biodiversity in forest carbon sequestration initiatives: not just a side benefit. *Current Opinion in Environmental Sustainability*, *1*(1), 55–60. https://doi.org/10.1016/j.cosust.2009.08.001

Dickey, D. A., & Fuller, W. A. (1979). Distribution of the Estimators for Autoregressive Time Series With a Unit Root. *Journal of the American Statistical Association*, *74*(366), 427–431. https://doi.org/10.2307/2286348

Dixon, R. K., Brown, S., Houghton, R. A., Solomon, A. M., Trexler, M. C., & Wisniewski, J. (1994). Carbon pools and flux of global forest ecosystems. *Science*, *263*(5144), 185–190. https://doi.org/10.1126/science.263.5144.185

Dormann, C. F., Elith, J., Bacher, S., Buchmann, C., Carl, G., Carré, G., … Lautenbach, S. (2013). Collinearity: A review of methods to deal with it and a simulation study evaluating their performance. Ecography, 36(1), 27–46. https://doi.org/10.1111/j.1600-0587.2012.07348.x

Erb, K. H., Kastner, T., Plutzar, C., Bais, A. L. S., Carvalhais, N., Fetzel, T., … Luyssaert, S. (2018). Unexpectedly large impact of forest management and grazing on global vegetation biomass. *Nature*, *553*(7686), 73–76. https://doi.org/10.1038/nature25138

Ferreira, J., Lennox, G. D., Gardner, T. A., Thomson, J. R., Berenguer, E., Lees, A. C., … Barlow, J. (2018). Carbon-focused conservation may fail to protect the most biodiverse tropical forests. *Nature Climate Change*, *8*(8), 744–749. https://doi.org/10.1038/s41558-018-0225-7

Fletcher, R., & Fortin, M. (2018). *Spatial ecology and conservation modeling*. Springer.

García-Palacios, P., Gross, N., Gaitán, J., & Maestre, F. T. (2018). Climate mediates the biodiversity–ecosystem stability relationship globally. *Proceedings of the National Academy of Sciences of the United States of America*, *115*(33), 8400–8405. https://doi.org/10.1073/pnas.1800425115

Gardner, T. A., Burgess, N. D., Aguilar-Amuchastegui, N., Barlow, J., Berenguer, E., Clements, T., … Vieira, I. C. G. (2012). A framework for integrating biodiversity concerns into national REDD+ programmes. *Biological Conservation*, *154*, 61–71. https://doi.org/10.1016/j.biocon.2011.11.018

Gatti, L. V., Basso, L. S., Miller, J. B., Gloor, M., Domingues, L. G., Cassol, H. L. G., … Neves, R. A. L. (2021). Amazonia as a carbon source linked to deforestation and climate change. *Nature*, *595*(July). https://doi.org/10.1038/s41586-021-03629-6

Kapos, V., Ravilious, C., Campbell, A., Dickson, B., Gibbs, H., Hansen, M., … Trumper, K. (2008). *Carbon and biodiversity: a demonstration atlas*. *UNEP-WCMC, Cambridge, UK.*

Kruid, S., Macedo, M. N., Gorelik, S. R., Walker, W., Moutinho, P., Brando, P. M., … Coe, M. T. (2021). Beyond Deforestation: Carbon Emissions From Land Grabbing and Forest Degradation in the Brazilian Amazon. *Frontiers in Forests and Global Change*, *4*(July). https://doi.org/10.3389/ffgc.2021.645282

Laurance, W. F., Fearnside, P. M., Laurance, S. G., Delamonica, P., Lovejoy, T. E., Rankin-de Merona, J. M., … Gascon, C. (1999). Relationship between soils and Amazon forest biomass. *Forest Ecology and Mangement*, *118*, 127–138. https://doi.org/10.1016/S0378-1127(98)00494-0

Legendre, P., & Legendre, L. F. J. (2012). *Numerical ecology*. Elsevier.

Magnago, L. F. S., Magrach, A., Laurance, W. F., Martins, S. V., Meira-Neto, J. A. A., Simonelli, M., & Edwards, D. P. (2015). Would protecting tropical forest fragments provide carbon and biodiversity cobenefits under REDD+? *Global Change Biology*, *21*(9), 3455–3468. https://doi.org/10.1111/gcb.12937

Melo, F. P. L., Pinto, S. R. R., Brancalion, P. H. S., Castro, P. S., Rodrigues, R. R.,

Aronson, J., & Tabarelli, M. (2013). Priority setting for scaling-up tropical forest restoration projects: Early lessons from the Atlantic forest restoration pact. *Environmental Science and Policy*, *33*, 395–404. https://doi.org/10.1016/j.envsci.2013.07.013

Murray, J. P., Grenyer, R., Wunder, S., Raes, N., & Jones, J. P. G. (2015). Spatial patterns of carbon, biodiversity, deforestation threat, and REDD+ projects in Indonesia. *Conservation Biology*, *29*(5), 1434–1445. https://doi.org/10.1111/cobi.12500

Myers, N., Mittermeier, R. A., Mittermeier, C. G., da Fonseca, G. A. B., & Kent, J. (2000). Biodiversity hotspots for conservation priorities. *Nature*, *403*(6772), 853–858. https://doi.org/10.1038/35002501

Pettorelli, N., Vik, J. O., Mysterud, A., Gaillard, J. M., Tucker, C. J., & Stenseth, N. C. (2005). Using the satellite-derived NDVI to assess ecological responses to environmental change. *Trends in Ecology and Evolution*. https://doi.org/10.1016/j.tree.2005.05.011

Phelps, J., Friess, D. A., & Webb, E. L. (2012). Win-win REDD+ approaches belie carbon-biodiversity trade-offs. *Biological Conservation*, *154*, 53–60. https://doi.org/10.1016/j.biocon.2011.12.031

Phelps, J., Webb, E. L., & Adams, W. M. (2012). Biodiversity co-benefits of policies to reduce forest-carbon emissions. *Nature Climate Change*, *2*(7), 497–503. https://doi.org/10.1038/nclimate1462

Pimm, S. L. (1984). The complexity and stability of ecosystems. *Nature*, *307*(5949), 321–326. https://doi.org/10.1038/307321a0

Pohlert, T. (2018). trend: Non-Parametric Trend Tests and Change-Point Detection. R package version 1.1.1. *Https://CRAN.R-Project.Org/Package=trend*.

Rezende, C. L., Scarano, F. R., Assad, E. D., Joly, C. A., Metzger, J. P., Strassburg, B. B. N., … Mittermeier, R. A. (2018). From hotspot to hopespot: An opportunity for the Brazilian Atlantic Forest. *Perspectives in Ecology and Conservation*, *16*(4), 208–214. https://doi.org/10.1016/j.pecon.2018.10.002

Ribeiro, M. C., Martensen, A. C., Metzger, J. P., Tabarelli, M., Scarano, F., & Fortin, M.-J. (2011). The Brazilian Atlantic Forest: a shrinking biodiversity hotspot. In *Biodiversity hotspots* (pp. 405–434). Springer.

Ribeiro, M. C., Metzger, J. P., Martensen, A. C., Ponzoni, F. J., & Hirota, M. M. (2009). The Brazilian Atlantic Forest: How much is left, and how is the remaining forest distributed? Implications for conservation. *Biological Conservation*, *142*(6), 1141–1153. https://doi.org/10.1016/j.biocon.2009.02.021

Saatchi, S., Houghton, R. A., Dos Santos Alvalá, R. C., Soares, J. V., & Yu, Y. (2007). Distribution of aboveground live biomass in the Amazon basin. *Global Change Biology*, *13*(4), 816–837. https://doi.org/10.1111/j.1365-2486.2007.01323.x

Sales, L. P., Galetti, M., & Pires, M. M. (2020). Climate and land-use change will lead to a faunal "savannization" on tropical rainforests. *Global Change Biology*, *26*(12), 7036–7044. https://doi.org/10.1111/gcb.15374

Sattler, D., Murray, L. T., Kirchner, A., & Lindner, A. (2014). Influence of soil and topography on aboveground biomass accumulation and carbon stocks of afforested pastures in South East Brazil. *Ecological Engineering*, *73*, 126–131. https://doi.org/10.1016/j.ecoleng.2014.09.003

Soto-Navarro, C., Ravilious, C., Arnell, A., De Lamo, X., Harfoot, M., Hill, S. L. L., … Kapos, V. (2020). Mapping co-benefits for carbon storage and biodiversity to inform conservation policy and action. *Philosophical Transactions of the Royal Society B: Biological Sciences*, *375*(1794). https://doi.org/10.1098/rstb.2019.0128

Spawn, S. A., Sullivan, C. C., Lark, T. J., & Gibbs, H. K. (2020). Harmonized global maps of above and belowground biomass carbon density in the year 2010. *Scientific Data*, *7*(1), 1–22. https://doi.org/10.1038/s41597-020-0444-4

Sullivan, M. J. P., Lewis, S. L., Affum-Baffoe, K., Castilho, C., Costa, F., Sanchez, A. C., … Phillips, O. L. (2020). Long-term thermal sensitivity of Earth's tropical forests. *Science*, *in press*(800), 869–874. https://doi.org/10.1126/science.aaw7578

Sullivan, M. J. P., Talbot, J., Lewis, S. L., Phillips, O. L., Qie, L., Begne, S. K., … Zemagho, L. (2017). Diversity and carbon storage across the tropical forest biome.

Scientific Reports, *7*(July 2016), 1–12. https://doi.org/10.1038/srep39102

Tabarelli, M., Pinto, L. P., Silva, J. M. C., Hirota, M., & Bedê, L. (2005). Challenges and Opportunities for Biodiversity Conservation in the Brazilian Atlantic Forest. *Conservation Biology*, *19*(3), 695–700. https://doi.org/https://doi.org/10.1111/j.1523-1739.2005.00694.x

UNEP-WCMC and IUCN (2022), Protected Planet: The World Database on Protected Areas (WDPA) and World Database on Other Effective Area-based Conservation Measures (WD-OECM) [Online], February 2022, Cambridge, UK: UNEP-WCMC and IUCN. Available at: www.protectedplanet.net.

Venter, O., & Koh, L. P. (2012). Reducing emissions from deforestation and forest degradation (REDD+): Game changer or just another quick fix? *Annals of the New York Academy of Sciences*, *1249*(1), 137–150. https://doi.org/10.1111/j.1749-6632.2011.06306.x

Verbesselt, J., Umlauf, N., Hirota, M., Holmgren, M., Van Nes, E. H., Herold, M., … Scheffer, M. (2016). Remotely sensed resilience of tropical forests. *Nature Climate Change*, *6*(11), 1028–1031. https://doi.org/10.1038/nclimate3108

Verdone, M., & Seidl, A. (2017). Time, space, place, and the Bonn Challenge global forest restoration target. *Restoration Ecology*, *25*(6), 903–911. https://doi.org/10.1111/rec.12512

Vilela, B., & Villalobos, F. (2015). letsR: a new R package for data handling and analysis in macroecology. *Methods in Ecology and Evolution*, *6*(10), 1229–1234. https://doi.org/https://doi.org/10.1111/2041-210X.12401

Wood, S. N. (2017). Generalized additive models: an introduction with R. New York: Chapman and Hall/CRC. https://doi.org/https://doi.org/10.1201/9781315370279

Wood, S. N., Pya, N., and Säfken, B. (2016). Smoothing Parameter and Model Selection for General Smooth Models. Journal of the American Statistical Association, 111(516), 1548–1563. https://doi.org/10.1080/01621459.2016.1180986

Xu, L., Saatchi, S. S., Yang, Y., Yu, Y., Pongratz, J., Bloom, A. A., … Schimel, D. (2021). Changes in global terrestrial live biomass over the 21st century. *Science Advances, 7*(27), eabe9829. https://doi.org/10.1126/sciadv.abe9829

TABLES

Table 1. Biodiversity and carbon content in hotspots and their proportion of unprotected area in high and low forest stability.

		High forest stability	Low forest stability
Biodiversity	spp	860 (58.50%)	896 (60.95%)
	Unprotected	29.65%	95.12%
Carbon	Carbon (MgC)	4,916,254,182.04 (40.90%)	1,274,955,021.08 (10.60%)
	Unprotected	75.72%	91.08%
Biodiversity-carbon	spp	860 (58.50%)	776 (52.79%)
	Carbon (MgC)	729,776,935.84 (6.06%)	7,823,610.29 (0.06%)
	Unprotected	25.32%	83.71%

FIGURES

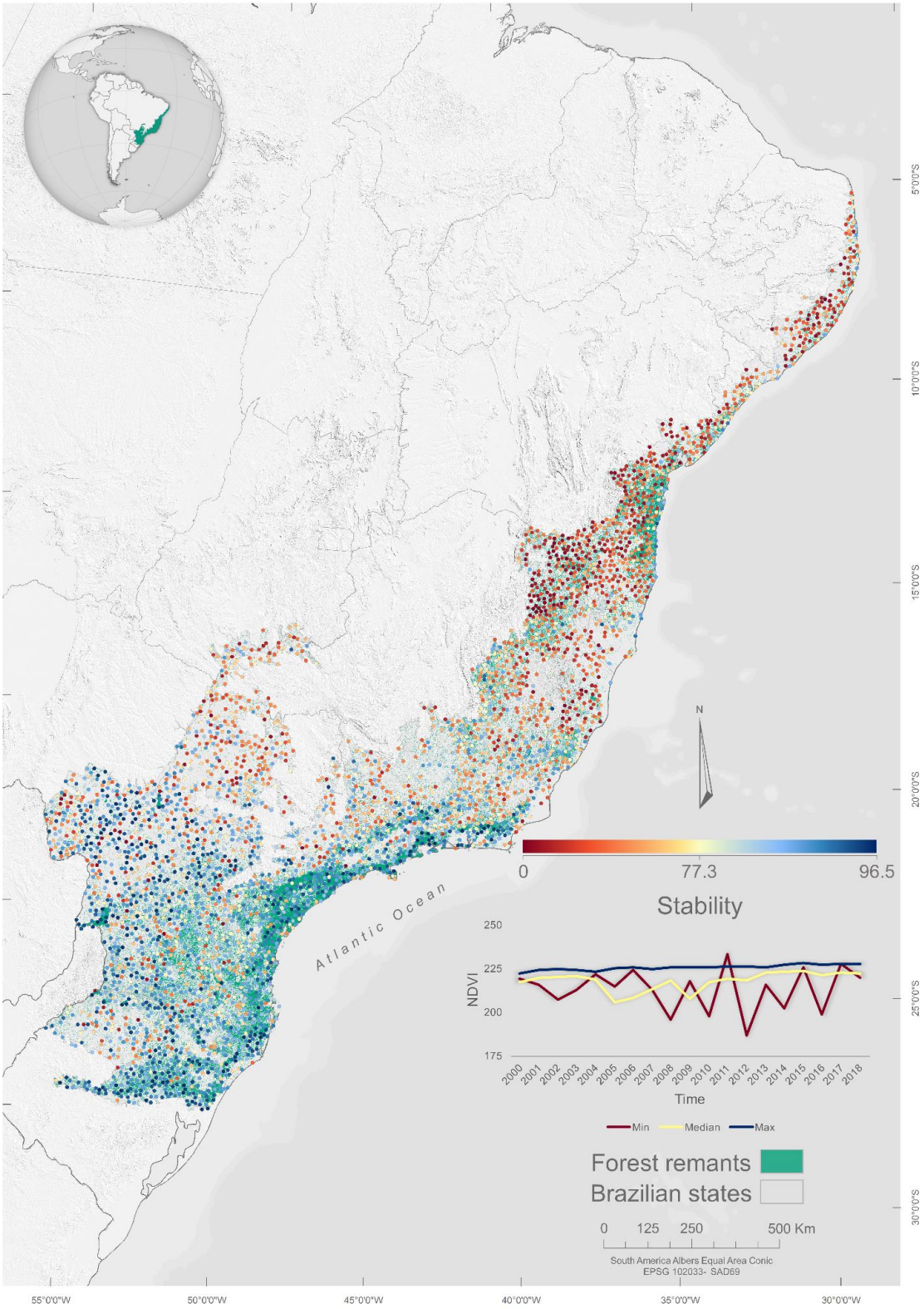

Figure 1. Distribution of 3,934 sample sites of old-growth forests in the Atlantic Forest. The color of the points represents its stability value that ranges from 0 (red) to 96.5 (blue) with a mean value of 77.3 (yellow). The graph shows the raw NDVI time-series of the points with the highest (blue), median (yellow) and lowest (red) stability. Forest remnants (green) are areas that remain classified as forests between 1985-2018, that is, forest with at least 33 years old.

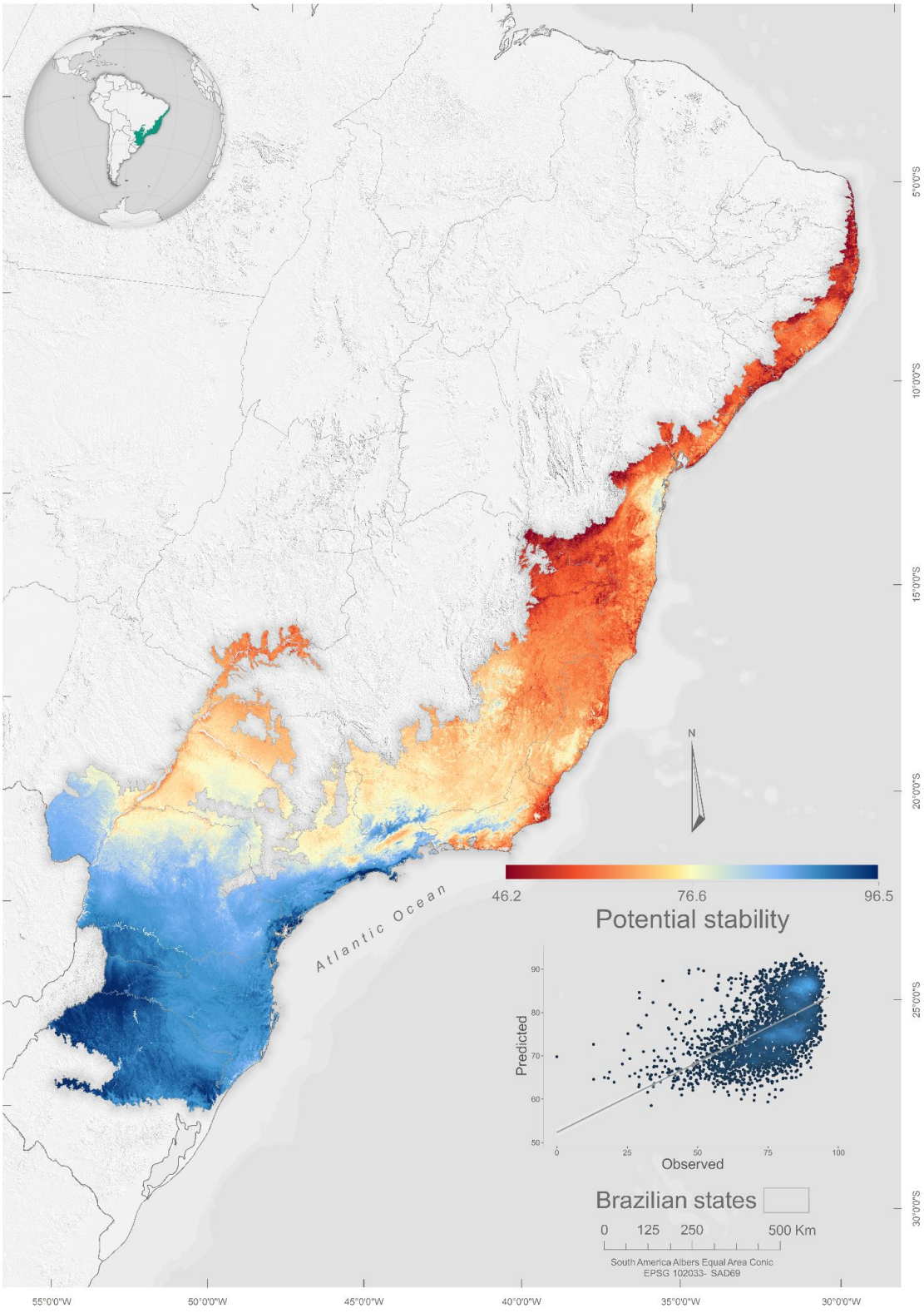

Figure 2. Prediction map of the potential stability of old-growth forests in Atlantic Forest ranges from 46.2 (red) to 96.5 (blue) with a mean value of 76.6 (yellow). The graph shows the linear relationship between predicted and observed stability (Pearson's correlation, r = 0.56).

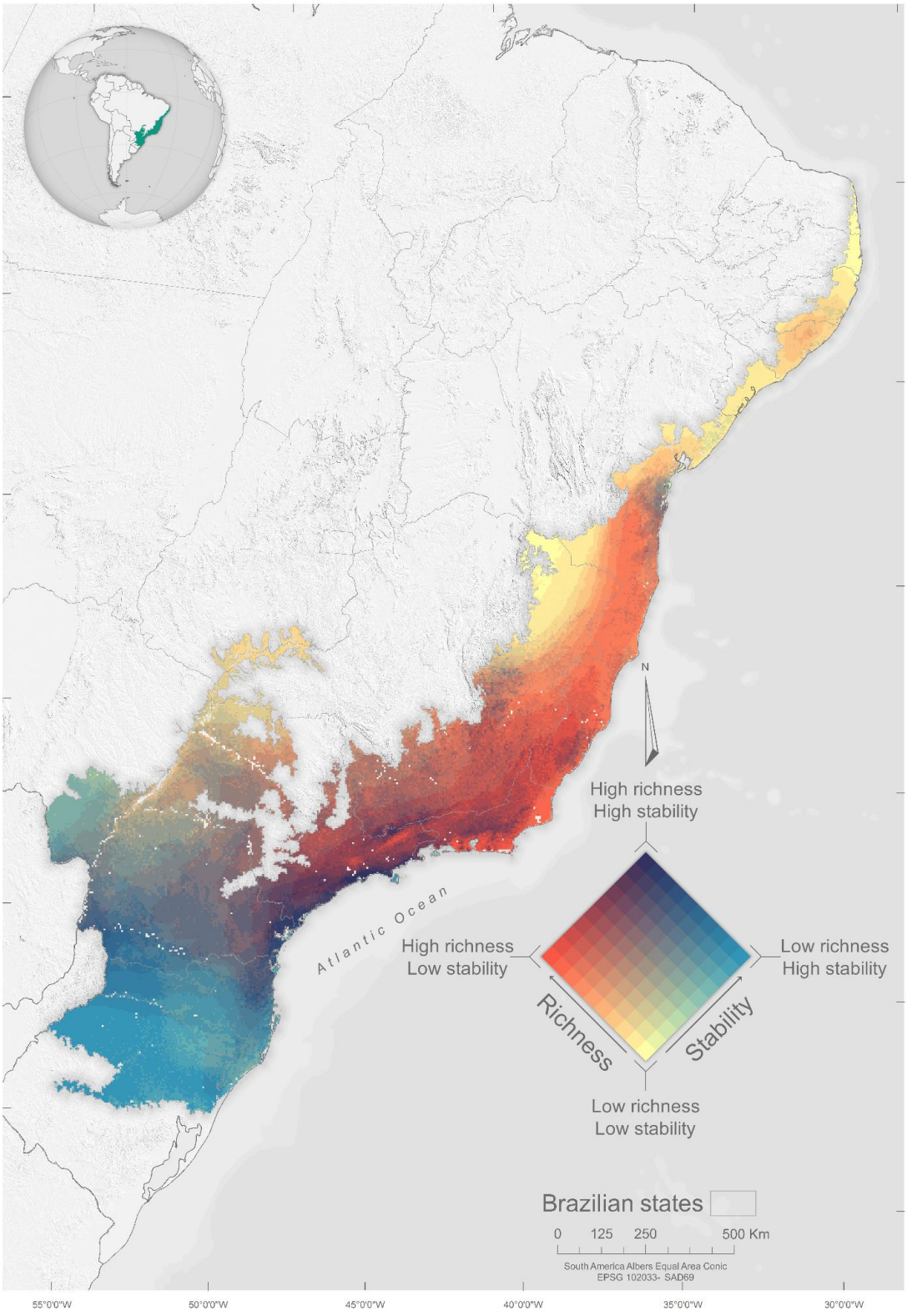

Figure 3. Bivariate map overlapping the 10% quantile classes of the species richness of forest-specialists (birds, mammals and amphibians) (yellow to red) and potential stability values (yellow to blue).

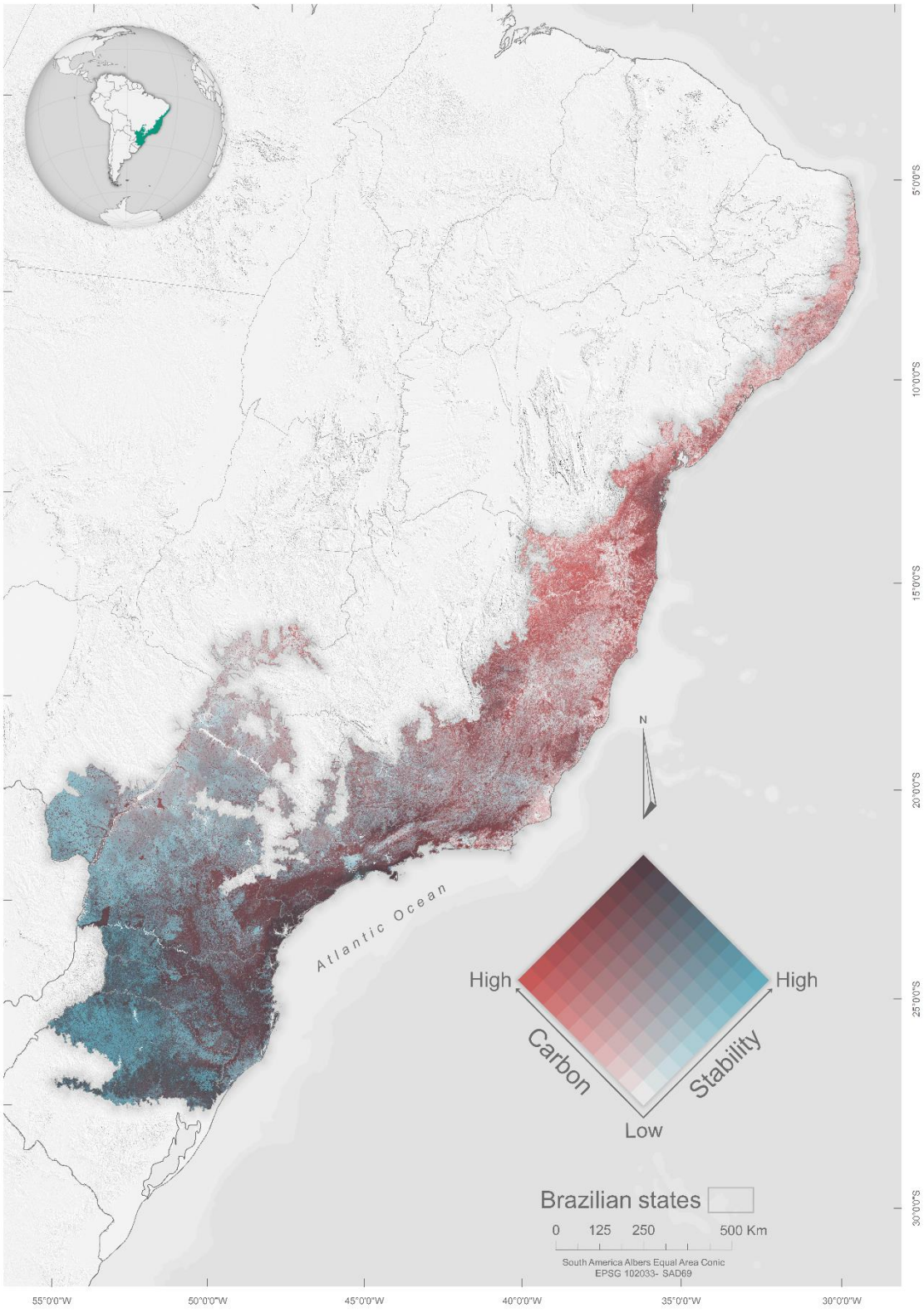

Figure 4. Bivariate map overlapping the 10% quantile classes of the carbon density (MgC/ha) (gray to red) and potential stability values (gray to blue).

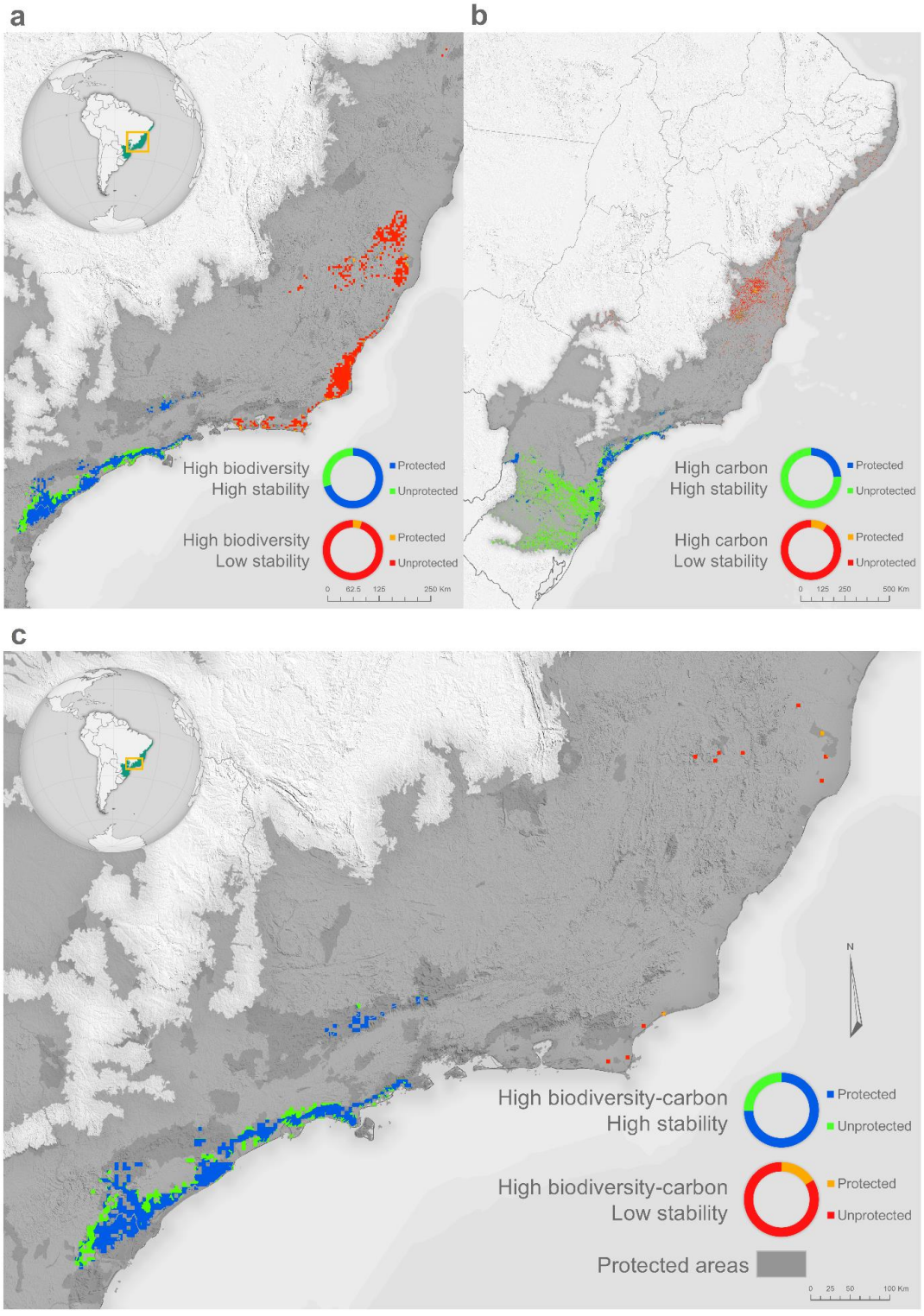

Figure 5. Hotspot maps showing areas of the highest (green and blue) and lowest (red and orange) 20% values of potential stability combined with the highest 20% values of biodiversity (a), carbon density (b), and the overlap areas of the biodiversity and carbon hotspots (c) where conservation co-benefit both. The three maps show four classes that represent high stability hotspots in protected (blue: 70.35% for biodiversity (a), 24.27% for carbon (b) and 74.68% for co-benefit (c) maps) and unprotected areas (green: 29.64% for biodiversity (a), 75.72% for carbon (b) and 25.31% for co-benefit (c) maps) and low stability hotspots in protected (orange: 4.88% for biodiversity (a), 8.92% for carbon (b) and 16.28% for co-benefit

(c) maps) and unprotected areas (red: 95.11% for biodiversity (a), 91.07% for carbon (b) and 83.71% for co-benefit (c) maps). Circular graphs show the proportion of protected and unprotected areas of the hotspots. Other protection areas are found as dark gray.

Supporting information

Biodiversity and carbon conservation under the ecosystem stability of tropical forests

Lucas Andrigo Maure[1,2], Milena Fiuza Diniz[3], Marco Túlio Pacheco Coelho[4], Paulo Guilherme Molin[5], Fernando Rodrigues da Silva[2], Erica Hasui[6]*

[1]Programa de Pós-graduação em Ecologia e Recursos Naturais (PPGERN), Universidade Federal de São Carlos, São Carlos-SP, Brazil

[2]Laboratório de Ecologia Teórica: Integrando Tempo, Biologia e Espaço (LET.IT.BE), Departamento de Ciências Ambientais, Universidade Federal de São Carlos, Sorocaba-SP, Brazil

[3]Departamento de Ecologia, Universidade Federal de Goiás, Goânia-GO, Brazil

[4]Swiss Federal Institute for Forest, Snow and Landscape, Birmensdorf, Switzerland

[5]Centro de Ciências da Natureza, Universidade Federal de São Carlos, Buri-SP, Brasil

[6]Laboratório de Ecologia de Fragmentos (EcoFrag), Instituto de Ciências da Natureza, Universidade Federal de Alfenas-MG, Brazil

***Corresponding author:** ericahasui@gmail.com

1. METHODS

1.1 Predictors

Climatic variables – we selected 21 climatic predictors, 19 bioclimatic variables and two additional variables of water vapor pressure and solar radiation, at the resolution of 30 seconds (~1 km) from the WorldClim v2.1 database (Fick & Hijmans, 2017).

Soil variables – we selected 15 variables that comprise physicochemical parameters of the soil at 250 m resolution and at 5 cm depth from the SoilGrid database (Hengl et al., 2017). Plant productivity is strongly influenced within a soil column of 0-16 cm (Goebes et al., 2019). Only for soil organic carbon stock in tons per ha (OCSTHA_30cm) the lowest available depth was at 30 cm.

Topography – we used 3 topographic variables. We obtained elevation data from SRTM Digital Elevation Database v4.1 (Jarvis, Reuter, Nelson, & Guevara, 2008) of the Consortium for Spatial Information (CGIAR-CSI) at a spatial resolution of 250 m. We used elevation data to calculate the two other topographic variables. We measured topographic heterogeneity by the elevation standard deviation in a spatial moving window of 3x3 cells. Topographic heterogeneity is an index for the elevation variability within an area (Amatulli et al., 2018). Because topographic heterogeneity is a driver of habitat diversity and, biotic and abiotic ecosystem processes such as water and nutrient availability, it is related to tropical forest structure, biomass and species distribution (Alves et al., 2010; Larkin, Vivian-smith, & Zedler, 2006; Muscarella, Kolyaie, Morton, Zimmerman, & Uriarte, 2020). We calculated topographic wetness index as $TWI = \ln(\alpha / \tan\beta + C)$, where α is flow accumulation, β is the slope and C is a constant of 0.001. By measuring the topographic control on hydrological processes, topographic wetness index expresses the terrain drainage and soil moisture and can predict vegetation type

and plant species richness, distribution, composition and growth (Kopecký & Čížková, 2010; Méndez-Toribio, Meave, Zermeño-Hernández, & Ibarra-Manríquez, 2016; Svenning, Kinner, Stallard, Engelbrecht, & Wright, 2004).

We reprojected all raster maps used in the response and predictor variables to South America Albers Equal Area Conic. We also resampled predictors data to a spatial resolution of 250 m using bilinear interpolation. All geoprocessing was performed using ArcGIS (10.6.1).

1.2 Potential stability map

The regression equation for potential stability map was: *stability* = 77.8416854 + (-0.3096654 * Isothermality) + 0.0381966 * Temperature Seasonality + (-0.0035819 * Mean Temperature of Coldest Quarter) + 0.0068351 * Annual Precipitation + (-0.0019555 * Absolute depth to bedrock) + 0.0258696 * Soil organic carbon stock.

2. DISCUSSION

In subtropical regions where temperature seasonality or the amplitude of the annual cycle of temperature is higher, plants have high efficiency of light use and present relatively low evapotranspiration. These plant and forest attributes may contribute to high canopy photosynthetic rates and constant intra and interannual NDVI of the forests, such as the forests in southern Atlantic Forest (Cristiano et al., 2014; Zhang et al., 2016).

On the other hand, isothemality, that is, the diurnal temperature oscillation relative to the annual temperature oscillations, decreases from north to south in the

Brazilian Atlantic Forest, along with the mean annual temperature ($r = 0.58$, $p < 0.001$; Pearson's correlation for sampling sites data). In this sense, forests in regions of high isothermality in the Brazilian Atlantic Forest are less stable due to the condition of physiological stress caused by constant elevated diurnal and annual temperatures. In tropical forests, plant evapotranspiration increases at elevated diurnal temperatures, triggering stomatal closure to reduce water loss (Doughty & Goulden, 2009; Goulden et al., 2004; Pau et al., 2018). Trees also display this ecophysiological response to avoid water loss in hydraulic stress due to the low precipitation.

In both cases of elevated diurnal temperatures and hydraulic stress, stomata closure constrains the photosynthesis rate and primary productivity and, for a prolonged time, increases the mortality risk of trees by carbon starvation or hydraulic failure (McDowell et al., 2018; Oliveira et al., 2021; Rowland et al., 2015). Therefore, temperature oscillation and precipitation ameliorate the stressful conditions that restrict productivity and promote the ecosystem stability of the old-growth forests in the Brazilian Atlantic Forest. The strong influence of the climate predictors on stability suggests a vulnerable condition of the old-growth forests to climate change.

Edaphic predictors also influence the spatial variation of stability, which increases with soil organic carbon content and decreases with depth to bedrock. Because carbon is a fundamental element in formation of plant cell and tissue, and for growth, soil organic carbon is positively associated with aboveground biomass of trees in tropical forests (Lambers, III, & Pons, 2008; Laurance et al., 1999). Moreover, soil organic carbon content presents a positive feedback relationship with plant production and is an important factor in controlling soil fertility (Jobbágy & Jackson, 2000).

APPENDICES:

Appendix S1. All the 39 predictors selected a priori and the effect of their category on plant productivity.

Category	Variable	Description	Effect on plant productivity
Climate			
	BIO1	Annual Mean Temperature	Temperature and precipitation affect plant productivity by ecophysiological responses that constrains photosynthesis. Higher temperature increases plant evaporation leading to stomatal closure reducing photosynthesis and the net primary productivity, forest growth, and above ground biomass (Baldocchi & Amthor, 2001; Clark, 2004; Cowling & Shin, 2006; Feeley, Joseph Wright, Nur Supardi, Kassim, & Davies, 2007; Sullivan et al., 2020). Water stress caused by low precipitation also increases the time of stomatal closure to avoid plant water loss, reducing plant productivity and growth. In extreme situations, water stress increases the mortality risk by hydraulic failure and carbon starvation (da Costa et al., 2010; McDowell et al., 2018, 2008; Nepstad, 2002; Oliveira et al., 2021).
	BIO2	Mean Diurnal Range (Mean of monthly (max temp - min temp))	
	BIO3	Isothermality (BIO2/BIO7) (×100)	
	BIO4	Temperature Seasonality (standard deviation ×100)	
	BIO5	Max Temperature of Warmest Month	
	BIO6	Min Temperature of Coldest Month	
	BIO7	Temperature Annual Range (BIO5-BIO6)	
	BIO8	Mean Temperature of Wettest Quarter	
	BIO9	Mean Temperature of Driest Quarter	
	BIO10	Mean Temperature of Warmest Quarter	
	BIO11	Mean Temperature of Coldest Quarter	
	BIO12	Annual Precipitation	
	BIO13	Precipitation of Wettest Month	
	BIO14	Precipitation of Driest Month	
	BIO15	Precipitation Seasonality (Coefficient of Variation)	
	BIO16	Precipitation of Wettest Quarter	
	BIO17	Precipitation of Driest Quarter	
	BIO18	Precipitation of Warmest Quarter	
	BIO19	Precipitation of Coldest Quarter	
	Vapr	Water vapor pressure (kPa)	
	Srad	Solar Radiation (kJ m-2 day-1)	
Soil			Edaphic chemical parameters determine nutrients availability, water content, and stressor conditions (Jakovac, Peña-Claros, Kuyper, & Bongers, 2015; Laurance et al., 1999; Poorter et al., 2016; Santiago-García, Finegan, & Bosque-Pérez, 2019). Whilst, edaphic physical parameters like soil texture control the roots growth and length, affecting plant nutrients and water uptake (Bengough, 2003; Bennett, Penman, Arndt, Roxburgh, & Bennett, 2020; Stirzaker, Passioura, & Wilms, 1996). Both physical and chemical soil parameters influence biomass and forest structure distribution, and recovery in second-growth tropical forests (Jakovac et al.,
	AWCtS	Derived saturated water content (volumetric fraction) teta-S	
	BDRLOG	Probability of occurrence of R horizon	
	BDTICM	Absolute depth to bedrock	
	BLDFIE	Bulk density (fine earth)	
	CECSOL	Cation exchange capacity (CEC)	
	CLYPPT	Clay content (0-2 micro meter) mass fraction	
	OCDENS	Soil organic carbon density in kg per cubic-m at depth 0.05 m	
	OCSTHA_30cm	Soil organic carbon stock in tons per ha	
	OCSTHA_sd2	Soil organic carbon stock	
	ORCDRC	Soil organic carbon content (fine earth fraction)	
	PHIHOX	Soil pH in H2O	

	PHIKCL	Soil pH x 10 in KCl	2015; Poorter et al., 2016; Santiago-García et al., 2019).
	SLTPPT	Silt content (2-50 micro meter) mass fraction	
	SNDPPT	Sand content (50-2000 micro meter) mass fraction	
	WWP	Derived available soil water capacity (volumetric fraction) until wilting point	
Topographic			Topography modulates climate and determine water and nutrient availability in soil affecting tree productivity, biomass and forest structure in the tropics (de Castilho et al., 2006; Ediriweera, Singhakumara, & Ashton, 2008; Kitayama & Aiba, 2002; Raich, Russell, & Vitousek, 1997; Sattler, Murray, Kirchner, & Lindner, 2014).
	Elevation	Altitude (m)	
	Topographic heterogeneity (TH)	Standard deviation of elevation measures the elevational variability within an area	
	Terrain wetness index (TWI)	Quantify topographic control on hydrological processes	

Appendix S2. Variance inflation factor (VIF) of selected predictors for analysis.

Predictor	VIF
BIO3	3.36
BIO4	4.93
BIO11	3.01
BIO12	1.85
BDTICM	1.92
OCSTHA_30cm	1.80

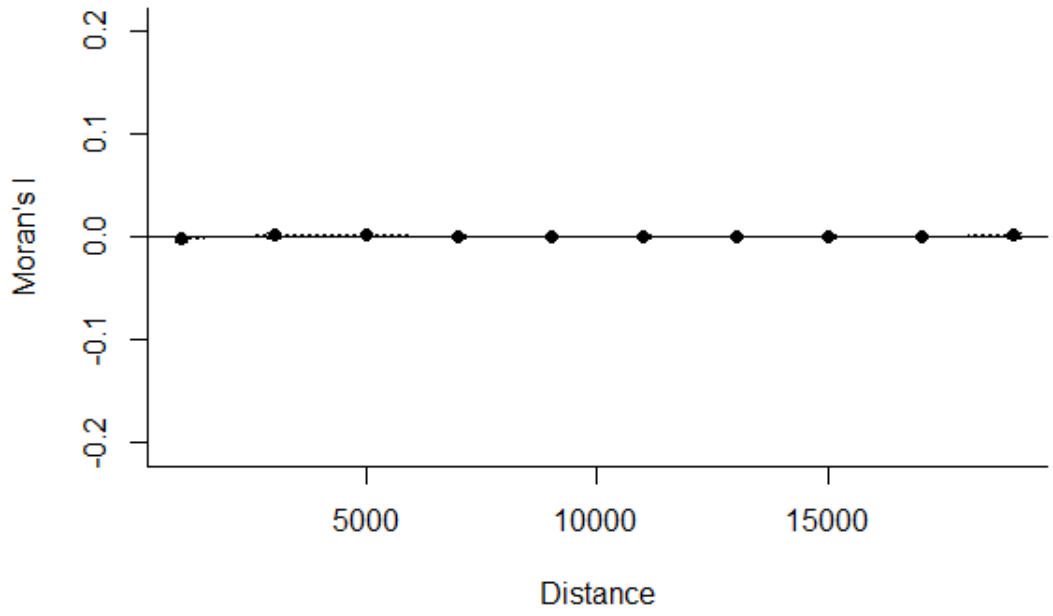

Appendix S3. Correlogram of the Moran's index for the residuals of the linear regression of selected predictors and stability indicating no spatial autocorrelation (p = 0.57) in a distance range of 20000 m between sample points.

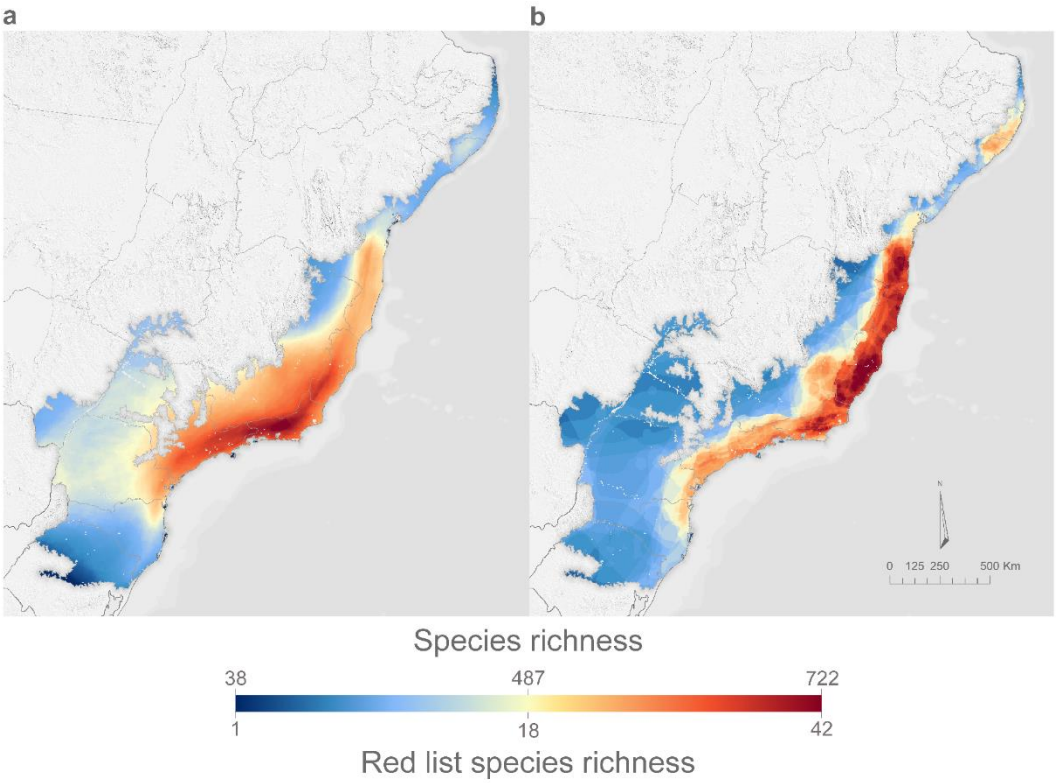

Appendix S4. Maps of species richness (a) and richness of threatened species (b). Threatened species are in the IUCN red list in the categories of critically endangered (CE), endangered (EN), and vulnerable (VU). Both maps were built using ranges of forest-specialist species of birds, mammals and amphibians from IUCN.

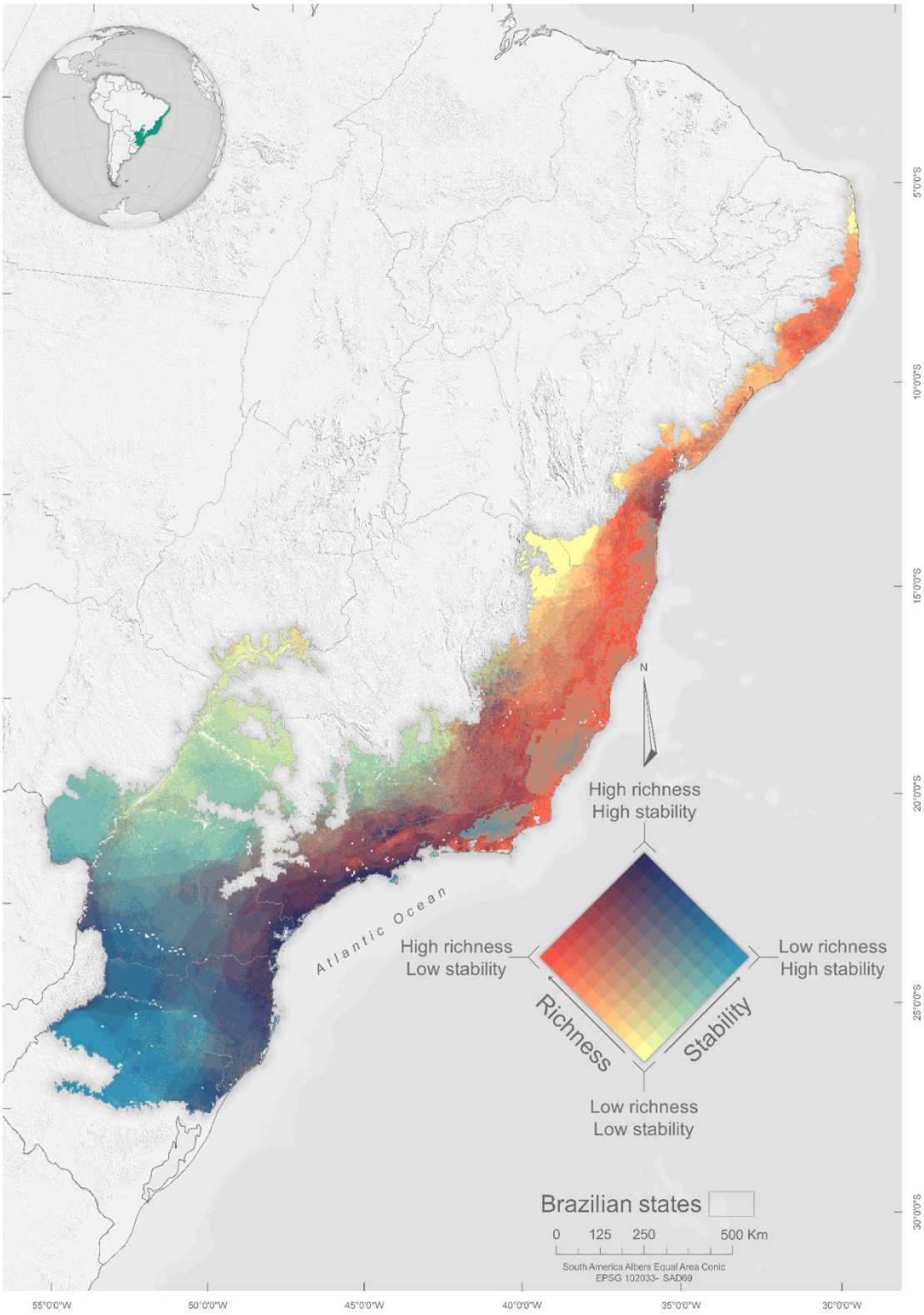

Appendix S5. Bivariate map of the combination of the 10% quantile classes of richness of threatened species (birds, mammals and amphibians) (yellow to red) and potential stability values (yellow to blue).

Appendix S6. Selection of 65 models emerging from the combination of the six predictors of stability.

Models	df	logLik	AICc	ΔAICc	weight
Stability ~ BDTICM + OCSTHA_M_30cm + BIO12 + BIO3 + BIO4	7	-14695.217	29404.463	0.000	0.719
Stability ~ BDTICM + OCSTHA_M_30cm + BIO11 + BIO12 + BIO3 + BIO4	8	-14695.207	29406.450	1.987	0.266
Stability ~ BDTICM + BIO12 + BIO3 + BIO4	6	-14700.532	29413.086	8.623	0.010
Stability ~ BDTICM + BIO11 + BIO12 + BIO3 + BIO4	7	-14700.064	29414.156	9.692	0.006
Stability ~ BDTICM + OCSTHA_M_30cm + BIO12 + BIO4	6	-14712.131	29436.284	31.820	0.000
Stability ~ BDTICM + OCSTHA_M_30cm + BIO11 + BIO12 + BIO4	7	-14712.126	29438.280	33.817	0.000
Stability ~ OCSTHA_M_30cm + BIO11 + BIO12 + BIO3 + BIO4	7	-14720.524	29455.077	50.613	0.000
Stability ~ BDTICM + BIO12 + BIO4	5	-14722.690	29455.395	50.932	0.000
Stability ~ BDTICM + BIO11 + BIO12 + BIO4	6	-14721.865	29455.752	51.289	0.000
Stability ~ BDTICM + OCSTHA_M_30cm + BIO11 + BIO12 + BIO3	7	-14721.100	29456.229	51.766	0.000
Stability ~ OCSTHA_M_30cm + BIO12 + BIO3 + BIO4	6	-14722.139	29456.300	51.837	0.000
Stability ~ BDTICM + BIO11 + BIO12 + BIO3	6	-14723.091	29458.203	53.740	0.000
Stability ~ BIO11 + BIO12 + BIO3 + BIO4	6	-14723.531	29459.083	54.619	0.000
Stability ~ BIO12 + BIO3 + BIO4	5	-14726.546	29463.108	58.645	0.000
Stability ~ BDTICM + OCSTHA_M_30cm + BIO12 + BIO3	6	-14730.035	29472.092	67.629	0.000
Stability ~ BDTICM + BIO12 + BIO3	5	-14734.295	29478.605	74.142	0.000
Stability ~ OCSTHA_M_30cm + BIO11 + BIO12 + BIO4	6	-14738.050	29488.121	83.658	0.000
Stability ~ OCSTHA_M_30cm + BIO12 + BIO4	5	-14739.621	29489.258	84.795	0.000
Stability ~ BDTICM + OCSTHA_M_30cm + BIO3 + BIO4	6	-14739.554	29491.130	86.667	0.000
Stability ~ BDTICM + OCSTHA_M_30cm + BIO11 + BIO3 + BIO4	7	-14739.371	29492.770	88.307	0.000
Stability ~ BIO11 + BIO12 + BIO4	5	-14745.094	29500.203	95.740	0.000
Stability ~ BIO12 + BIO4	4	-14748.935	29505.880	101.417	0.000
Stability ~ OCSTHA_M_30cm + BIO3 + BIO4	5	-14764.286	29538.586	134.123	0.000
Stability ~ OCSTHA_M_30cm + BIO11 + BIO3 + BIO4	6	-14763.776	29539.574	135.111	0.000
Stability ~ BIO11 + BIO12 + BIO3	5	-14766.530	29543.076	138.613	0.000
Stability ~ OCSTHA_M_30cm + BIO11 + BIO12 + BIO3	6	-14766.350	29544.721	140.258	0.000
Stability ~ BDTICM + OCSTHA_M_30cm + BIO4	5	-14768.316	29546.647	142.183	0.000
Stability ~ BDTICM + OCSTHA_M_30cm + BIO11 + BIO4	6	-14768.020	29548.061	143.598	0.000
Stability ~ BDTICM + BIO11 + BIO3 + BIO4	6	-14773.427	29558.875	154.412	0.000
Stability ~ BDTICM + BIO3 + BIO4	5	-14774.489	29558.993	154.530	0.000
Stability ~ BDTICM + OCSTHA_M_30cm + BIO11 + BIO3	6	-14773.535	29559.091	154.628	0.000
Stability ~ BDTICM + OCSTHA_M_30cm + BIO3	5	-14781.205	29572.426	167.963	0.000
Stability ~ BDTICM + OCSTHA_M_30cm + BIO11 + BIO12	6	-14789.859	29591.740	187.277	0.000
Stability ~ BIO11 + BIO3 + BIO4	5	-14791.972	29593.959	189.496	0.000
Stability ~ OCSTHA_M_30cm + BIO4	4	-14793.455	29594.920	190.457	0.000
Stability ~ OCSTHA_M_30cm + BIO11 + BIO4	5	-14793.084	29596.183	191.720	0.000
Stability ~ BIO3 + BIO4	4	-14795.836	29599.683	195.220	0.000
Stability ~ BDTICM + BIO11 + BIO12	5	-14796.799	29603.613	199.150	0.000

Stability ~ BDTICM + BIO11 + BIO3	5	-14800.051	29610.117	205.654	0.000
Stability ~ OCSTHA_M_30cm + BIO12 + BIO3	5	-14809.431	29628.877	224.414	0.000
Stability ~ BIO12 + BIO3	4	-14811.604	29631.219	226.755	0.000
Stability ~ BDTICM + BIO3	4	-14815.685	29639.380	234.917	0.000
Stability ~ OCSTHA_M_30cm + BIO11 + BIO3	5	-14820.523	29651.061	246.598	0.000
Stability ~ BDTICM + OCSTHA_M_30cm + BIO12	5	-14831.280	29672.574	268.111	0.000
Stability ~ BDTICM + BIO11 + BIO4	5	-14832.163	29674.342	269.879	0.000
Stability ~ BDTICM + BIO4	4	-14834.466	29676.942	272.479	0.000
Stability ~ BIO11 + BIO3	4	-14837.608	29683.227	278.763	0.000
Stability ~ BIO11 + BIO4	4	-14849.043	29706.097	301.633	0.000
Stability ~ BDTICM + BIO12	4	-14852.480	29712.971	308.507	0.000
Stability ~ BIO4	3	-14854.881	29715.768	311.305	0.000
Stability ~ OCSTHA_M_30cm + BIO3	4	-14861.223	29730.457	325.994	0.000
Stability ~ OCSTHA_M_30cm + BIO11 + BIO12	5	-14865.085	29740.186	335.723	0.000
Stability ~ BIO11 + BIO12	4	-14867.642	29743.294	338.831	0.000
Stability ~ BIO3	3	-14888.717	29783.440	378.976	0.000
Stability ~ BDTICM + OCSTHA_M_30cm + BIO11	5	-14889.674	29789.364	384.901	0.000
Stability ~ BDTICM + OCSTHA_M_30cm	4	-14942.499	29893.008	488.544	0.000
Stability ~ BDTICM + BIO11	4	-14970.326	29948.661	544.198	0.000
Stability ~ OCSTHA_M_30cm + BIO11	4	-14980.585	29969.181	564.717	0.000
Stability ~ BIO11	3	-15046.958	30099.923	695.459	0.000
Stability ~ OCSTHA_M_30cm + BIO12	4	-15051.936	30111.882	707.418	0.000
Stability ~ BIO12	3	-15079.802	30165.610	761.147	0.000
Stability ~ BDTICM	3	-15101.268	30208.542	804.079	0.000
Stability ~ OCSTHA_M_30cm	3	-15222.126	30450.257	1045.794	0.000
Stability ~ NA + NA + NA + NA + NA + NA	2	-15464.498	30932.999	1528.536	0.000

Appendix S7. Averaged coefficients of predictors (BIO3 = isothermality, BIO4 = temperature seasonality, BIO11 = mean temperature of coldest quarter, BIO12 = annual precipitation, BDTICM = absolute depth to bedrock, and OCSTHA_30cm = soil organic carbon stock in tons per ha) of the best performing models for stability.

	B	***SE***	***t***	***P***
Intercept	77.841	4.633	16.796	< 0.001 ***
BDTICM	-0.002	0.000	7.292	< 0.001***
OCSTHA_30cm	0.026	0.008	3.218	0.001 **
BIO12	0.007	0.001	9.454	< 0.001 ***
BIO3	-0.310	0.053	5.822	< 0.001 ***
BIO4	0.038	0.005	8.005	< 0.001***
BIO11	-0.004	0.048	0.075	0.940

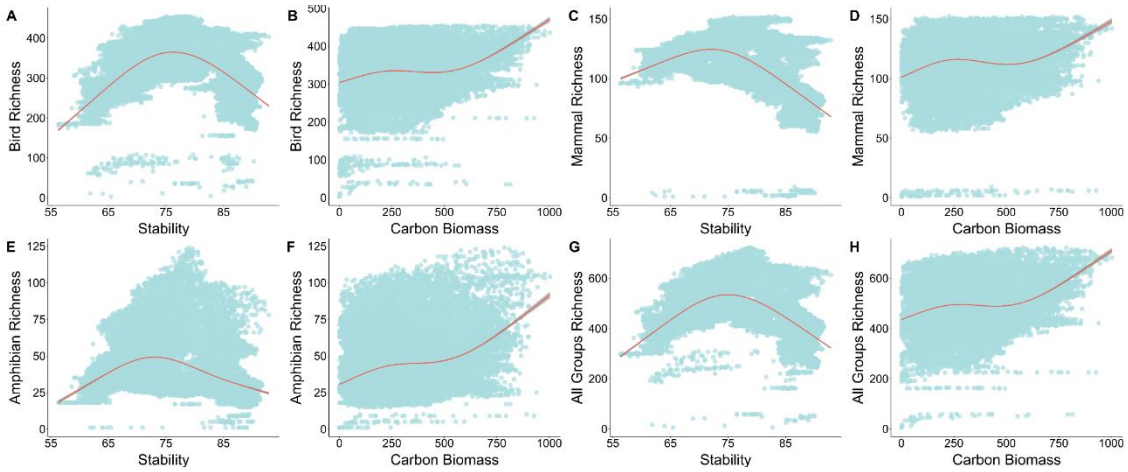

Appendix S8. Richness of birds, mammals, amphibians and all groups related to stability (A, C, E and G) and carbon biomass (carbon density (MgC/ha)) (B, D, F, and H). Red line represents the smoothed trend fitted by a generalized additive model (GAM) and confidence interval is given as shade.

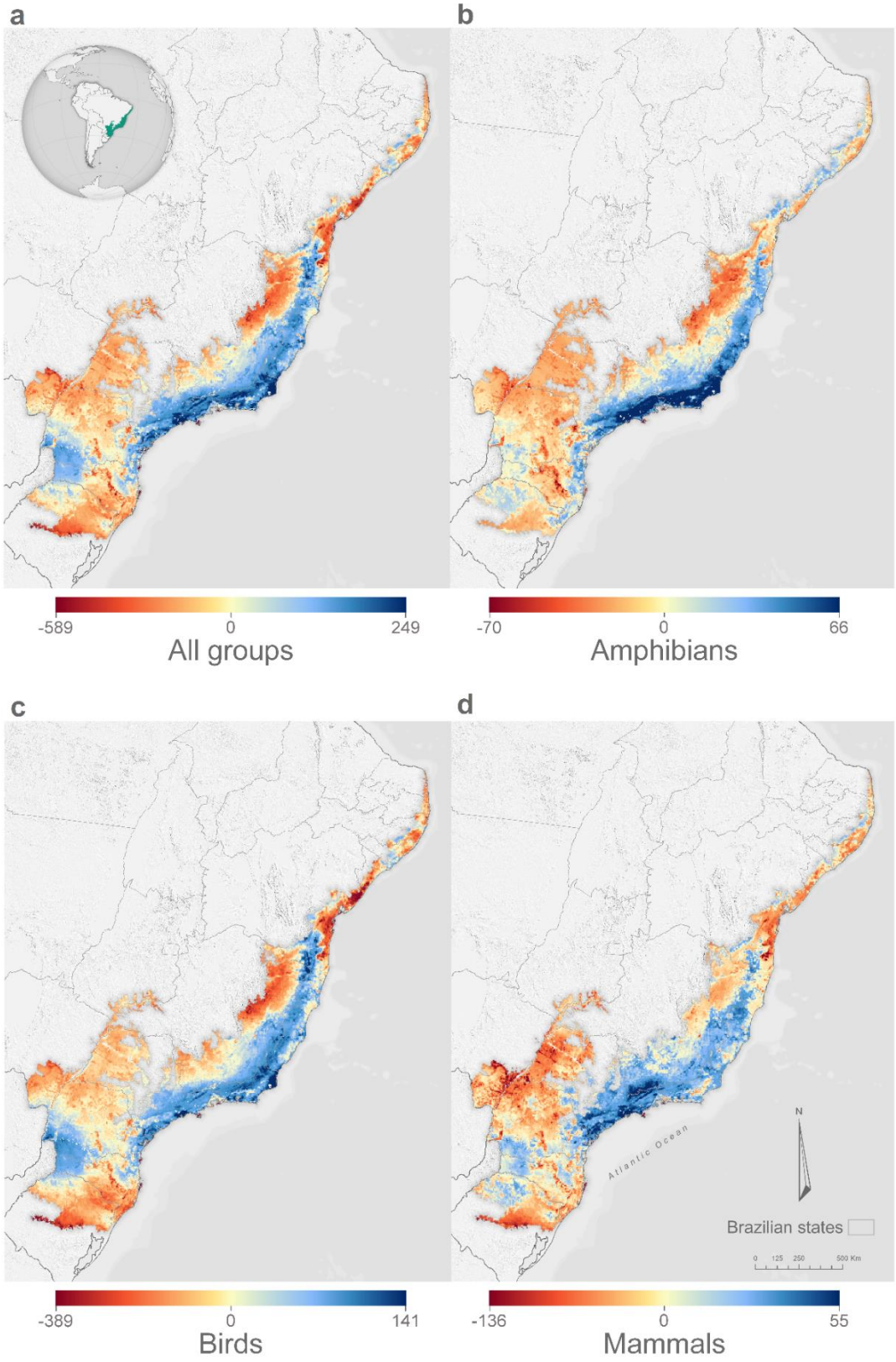

Appendix S9. Uncertainty maps for all groups (a), amphibians (b), birds (c) and mammals (d). The uncertainty represents the residuals of the generalized additive model (GAM). The negative values mean overestimation and positive, underestimation of the effect of stability and carbon density on distribution of species richness of each and all taxonomic groups.

REFERENCES

Alves, L. F., Vieira, S. A., Scaranello, M. A., Camargo, P. B., Santos, F. A. M., Joly, C. A., & Martinelli, L. A. (2010). Forest structure and live aboveground biomass variation along an elevational gradient of tropical Atlantic moist forest (Brazil). Forest Ecology and Management, 260(5), 679–691. https://doi.org/10.1016/j.foreco.2010.05.023

Amatulli, G., Domisch, S., Tuanmu, M. N., Parmentier, B., Ranipeta, A., Malczyk, J., & Jetz, W. (2018). Data Descriptor: A suite of global, cross-scale topographic variables for environmental and biodiversity modeling. Scientific Data, 5, 1–15. https://doi.org/10.1038/sdata.2018.40

Baldocchi, D. D., & Amthor, J. S. (2001). Canopy photosynthesis: history, measurements, and models. In Terrestrial global productivity (pp. 9–31). ACADEMIC PRESS.

Bengough, A. G. (2003). Root Growth and Function in Relation to Soil Structure, Composition, and Strength BT - Root Ecology. In H. de Kroon & E. J. W. Visser (Eds.) (pp. 151–171). Berlin, Heidelberg: Springer Berlin Heidelberg. https://doi.org/10.1007/978-3-662-09784-7_6

Bennett, A. C., Penman, T. D., Arndt, S. K., Roxburgh, S. H., & Bennett, L. T. (2020). Climate more important than soils for predicting forest biomass at the continental scale. Ecography, 1–14. https://doi.org/10.1111/ecog.05180

Clark, D. A. (2004). Sources or sinks? The responses of tropical forests to current and future climate and atmospheric composition. Philosophical Transactions of the Royal Society B: Biological Sciences, 359(1443), 477–491. https://doi.org/10.1098/rstb.2003.1426

Cowling, S. A., & Shin, Y. (2006). Simulated ecosystem threshold responses to co-varying temperature, precipitation and atmospheric CO2 within a region of Amazonia. Global Ecology and Biogeography, 0(0), 060807052106001-??? https://doi.org/10.1111/j.1466-822x.2006.00256.x

Cristiano, P. M., Madanes, N., Campanello, P. I., Di Francescantonio, D.,

Rodríguez, S. A., Zhang, Y. J., … Goldstein, G. (2014). High NDVI and Potential canopy photosynthesis of South American subtropical forests despite seasonal changes in leaf area index and air temperature. *Forests*, *5*(2), 287–308. https://doi.org/10.3390/f5020287

da Costa, A. C. L., Galbraith, D., Almeida, S., Portela, B. T. T., da Costa, M., de Athaydes Silva Junior, J., … Meir, P. (2010). Effect of 7 yr of experimental drought on vegetation dynamics and biomass storage of an eastern Amazonian rainforest. New Phytologist, 187(3), 579–591. https://doi.org/10.1111/j.1469-8137.2010.03309.x

de Castilho, C. V., Magnusson, W. E., de Araújo, R. N. O., Luizão, R. C. C., Luizão, F. J., Lima, A. P., & Higuchi, N. (2006). Variation in aboveground tree live biomass in a central Amazonian Forest: Effects of soil and topography. Forest Ecology and Management, 234(1–3), 85–96. https://doi.org/10.1016/j.foreco.2006.06.024

Doughty, C. E., & Goulden, M. L. (2009). Are tropical forests near a high temperature threshold? *Journal of Geophysical Research: Biogeosciences*, *114*(1), 1–12. https://doi.org/10.1029/2007JG000632

Ediriweera, S., Singhakumara, B. M. P., & Ashton, M. S. (2008). Variation in canopy structure, light and soil nutrition across elevation of a Sri Lankan tropical rain forest. Forest Ecology and Management, 256(6), 1339–1349. https://doi.org/10.1016/j.foreco.2008.06.035

Feeley, K. J., Joseph Wright, S., Nur Supardi, M. N., Kassim, A. R., & Davies, S. J. (2007). Decelerating growth in tropical forest trees. Ecology Letters, 10(6), 461–469. https://doi.org/10.1111/j.1461-0248.2007.01033.x

Fick, S. E., & Hijmans, R. J. (2017). WorldClim 2: new 1-km spatial resolution climate surfaces for global land areas. International Journal of Climatology, 37(12), 4302–4315. https://doi.org/doi:10.1002/joc.5086

Goebes, P., Schmidt, K., Seitz, S., Both, S., Bruelheide, H., Erfmeier, A., … Kühn, P. (2019). The strength of soil-plant interactions under forest is related to a Critical Soil Depth. Scientific Reports, 9(8635), 1–12. https://doi.org/10.1038/s41598-019-45156-5

Goulden, M. L., Miller, S. D., Da Rocha, H. R., Menton, M. C., De Freitas, H. C., E Silva Figueira, A. M., & Dias De Sousa, C. A. (2004). Diel and seasonal patterns of tropical forest CO2 exchange. *Ecological Applications*, *14*(4 SUPPL.), 42–54. https://doi.org/10.1890/02-6008

Hengl, T., De Jesus, J. M., Heuvelink, G. B. M., Gonzalez, M. R., Kilibarda, M., Blagotić, A., … Kempen, B. (2017). SoilGrids250m: Global gridded soil information based on machine learning. PLoS ONE, 12(2), 1–40. https://doi.org/10.1371/journal.pone.0169748

Jakovac, C. C., Peña-Claros, M., Kuyper, T. W., & Bongers, F. (2015). Loss of secondary-forest resilience by land-use intensification in the Amazon. Journal of Ecology, 103(1), 67–77. https://doi.org/10.1111/1365-2745.12298

Jarvis, A., Reuter, H., Nelson, A., & Guevara, E. (2008). Hole-filled SRTM for the globe version 3, from the CGIAR-CSI SRTM 90m database. See Http://Srtm. Csi. Cgiar. Org.

Jobbágy, E. G., & Jackson, R. B. (2000). The vertical distribution of soil organic carbon and its relation to climate and vegetation. *Ecological Applications*, *10*(2), 423–436. https://doi.org/doi:10.1890/1051-0761(2000)010[0423:TVDOSO]2.0.CO;2

Kitayama, K., & Aiba, S. I. (2002). Ecosystem structure and productivity of tropical rain forests along altitudinal gradients with contrasting soil phosphorus pools on Mount Kinabalu,Borneo. Journal of Ecology, 90(1), 37–51. https://doi.org/10.1046/j.0022-0477.2001.00634.x

Kopecký, M., & Čížková, Š. (2010). Using topographic wetness index in vegetation ecology: Does the algorithm matter? Applied Vegetation Science, 13(4), 450–459. https://doi.org/10.1111/j.1654-109X.2010.01083.x

Lambers, H., III, F. S. C., & Pons, T. L. (2008). *Plant physiological ecology*. https://doi.org/10.1007/978-3-030-29639-1

Larkin, D., Vivian-smith, G., & Zedler, J. (2006). Topographic heterogeneity theory and ecological restoration. In D. A. Falk, M. A. Palmer, & J. B. Zedler (Eds.),

Foundations of Restoration Ecology (pp. 142–164).

Laurance, W. F., Fearnside, P. M., Laurance, S. G., Delamonica, P., Lovejoy, T. E., Rankin-de Merona, J. M., … Gascon, C. (1999). Relationship between soils and Amazon forest biomass. Forest Ecology and Mangement, 118, 127–138. https://doi.org/10.1016/S0378-1127(98)00494-0

McDowell, N., Allen, C. D., Anderson-Teixeira, K., Brando, P., Brienen, R., Chambers, J., … Xu, X. (2018). Drivers and mechanisms of tree mortality in moist tropical forests. New Phytologist, 219(3), 851–869. https://doi.org/10.1111/nph.15027

McDowell, N., Pockman, W. T., Allen, C. D., Breshears, D. D., Cobb, N., Kolb, T., … Yepez, E. A. (2008). Mechanisms of plant survival and mortality during drought: Why do some plants survive while others succumb to drought? New Phytologist. https://doi.org/10.1111/j.1469-8137.2008.02436.x

Méndez-Toribio, M., Meave, J. A., Zermeño-Hernández, I., & Ibarra-Manríquez, G. (2016). Effects of slope aspect and topographic position on environmental variables, disturbance regime and tree community attributes in a seasonal tropical dry forest. Journal of Vegetation Science, 27(6), 1094–1103. https://doi.org/10.1111/jvs.12455

Muscarella, R., Kolyaie, S., Morton, D. C., Zimmerman, J. K., & Uriarte, M. (2020). Effects of topography on tropical forest structure depend on climate context. Journal of Ecology, 108(1), 145–159. https://doi.org/10.1111/1365-2745.13261

Nepstad, D. C. (2002). The effects of partial throughfall exclusion on canopy processes, aboveground production, and biogeochemistry of an Amazon forest. Journal of Geophysical Research, 107(D20), 1–18. https://doi.org/10.1029/2001jd000360

Oliveira, R. S., Eller, C. B., Barros, F. de V., Hirota, M., Brum, M., & Bittencourt, P. (2021). Linking plant hydraulics and the fast-slow continuum to understand resilience to drought in tropical ecosystems. New Phytologist. https://doi.org/10.1111/nph.17266

Pau, S., Detto, M., Kim, Y., & Still, C. J. (2018). Tropical forest temperature thresholds for gross primary productivity. *Ecosphere*, *9*(7), 1–12. https://doi.org/10.1002/ecs2.2311

Poorter, L., Bongers, F., Aide, T. M., Almeyda Zambrano, A. M., Balvanera, P., Becknell, J. M., … Rozendaal, D. M. A. (2016). Biomass resilience of Neotropical secondary forests. Nature, 530(7589), 211–214. https://doi.org/10.1038/nature16512

Raich, J. W., Russell, A. E., & Vitousek, P. M. (1997). Primary productivity and ecosystem development along an elevational gradient on Mauna Loa, Hawai'i. Ecology, 78(3), 707–721. https://doi.org/10.1890/0012-9658(1997)078[0707:PPAEDA]2.0.CO;2

Rowland, L., Da Costa, A. C. L., Galbraith, D. R., Oliveira, R. S., Binks, O. J., Oliveira, A. A. R., … Meir, P. (2015). Death from drought in tropical forests is triggered by hydraulics not carbon starvation. *Nature*, *528*(7580), 119–122. https://doi.org/10.1038/nature15539

Santiago-García, R. J., Finegan, B., & Bosque-Pérez, N. A. (2019). Soil is the main predictor of secondary rain forest estimated aboveground biomass across a Neotropical landscape. Biotropica, 51(1), 10–17. https://doi.org/10.1111/btp.12621

Sattler, D., Murray, L. T., Kirchner, A., & Lindner, A. (2014). Influence of soil and topography on aboveground biomass accumulation and carbon stocks of afforested pastures in South East Brazil. Ecological Engineering, 73, 126–131. https://doi.org/10.1016/j.ecoleng.2014.09.003

Stirzaker, R. J., Passioura, J. B., & Wilms, Y. (1996). Soil structure and plant growth: Impact of bulk density and biopores. Plant and Soil, 185(1), 151–162. https://doi.org/10.1007/BF02257571

Sullivan, M. J. P., Lewis, S. L., Affum-Baffoe, K., Castilho, C., Costa, F., Sanchez, A. C., … Phillips, O. L. (2020). Long-term thermal sensitivity of Earth's tropical forests. Science, in press (800), 869–874. https://doi.org/10.1126/science.aaw7578

Svenning, J. C., Kinner, D. A., Stallard, R. F., Engelbrecht, B. M. J., & Wright, S. J. (2004). Ecological determinism in plant community structure across a tropical forest landscape. Ecology, 85(9), 2526–2538. https://doi.org/10.1890/03-0396

Zhang, Y.-J., Cristiano, P. M., Zhang, Y.-F., Campanello, P. I., Tan, Z.-H., Zhang, Y.-P., … Goldstein, G. (2016). Carbon Economy of Subtropical Forests - Tropical Tree Physiology: Adaptations and Responses in a Changing Environment. In G. Goldstein & L. S. Santiago (Eds.) (pp. 337–355). Cham: Springer International Publishing. https://doi.org/10.1007/978-3-319-27422-5_16

CAPÍTULO III

Conservation of biodiversity and carbon stocks under the effect of climate change on ecosystem stability of tropical forests

Lucas Andrigo Maure, Milena Fiuza Diniz, Marco Túlio Pacheco Coelho, Bruno Roberto Ribeiro, Paulo Guilherme Molin, Fernando Rodrigues da Silva, Erica Hasui

Conservation of biodiversity and carbon stocks under the effect of climate change on ecosystem stability of tropical forests

Lucas Andrigo Maure[1,2], Milena Fiuza Diniz[3], Marco Túlio Pacheco Coelho[4], Bruno R. Ribeiro[3], Paulo Guilherme Molin[5], Fernando Rodrigues da Silva[2], Erica Hasui[6]*

[1]Programa de Pós-graduação em Ecologia e Recursos Naturais (PPGERN), Universidade Federal de São Carlos, São Carlos-SP, Brazil

[2]Laboratório de Ecologia Teórica: Integrando Tempo, Biologia e Espaço (LET.IT.BE), Departamento de Ciências Ambientais, Programa de Pós-graduação em Ecologia e Recursos Naturais (PPGERN), Universidade Federal de São Carlos, Sorocaba-SP, Brazil

[3]Departamento de Ecologia, Universidade Federal de Goiás, Goânia-GO, Brazil

[4]Swiss Federal Institute for Forest, Snow and Landscape, Birmensdorf, Switzerland

[5]Centro de Ciências da Natureza, Universidade Federal de São Carlos, Buri-SP, Brasil

[6]Laboratório de Ecologia de Fragmentos (EcoFrag), Instituto de Ciências da Natureza, Universidade Federal de Alfenas, Alfenas-MG, Brazil

*Corresponding author: ericahasui@gmail.com

Abstract

Protection and restoration of tropical forests focusing on enhancing biodiversity conservation and carbon storage are effective nature-based solutions in the face of the current biodiversity and climate crises. Climate change may affect the ecological stability of forests (i.e., the ability of the ecosystem to maintain its function over time), altering their capacity to maintain biodiversity and stock carbon. Here we identified priority areas for forest protection and restoration taking into account the effects of climate change on the stability of old-growth forests in the Brazilian Atlantic Forest. We used the random forest algorithm to model the influence of the current and future climate conditions on old-growth forest stability. We identified hotspots for forest protection and restoration by overlapping the map of forest stability change with maps of vertebrate richness and carbon density and accumulation. Climate explains 43.52% of the stability variance of old-growth forests and predicted versus observed data were highly correlated ($r = 0.95$). The relative change of forest stability due to climate change ranged from -21% to 106% and showed a heterogeneous spatial distribution. Most species and carbon amounts of protection hotspots were found in unprotected areas that are predicted to lose forest stability. In turn, most of the carbon accumulation potential and species in restoration hotspots are in areas where forest stability is predicted to improve. However, the low spatial overlap of biodiversity and carbon in hotspots for protection and restoration means that co-benefit is limited and conservation has to face trade-offs in the Atlantic Forest. Thus, the ecosystem-based approach presented here can help guide conservation decisions under the effect of climate change on old-growth forest stability.

Keywords: random forest, carbon density, carbon accumulation potential, conservation trade-offs, Atlantic Forest, old-growth forests, protected area, forest restoration

1. INTRODUCTION

Forest protection reduces carbon emissions and promotes its sequestration from the atmosphere effectively offering a solution for biodiversity conservation and climate change mitigation (Gibson et al., 2011; Lennox et al., 2018; Matos et al., 2020; Noon et al., 2021; Pettorelli et al., 2021). However, studies focusing on biodiversity-carbon conservation have not yet taken into account the effect of climate change on the spatial distribution of tropical forests' stability (i.e., the ability of the ecosystem to maintain primary productivity over time).

The establishment of protected areas targeting both biodiversity and carbon conservation has been a hotly debated theme due to uncertainties about their spatial correlation (Di Marco et al., 2018; Ferreira et al., 2018). Although biodiversity and carbon are globally correlated, this correlation is known to weaken at finer scales, limiting the ideal scenario of conservation co-benefits (Di Marco et al., 2018; Strassburg et al., 2010). Protecting only carbon-rich areas may impair biodiversity, which undermine international conservation agendas, such as Reducing Emissions from Deforestation and Forest Degradation (REDD+) and post-2020 global biodiversity framework (Ferreira et al., 2018). When there is a weak biodiversity-carbon spatial association, a trade-off scenario arises, making decisions for conservation between biodiversity and carbon stocks a task not only challenging but mandatory (Gardner et al., 2012; Phelps, Friess, & Webb, 2012; Phelps, Webb, & Adams, 2012). In addition, as carbon accumulation potential is unevenly distributed across space, trade-off

scenarios may also affect the establishment of forest restoration areas that also aim to benefit biodiversity (Cook-Patton et al., 2020).

For both conservation scenarios of co-benefit and trade-off, an ecosystem-based approach can support the identification of areas for forest protection and restoration according to alterations in forest stability caused by climate change. For example, forest conservation and restoration can be optimized in areas where climate change promotes stability gains. On the one hand, areas with gains in forest stability may be considered refuges for biodiversity and/or carbon stock. Stable forests can withstand perturbations, maintaining primary productivity, prolongating carbon residence time, and supporting higher species richness. On the other hand, locations where climate change promotes loss of forest stability may be considered vulnerable areas for biodiversity and/or carbon stock because they are unable to maintain primary productivity under perturbations, which could lead to species loss and carbon emission (Deere et al., 2018; Ferreira et al., 2018; Gatti et al., 2021; Sales, Galetti, & Pires, 2020).

Thus, the spatial distribution pattern of forest stability change (gain or loss) can assist decisions for conservation under climate change by indicating more or less suitable areas for biodiversity and carbon stocks. This approach would be highly relevant for regions with great and threatened species richness, and biomass erosion due to forest degradation by constant perturbations such as the Brazilian Atlantic Forest (Brooks et al., 2002; de Lima et al., 2020; Rezende et al., 2018; Ribeiro et al., 2009, 2011; Soto-Navarro et al., 2020).

Here, we used machine learning to predict the effect of climate change on the distribution of the old-growth forests stability. Based on stability change, we identified priority areas for forest conservation and restoration focusing on biodiversity and carbon stock. Using remote sensing data and geoprocessing tools, we selected 3,934

sites of old-growth forest across the Brazilian Atlantic Forest to model the effect of climate predictors on forest stability measured by primary productivity. With the fitted model, we predicted the current and future (2100) climate-driven forest stability across space. Then, we obtained a map of the relative change between future and current forest stability, which we overlapped with species richness maps of forest-specialist vertebrates, carbon density, and carbon accumulation by natural regrowth. We identified as protection hotspots the areas that simultaneously presented the highest values of biodiversity and/or carbon density and the highest values of either forest stability gain or loss. After verifying the protection status, we recommended forest management for the stability loss hotspots covered by protected areas. However, protection hotspots showing gain in forest stability and not covered by protected areas would be of higher relevance for forest protection, while unprotected areas of forest stability loss would be of higher relevance for both forest protection and management. In turn, we located restoration hotspots where there was an overlap among the highest values of biodiversity, carbon accumulation potential, and either gains or losses in forest stability. Thus, our ecosystem-based approach can potentially mitigate the effect of climate change on species loss by directly advising restoration projects and designing and/or identifying protection areas that optimizes both biodiversity conservation and carbon stock.

2. METHODS

2.1 Study area

Our study area consists of the Brazilian Atlantic Forest, a South American biome that has a long history of forest devastation and fragmentation. Currently, only ~28% of the

Atlantic Forest surface (c. 1.5 million km2) is covered by native vegetation (Rezende et al., 2018). Its forest remnants frequently face logging, hunting, grazing, and fire that severely impact their biodiversity and ecosystems (Barlow et al., 2016; de Lima et al., 2020; Erb et al., 2018; Ribeiro et al., 2011; Tabarelli et al., 2005). The forest devastation associated with a high biodiversity, endemism, and threatened species makes the Atlantic Forest one of the most important domains for conservation (Myers et al., 2000). Although the Atlantic Forest native cover area has remained relatively constant over the last 30 years, this apparent stability has masked an important process of forest cover rejuvenation from which the loss of older forest has been offset by gains in younger native forest cover (Rosa et al., 2021).

2.2 Data

Sampling sites of old-growth forests – We identified forest remnants with a minimum of 33 years old using classified images from 1985 to 2018 at 30 m resolution from MapBiomas v4.0 (http://mapbiomas.org/). We overlaid the forest map with a gridded map at the same 250 m resolution of MODIS images to obtain data about forest productivity. Subsequently we selected as sampling sites only cells totally covered by forests, avoiding cells covered by other land uses. A total of 14,569 cells out of 920,603 remained after we performed a random selection of cells with a minimum arbitrary distance of 5 km to each other to reduce the number of sampling sites and improve computational tractability.

Response variable – We used the Normalized Difference Vegetation Index (NDVI) to measure stability of the primary productivity of old-growth forests through interannual time series of 19 years, time range of available images (De Keersmaecker, Lhermitte, & Honnay, 2014; García-Palacios, Gross, Gaitán, & Maestre, 2018). Derived from satellite images, NDVI is a vegetation index used as an indicator of primary productivity and biomass due to its sensitivity to photosynthetically active biomass (Caughlin et al., 2020; Pettorelli et al., 2005; Saatchi et al., 2007). We obtained NDVI data from MODIS sensor images at 250 m resolution available in the GLAM Project (http://pekko.geog.umd.edu/usda/test/), in which values from observation error were excluded. For the interannual time series, we used mean NDVI values for each year between 2000-2018 calculated with all 23 available images per year. Mean NDVI values in the interannual time series avoids intra-annual variations caused by the seasonality of the plant productivity phenology, which may influence our main objective to detect long-term variations in primary productivity.

To measure forest stability, we calculate the total standard deviation of the detrended interannual NDVI time series (De Keersmaecker et al., 2014). We detrended all time series by a second-order difference in which stationarity was tested using the Augmented Dickey Fuller test (ADF; Dickey & Fuller, 1979) from the 'trend' R package (Pohlert, 2018). Nonstationary time series may bias standard deviation values due to long-term or stochastic trends and they were excluded from analyses, reducing the dataset to 8,974 sampling sites (De Keersmaecker et al., 2014). Since high values of standard deviation indicate low forest stability, we rescaled standard deviation values to range from 0 to 100 so that higher values indicate higher forest stability. Finally, we promote regular distribution of the sites by applying a new random selection based on a minimum distance of 10 km, which is the mean distance between all sites. Regular

spatial distribution of the samples promotes a gradient-wide range of the variable values and avoids spatial autocorrelation (Dale & Fortin, 2014; Fletcher & Fortin, 2018). At last, we obtained a dataset of 3,934 sites of old-growth forest area with stationary time series and regularly distributed across the Brazilian Atlantic Forest (Figure S1).

2.4 Modeling climate and forest stability relationships

We used the random forest algorithm to model the relationships between climate and forest stability and to spatially predict the current and future climate-driven forest stability in the Atlantic Forest (Breiman, 2001). Random forest is a machine-learning model robust to overfitting that handles complex non-linear and non-monotonic relationships between response variables and numerous predictors in regression analyses (Breiman, 2001; Liaw & Wiener, 2002). It has a high predictive accuracy and has been used to predict the spatial distribution of biomass, carbon accumulation potential, and biomes (Aleman et al., 2020; Bennett et al., 2020; Cook-patton et al., 2020; Harris et al., 2021). Random forest was also applied to identify the predictors importance in spatial variation of biodiversity-carbon correlation, carbon stock, woody-biomass, and drought impacts in tropical forests (Di Marco et al., 2018; Ross et al., 2021; Schwartz, Budsock, & Uriarte, 2019; Sullivan et al., 2020).

To model the effect of climate on spatial distribution of forest stability we used all the 19 bioclimatic variables (Table S1) at the resolution of 30 seconds (~1 km) available on WorldClim v2.1 database (Fick & Hijmans, 2017). We performed a principal component analysis (PCA) with centered and normalized data to reduce dimensionality and correlation of bioclimatic variables. Based on the cumulative proportion of variance explained, we choose as forest stability predictors the first nine

axes of the PCA, corresponding to 99.5% of the bioclimatic data (Table S2, Figure S2). For random forest model tuning, we first used a 10-fold cross validation to find model's hyperparameters that maximize the coefficient of determination (r^2). These tuning parameters were: five predictors as minimum node size, one predictor at each tree split (mtry = 1), and a forest of 1000 trees (ntree) (Figure S3). The residuals of the model with these parameters showed no spatial autocorrelation (Figure S4).

Then, a final random forest model was tuned to produce 959 trees, which generates the minimum out-of-bag error rates in a total of 1000 trees (Liaw & Wiener, 2002). To evaluate the models' performance, we estimate the coefficient of determination (r^2) and the root-mean-square error (RMSE) between predicted and observed forest stability data. We also used a Pearson's correlation for a linear relationship between values of predicted forest stability map and observed forest stability data to estimate the predictive power of the model. We used the predictors importance, calculated as the average increase in node purity across all decision trees, to indicate the influence of the predictor on forest stability. Analyses were performed in R (R Core Team, 2020) using the packages 'RStoolbox' (Leutner et al., 2017) for bioclimatic PCA; 'spatialRF' (Benito, 2021) and 'ranger' (Wright & Ziegler, 2017) for model tuning and spatial autocorrelation test; 'randomForest' (Liaw & Wiener, 2002) for random forest model; and 'caret' (Kuhn et al., 2021) for evaluation of models' performance.

2.5 Mapping current, future, and relative change of forest stability

We used the final random forest model to predict the distribution of forest stability across the Atlantic Forest for the current and future periods. For the future prediction

map, we used the bioclimatic data of 2.5 minutes (~5km) of spatial resolution of the CMIP6 projection for the 2080 - 2100 period, available at WorldClim v2.1 database (Fick & Hijmans, 2017). We choose two global climate models, the MRI-ESM2-0 and the Shared Socio-economic Pathway 3-7.0 (SSP3-7.0). They were chosen because the first model presents the median value of the equilibrium climate sensitivity between the available models while the second one indicates a moderate scenario of the increase in the future CO2 emissions. These data were resampled to 1 km resolution using bilinear interpolation to fit current climate data.

To predict forest stability in the future, we used the loadings of the current bioclimatic PCA axes to reproduce an equivalent future bioclimatic PCA. First, we normalized and centered all future variables. Then, each variable was multiplied by the loading of the referent variable of the current bioclimatic PCA and all multiplications were summed in an equation, reproducing the future PCA axis. This process was repeated to reproduce each of the nine PCA axes. We reproduce the PCA axes of the future because the loadings of the future bioclimatic PCA are different from those of the current bioclimatic PCA. Therefore, the correlations between future bioclimatic variables are different from those of the current variables, which we modeled the relationship with forest stability. To map the relative change in forest stability, we subtracted the future map by the current map dividing by the current map multiplied by 100. Thus, the relative change map expresses the magnitude of the difference between future and current forest stability in percentage, so that negative values mean forest stability loss and positive values indicate forest stability gain.

2.6 Bivariate and hotspot maps of biodiversity and carbon stock

We used bivariate maps to visualize the spatial overlap between biodiversity, carbon stock, carbon accumulation, and forest stability change, as well as to find protection and restoration hotspots. We also evaluated the correlation between species richness of each taxon (birds, mammals, and amphibians) and all groups, and forest stability change, carbon stock and accumulation potential using Spearman's rank (r_S) correlation coefficient.

Biodiversity and forest stability change – We build species richness maps using range data of birds (n = 732), mammals (n = 293), and amphibians (n = 445) of Brazil restricted to the Atlantic Forest from the International Union for Conservation of Nature database (IUCN, www.iucnredlist.org; bird's ranges from BirdLife International). These species are occupant of all forest habitats categories according to the IUCN habitat type scheme, they can be classified as forest-specialists and are more vulnerable to forest perturbations (Sales et al., 2020). The species' range was converted to a species richness map at 5 km resolution for each taxon using the R package 'lestR' (Vilela & Villalobos, 2015). The richness map of the three taxa were highly correlated (Pearson's $r > 0.94$) and we obtain a single map of the total species richness summing them (Figure S5a). After resampling the map of forest stability change to 5 km resolution using bilinear interpolation to fit the species richness map, we classified both maps in ten classes by 10% quantiles to create a bivariate choropleth map. Given species richness may omit species of high conservation concern, we also built a bivariate map for threatened forest-specialist species (IUCN's category critically endangered, endangered, and vulnerable). Species richness and threatened species richness (Figure S5b) maps had a high correlation (Pearson's r = 0.89) and we moved the bivariate map of the threatened species richness to supporting information (Figure S6).

Carbon density, carbon accumulation potential, and forest stability change – Using bilinear interpolation we resample to 1 km resolution a harmonized global map of aboveground biomass carbon density (MgC/ha) for the reference year 2010 at ~328 m resolution (Spawn et al., 2020). We also used a global map at ~1 km resolution of carbon accumulation potential density per year ($MgC/ha^{-1}/y^{-1}$) of aboveground biomass by natural regrowth for the thirty first years of regeneration (Cook-Patton et al., 2020). This map represents carbon accumulation only for reforestation opportunities, excluding areas of native grasslands and croplands (Griscom et al., 2017). We reclassified the maps of carbon density, carbon accumulation, and forest stability change in ten classes of 10% quantiles. We then combined each carbon map with forest stability change in bivariate choropleth maps.

Hotspot maps – We mapped hotspots for forest protection and restoration that could benefit biodiversity, carbon density, and carbon accumulation under extremes of forest stability loss and gain due to climate change. Using the respective bivariate maps, we identified the protection hotspots for biodiversity, carbon density, and biodiversity-carbon density, which are the overlapping hotspots of both. Similarly, we identified the restoration hotspots for carbon accumulation and biodiversity-carbon accumulation, which are also the overlapping hotspots of both. Hotspot maps highlighted areas where the highest 20% values of biodiversity, carbon density, and carbon accumulation overlapped with the highest and lowest 20% values of the relative change in forest stability (Armenteras, Rodríguez, & Retana, 2015, Soto-Navarro 2020).

We quantified the species number and carbon stock for the two classes of forest stability (loss and gain) of each map for protection hotspots. Using the original dataset, we quantified carbon stock in absolute values of MgC by multiplying the total MgC/ha value in each of the two protection hotspots classes by 10.77, which is the pixel area in ha of carbon density dataset. We also quantified the proportions of the hotspots located in protected and unprotected areas, according to the World Database on Protected Areas (WDPA) (UNEP-WCMC & IUCN, 2022). Each map of protection hotspots has four classes highlighting areas of forest stability gain: (1) currently protected and (2) unprotected, considered as refuge for high biodiversity and/or carbon storage that are suitable for protection; and areas of forest stability loss: (3) currently protected but where forest management is required and (4) unprotected, considered as vulnerable areas for high biodiversity and/or carbon storage where forest protection and management are recommended.

For the two classes of forest stability loss and gain in the maps of restoration hotspots, we quantified the species number and carbon accumulation. We used the original dataset to quantify carbon accumulation in absolute values of MgC per year by multiplying the total MgC/ha value in each of the two restoration hotspots classes by 54.66, which is the pixel area in ha of carbon density dataset. Because the carbon accumulation dataset was designed for the first thirty years of regeneration (Cook-Patton et al., 2020), we multiply the absolute value of MgC per year by 30 to obtain the total carbon accumulation in thirty years of natural forest regrowth. The two classes of each map of restoration hotspots highlight areas of forest stability gain, considered as refuge for biodiversity and/or carbon accumulation of new forests in the future; and areas of forest stability loss, considered as vulnerable areas for biodiversity and/or

carbon accumulation of new forests in the future where forest management is recommended.

A general framework of the methods is given as supporting information (Figure S7).

3. RESULTS

3.1 Model performance

Forest stability of old-growth forests spatially ranged from 0 to 96.5 and increased from north to south across the Atlantic Forest (Figure S1). The fitted model with the lowest out-of-bag error rates (± 9.27%) explains 43.52% of the forest stability variance. The performance evaluation of this model presented a $r^2 = 0.90$ and a RMSE of ± 4.49 between predicted and observed forest stability. However, Pearson's test showed a high correlation ($r = 0.95$) between predicted and observed values of forest stability (Figure 1a). The predictors' importance showed that the spatial distribution of the forest stability was mostly influenced by PCA1 and PCA3 (Figure S8). PCA1 was mainly positively represented by mean temperature of coldest quarter and annual mean temperature, and negatively by temperature seasonality and precipitation of driest quarter. PCA3 was mainly positively represented by annual precipitation and precipitation of wettest quarter, and negatively by mean diurnal range and temperature annual range (Table S3).

3.2 Current, future and relative change of forest stability

Both current and future forest stability prediction also showed a spatial distribution increasing from north to south across the Atlantic Forest (Figure 1a and 1b). Higher values of current forest stability were found mainly over the Brazilian south and southeast coast, in isolated areas of the southern region interior, and in a narrow strip along the coast of Bahia state (Figure 1a). For future forest stability, higher values of the coast were concentrated mainly at São Paulo state in the south of the biome (Figure 1b). Lowest values of both current and future forest stability occur at inland areas between Minas Gerais and Bahia states in the Atlantic Forest northern region (Figure 1a and 1b). However, these were also the larger areas where it is predicted to have the highest gain of the relative change in forest stability, which generally presents high spatial variation ranging from -21% to 106% (Figure 1c). The loss of forest stability was also predicted to occur throughout the Atlantic Forest, but the largest losses are located in its northern region, specifically on the coast of Bahia state and in between the Jequitinhonha and Mucuri valleys in Minas Gerais state.

3.3 Protection bivariate and hotspots maps

High levels of biodiversity (represented here by species richness of forest-specialist vertebrates) and forest stability gain were found at Minas Gerais and Espírito Santo states and along the southern region coast (Figure 2). Biodiversity hotspot with forest stability gain covers 4.23% of the Brazilian Atlantic Forest harboring 1011 species (68.77%) (Figure 4a, Table 1). However, 96.88% of this hotspot is unprotected. High carbon density and forest stability gain is also found mainly in the central region of the Atlantic Forest (Figure 3). Carbon hotspots covered only 1.94% of the Atlantic Forest and stocks 1,184,927,504 MgC, representing 9.85% of all carbon found in old-growth

forest areas (Figure 4b, Table 1). Of the total hotspot areas of high carbon density and forest stability gain, 90.83% are in unprotected areas. Covering only 0.31% of the Atlantic Forest, biodiversity-carbon density hotspots overlapping with higher forest stability gain were found in Minas Gerais and Espírito Santo states (Figure 4c, Table 1). These areas harbor 967 species (65,78%) and 120,058,129 MgC (1%), and were most unprotected (86.09%).

Areas of higher biodiversity (Figure 2) and carbon density (Figures 3) overlapped with forest stability loss were located along the southern region coast, especially in the Serra do Mar ecoregion at São Paulo state. These areas were also found at the Bahia state coast in the north region of the Atlantic Forest, but mainly for carbon density. The hotspots of higher biodiversity and forest stability loss extends over 2.11% of the Atlantic Forest and contain 1085 species (73.81%) (Figure 4a, Table 1). Around 81% of this hotspot with great biodiversity in a vulnerable habitat is unprotected. Occupying 5.17% of the Atlantic Forest, hotspots of higher carbon density and forest stability loss stock 3,511,992,885 MgC, representing 29.19% of the carbon in old-growth forests (Figure 4b, Table 1). This hotspot has 75.08% of its total in unprotected areas. In turn, areas that combine hotspots of biodiversity and carbon density in forest stability loss cover 0.57% of the Atlantic Forest. Containing 1066 species (72.52%) and 355,627,412 MgC (2.95%), biodiversity-carbon hotspots overlapping with forest stability loss occur mainly at the Serra do Mar ecoregion in São Paulo state and in the Espírito Santo state, in which 63.96% of its total is unprotected (Figure 4c, Table 1). Overall, biodiversity-carbon hotspots presented low spatial overlap, representing only 6.55% of the total area of biodiversity and carbon stock hotspots.

3.4 Restoration bivariate and hotspots maps

High carbon accumulation potential by natural forest regrowth and forest stability gain overlapped mainly over the central region of the Atlantic Forest and across the northern region (Figure 5). The hotspots for this class ranges over 4.29% of the Brazilian Atlantic Forest and have the potential to accumulate 640,098,374 MgC in the first thirty years of natural forest regrowth, 11.20% of total carbon accumulation in this period for the entire study area (Figure 6a, Table 1). Areas where biodiversity-carbon accumulation hotspots overlap with forest stability gain were found in the central region mainly between Minas Gerais and Espírito Santo states, but also in the Rio de Janeiro states. Occupying 1.68% of the study area, these hotspots can harbor 933 species (63.47%) and accumulate 253,663,906 MgC (4.44%) (Figure 6b, Table 1). Areas of high carbon accumulation and forest stability loss also occur across the central and northern regions (Figure 5). Their hotspot areas can accumulate a total of 160,771,323 MgC in 1.10% of the Brazilian Atlantic Forest, which represents 2.81% of the total carbon accumulation (Figure 6a, Table 1). Found mainly in Rio de Janeiro and Espírito Santo states, areas where biodiversity-carbon accumulation hotspots overlap with forest stability loss extends over 0.14% of the study area but can harbor 923 species (62.79%) and accumulate 21,058,789 MgC (0.37%) (Figure 6b, Table 1). Overall, the carbon accumulated in restoration hotspots increased its stock by 14.57% considering the amount stored in carbon density hotspots.

3.5 Biodiversity, carbon and forest stability change correlation

Mammals richness (Figure S9b, Table S4) and carbon accumulation (Figure S10b, Table S4) had the highest positive relationship with forest stability change, indicating

that they would be the main beneficiated of forest stability gain. However, carbon density was negatively associated with forest stability change (Figure S10b, Table S4). Each taxon and all groups were positively correlated more with carbon accumulation (Figure S11a-d, Table S4) than carbon density (Figure S12a-d, Table S4). These results suggest that forest restoration would benefit biodiversity more than forest protection. Amphibian species richness was highly related to carbon density (Figure S12c, Table S4) while mammals to carbon accumulation (Figure S11b, Table S4).

4. DISCUSSION

The effect of climate change on old-growth forest stability makes it necessary to rethink current areas for forest protection and restoration in the Brazilian Atlantic Forest when focusing on biodiversity conservation and carbon stocks. The ecosystem-based approach presented here provides new insights for spatial planning and decision making for forest protection and restoration under climate change. Our mapping highlights refuge areas where gains in forest stability can enhance biodiversity and carbon conservation. Protection or restoration of these areas are likely to deliver benefits for biodiversity and carbon at lowest management cost due to their ability to maintain primary productivity. However, biodiversity and carbon stock may be at risk in areas of forest stability loss. Under forest stability loss, forest protection or restoration may require management and conservation actions to avoid carbon emission and species loss due to forests' vulnerability to perturbations as a consequence of climate change. Our results demonstrated that conservation co-benefit biodiversity and carbon only in small areas both for protection and restoration hotspots. Thus, biodiversity and carbon stocks conservation should follow a trade-off approach in the Atlantic Forest. For such, our

results can help decisions by indicating important areas for protection and restoration considering the effect of climate change on forest ecosystems.

4.1 Forest stability change

While current and future predictions of forest stability generally increase from north to south throughout the Atlantic Forest, the relative change of forest stability has high spatial variation. This pattern of spatial heterogeneity may be a result of the local climate and topographic variations (Ackerly et al., 2010; Hamann et al., 2015). The heterogeneity at finer scales provides a spatial buffer against climate change due to the occurrence of a nearby climate refuge for biological conservation (Ackerly et al., 2010). Thus, our results suggest such a spatial buffer but for forest ecosystems in the face of climate change, alternating areas of forest stability loss with an adjacent area of forest stability gain across the Atlantic Forest.

In areas of forest stability gain, climate change may provide optimal conditions and resources to physiological performance of plants, contributing to maintaining forest primary productivity constant over time. Instead, in areas of forest stability loss, the exact opposite can occur. For example, both elevated temperature and low water availability, which increases plant evapotranspiration and hydraulic stress, respectively, can prolongate stomatal closure constraining photosynthesis rate and primary productivity in tropical forests (McDowell et al., 2018; Oliveira et al., 2021). As global temperatures rise, climate change is predicted to increase the frequency of heatwaves and warmer drought events that put trees under conditions of physiological stress and vulnerability (Fontes et al., 2018). In extreme cases, these events can drive tree mortality in tropical forests by hydraulic failure and carbon starvation, drought-fire

interactions, or even by insect attack due to the weakening of their defenses (Brando et al., 2014; Hartmann et al., 2022; McDowell et al., 2018).

4.2 Biodiversity and carbon under forest stability change

Biodiversity, carbon stocks, and carbon accumulation combined with forest stability change have high spatial variation. The spatial alternation between loss and gain of forest stability overlapping high biodiversity is found mainly along the coast and in the interior of the Atlantic Forest southern region. This result is expected because southern coast comprises the highly rich ecoregion of Serra do Mar, a center of endemism where also concentrate the greater species number for reactive conservation actions in the Neotropics (Ribeiro et al., 2009, 2011; Soto-Navarro et al., 2020). High carbon stocks with spatial alternation of forest stability occurs mainly at central interior and northern coast regions, while in south and Serra do Mar ecoregion predominates forest stability loss. These regions contain great proportions of forest cover and, therefore, high carbon density in aboveground biomass (Rezende et al., 2018; Ribeiro et al., 2009; Soto-Navarro et al., 2020). Although carbon accumulation potential and forest stability change also present spatial heterogeneity, larger areas of higher values for both are noticed in the central and northern regions. These regions have low forest cover due to advanced deforestation and are the most important regions of the tropics with restoration opportunities that benefit biodiversity conservation and climate change mitigation (Brancalion et al., 2019; Cook-Patton et al., 2020; Rezende et al., 2018; Strassburg et al., 2020).

As biodiversity and aboveground biomass are closely related to forest habitats in the tropics, their integrity is likely to be directly affected by the effect of climate change

on forest ecosystems. Thus, forests in areas of stability gain can be considered refuges for biodiversity and carbon stock due to its ability to maintain primary productivity. In turn, forest stability loss can make these habitats more vulnerable to perturbations, challenging the capacity of forest to sustain species and carbon stocks (Deere et al., 2018; Ferreira et al., 2018; Gatti et al., 2021; Sales et al., 2020). Forest perturbations due to changes in climate conditions may drive a turnover of vertebrate species in tropical forest, in which forest-specialists are expected to face local extinctions due to drastic decrease in their suitable range (Sales et al., 2020). In addition, perturbations may lead tropical forests to change from sinks to sources of carbon to the atmosphere (Aragão et al., 2018; Gatti et al., 2021; Hartmann et al., 2022; Sullivan et al., 2020; Xu et al., 2021). Thus, the capacity of climate change mitigation by ecosystems is reduced, once it depends on the forest stability of carbon stocks (Díaz, Hector, & Wardle, 2009).

4.3 Priority areas for conservation

Unprotected hotspots with extreme values of forest stability loss and gain are highly recommended for protection due to its potential for conservation of higher levels of biodiversity and/or carbon density. In the Brazilian Atlantic Forest, hotspots at forest stability gain have the largest proportion of unprotected areas (96.88% for biodiversity, 90.83% for carbon stocks, and 86.09% for both). As forest stability is expected to increase in these areas, low forest management would be required, making conservation more cost-effective. Moreover, protecting larger fragments and those close to the sources can increase the potential of biodiversity-carbon conservation (Magnago et al., 2015). However, because protection hotspots at forest stability gain harbor more species than aboveground biomass, our results show that protecting their forests will benefit

biodiversity more than carbon stocks, mainly in hotspots of biodiversity-carbon overlap where conservation co-benefit both.

Biodiversity would also be the main beneficiary in the protection at forest stability loss areas. Although protection hotspots of high biodiversity in forest stability gain is twice as large, areas of high biodiversity in forest stability loss contains the majority of the forest-specialist vertebrate species (n = 1085, 73.81%) which is also true for the co-benefit hotspots (n = 1066, 72.52%). However, relative to the total of the carbon stored in aboveground biomass of old-growth forests in the Brazilian Atlantic Forests, a large carbon stock is found in its hotspots of forest stability loss (3,511,992,885 MgC, 29.19%). Considering that forests are predicted to lose stability in biodiversity, carbon, and co-benefit hotspots, it is worrying that most of their areas are unprotected. Due to the forest stability loss of the forests to climate change, protection of these areas and management of their forests is necessary for future biodiversity and carbon stocks conservation. For protected areas, however, only forest management may be required.

4.4 Priority areas for forest restoration

In addition to highlighting areas for forest protection, the ecosystem-based approach presented here can also optimize forest restoration by natural regrowth with a focus on future conservation of biodiversity and carbon stock under climate change. In the future, restored forests can be more resistant to perturbations and low management is required where climate change promotes increase in forest stability. Thus, the high potential for carbon sequestration and storage (640,098,374 MgC, 11.20%) of these areas could make forest regrowth more efficient and a cost-effective climate change mitigation by

natural solutions. Although restoration in areas of biodiversity-carbon hotspots at forest stability gain does not result in the accumulation of great amounts of carbon (253,663,906 MgC, 4.44%), it can highly benefit biodiversity (*n* = 933, 63.47%). In turn, forest management may be necessary for restoration to maintain carbon accumulation potential and its storage (160,771,323 MgC, 2.81%) where climate change causes forest stability loss. The difference between biodiversity and carbon storage is greater where their hotspots overlap at forest stability loss and, despite its small size, these areas can harbor a large number of species (*n* = 923, 62.79%).

Overall, hotspots for forest restoration show an important role for both carbon sequestration and storage. Along with carbon density hotspots, thirty years of natural forest regrowth in restoration hotspots for carbon accumulation can increase 14.57% the total carbon stock in Brazilian Atlantic Forest. In addition, these areas have the potential to harbor a great number of forest-specialist vertebrate species. However, some issues can make the conservation value of regrowth forests in the future questionable, such as uncertainties regarding succession pathways in second-growth tropical forests (Arroyo-Rodríguez et al., 2017; Chazdon et al., 2007). Also, second-growth forest cannot conserve some primary forest species and may not help mitigate species loss in tropical forests (Barlow, Mestre, Gardner, & Peres, 2007; Gibson et al., 2011). Moreover, the effects of climate and land-use changes along with disturbances promoted by them will directly affect carbon balance in tropical forests (Elias et al., 2020).

Nevertheless, there is evidence that second-growth tropical forests have great potential for co-benefit biodiversity conservation and carbon storage (Ferreira et al., 2018; Matos et al., 2020). Second-growth forests can recover not only high proportions of the species richness and composition but also threatened and endemic species found in primary forests (Chazdon et al., 2009; Lennox et al., 2018; Matos et al., 2020;

Rozendaal et al., 2019). With high rates of carbon sequestration per year, regrowth forests are also able to accumulate great amounts of carbon in aboveground biomass compared to the primary forests, which recovery can be faster than plant diversity (Lennox et al., 2018; Martin, Newton, & Bullock, 2013; Matos et al., 2020; Poorter et al., 2016). Moreover, the total carbon stored by second-growth forests has a great potential to balance anthropogenic emissions from fossil fuel and industrial production (Chazdon et al., 2016). Therefore, although primary forests have an irreplaceable value for conservation, forest restoration by natural regrowth is an important auxiliary strategy with high potential to restrain species loss and climate change, especially in highly fragmented landscapes such as in the Atlantic Forest.

4.5 Biodiversity and carbon overlap

Our results also show that biodiversity and carbon in hotspots for protection and restoration have low spatial overlap in the Brazilian Atlantic Forest. Protection could co-benefit both biodiversity and carbon stock in small and sparsely distributed areas which represent only 6.55% of the two hotspots, where they overlap. The same is true for forest restoration, which could co-benefit biodiversity and carbon stock in 15.60% of the hotspots for biodiversity and carbon accumulation. Because we performed this study within the Atlantic Forest limits, this finding was expected once spatial correlation between biodiversity and carbon density decreases from global to regional scales (Armenteras, Rodríguez, & Retana, 2015; Di Marco et al., 2018). Therefore, synergy in biodiversity-carbon conservation is limited in the Brazilian Atlantic Forest under the effects of climate change on forest stability. Thus, decisions should follow a

trade-off approach both for protection and restoration strategies (Gardner et al., 2012; Phelps, Friess, et al., 2012; Phelps, Webb, et al., 2012).

4.6 Warnings

Overall, our ecosystem-based approach for biodiversity and carbon stock conservation recommends areas of forest stability gain for forest protection and restoration by natural regrowth, and areas of forest stability loss for both but forest management is required to avoid species loss and carbon emissions. However, it is important to emphasize some caveats. Despite forest stability gain, its areas in central and northern regions of the Atlantic Forest are located in current and future low forest stability compared to other regions. The same is true for areas of forest stability loss in regions of current and future high forest stability such as the southern Atlantic Forest. Otherwise, there are areas of gain and loss in regions of current and future high and low values of stability which represent a real increase and a worrying decline of forests' stability in the future, respectively. Thus, the regional context of the relative change of forest stability should also account in conservation decisions via forest protection or restoration strategies. Also, the use of range maps of species to build the species richness map at high resolution on a broad scale can overestimate the local species number (Hurlbert & Jetz, 2007). This overestimation can explain our findings of higher species richness compared to carbon amount in protection and restoration hotspots.

5. CONCLUSION

In the Brazilian Atlantic Forest, climate can explain the spatial distribution of forest stability of the old-growth forests which increase from north to south. Our results show where biodiversity, carbon stocks, and its accumulation would be beneficiated or undermined in the future by forest stability gain or loss caused by climate change. Most species and carbon stocks found in hotspots for conservation are in unprotected areas predicted to lose forest stability. In hotspots for restoration, however, most of the carbon that could be stored in the first thirty years of natural forest regrowth is found at stability gain, as in areas with combination with biodiversity hotspots. In addition to the low spatial overlap between biodiversity and carbon stock, protecting and restoring the hotspots found here would benefit biodiversity more than carbon storage. Therefore, trade-offs cannot be avoided when identifying priority areas for protection and restoration of biodiversity and carbon stocks in the Brazilian Atlantic Forest under the effects of climate change on forest stability. The ecosystem-based approach presented here can help decisions by indicating unprotected areas of forest stability loss as priority areas for forest protection and management that contain high biodiversity and/or carbon stocks. Also, this approach indicates for forest restoration both areas of forest stability gain and loss with high potential for carbon accumulation and/or biodiversity. However, areas of forest stability loss may require management of their forests. Thus, this planning for forest protection and restoration considering the response of forest ecosystems to climate change can help avoid species loss and carbon emission, contributing to mitigate both biodiversity and climate crises.

ACKNOWLEDGMENTS

Lucas Andrigo Maure thanks CNPq for Ph.D funding (141218/2018-5).

AUTHOR'S CONTRIBUTIONS

All authors conceived the study and designed methodology; LAM collected and analyzed the data, interpreted the results and led the writing of the manuscript. All authors contributed critically to the drafts and gave final approval for publication.

CONFLICT OF INTEREST

The authors declare no conflict of interest.

DATA AVAILABILITY

The data that support the findings of this study are openly available in [repository name] at http://doi.org/[doi], reference number [reference number].

REFERENCES

Ackerly, D. D., Loarie, S. R., Cornwell, W. K., Weiss, S. B., Hamilton, H., Branciforte, R., & Kraft, N. J. B. (2010). The geography of climate change: Implications for conservation biogeography. *Diversity and Distributions*. https://doi.org/10.1111/j.1472-4642.2010.00654.x

Aleman, J. C., Fayolle, A., Favier, C., Staver, A. C., Dexter, K. G., Ryan, C. M., … Swaine, M. D. (2020). Floristic evidence for alternative biome states in tropical Africa. *Proceedings of the National Academy of Sciences of the United States of America*, *117*(45), 28183–28190. https://doi.org/10.1073/pnas.2011515117

Aragão, L. E. O. C., Anderson, L. O., Fonseca, M. G., Rosan, T. M., Vedovato, L. B., Wagner, F. H., … Saatchi, S. (2018). 21st Century drought-related fires counteract the decline of Amazon deforestation carbon emissions. *Nature Communications*,

9(1), 1–12. https://doi.org/10.1038/s41467-017-02771-y

Armenteras, D., Rodríguez, N., & Retana, J. (2015). National and regional relationships of carbon storage and tropical biodiversity. *Biological Conservation*, *192*, 378–386. https://doi.org/10.1016/j.biocon.2015.10.014

Arroyo-Rodríguez, V., Melo, F. P. L., Martínez-Ramos, M., Bongers, F., Chazdon, R. L., Meave, J. A., … Tabarelli, M. (2017). Multiple successional pathways in human-modified tropical landscapes: new insights from forest succession, forest fragmentation and landscape ecology research. *Biological Reviews*, *92*(1), 326–340. https://doi.org/10.1111/brv.12231

Barlow, J., Lennox, G. D., Ferreira, J., Berenguer, E., Lees, A. C., Nally, R. Mac, … Gardner, T. A. (2016). Anthropogenic disturbance in tropical forests can double biodiversity loss from deforestation. *Nature*, *535*(7610), 144–147. https://doi.org/10.1038/nature18326

Barlow, J., Mestre, L. A. M., Gardner, T. A., & Peres, C. A. (2007). The value of primary, secondary and plantation forests for Amazonian birds. *Biological Conservation*, *136*(2), 212–231. https://doi.org/10.1016/j.biocon.2006.11.021

Benito, B. M. (2021). spatialRF: Easy Spatial Regression with Random Forest. R package version 1.1.0. https://doi.org/10.5281/zenodo.4745208

Bennett, A. C., Penman, T. D., Arndt, S. K., Roxburgh, S. H., & Bennett, L. T. (2020). Climate more important than soils for predicting forest biomass at the continental scale. *Ecography*, 1–14. https://doi.org/10.1111/ecog.05180

Brancalion, P. H. S., Niamir, A., Broadbent, E., Crouzeilles, R., Barros, F. S. M., Almeyda Zambrano, A. M., … Chazdon, R. L. (2019). Global restoration opportunities in tropical rainforest landscapes. *Science Advances*, *5*(7), 1–12. https://doi.org/10.1126/sciadv.aav3223

Brando, P. M., Balch, J. K., Nepstad, D. C., Morton, D. C., Putz, F. E., Coe, M. T., … Soares-Filho, B. S. (2014). Abrupt increases in Amazonian tree mortality due to drought-fire interactions. *Proceedings of the National Academy of Sciences of the United States of America*, *111*(17), 6347–6352.

https://doi.org/10.1073/pnas.1305499111

Breiman, L. (2001). Random Forests. *Machine Learning*, *45*(1), 5–32. https://doi.org/10.1023/A:1010933404324

Brooks, T. M., Mittermeier, R. A., Mittermeier, C. G., Da Fonseca, G. A. B., Rylands, A. B., Konstant, W. R., … Hilton-Taylor, C. (2002). Habitat Loss and Extinction in the Hotspots of Biodiversity. *Conservation Biology*, *16*(4), 909–923. https://doi.org/10.1046/j.1523-1739.2002.00530.x

Caughlin, T. T., Barber, C., Asner, G. P., Glenn, N. F., Bohlman, S. A., & Wilson, C. H. (2020). Monitoring tropical forest succession at landscape scales despite uncertainty in Landsat time series. *Ecological Applications*, (February 2020), 0–3. https://doi.org/10.1002/eap.2208

Chazdon, R. L., Broadbent, E. N., Rozendaal, D. M. A., Bongers, F., Zambrano, A. M. A., Aide, T. M., … Poorter, L. (2016). Carbon sequestration potential of second-growth forest regeneration in the Latin American tropics. *Science Advances*, *2*(5). https://doi.org/10.1126/sciadv.1501639

Chazdon, R. L., Letcher, S. G., Van Breugel, M., Martínez-Ramos, M., Bongers, F., & Finegan, B. (2007). Rates of change in tree communities of secondary Neotropical forests following major disturbances. *Philosophical Transactions of the Royal Society B: Biological Sciences*, *362*(1478), 273–289. https://doi.org/10.1098/rstb.2006.1990

Chazdon, R. L., Peres, C. A., Dent, D., Sheil, D., Lugo, A. E., Lamb, D., … Miller, S. E. (2009). The potential for species conservation in tropical secondary forests. *Conservation Biology*, *23*(6), 1406–1417. https://doi.org/10.1111/j.1523-1739.2009.01338.x

Cook-Patton, S. C., Leavitt, S. M., Gibbs, D., Harris, N. L., Lister, K., Anderson-Teixeira, K. J., … Griscom, B. W. (2020). Mapping carbon accumulation potential from global natural forest regrowth. *Nature*, *585*(7826), 545–550. https://doi.org/10.1038/s41586-020-2686-x

Dale, M. R. T., & Fortin, M.-J. (2014). *Spatial analysis: a guide for ecologists*.

Cambridge University Press.

De Keersmaecker, W., Lhermitte, S., & Honnay, O. (2014). How to measure ecosystem stability ? An evaluation of the reliability of stability metrics based on remote sensing time series across the major global ecosystems. *Global Change Biology*, 2149–2161. https://doi.org/10.1111/gcb.12495

de Lima, R. A. F., Oliveira, A. A., Pitta, G. R., de Gasper, A. L., Vibrans, A. C., Chave, J., … Prado, P. I. (2020). The erosion of biodiversity and biomass in the Atlantic Forest biodiversity hotspot. *Nature Communications*, *11*(1), 6347. https://doi.org/10.1038/s41467-020-20217-w

Deere, N. J., Guillera-Arroita, G., Baking, E. L., Bernard, H., Pfeifer, M., Reynolds, G., … Struebig, M. J. (2018). High Carbon Stock forests provide co-benefits for tropical biodiversity. *Journal of Applied Ecology*, *55*(2), 997–1008. https://doi.org/10.1111/1365-2664.13023

Di Marco, M., Watson, J. E. M., Currie, D. J., Possingham, H. P., & Venter, O. (2018). The extent and predictability of the biodiversity–carbon correlation. *Ecology Letters*, *21*(3), 365–375. https://doi.org/10.1111/ele.12903

Díaz, S., Hector, A., & Wardle, D. A. (2009). Biodiversity in forest carbon sequestration initiatives: not just a side benefit. *Current Opinion in Environmental Sustainability*, *1*(1), 55–60. https://doi.org/10.1016/j.cosust.2009.08.001

Dickey, D. A., & Fuller, W. A. (1979). Distribution of the Estimators for Autoregressive Time Series With a Unit Root. *Journal of the American Statistical Association*, *74*(366), 427–431. https://doi.org/10.2307/2286348

Elias, F., Ferreira, J., Lennox, G. D., Berenguer, E., Ferreira, S., Schwartz, G., … Barlow, J. (2020). Assessing the growth and climate sensitivity of secondary forests in highly deforested Amazonian landscapes. *Ecology*, *101*(3). https://doi.org/10.1002/ecy.2954

Erb, K. H., Kastner, T., Plutzar, C., Bais, A. L. S., Carvalhais, N., Fetzel, T., … Luyssaert, S. (2018). Unexpectedly large impact of forest management and grazing on global vegetation biomass. *Nature*, *553*(7686), 73–76.

https://doi.org/10.1038/nature25138

Ferreira, J., Lennox, G. D., Gardner, T. A., Thomson, J. R., Berenguer, E., Lees, A. C., … Barlow, J. (2018). Carbon-focused conservation may fail to protect the most biodiverse tropical forests. *Nature Climate Change*, *8*(8), 744–749. https://doi.org/10.1038/s41558-018-0225-7

Fick, S. E., & Hijmans, R. J. (2017). WorldClim 2: new 1-km spatial resolution climate surfaces for global land areas. *International Journal of Climatology*, *37*(12), 4302–4315. https://doi.org/doi:10.1002/joc.5086

Fletcher, R., & Fortin, M. (2018). *Spatial ecology and conservation modeling*. Springer.

Fontes, C. G., Dawson, T. E., Jardine, K., McDowell, N., Gimenez, B. O., Anderegg, L., … Chambers, J. Q. (2018). Dry and hot: The hydraulic consequences of a climate change–type drought for Amazonian trees. *Philosophical Transactions of the Royal Society B: Biological Sciences*, *373*(1760). https://doi.org/10.1098/rstb.2018.0209

García-Palacios, P., Gross, N., Gaitán, J., & Maestre, F. T. (2018). Climate mediates the biodiversity–ecosystem stability relationship globally. *Proceedings of the National Academy of Sciences of the United States of America*, *115*(33), 8400–8405. https://doi.org/10.1073/pnas.1800425115

Gardner, T. A., Burgess, N. D., Aguilar-Amuchastegui, N., Barlow, J., Berenguer, E., Clements, T., … Vieira, I. C. G. (2012). A framework for integrating biodiversity concerns into national REDD+ programmes. *Biological Conservation*, *154*, 61–71. https://doi.org/10.1016/j.biocon.2011.11.018

Gatti, L. V., Basso, L. S., Miller, J. B., Gloor, M., Domingues, L. G., Cassol, H. L. G., … Neves, R. A. L. (2021). Amazonia as a carbon source linked to deforestation and climate change. *Nature*, *595*(July). https://doi.org/10.1038/s41586-021-03629-6

Gibson, L., Lee, T. M., Koh, L. P., Brook, B. W., Gardner, T. A., Barlow, J., … Sodhi, N. S. (2011). Primary forests are irreplaceable for sustaining tropical biodiversity. *Nature*, *478*(7369), 378–381. https://doi.org/10.1038/nature10425

Griscom, B. W., Adams, J., Ellis, P. W., Houghton, R. A., Lomax, G., Miteva, D. A., … Fargione, J. (2017). Natural climate solutions. *Proceedings of the National Academy of Sciences of the United States of America*, *114*(44), 11645–11650. https://doi.org/10.1073/pnas.1710465114

Hamann, A., Roberts, D. R., Barber, Q. E., Carroll, C., & Nielsen, S. E. (2015). Velocity of climate change algorithms for guiding conservation and management. *Global Change Biology*, *21*(2), 997–1004. https://doi.org/10.1111/gcb.12736

Harris, N. L., Gibbs, D. A., Baccini, A., Birdsey, R. A., de Bruin, S., Farina, M., … Tyukavina, A. (2021). Global maps of twenty-first century forest carbon fluxes. *Nature Climate Change*. https://doi.org/10.1038/s41558-020-00976-6

Hartmann, H., Bastos, A., Das, A. J., Esquivel-Muelbert, A., Hammond, W. M., Martínez-Vilalta, J., … Allen, C. D. (2022). Climate Change Risks to Global Forest Health: Emergence of Unexpected Events of Elevated Tree Mortality Worldwide. *Annual Review of Plant Biology*. https://doi.org/10.1146/annurev-arplant-102820-012804

Hurlbert, A. H., & Jetz, W. (2007). Species richness, hotspots, and the scale dependence of range maps in ecology and conservation. *Proceedings of the National Academy of Sciences of the United States of America*, *104*(33), 13384–13389. https://doi.org/10.1073/pnas.0704469104

Kuhn, M., Wing, J., Weston, S., Williams, A., Keefer, C., Engelhardt, A., … Team, R. C. (2021). Caret: Classification and Regression Training. *R Package Version*.

Lennox, G. D., Gardner, T. A., Thomson, J. R., Ferreira, J., Berenguer, E., Lees, A. C., … Barlow, J. (2018). Second rate or a second chance? Assessing biomass and biodiversity recovery in regenerating Amazonian forests. *Global Change Biology*, *24*(12), 5680–5694. https://doi.org/10.1111/gcb.14443

Leutner, B., Horning, N., Schwalb-Willmann, J., & Hijmans, R. J. (2017). RStoolbox: tools for remote sensing data analysis. *R Package Version 0.1*, *7*.

Lewis, S. L., Edwards, D. P., & Galbraith, D. (2015). Increasing human dominance of tropical forests. *Science*, *349*(6250), 827–832.

Liaw, A., & Wiener, M. (2002). Classification and regression by randomForest. *R News*, *2*(3), 18–22.

Loarie, S. R., Duffy, P. B., Hamilton, H., Asner, G. P., Field, C. B., & Ackerly, D. D. (2009). The velocity of climate change. *Nature*, *462*(7276), 1052–1055. https://doi.org/10.1038/nature08649

Magnago, L. F. S., Magrach, A., Laurance, W. F., Martins, S. V., Meira-Neto, J. A. A., Simonelli, M., & Edwards, D. P. (2015). Would protecting tropical forest fragments provide carbon and biodiversity cobenefits under REDD+? *Global Change Biology*, *21*(9), 3455–3468. https://doi.org/10.1111/gcb.12937

Martin, P. A., Newton, A. C., & Bullock, J. M. (2013). Carbon pools recover more quickly than plant biodiversity in tropical secondary forests. *Proceedings of the Royal Society B: Biological Sciences*, *280*(1773). https://doi.org/10.1098/rspb.2013.2236

Matos, F. A. R., Magnago, L. F. S., Aquila Chan Miranda, C., de Menezes, L. F. T., Gastauer, M., Safar, N. V. H., … Edwards, D. P. (2020). Secondary forest fragments offer important carbon and biodiversity cobenefits. *Global Change Biology*, *26*(2), 509–522. https://doi.org/10.1111/gcb.14824

McDowell, N., Allen, C. D., Anderson-Teixeira, K., Brando, P., Brienen, R., Chambers, J., … Xu, X. (2018). Drivers and mechanisms of tree mortality in moist tropical forests. *New Phytologist*, *219*(3), 851–869. https://doi.org/10.1111/nph.15027

Myers, N., Mittermeier, R. A., Mittermeier, C. G., da Fonseca, G. A. B., & Kent, J. (2000). Biodiversity hotspots for conservation priorities. *Nature*, *403*(6772), 853–858. https://doi.org/10.1038/35002501

Noon, M. L., Goldstein, A., Ledezma, J. C., Roehrdanz, P. R., Cook-Patton, S. C., Spawn-Lee, S. A., … Turner, W. R. (2021). Mapping the irrecoverable carbon in Earth's ecosystems. *Nature Sustainability*. https://doi.org/10.1038/s41893-021-00803-6

Oliveira, R. S., Eller, C. B., Barros, F. de V., Hirota, M., Brum, M., & Bittencourt, P. (2021). *Linking plant hydraulics and the fast-slow continuum to understand*

resilience to drought in tropical ecosystems. *New Phytologist*. https://doi.org/10.1111/nph.17266

Pettorelli, N., Graham, N. A. J., Seddon, N., da Cunha Bustamante, M., Lowton, M. J., Sutherland, W. J., … Barlow, J. (2021). Time to integrate global climate change and biodiversity science-policy agendas. *Journal of Applied Ecology*, *n/a*(n/a). https://doi.org/https://doi.org/10.1111/1365-2664.13985

Pettorelli, N., Vik, J. O., Mysterud, A., Gaillard, J. M., Tucker, C. J., & Stenseth, N. C. (2005). Using the satellite-derived NDVI to assess ecological responses to environmental change. *Trends in Ecology and Evolution*. https://doi.org/10.1016/j.tree.2005.05.011

Phelps, J., Friess, D. A., & Webb, E. L. (2012). Win-win REDD+ approaches belie carbon-biodiversity trade-offs. *Biological Conservation*, *154*, 53–60. https://doi.org/10.1016/j.biocon.2011.12.031

Phelps, J., Webb, E. L., & Adams, W. M. (2012). Biodiversity co-benefits of policies to reduce forest-carbon emissions. *Nature Climate Change*, *2*(7), 497–503. https://doi.org/10.1038/nclimate1462

Pohlert, T. (2018). trend: Non-Parametric Trend Tests and Change-Point Detection. R package version 1.1.1. *Https://CRAN.R-Project.Org/Package=trend*.

Poorter, L., Bongers, F., Aide, T. M., Almeyda Zambrano, A. M., Balvanera, P., Becknell, J. M., … Rozendaal, D. M. A. (2016). Biomass resilience of Neotropical secondary forests. *Nature*, *530*(7589), 211–214. https://doi.org/10.1038/nature16512

R Core Team. (2020). R: A language and environment for statistical computing. *R Foundation for Statistical Computing, Vienna, Austria.*

Rezende, C. L., Scarano, F. R., Assad, E. D., Joly, C. A., Metzger, J. P., Strassburg, B. B. N., … Mittermeier, R. A. (2018). From hotspot to hopespot: An opportunity for the Brazilian Atlantic Forest. *Perspectives in Ecology and Conservation*, *16*(4), 208–214. https://doi.org/10.1016/j.pecon.2018.10.002

Ribeiro, M. C., Metzger, J. P., Martensen, A. C., Ponzoni, F. J., & Hirota, M. M. (2009). The Brazilian Atlantic Forest: How much is left, and how is the remaining forest distributed? Implications for conservation. *Biological Conservation*, *142*(6), 1141–1153. https://doi.org/10.1016/j.biocon.2009.02.021

Ribeiro, M., Martensen, A., Metzger, J., Tabarelli, M., Scarano, F., & Fortin, M.-J. (2011). The Brazilian Atlantic Forest: A Shrinking Biodiversity Hotspot. In *Biodiversity Hotspots: Distribution and Protection of Conservation Priority Areas* (pp. 405–434). https://doi.org/10.1007/978-3-642-20992-5_21

Rosa, M. R., Brancalion, P. H. S., Crouzeilles, R., Tambosi, L. R., Piffer, P. R., Lenti, F. E. B., … Metzger, J. P. (2021). Hidden destruction of older forests threatens Brazil's Atlantic Forest and challenges restoration programs. Science Advances, 7, eabc4547.

Ross, C. W., Hanan, N. P., Prihodko, L., Anchang, J., Ji, W., & Yu, Q. (2021). Woody-biomass projections and drivers of change in sub-Saharan Africa. *Nature Climate Change*, *11*(5), 449–455. https://doi.org/10.1038/s41558-021-01034-5

Rozendaal, D. M. A., Bongers, F., Aide, T. M., Alvarez-Dávila, E., Ascarrunz, N., Balvanera, P., … Poorter, L. (2019). Biodiversity recovery of Neotropical secondary forests. *Science Advances*, *5*(3). https://doi.org/10.1126/sciadv.aau3114

Saatchi, S., Houghton, R. A., Dos Santos Alvalá, R. C., Soares, J. V., & Yu, Y. (2007). Distribution of aboveground live biomass in the Amazon basin. *Global Change Biology*, *13*(4), 816–837. https://doi.org/10.1111/j.1365-2486.2007.01323.x

Sales, L. P., Galetti, M., & Pires, M. M. (2020). Climate and land-use change will lead to a faunal "savannization" on tropical rainforests. *Global Change Biology*, *26*(12), 7036–7044. https://doi.org/10.1111/gcb.15374

Schwartz, N. B., Budsock, A. M., & Uriarte, M. (2019). Fragmentation, forest structure, and topography modulate impacts of drought in a tropical forest landscape. *Ecology*, *100*(6). https://doi.org/10.1002/ecy.2677

Soto-Navarro, C., Ravilious, C., Arnell, A., De Lamo, X., Harfoot, M., Hill, S. L. L., … Kapos, V. (2020). Mapping co-benefits for carbon storage and biodiversity to

inform conservation policy and action. *Philosophical Transactions of the Royal Society B: Biological Sciences*, *375*(1794). https://doi.org/10.1098/rstb.2019.0128

Spawn, S. A., Sullivan, C. C., Lark, T. J., & Gibbs, H. K. (2020). Harmonized global maps of above and belowground biomass carbon density in the year 2010. *Scientific Data*, *7*(1), 1–22. https://doi.org/10.1038/s41597-020-0444-4

Strassburg, B. B. N., Iribarrem, A., Beyer, H. L., Cordeiro, C. L., Crouzeilles, R., Jakovac, C. C., … Visconti, P. (2020). Global priority areas for ecosystem restoration. *Nature*, (August 2019). https://doi.org/10.1038/s41586-020-2784-9

Strassburg, B. B. N., Kelly, A., Balmford, A., Davies, R. G., Gibbs, H. K., Lovett, A., … Rodrigues, A. S. L. (2010). Global congruence of carbon storage and biodiversity in terrestrial ecosystems. *Conservation Letters*. https://doi.org/10.1111/j.1755-263X.2009.00092.x

Sullivan, M. J. P., Lewis, S. L., Affum-Baffoe, K., Castilho, C., Costa, F., Sanchez, A. C., … Phillips, O. L. (2020). Long-term thermal sensitivity of Earth's tropical forests. *Science, in press*(800), 869–874. https://doi.org/10.1126/science.aaw7578

Tabarelli, M., Pinto, L. P., Silva, J. M. C., Hirota, M., & Bedê, L. (2005). Challenges and Opportunities for Biodiversity Conservation in the Brazilian Atlantic Forest. *Conservation Biology*, *19*(3), 695–700. https://doi.org/https://doi.org/10.1111/j.1523-1739.2005.00694.x

Vilela, B., & Villalobos, F. (2015). letsR: a new R package for data handling and analysis in macroecology. *Methods in Ecology and Evolution*, *6*(10), 1229–1234. https://doi.org/https://doi.org/10.1111/2041-210X.12401

Wright, M. N., & Ziegler, A. (2017). ranger: A Fast Implementation of Random Forests for High Dimensional Data in C++ and R. *Journal of Statistical Software*, *77(1)*, 1–17. https://doi.org/10.18637/jss.v077.i01

Xu, L., Saatchi, S. S., Yang, Y., Yu, Y., Pongratz, J., Bloom, A. A., … Schimel, D. (2021). Changes in global terrestrial live biomass over the 21st century. *Science Advances*, *7*(27), eabe9829. https://doi.org/10.1126/sciadv.abe9829

FIGURES

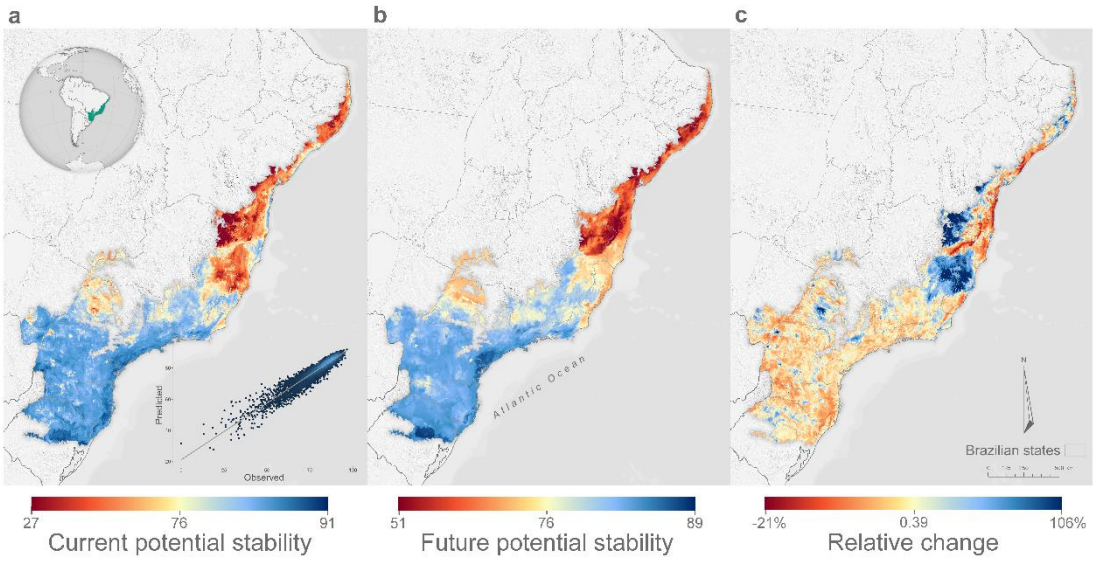

Figure 1. Prediction of forest stability by current (a) and future (2100) periods (b). (c) shows the percentage of relative change in forest stability due to climate change. The density graph in (a) illustrates the Pearsons' correlation (r = 0.95) between observed and current forest stability data predicted by random forest model.

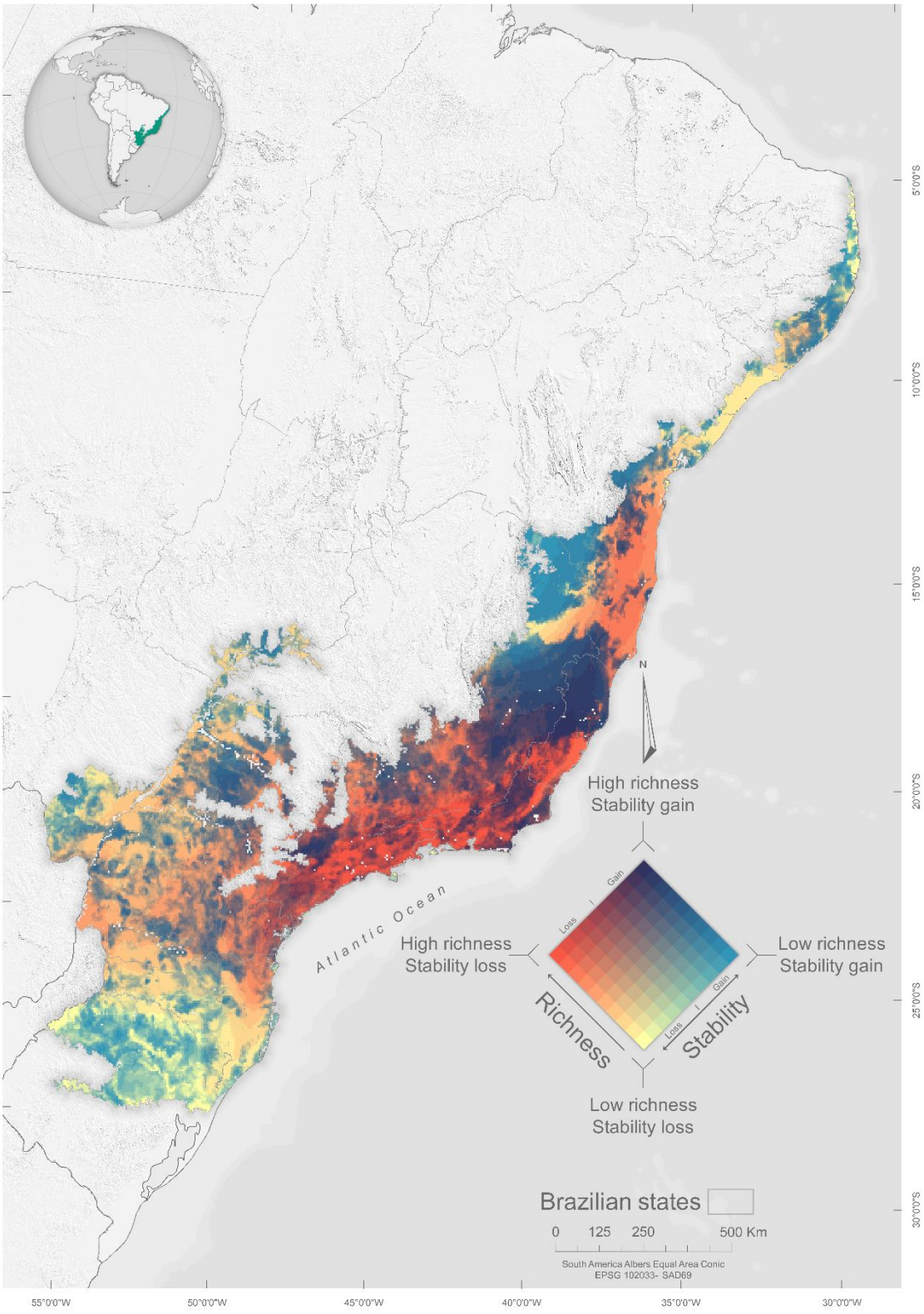

Figure 2. Bivariate map overlapping the 10% quantile classes of the values of species richness of forest-specialist vertebrates (birds, mammals, and amphibians; yellow to red) and relative change of forest stability (yellow to blue). Forest stability loss increases from the fifth to the first quantile and forest stability gain from the sixth to the tenth quantile.

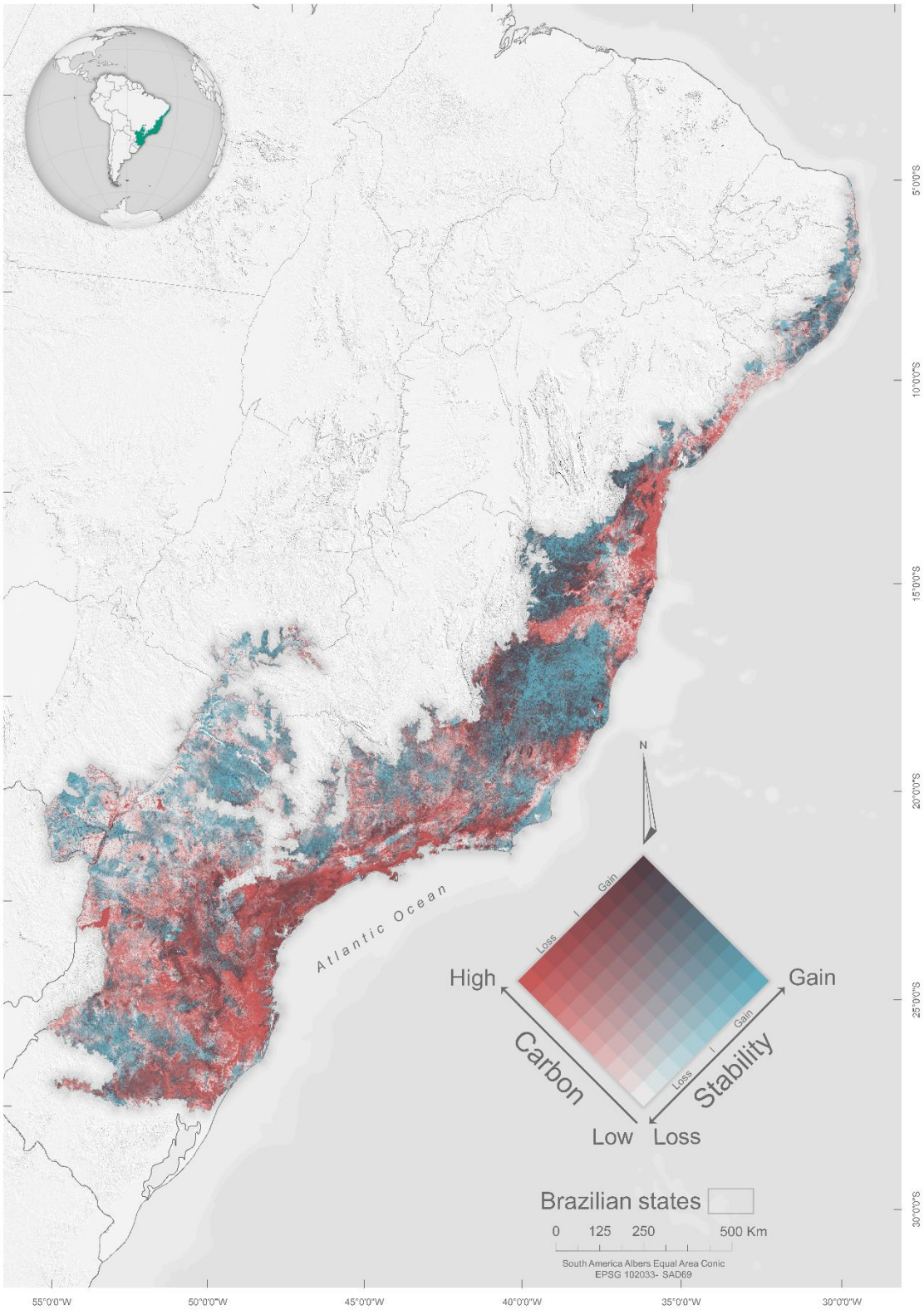

Figure 3. Bivariate map overlapping the 10% quantile classes of the values of carbon density (MgC/ha; gray to red) and relative change of forest stability (gray to blue). Forest stability loss increases from the fifth to the first quantile and forest stability gain from the sixth to the tenth quantile.

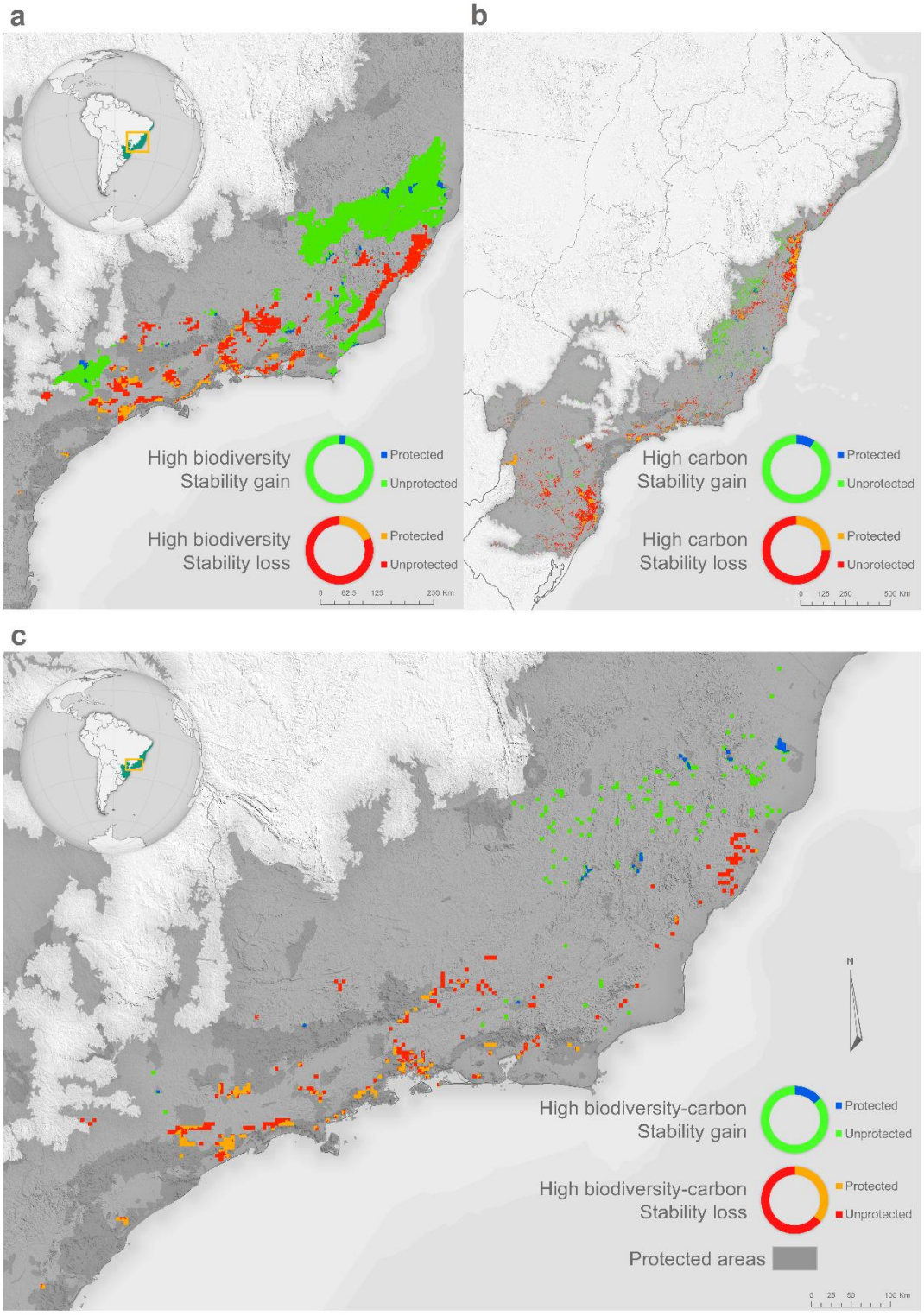

Figure 4. Maps of protection hotspots showing areas of the highest 20% values of forest stability gain (green and blue) and loss (red and orange) combined with the highest 20% values of biodiversity (a), carbon density (b), and the overlap areas of the biodiversity and carbon hotspots (c) where conservation co-benefit both. The three maps show four classes that represent forest stability gain in protected (blue - 3.12% for biodiversity (a), 9.17% for carbon (b) and 13.91% for co-benefit (c) maps) and unprotected areas (green - 96.88% for biodiversity (a), 90.83% for carbon (b) and 86.09% for co-benefit (c) maps),

and forest stability loss in protected (orange - 18.94% for biodiversity (a), 24.92% for carbon (b) and 36.03% for co-benefit (c) maps) and unprotected areas (red - 81.06% for biodiversity (a), 75.08% for carbon (b) and 63.96% for co-benefit (c) maps). Circular graphs show the proportion of protected and unprotected areas of the hotspots. Other protection areas are found as dark gray.

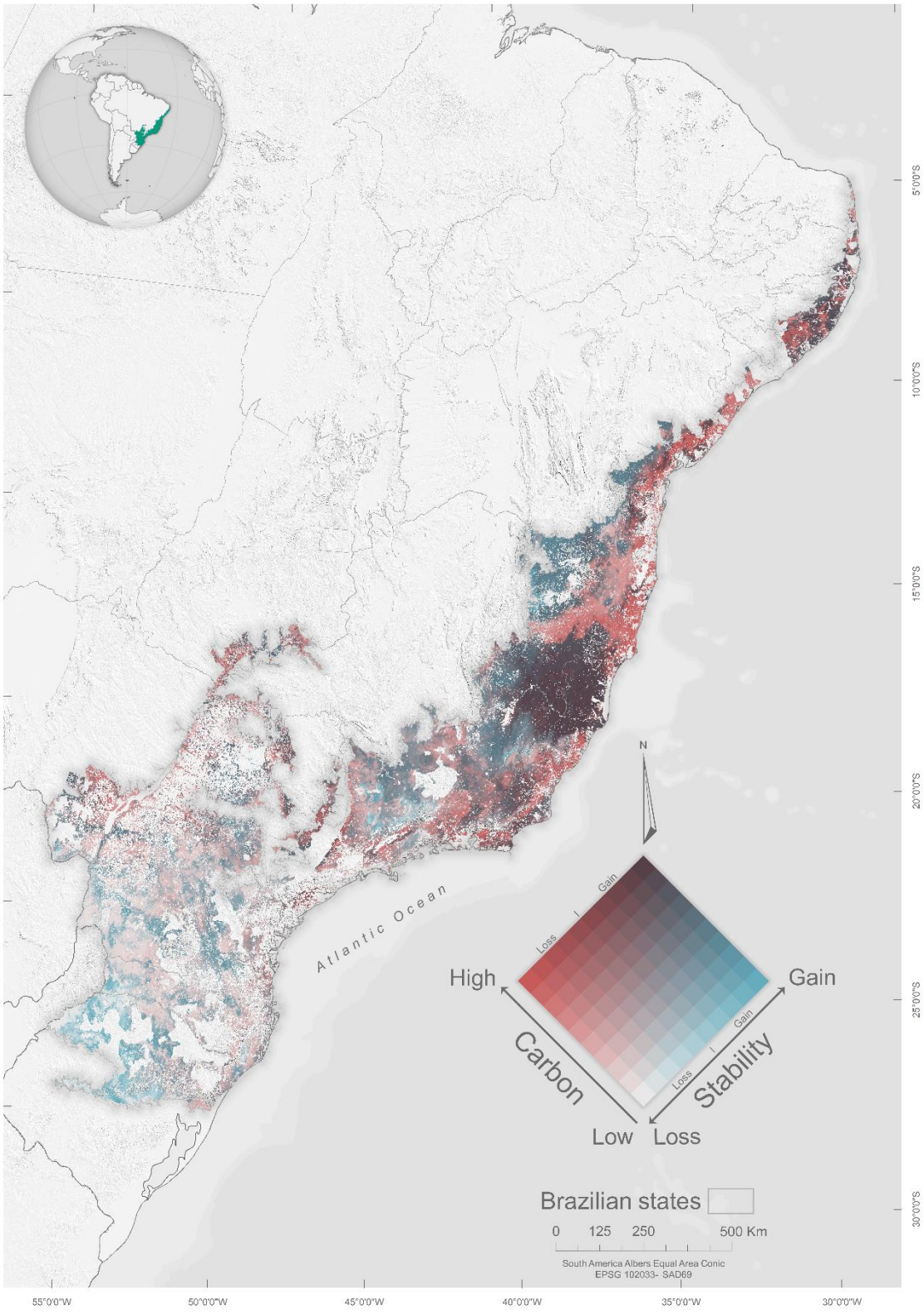

Figure 5. Bivariate map overlapping the 10% quantile classes of the values of carbon accumulation potential ($MgC/ha^{-1}/y^{-1}$; gray to red) and relative change of forest stability (gray to blue). Forest stability loss increases from the fifth to the first quantile and forest stability gain from the sixth to the tenth quantile. This map displays only areas for reforestation opportunities according to Griscom et al., (2017).

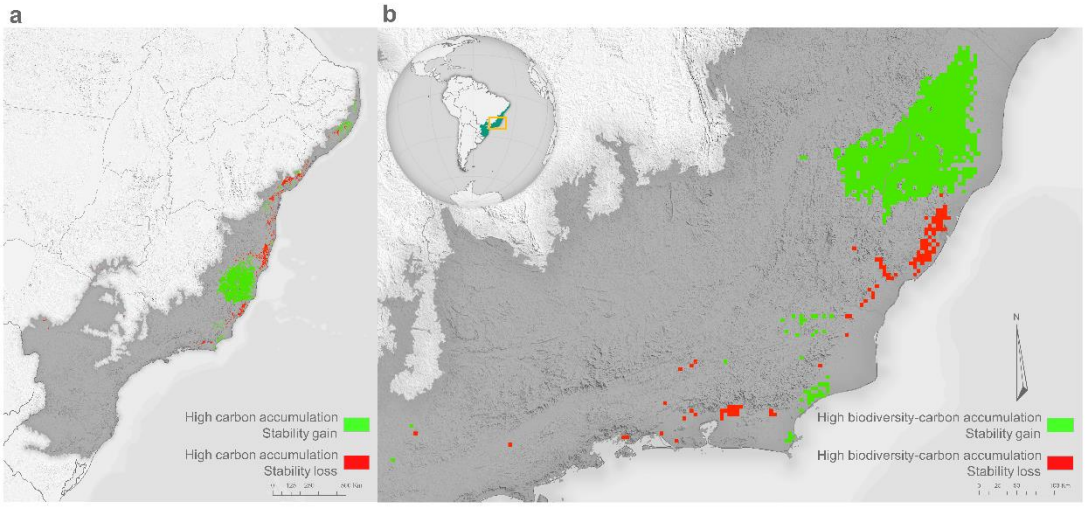

Figure 6. Maps of restoration hotspots showing areas of the highest 20% values of forest stability gain (green) and loss (red) combined with the highest 20% values of carbon accumulation potential (MgC/ha^{-1}/y^{-1}) (a) and the overlap areas values of biodiversity and carbon accumulation potential hotspots at highest 20% values of forest stability gain (green) and loss (red) (c) where conservation co-benefit both. This map displays only areas for reforestation opportunities according to Griscom et al., (2017).

TABLES

Table 1. Biodiversity and carbon content in protection and restoration hotspots in forest stability gain and loss for biodiversity, carbon and biodiversity-carbon scenarios.

PROTECTION HOTSPOTS		
Scenarios	**Forest stability gain**	**Forest stability loss**
Biodiversity	1011 spp (68.77%)	1085 spp (73.81%)
Carbon	1,184,927,504 MgC (9.85%)	3,511,992,885 MgC (29.19%)
Biodiversity -Carbon	967 spp (65,78%) - 120,058,129 MgC (1%)	1066 spp (72.52%) - 355,627,412 MgC (2.95%)

RESTORATION HOTSPOTS		
Scenarios	**Forest stability gain**	**Forest stability loss**
Carbon	640,098,374 MgC (11.20%)	160,771,323 MgC (2.81%)
Biodiversity -Carbon	933 spp (63.47%) - 253,663,906 MgC (4.44%)	934 spp (63.47%) - 21,058,789 MgC (0.37%)

Supporting information

Conservation of biodiversity and carbon stocks under the effect of climate change on ecosystem stability of tropical forests

Lucas Andrigo Maure[1,2], Milena Fiuza Diniz[3], Marco Túlio Pacheco Coelho[4], Bruno Roberto Ribeiro[3], Paulo Guilherme Molin[5], Fernando Rodrigues da Silva[2], Erica Hasui[6]*

[1]Programa de Pós-graduação em Ecologia e Recursos Naturais (PPGERN), Universidade Federal de São Carlos, São Carlos-SP, Brazil

[2]Laboratório de Ecologia Teórica: Integrando Tempo, Biologia e Espaço (LET.IT.BE), Departamento de Ciências Ambientais, Programa de Pós-graduação em Ecologia e Recursos Naturais (PPGERN), Universidade Federal de São Carlos, Sorocaba-SP, Brazil

[3]Departamento de Ecologia, Universidade Federal de Goiás, Goânia-GO, Brazil

[4]Swiss Federal Institute for Forest, Snow and Landscape, Birmensdorf, Switzerland

[5]Centro de Ciências da Natureza, Universidade Federal de São Carlos, Buri-SP, Brasil

[6]Laboratório de Ecologia de Fragmentos (EcoFrag), Instituto de Ciências da Natureza, Universidade Federal de Alfenas, Alfenas-MG, Brazil

*Corresponding author: ericahasui@gmail.com

TABLES

Table S1. All the 19 bioclimatic variables and the effect of climate on plant productivity.

Variable	Description	Effect on plant productivity
BIO1	Annual Mean Temperature	Temperature and precipitation affect plant productivity by ecophysiological responses that constrains photosynthesis. Higher temperature increases plant evaporation leading to stomatal closure reducing photosynthesis and the net primary productivity, forest growth, and above ground biomass (Baldocchi & Amthor, 2001; Clark, 2004; Cowling & Shin, 2006; Feeley, Joseph Wright, Nur Supardi, Kassim, & Davies, 2007; Sullivan et al., 2020). Water stress caused by low precipitation also increases the time of stomatal closure to avoid plant water loss, reducing plant productivity and growth. In extreme situations, water stress increases the mortality risk by hydraulic failure and carbon starvation (da Costa et al., 2010; McDowell et al., 2018, 2008; Nepstad, 2002; Oliveira et al., 2021).
BIO2	Mean Diurnal Range (Mean of monthly (max temp - min temp))	
BIO3	Isothermality (BIO2/BIO7) (×100)	
BIO4	Temperature Seasonality (standard deviation ×100)	
BIO5	Max Temperature of Warmest Month	
BIO6	Min Temperature of Coldest Month	
BIO7	Temperature Annual Range (BIO5-BIO6)	
BIO8	Mean Temperature of Wettest Quarter	
BIO9	Mean Temperature of Driest Quarter	
BIO10	Mean Temperature of Warmest Quarter	
BIO11	Mean Temperature of Coldest Quarter	
BIO12	Annual Precipitation	
BIO13	Precipitation of Wettest Month	
BIO14	Precipitation of Driest Month	
BIO15	Precipitation Seasonality (Coefficient of Variation)	
BIO16	Precipitation of Wettest Quarter	
BIO17	Precipitation of Driest Quarter	
BIO18	Precipitation of Warmest Quarter	
BIO19	Precipitation of Coldest Quarter	

Table S2. Standard deviation, proportion of variance and cumulative proportion of the PCA components.

	Standard deviation	Proportion of Variance	Cumulative Proportion
Comp.1	2.9918948	0.4711281	0.4711281
Comp.2	2.0932238	0.2306098	0.7017379
Comp.3	1.4812122	0.1154731	0.817211
Comp.4	1.3896191	0.1016337	0.9188448
Comp.5	0.88674853	0.04138542	0.96023021
Comp.6	0.56808144	0.01698508	0.97721529
Comp.7	0.41456792	0.009045608	0.986260902
Comp.8	0.319457843	0.005371227	0.991632129
Comp.9	0.266688816	0.003743312	0.99537544
Comp.10	0.168317951	0.001491102	0.996866542
Comp.11	0.156685371	0.001292121	0.998158664
Comp.12	0.111772887	0.000657536	0.998816199
Comp.13	0.091091664	0.000436721	0.99925292
Comp.14	0.083517031	0.00036711	0.99962003
Comp.15	0.070960788	0.000265023	0.999885053
Comp.16	3.39E-02	6.05E-05	1.00E+00
Comp.17	2.92E-02	4.50E-05	1.00E+00
Comp.18	1.34E-02	9.50E-06	1.00E+00
Comp.19	1.95E-05	2.01E-11	1.00E+00

Table S3. PCAs **l**oadings showing the representation of each bioclimate variable on components.

	Comp. 1	Comp. 2	Comp. 3	Comp. 4	Comp. 5	Comp. 6	Comp. 7	Comp. 8	Comp. 9	Comp. 10	Comp. 11	Comp. 12	Comp. 13	Comp. 14	Comp. 15	Comp. 16	Comp. 17	Comp. 18	Comp. 19
BIO1	0.31	0.10	0.06	0.19	0.02	0.01	0.09	0.07	0.19	0.03	0.11	0.05	0.21	0.41	0.15	0.19	0.56	0.45	0.00
BIO2	-0.09	-0.27	-0.31	0.37	-0.41	-0.17	0.05	0.03	-0.03	-0.06	-0.04	-0.07	0.01	0.19	0.02	-0.65	0.13	-0.03	0.00
BIO3	0.26	-0.12	-0.06	-0.10	-0.57	-0.44	0.05	0.00	0.10	0.14	0.24	0.36	0.03	-0.22	-0.08	0.31	-0.12	0.01	0.00
BIO4	-0.29	0.04	-0.10	0.31	0.14	0.26	-0.17	-0.27	0.05	0.14	0.36	0.50	0.22	-0.16	-0.10	-0.01	0.25	-0.27	0.00
BIO5	0.23	0.10	-0.06	0.49	-0.05	0.19	-0.02	0.21	0.12	0.05	-0.15	-0.18	-0.30	-0.50	-0.12	0.12	0.12	0.03	-0.40
BIO6	0.30	0.19	0.16	-0.04	0.06	0.02	0.02	0.10	0.11	0.10	0.02	0.02	-0.10	-0.34	-0.13	-0.34	0.16	0.01	0.72
BIO7	-0.22	-0.17	-0.24	0.40	-0.12	0.11	-0.04	0.02	-0.05	-0.09	-0.13	-0.15	-0.08	0.08	0.09	0.52	-0.12	0.00	0.56
BIO8	0.26	-0.01	-0.02	0.26	0.38	-0.54	-0.47	-0.07	-0.45	-0.01	-0.03	0.04	0.01	0.00	0.03	0.01	0.00	0.00	0.00
BIO9	0.27	0.18	0.16	0.11	-0.23	0.21	0.34	-0.60	-0.49	-0.21	-0.05	-0.01	-0.01	-0.02	-0.01	0.01	0.00	0.00	0.00
BIO10	0.26	0.16	0.05	0.35	0.11	0.15	0.04	0.05	0.22	0.06	0.14	0.17	0.13	0.23	-0.01	-0.16	-0.72	0.16	0.00
BIO11	0.32	0.08	0.09	0.07	0.00	-0.05	0.11	0.14	0.15	-0.03	-0.04	-0.10	0.08	0.27	0.10	0.10	0.08	-0.84	0.00
BIO12	-0.22	0.03	0.46	0.18	-0.10	-0.13	0.06	0.21	0.01	-0.31	-0.29	0.14	0.50	-0.30	0.30	-0.02	-0.03	0.02	0.00
BIO13	0.01	-0.35	0.43	0.07	-0.10	0.16	-0.13	0.16	-0.21	0.04	0.64	-0.36	-0.01	-0.05	0.12	-0.01	-0.02	0.00	0.00
BIO14	-0.24	0.29	0.14	0.10	-0.06	-0.08	0.23	0.22	-0.30	0.49	-0.01	0.23	-0.38	0.11	0.42	-0.03	0.01	-0.02	0.00
BIO15	0.21	-0.36	-0.01	-0.08	-0.06	0.27	-0.11	-0.06	-0.14	0.64	-0.39	-0.05	0.38	-0.05	0.05	0.00	-0.03	0.00	0.00
BIO16	0.02	-0.35	0.44	0.06	-0.06	0.14	-0.13	0.11	-0.03	-0.13	-0.27	0.43	-0.37	0.27	-0.38	0.02	0.06	-0.01	0.00
BIO17	-0.24	0.29	0.12	0.12	-0.07	-0.17	0.16	0.18	-0.20	0.23	0.02	-0.24	0.28	0.14	-0.69	0.08	0.01	0.00	0.00
BIO18	-0.13	-0.33	0.24	0.19	0.32	-0.36	0.42	-0.41	0.35	0.21	-0.02	-0.14	-0.12	-0.08	-0.02	0.02	0.00	0.00	0.00
BIO19	-0.14	0.33	0.29	0.03	-0.34	-0.06	-0.55	-0.38	0.32	0.14	-0.11	-0.23	-0.11	0.12	0.08	-0.02	-0.01	0.00	0.00

Table S4. Spearman rank (r_S) correlation coefficients between species richness (Birds, mammals, amphibians and all groups) Stability change, Carbon density (MgC/ha) and Carbon accumulation (MgC/ha-1/y-1).

	Birds		*Mammals*		*Amphibians*		*All groups*		*Carbon density*		*Carbon accumulation*	
	r_S	*p*	r_S	*p*	r_S	*p*	r_S	*p*	r_S	*p*	r_S	*p*
Stability change	0.00	0.959	0.20	<0.001	0.027	<0.001	0.04	<0.001	-0.16	<0.001	0.15	<0.001
Carbon density	0.13	<0.001	0.15	<0.001	0.29	<0.001	0.17	<0.001	-	-	-	-
Carbon accumulation	0.23	<0.001	0.53	<0.001	0.52	<0.001	0.37	<0.001	-	-	-	-

FIGURES

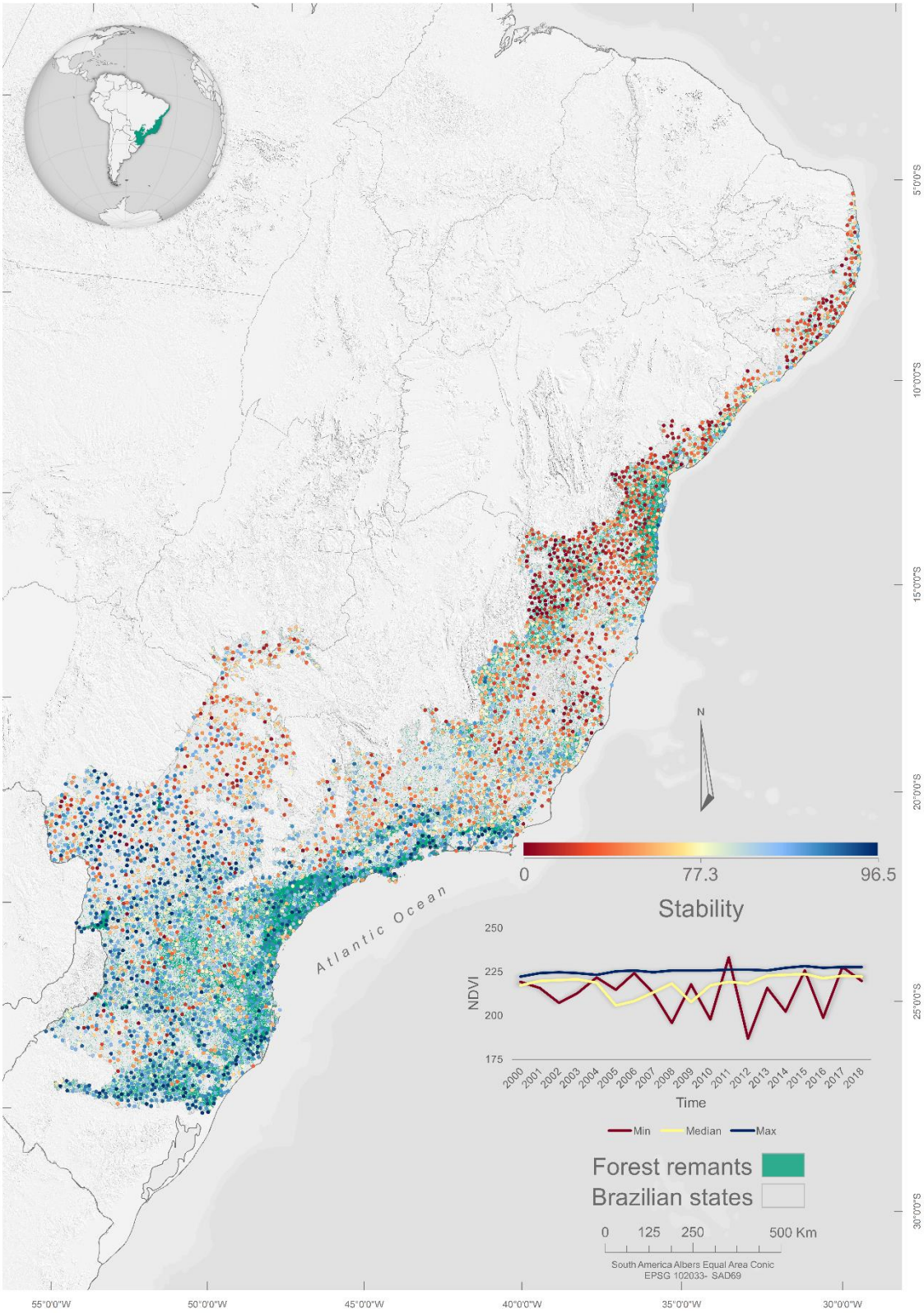

Figure S1. Distribution of 3,934 sample sites of old-growth forests in the Atlantic Forest. The color of the points represents its stability value that ranges from 0 (red) to 96.5 (blue) with a mean value of 77.3

(yellow). The graph shows the raw NDVI time-series of the points with the highest (blue), median (yellow) and lowest (red) stability. Forest remnants (green) are areas that remain classified as forests between 1985-2018, that is, forest with at least 33 years old.

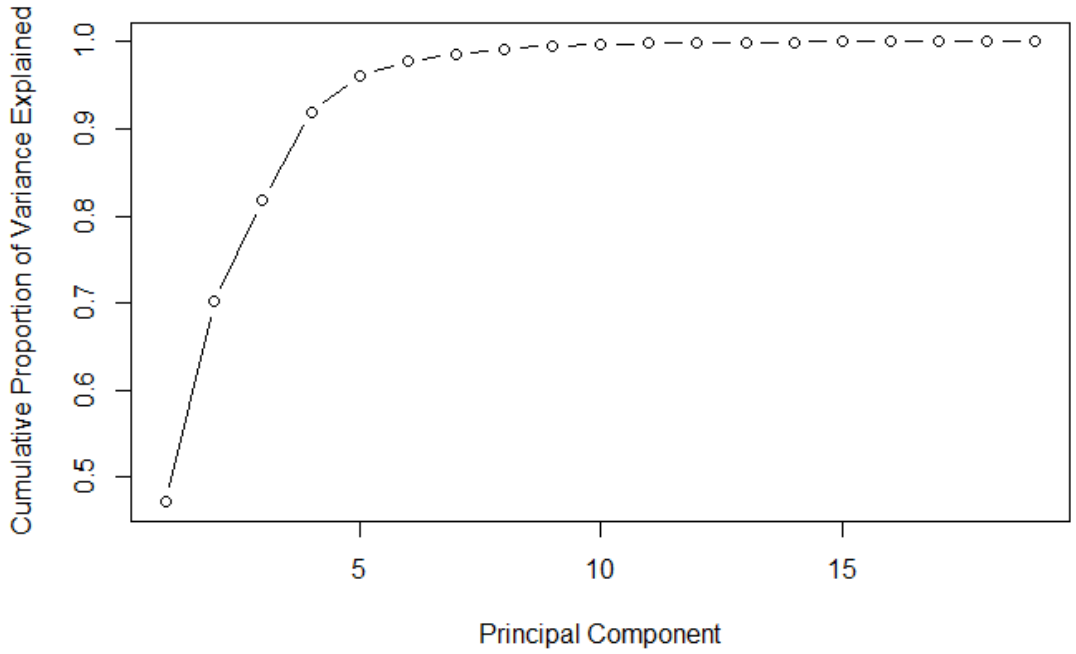

Figure S2. Cumulative proportion of variance of the PCAs.

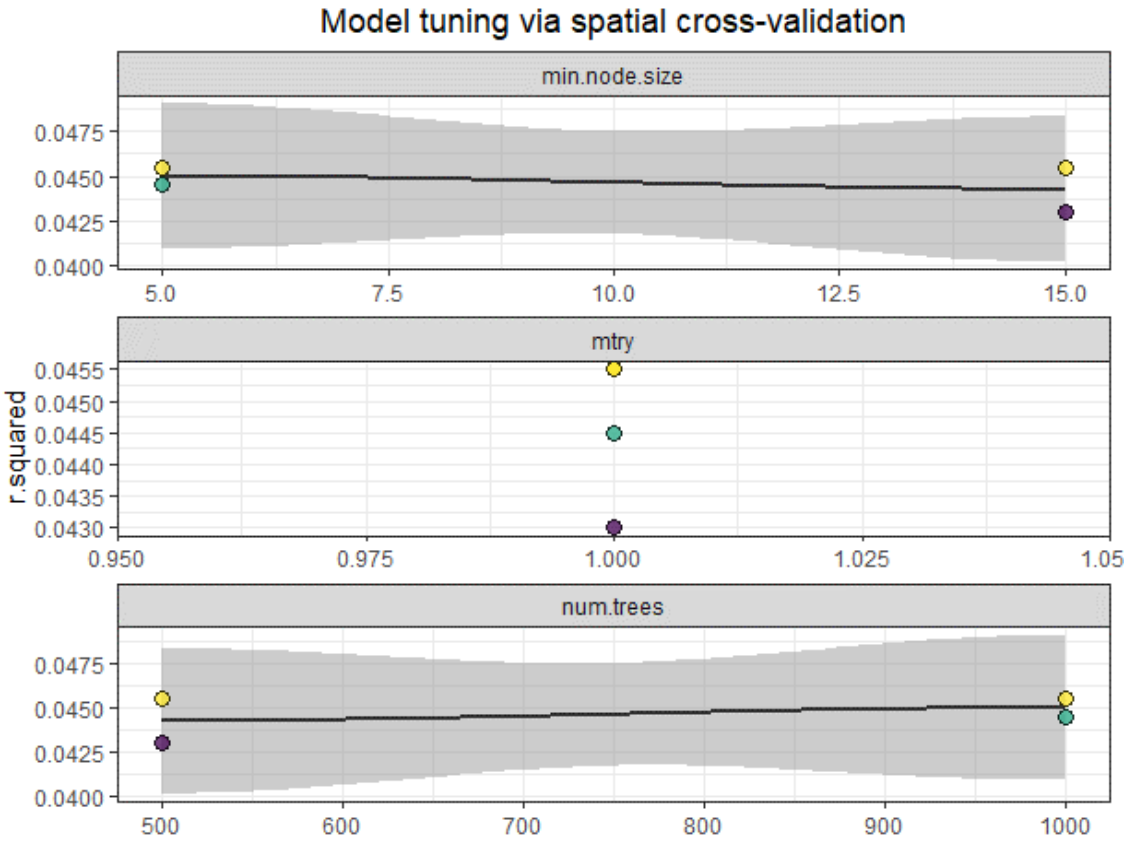

Figure S3. Graphics showing the maximization of the coefficient of determination (r^2) by the hyperparameters of minimum node size (above), predictors at each tree split (mtry) (middle) and number of trees in the forest (below).

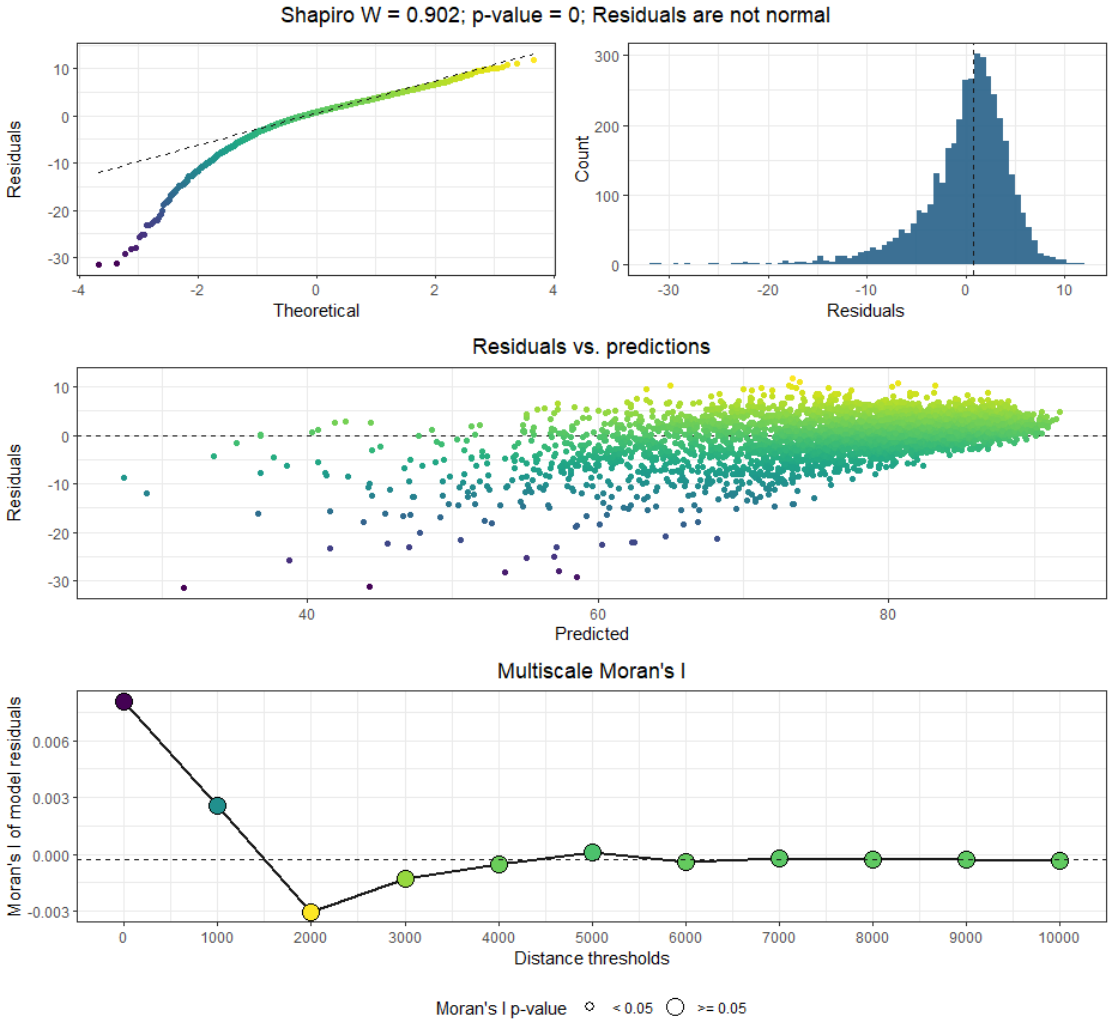

Figure S4. Residuals of the tuned model displaying the normality test (above), relationship between the residuals and the fitted values (middle) and Moran's I of the residuals (below) which shows no evidence ($p >= 0.05$) for spatial correlation across distance thresholds between 0 and 10000 m.

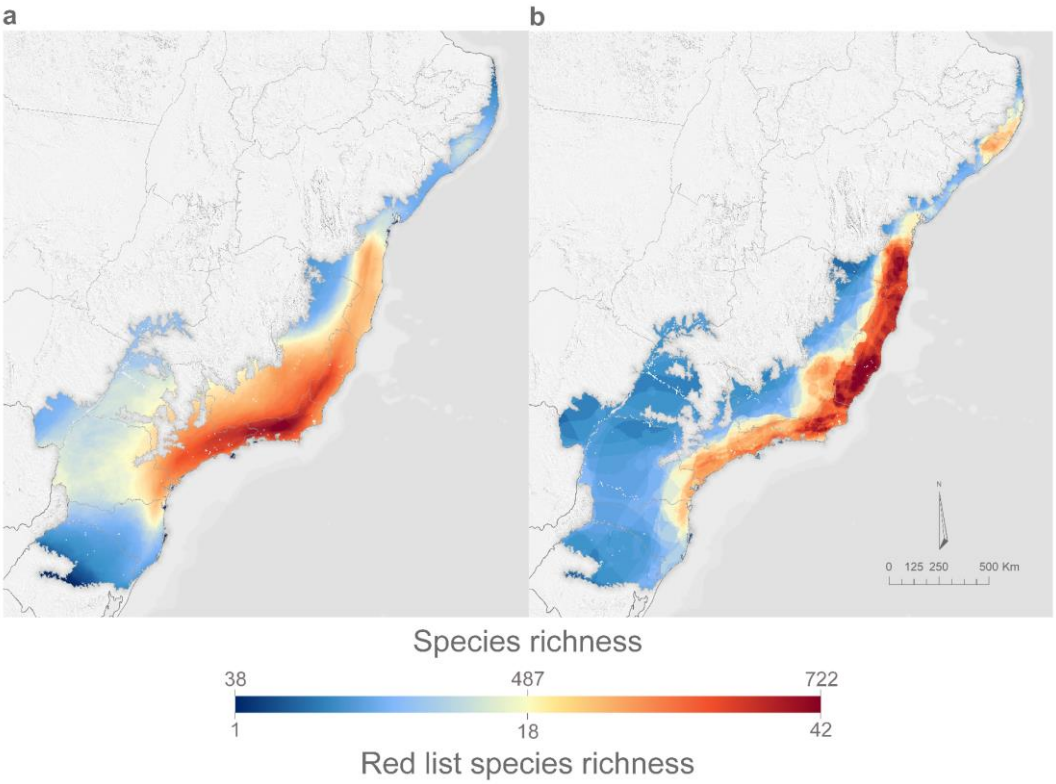

Figure S5. Maps of species richness (a) and richness of threatened species (b). Threatened species are in the IUCN red list in the categories of critically endangered (CE), endangered (EN), and vulnerable (VU). Both maps were built using ranges of forest-specialist species of birds, mammals and amphibians from IUCN.

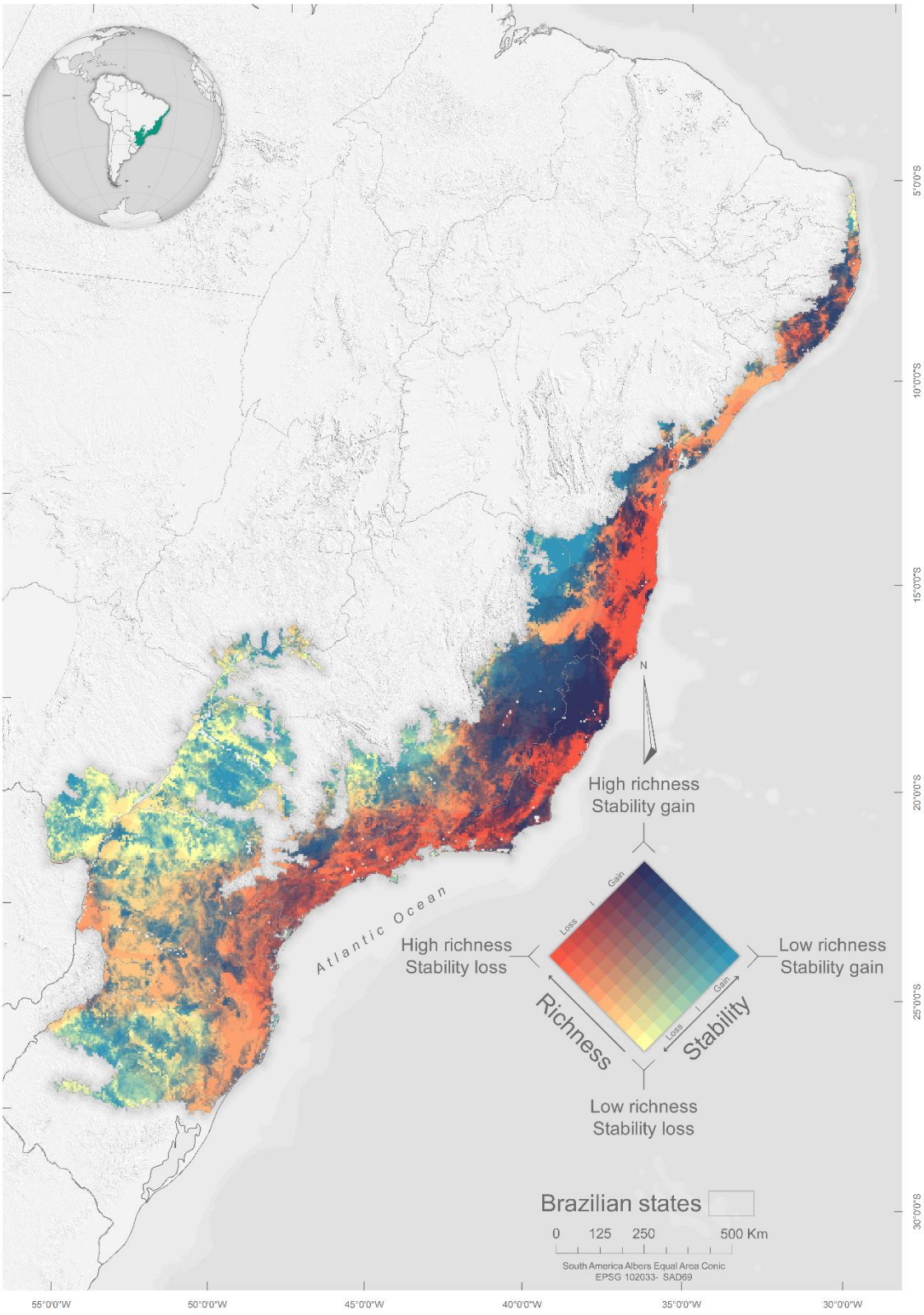

Figure S6. Bivariate map of the combination of the 10% quantile classes of the values of species richness of threatened forest-specialist vertebrates (birds, mammals and amphibians) (yellow to red) and relative change of stability (yellow to blue). Stability loss increases from the fifth to the first quantile and stability gain from the sixth to the tenth quantile.

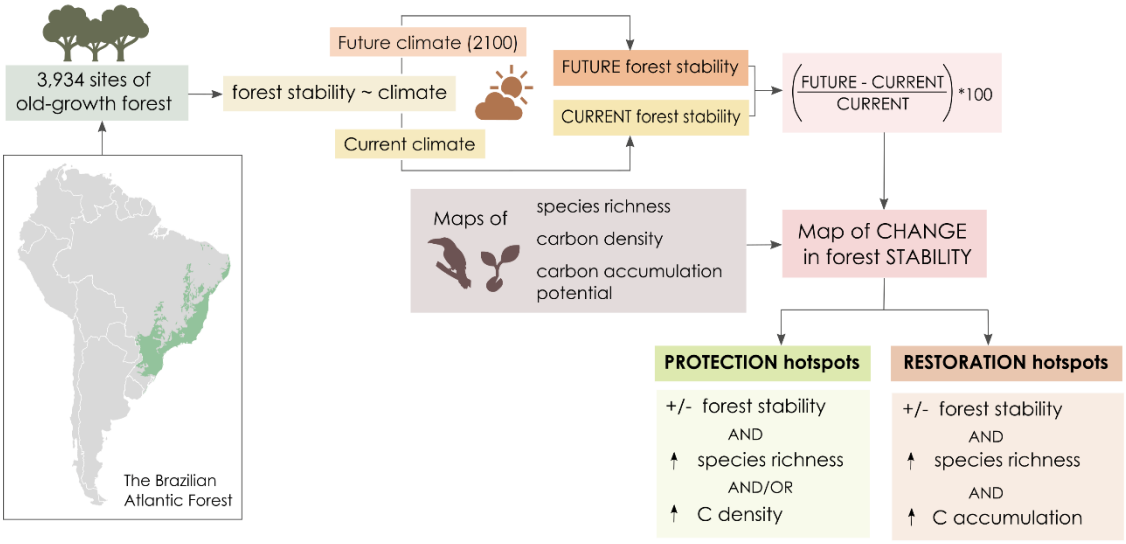

Figure S7. General framework of the methods.

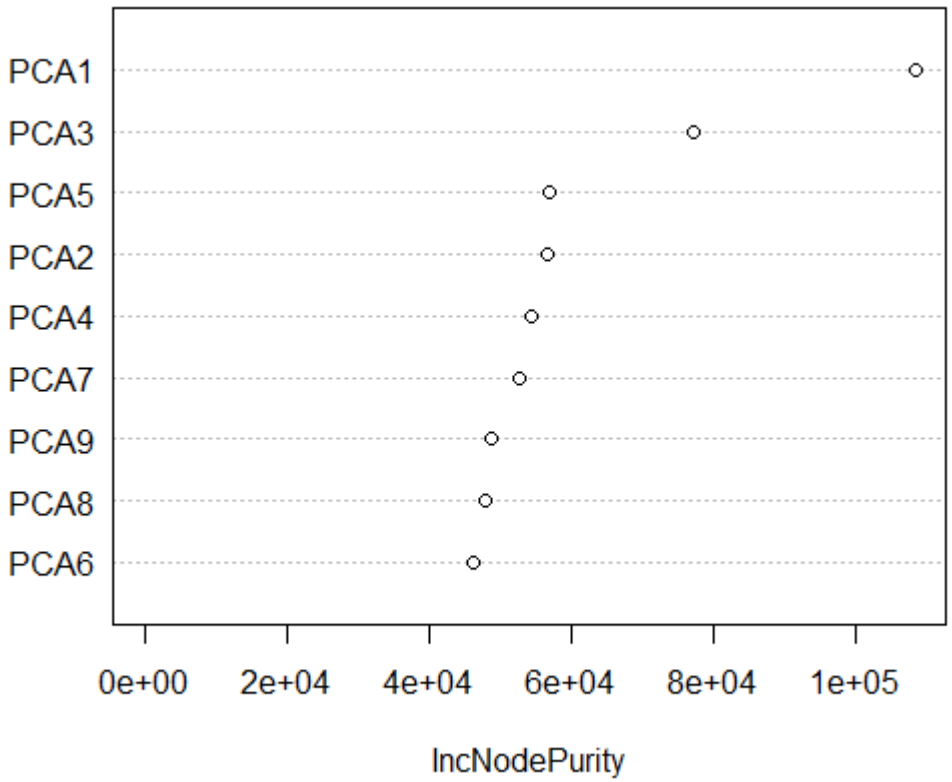

Figure S8. Predictors importance calculated as the average increase in node purity across all decision trees indicating the influence of the predictor on stability.

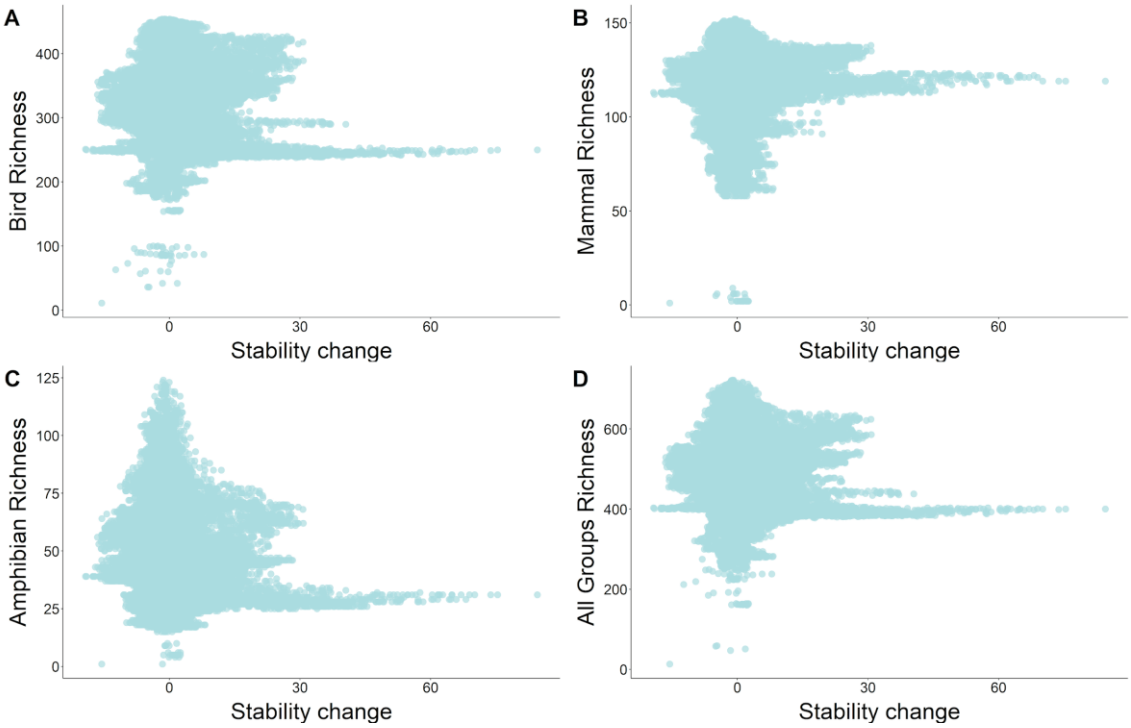

Figure S9. Scatter plot illustrating the relationship between forest stability change and species richness of birds (a), mammals (b), amphibians (c) and all groups (d).

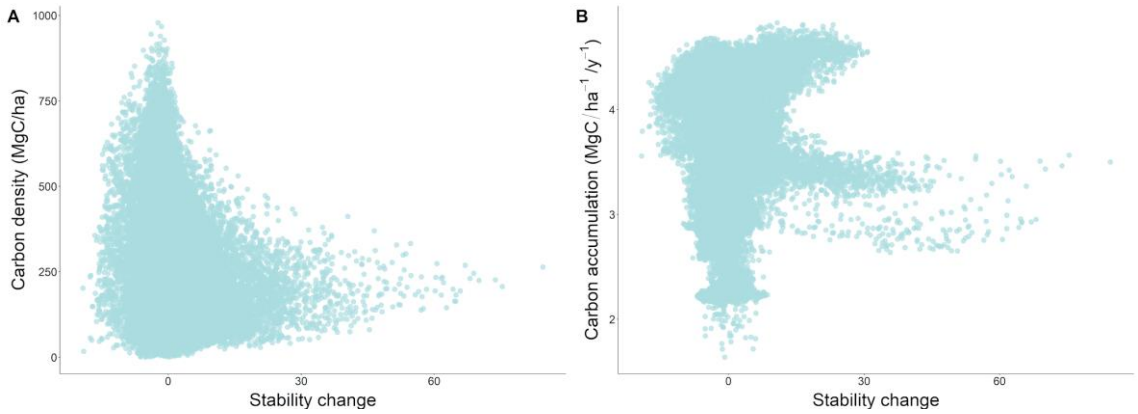

Figure S10. Scatter plot illustrating the relationship between forest stability change, carbon density (a) and carbon accumulation (b).

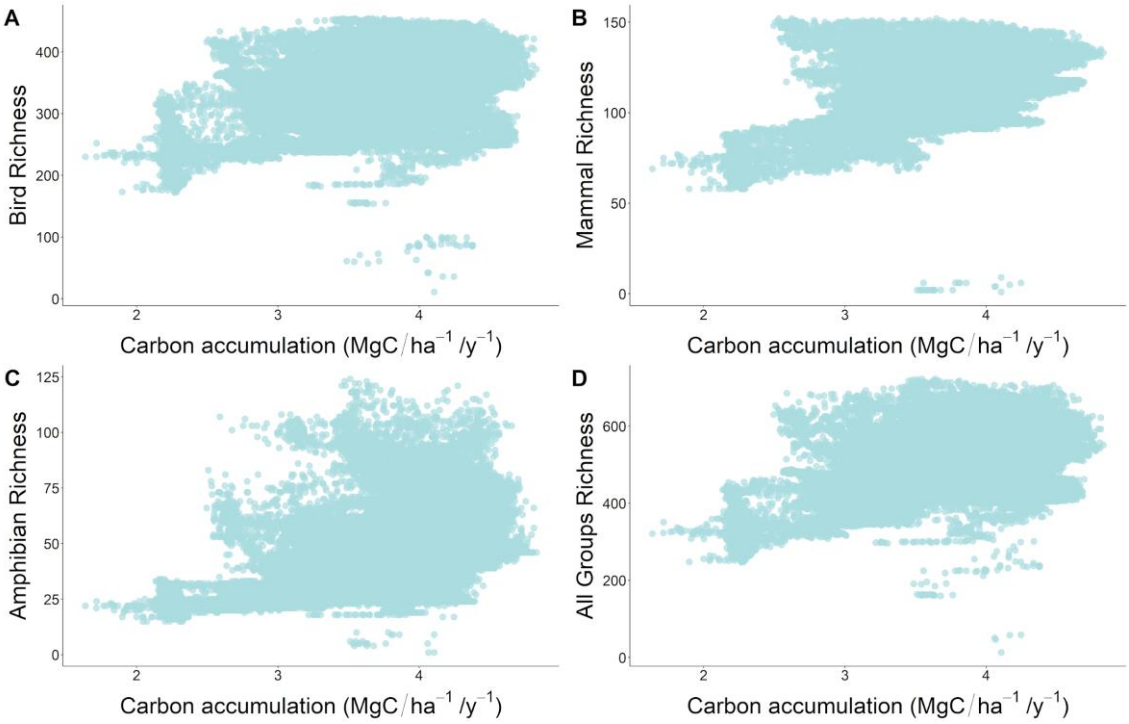

Figure S11. Scatter plot illustrating the relationship between carbon accumulation and species richness of birds (a), mammals (b), amphibians (c) and all groups (d).

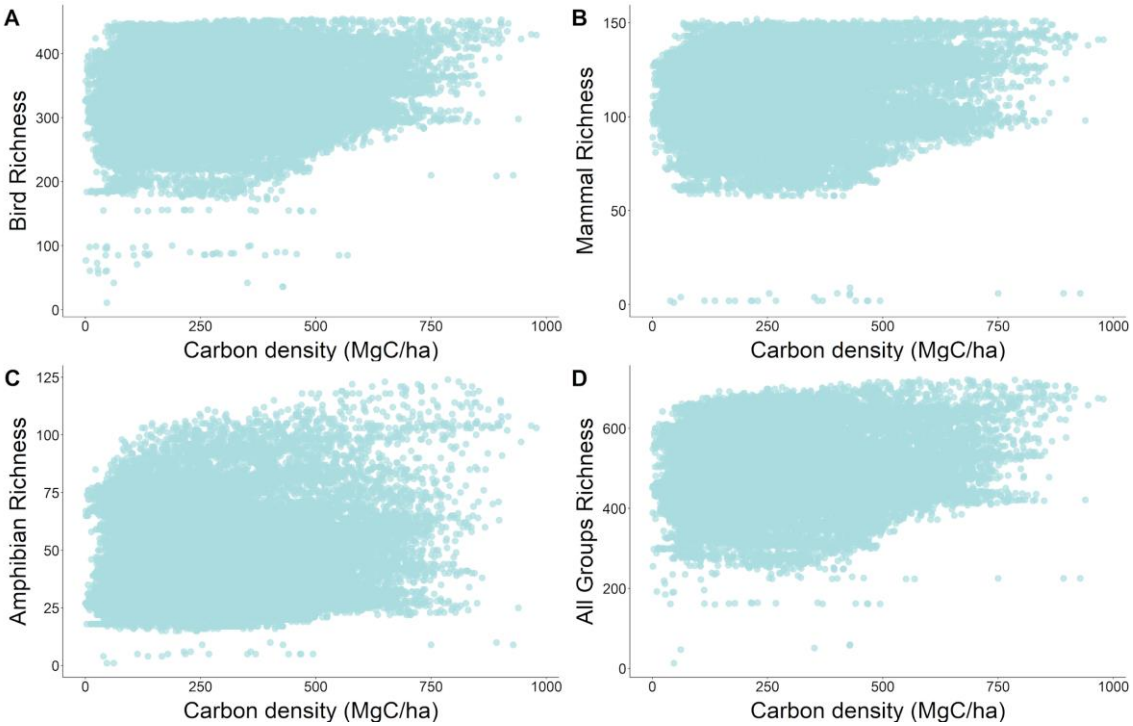

Figure S12. Scatter plot illustrating the relationship between carbon density and species richness of birds (a), mammals (b), amphibians (c) and all groups (d).

REFERENCES

Baldocchi, D. D., & Amthor, J. S. (2001). Canopy photosynthesis: history, measurements, and models. In Terrestrial global productivity (pp. 9–31). ACADEMIC PRESS.

Clark, D. A. (2004). Sources or sinks? The responses of tropical forests to current and future climate and atmospheric composition. Philosophical Transactions of the Royal Society B: Biological Sciences, 359(1443), 477–491. https://doi.org/10.1098/rstb.2003.1426

Cowling, S. A., & Shin, Y. (2006). Simulated ecosystem threshold responses to co-varying temperature, precipitation and atmospheric CO2 within a region of Amazonia. Global Ecology and Biogeography, 0(0), 060807052106001-??? https://doi.org/10.1111/j.1466-822x.2006.00256.x

da Costa, A. C. L., Galbraith, D., Almeida, S., Portela, B. T. T., da Costa, M., de Athaydes Silva Junior, J., … Meir, P. (2010). Effect of 7 yr of experimental drought on vegetation dynamics and biomass storage of an eastern Amazonian rainforest. New Phytologist, 187(3), 579–591. https://doi.org/10.1111/j.1469-8137.2010.03309.x

Feeley, K. J., Joseph Wright, S., Nur Supardi, M. N., Kassim, A. R., & Davies, S. J. (2007). Decelerating growth in tropical forest trees. Ecology Letters, 10(6), 461–469. https://doi.org/10.1111/j.1461-0248.2007.01033.x

McDowell, N., Allen, C. D., Anderson-Teixeira, K., Brando, P., Brienen, R., Chambers, J., … Xu, X. (2018). Drivers and mechanisms of tree mortality in moist tropical forests. New Phytologist, 219(3), 851–869.

https://doi.org/10.1111/nph.15027

McDowell, N., Pockman, W. T., Allen, C. D., Breshears, D. D., Cobb, N., Kolb, T., … Yepez, E. A. (2008). Mechanisms of plant survival and mortality during drought: Why do some plants survive while others succumb to drought? New Phytologist. https://doi.org/10.1111/j.1469-8137.2008.02436.x

Nepstad, D. C. (2002). The effects of partial throughfall exclusion on canopy processes, aboveground production, and biogeochemistry of an Amazon forest. Journal of Geophysical Research, 107(D20), 1–18. https://doi.org/10.1029/2001jd000360

Oliveira, R. S., Eller, C. B., Barros, F. de V., Hirota, M., Brum, M., & Bittencourt, P. (2021). Linking plant hydraulics and the fast-slow continuum to understand resilience to drought in tropical ecosystems. New Phytologist. https://doi.org/10.1111/nph.17266

Sullivan, M. J. P., Lewis, S. L., Affum-Baffoe, K., Castilho, C., Costa, F., Sanchez, A. C., … Phillips, O. L. (2020). Long-term thermal sensitivity of Earth's tropical forests. Science, in press (800), 869–874. https://doi.org/10.1126/science.aaw7578

CONCLUSÃO GERAL

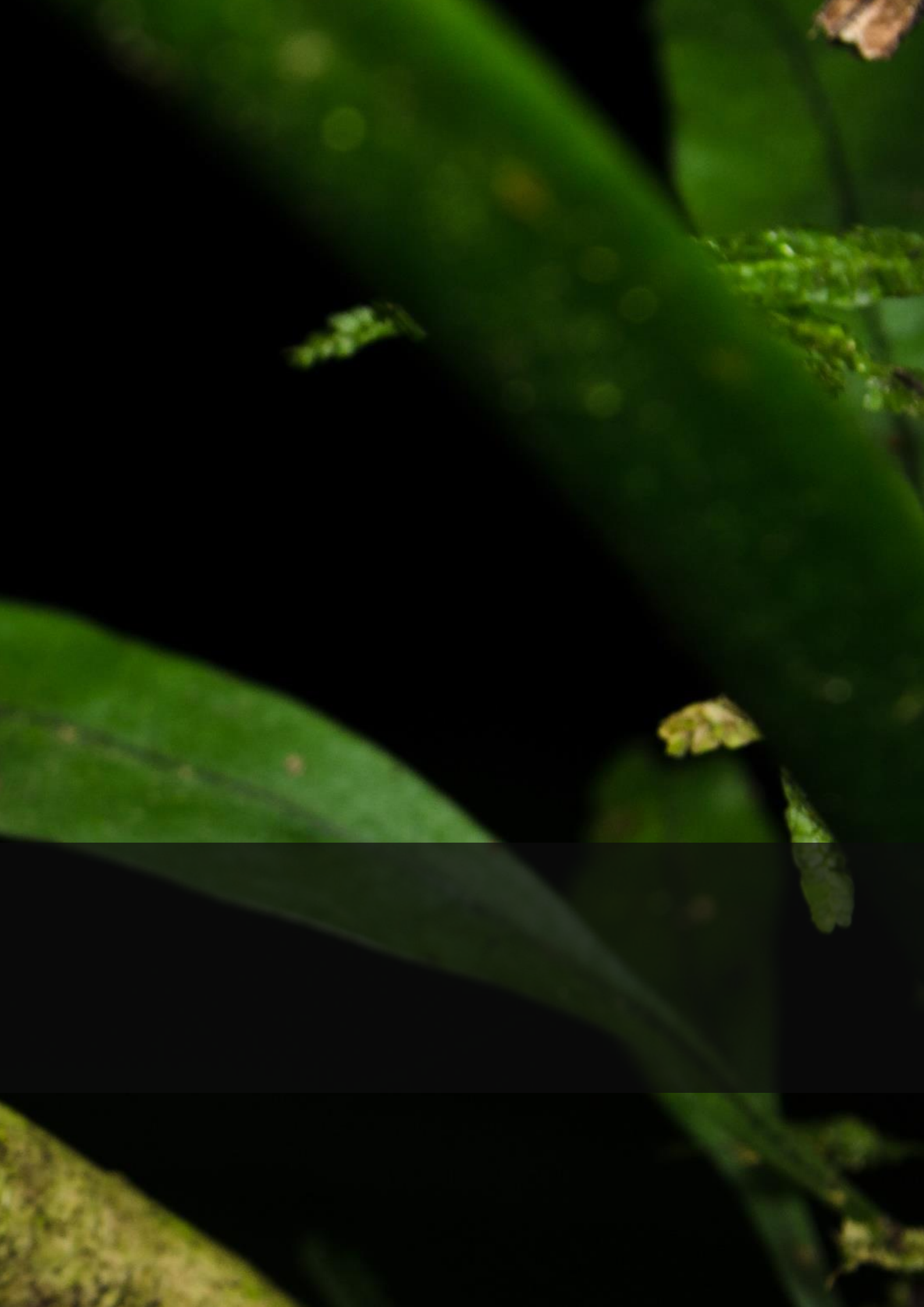

Ao fim dessa tese, concluímos que:

Capítulo I | Predicting resilience and stability of early second-growth forests

- A resiliência de florestas secundárias iniciais foi negativamente influenciada principalmente pela isotermalidade, ou seja, a oscilação diurna em relação a oscilação da temperatura anual. Por sua vez, a estabilidade dessas florestas esteve positivamente associada principalmente com a probabilidade de ocorrência da rocha matriz, a precipitação anual e a sazonalidade da precipitação.
- Os mapas preditivos tanto da resiliência quanto da estabilidade mostram um padrão de distribuição espacial geral cujos valores aumentam do norte ao sul ao longo Mata Atlântica brasileira. No entanto, uma área isolada de altos valores de resiliência e estabilidade é encontrada no sul da Bahia.
- Desse modo, devido ao baixo potencial ecossistêmico resultante das condições ambientais e aos recursos disponíveis, a restauração florestal em áreas de baixa resiliência e estabilidade pode requerer praticas ativas.

Capítulo II | Biodiversity and carbon conservation under the ecosystem stability of tropical forests

- De modo geral, a estabilidade ecossistêmica de florestas tardias observada concentra seus valores mais baixos na região norte e seus valores mais altos na região sul da Mata Atlântica. Esse padrão de distribuição foi positivamente influenciado principalmente pela sazonalidade da temperatura, estoque de carbono orgânico do solo e precipitação anual, e negativamente pela isotermalidade e profundidade da rocha matriz.
- Maiores extensões de grande número de espécies se encontram em áreas de baixa estabilidade enquanto altas densidades de carbono ocorrem em áreas de maior estabilidade, assim como a área em que tanto alta biodiversidade e estoques de carbono se sobrepõem. Grande parte das áreas prioritárias para a conservação da biodiversidade e de estoque de carbono de baixa estabilidade florestal está desprotegida.
- Devido à baixa sobreposição especial entre as áreas de maior riqueza de espécies e densidade de carbono, a conservação de ambos na Mata Atlântica apresenta um

cenário de trade-off. Nesse caso, as decisões sobre proteção e manejo podem seguir a abordagem baseada no ecossistema apresentada aqui. Assim, visando a conservação da biodiversidade ou estoques de carbono, áreas de alta estabilidade florestal desprotegidas seriam prioritárias para proteção. Por outro lado, áreas de baixa estabilidade florestal desprotegidas seriam prioritárias para proteção e manejo florestal, enquanto áreas protegidas, para manejo.

Capítulo III | Conservation of biodiversity and carbon stocks under the effect of climate change on ecosystem stability of tropical forests

- O clima pode explicar a distribuição da estabilidade ecossistêmica das florestas tardias. Em decorrência das mudanças climáticas, a distribuição espacial entre as áreas de ganho e perda de estabilidade florestal apresenta um padrão heterogêneo ao longo da Mata Atlântica. Essa predição pode indicar áreas adequadas para a proteção e restauração florestal visando a conservação futura da biodiversidade e estoques de carbono em um contexto de mudanças climáticas.
- Grande parte das espécies e do estoque de carbono em áreas prioritárias para proteção está em áreas de perda de estabilidade florestal, cuja maior proporção se encontra desprotegida. Por outro lado, áreas prioritárias para restauração com grande potencial de acúmulo de carbono e de conservação da biodiversidade se encontram em áreas de ganho de estabilidade, mas a maior proporção está desprotegida. Embora o estoque de carbono e seu acúmulo apresentem números importantes, proteger e restaurar áreas prioritárias tanto de ganho quanto de perda de estabilidade beneficiaria mais a biodiversidade do que estoques de carbono.
- Considerando a baixa sobreposição espacial entre altos valores de riqueza de espécies e densidade de carbono em um contexto de mudança de estabilidade florestal por conta das mudanças climáticas, a conservação de ambos na Mata Atlântica enfrenta um cenário de trade-off. Assim, decisões sobre áreas de proteção e restauração com foco na conservação futura de cada um, pode se apoiar na abordagem ecossistêmica sugerida nesse trabalho. Desse modo, áreas que se encontram desprotegidas e com previsão de perda de estabilidade seriam prioritárias para proteção e manejo. Pelo potencial em beneficiar a biodiversidade e aumentar o estoque de carbono, a restauração

florestal seria indicada tanto para áreas de ganho quanto para de perda de estabilidade, embora esta última exija manejo florestal.

Considerações finais |

Em síntese, nessa tese testamos o efeito de preditores ambientais no potencial ecossistêmico de florestas iniciais e tardias da Mata Atlântica. Com a modelagem da distribuição espacial da resiliência e estabilidade, destacamos áreas apropriadas e prioritárias para a proteção e restauração florestal. Essas áreas possuem grande potencial para a conservação atual da biodiversidade e estoques de carbono. Também, para a conservação futura de ambos, considerando o efeito das mudanças climáticas nos ecossistemas florestais. No entanto, muitas dessas áreas necessitam de proteção e manejo florestal. Assim, essa abordagem baseada no ecossistema fornece uma nova visão para a tomada de decisões acerca da conservação, contribuindo para a redução da perda de espécies e das mudanças climáticas.

FOTOGRAFIAS

Rafael Mitsuo